Ph.D. Thesis

Chemical Engineering

CONVECTIVE AND BOILING HEAT TRANSFER FROM A VIBRATING SURFACE

KRISHAN KUMAR NANGIA

ABSTRACT

Convective and boiling heat transfer from a vertically oscillating, horizontal platinum wire to water and methanol were studied. The wire diameter was 0.01 in. and temperatures covered were 118.4° and 170.6°F for water and 95°F for methanol. The range of frequency varied from 20 to 80 CPS and amplitude from 0.035 to 0.08 in. An increase in heat flux up to ten-fold was observed for vibration-induced forced convection. This effect diminished with increasing temperature difference. A mathematical model was solved to determine the boundary between convective and boiling heat transfer regions.

Various aspects of bubble behaviour on vibrating surfaces were investigated for water at 212°F. The generating period for bubbles and their diameter at break-off were found to follow normal distribution under vibrations. For a single isolated bubble the buoyancy and interfacial tension forces dominated the force balance on a stationary surface. For a vibrating surface, the additional drag and inertia initiated the cyclic fluctuations in bubble dimensions and the forces. The overall growth rate was faster and bubbles departed earlier.

CONVECTIVE AND BOILING HEAT TRANSFER FROM A VIBRATING SURFACE

K.K. NANGIA

CONVECTIVE AND BOILING HEAT TRANSFER FROM A VIBRATING SURFACE

by

KRISHAN KUMAR NANGIA, B. Chem. Eng.

A thesis submitted to the Faculty of Graduate
Studies and Research in partial fulfilment
of the requirements for the degree of
Doctor of Philosophy

Chemical Engineering Department,
McGill University,
Montreal.

March 31st, 1968.

ACKNOWLEDGEMENTS

The author expresses his sincere appreciation to Dr. W.Y. Chon for his continued interest in directing this research.

The author is also indebted to:

Dr. M.E. Weber for his interest and many suggestions during the course of this investigation.

Fellow graduate students especially B.B. Pruden and M.S. Monga, who gave freely of their time and were always available for useful dicussions.

The National Research Council of Canada for financial assistance in the form of studentships.

Mr. A. Krish for his help and cooperation in the fabrication of the experimental apparatus.

Mr. A. Nowacki for his assistance in the high speed photographic work.

Miss Hildegard Schroeder for typing the manuscript.

Finally, to express his sentiments toward his parents, the author is unable to find words.

TABLE OF CONTENTS

PART III. DYNAMICS OF BOILING BUBBLES FROM VIBRATING SURFACES IN SATURATED NUCLEATE BOILING OF WATER

LIST OF ILLUSTRATIONS

Page

Page

Part II

Part III.

LIST OF TABLES

PRESENT INVESTIGATION

Part I

GENERAL INTRODUCTION

There has been a growing interest in the effects of oscillation on transport phenomenon, particularly on convective and boiling heat transfer. Substantial improvements in such processes as heat exchange, sublimation, drying-dissolution and many nuclear applications may be brought by the use of pulsations or vibrations. In some special cases, the use of vibration or sound to increase the rate of heat or mass transfer is especially attractive since it can eliminate the possibility of chemical or bacteriological contamination e.g. in artificial kidney machines.

A considerable amount of investigation has been carried out in the field of natural convection heat transfer from a vibrating surface. However, the data for heat transfer to two phase systems under vibrational conditions have been extremely limited.

Although some work has been carried out on the effects of ultrasonic vibrations on burnout heat flux, there has been no emphasis on exploring the effects of surface vibration in the region of nucleate boiling where the interactions of vibration attribute to the change in bubble activity near the heat transfer surface.

The results of the present investigation are presented in two main sections. The first part deals with the measurements and correlations of the heat transfer data for three distinct regions which occur when the heat transfer surface is subjected to vertical oscillations in subcooled boiling of water and methanol. The second part considers the study of bubble dynamics from vibrating heat transfer surface in saturated nucleate boiling of water. The statistical properties of bubble growing from natural active site on pulsating wire and the forces which act during the growth of bubbles from artificial active site on a vibrating heat transfer surface are included. The results are computed and compared to the non-vibrating case.

LITERATURE REVIEW

INTRODUCTION

Natural Convection:

The influence of vibrations upon the rate of heat transfer by free convection from a heated surface can be investigated experimentally by two different methods. These may be acoustic vibrations in the fluid media, or an oscillatory motion impressed upon a heat transfer surface. These methods are similar in that they create an oscillating relative velocity vector between a heated surface and a fluid medium. The two methods are directly comparable if the wavelength of sound is large relative to the characteristic dimensions of the surface employed.

The interaction between vibrations and free convection has been studied for flat plates and cylinders, for different orientations of the vibration vector relative to these surfaces, for different ranges of amplitude and frequency of vibration, and for different magnitudes of the temperature difference. For practical reasons the geometry that has been most frequently studied is that of a horizontal cylinder subjected to vibrations whose directions are normal to the longitudinal axis of the cylinder. It has been shown experimentally that transverse vibrations of sufficient intensity cause large increases in the rate of heat transfer from heated horizontal cylinders. In order to explain the interaction between transverse vibrations and free convection from horizontal cylinders, several different hypothesis have been proposed which are discussed in the corresponding part of this section.

Boiling Heat Transfer:

The first scientific study of boiling was done by Nukiyama(1) in 1934 in Japan. He submerged a horizontal platinum wire in water at 212°F and heated it electrically to cause boiling. The wire also served as a resistance thermometer. Nukiyama's boiling curve is shown in Figure 1. A similar trend holds for all liquids although the specific values for the coordinates depend on the kind of liquid, the pressure and other factors.

The phenomenon of boiling is complex because three distinctly different regimes exist: Nucleate, transition, and film boiling. The change from one regime to another is accompanied by marked changes in the hydrodynamic and thermal state of the system. These regimes are illustrated in Figure 1. When the temperature of the heating surface is below the fluid saturation temperature, heat is transferred by convection, forced or natural, depending on the conditions. This non-boiling regime (AB) has been extensively investigated and equations have been derived which permit the prediction of heat transfer rates. Nucleate boiling (BC) starts when the temperature of the surface exceeds the saturation by a few degrees. Adjacent to the surface a thin layer of superheated liquid is formed in which bubbles nucleate and grow from some preferred spots on the surface. The thermal resistance of this superheated liquid film is greatly reduced by the agitation produced by the bubbles. As the wall temperature is increased, more bubbles appear

FIGURE 1

A TYPICAL CURVE OF HEAT FLUX DENSITY
VERSUS SURFACE TEMPERATURE IN BOILING

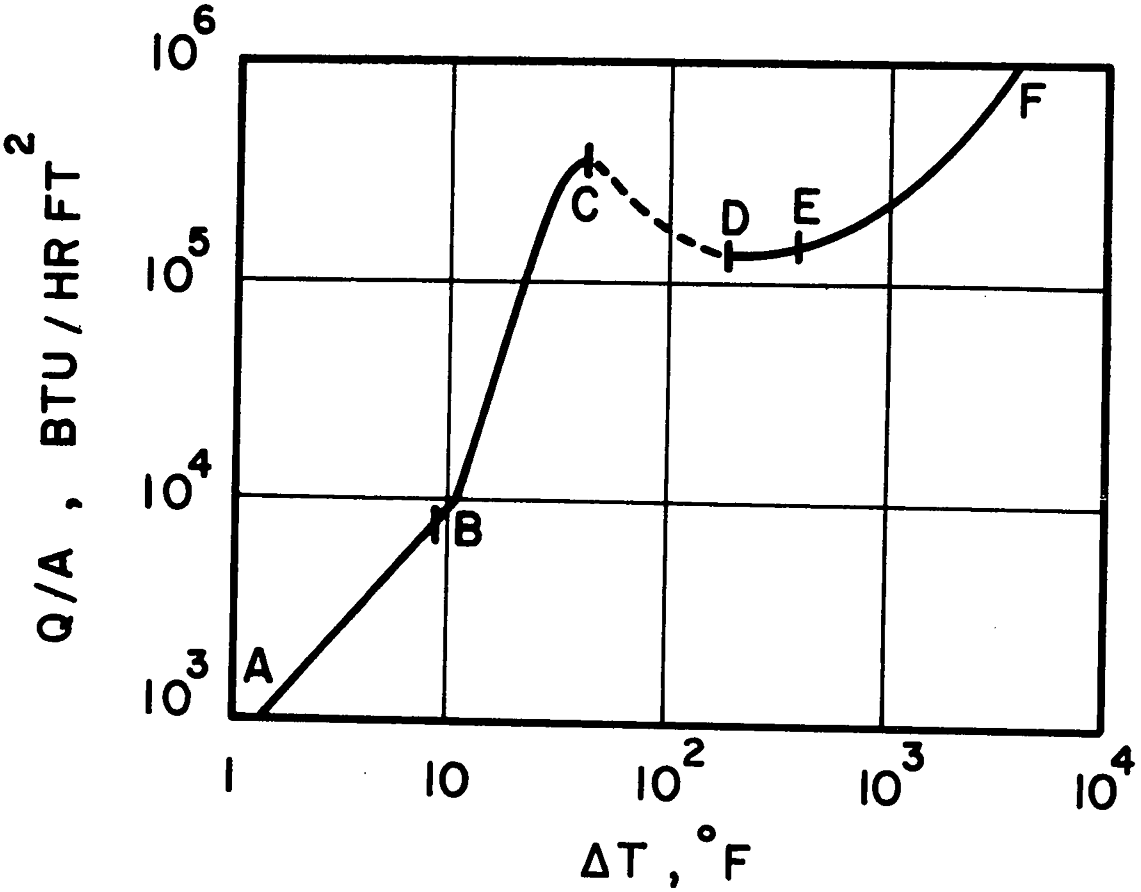
Q/A , BTU / HR FT^2
10^6
10^5
10^4
10^3
1
10
10^2
10^3
10^4
ΔT , °F
A
B
C
D
E
F

on the surface and the heat flux subsequently increases. However, as the temperature is further increased, bubbles become so numerous that their motions start to interact. Under these conditions the nucleate heat flux reaches its peak.

WestWater and Santangello(2) have found that in the region (CD) which is often referred to as transition boiling, no liquid-solid contact exists. The surface is blanketed by an irregular film of vapour which is in violent motion. In transition boiling an increase of temperature is followed by a decrease of heat flux until a minimum value is reached at which point film boiling starts. This new regime is characterised by an orderly discharge of large bubbles with a regular frequency and at regular intervals. In the film boiling region the heat flux increases with an increase of temperature but at a much slower rate than in nucleate boiling. Subsequently, at high heat transfer rates, the temperature of the heating surface can exceed the melting temperature and burnout occurs. Thus it is of great practical importance to operate in the nucleate boiling region because of the favourable heat transfer.

Experimental and theoretical investigations in the field of nucleate boiling heat transfer have indicated that the flow of heat is partly from the surface to the liquid through the boundary layer and partly by latent heat transported through the vapour bubbles. However, photographic studies on subcooled boiling by Gunther and Kreith(3), Rohsenow and Clark(4), and others have proved that the transfer of heat in lower and intermediate heat flux boiling regions, takes place primarily through the boundary layer, the transport by latent heat being negligible. As the large heat fluxes obtained cannot be explained on the basis of thermal conduction through the superheated layer, it has been postulated that random microconvection is created in the boundary layer by bubble dynamics, reducing thus the high thermal resistance of boundary layer considerably.

The above explanation, however, is not valid over the complete range of saturated nucleate boiling. In the discrete bubble region, i.e. for small temperature differences, the heat transfer is largely through the boundary layer. Both the bubble population and bubble emission frequency increase considerably with increasing temperature difference. When the heat flux reaches around 80% of its critical value, it is likely that the latent heat transport becomes dominant over other modes of heat flow.

Based on the above findings it is reasonable to assume that any external agitation which affects the thermal boundary layer, or any device to increase the bubble population or bubble emission frequency, would enhance the heat flux in subcooled boiling and in the lower range of saturated boiling. Westwater(5), in his microscopic studies of bubble growth, found that the heat transfer coefficient for a bubble decreases as the bubble grows; the typical variation of heat transfer coefficient, h, with time being as follows:

θ Secs.	h Btu/(hr)(ft^2)^{o}F
10^{-4}	2400-8400
10^{-3}	379-1900
10^{-2}	57-420

From these observations, he concluded that any mechanism to remove bubbles from the surface when they are young would increase the heat flux. Schweppe and Foust(6), Robinson and Katz(7) and others showed that agitation of the liquid increased the heat flux in the lower nucleate boiling region but had little effect near the peak heat flux. In all the work the agitation was imparted to the bulk of the fluid. The effect of turbulence in the boundary layer alone was not considered. Furthermore, no extensive study of the behaviour of bubbles under vibrational conditions had ever been undertaken.

Streaming in the vicinity of a cylinder under conditions of Isothermal Vibration:

When a fluid is set into oscillation, as in the presence of a sound wave or an oscillating body or boundary, steady streaming motions are generated under certain conditions. These steady currents, which are superimposed upon the vibratory motion, are referred to as acoustic streaming. The form and intensity of acoustic streaming depend upon the geometry of the surface, the properties of the fluid and the parameters of vibration. So far the geometry which has been studied is that of a circular cylinder subjected to vibrations in a direction normal to the longitudinal axis of the cylinder. In spite of considerable research efforts, broad generalizations over wide ranges of the controlling parameters cannot be made, due to the complexity of the problem.

Andrade(8), in 1931, carried out some experiments with cylindrical obstacles kept at an antinode in the standing wave tube under suitable conditions. Using smoke as the indicating medium he observed that at a suitable intensity a vortex motion with four loops as shown in Figure 2, is formed around the cylinder and the direction of streaming is away from the surface along the line of sound propagation which passes through the centre of the cylinder. At a fixed intensity the size of the cylinder has an effect on the size of the vortex motion. At large intensities of vibration the general circulation between node and antinode is the predominating factor, the vortex system around the particles being ill formed or supressed; at medium intensities the vortex systems are strong and well formed; at low intensities they are very feeble. These experiments were conducted with a rod of diameter 0.237 cm

FIGURE 2

STREAMING AROUND A CIRCULAR CYLINDER

IN A STANDING WAVE TUBE (AFTER ANDRADE)

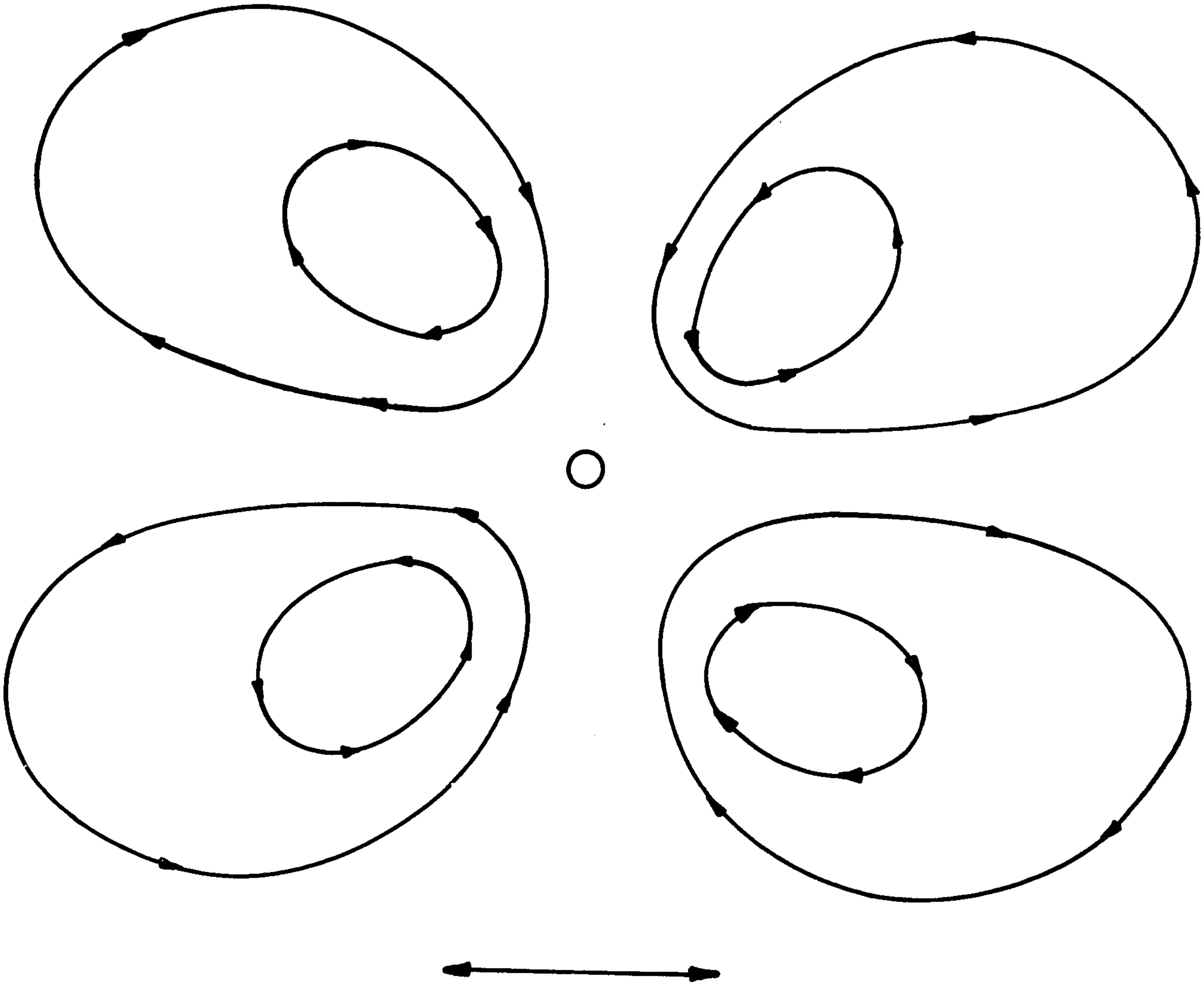

and a frequency of 512 CPS, which was the resonant frequency for that particular system. The first mathematical solution of the problem of streaming motion around a cylinder was obtained by Schlichting(9). This solution predicted that there would be two distinct regions of streaming in each quadrant around the cylinder; a thin layer next to the cylinder with streaming directed towards the surface along the propagation axis (called the D.C. boundary layer, $\delta_{D.C}$), and an outer streaming in the region radially further from the axis. The outer region forms a vortex when the fluid is bounded, but, in unlimited space the outer core moves to infinity as shown in Figure 3. According to Schlichting(9), the thickness of the D.C. boundary layer is proportional to that of A.C. boundary layer, $\delta_{A.C}$, as defined by $(\frac{v}{\omega})^{1/2}$. When the kinematic viscosity of the fluid is increased or the frequency of oscillation is reduced so that $\frac{\delta_{A.C}}{D} > 10^{-1}$, it is no longer appropriate to analyse the flow with laminar boundary layer theory and the full Navier-Stokes equations must be used. Schlichting obtained corroborating experimental evidence for his analytical results by vibrating a circular cylinder in water.

In a study conducted by West(10) thin lamina and small cylinders were vibrated in air and water. He reported that at a frequency of 550 cycles per second and with an amplitude of less than 0.04 cm, the circulation around a pin of diameter 0.077 cm was very similar to that shown in Figure 4. With an increase in amplitude to 0.045 cm, however, this circulation had shrunk to a region near the cylindrical surface and around it was a vigorous circulation in the opposite sense as shown in Figure 5. The second type of circulation takes place according to the above data when the Reynolds number,

FIGURE 3

STREAMING AROUND A CIRCULAR CYLINDER
IN UNLIMITED SPACE (AFTER SCHLICHTING)

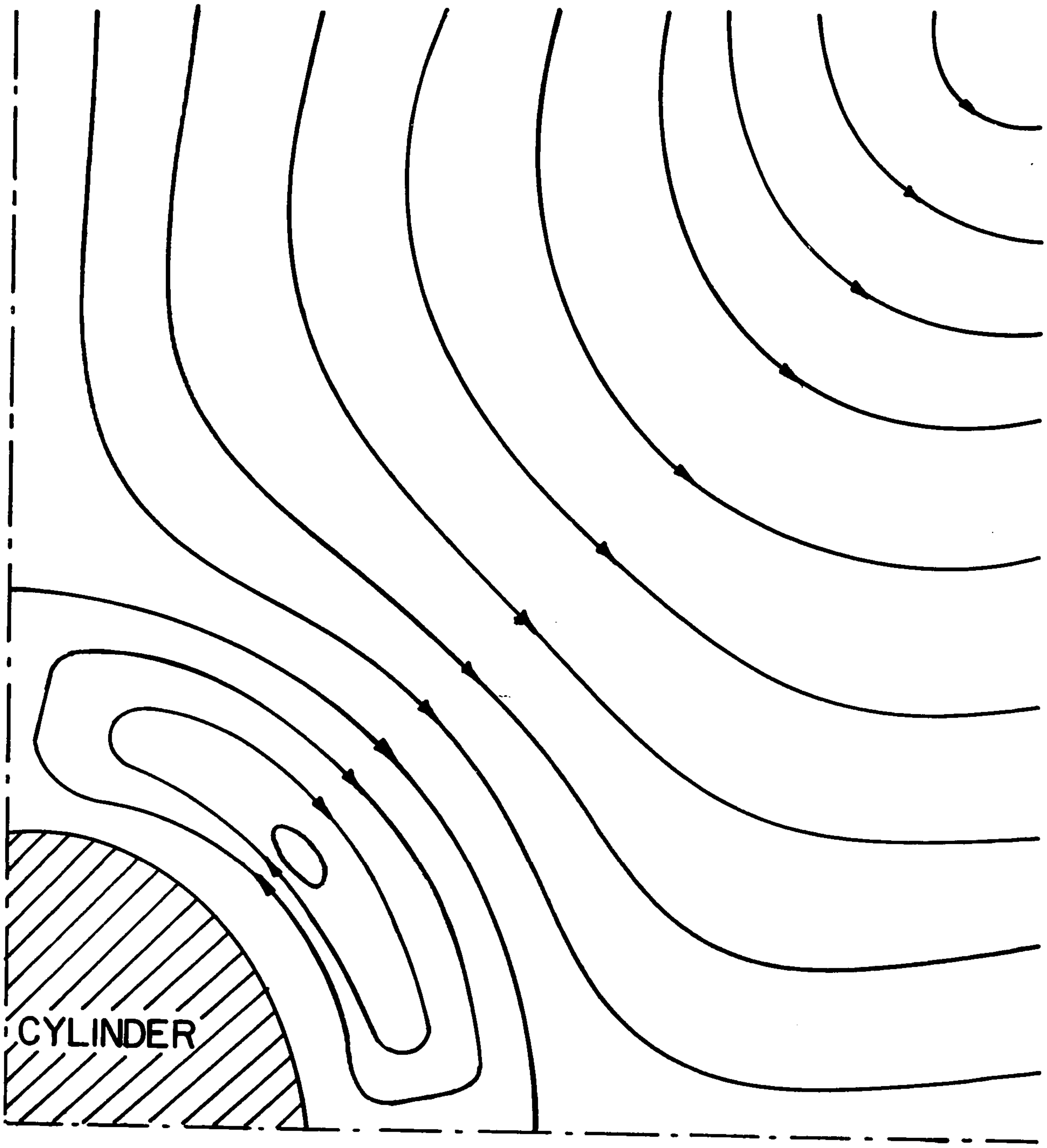

DIRECTION OF OSCILLATION

FIGURE 4

STREAMING AROUND A VIBRATING CYLINDER (AFTER WEST)

FREQUENCY = 550 CPS

AMPLITUDE < 0.04 CM

DIAMETER OF CYLINDER = 0.077 CM

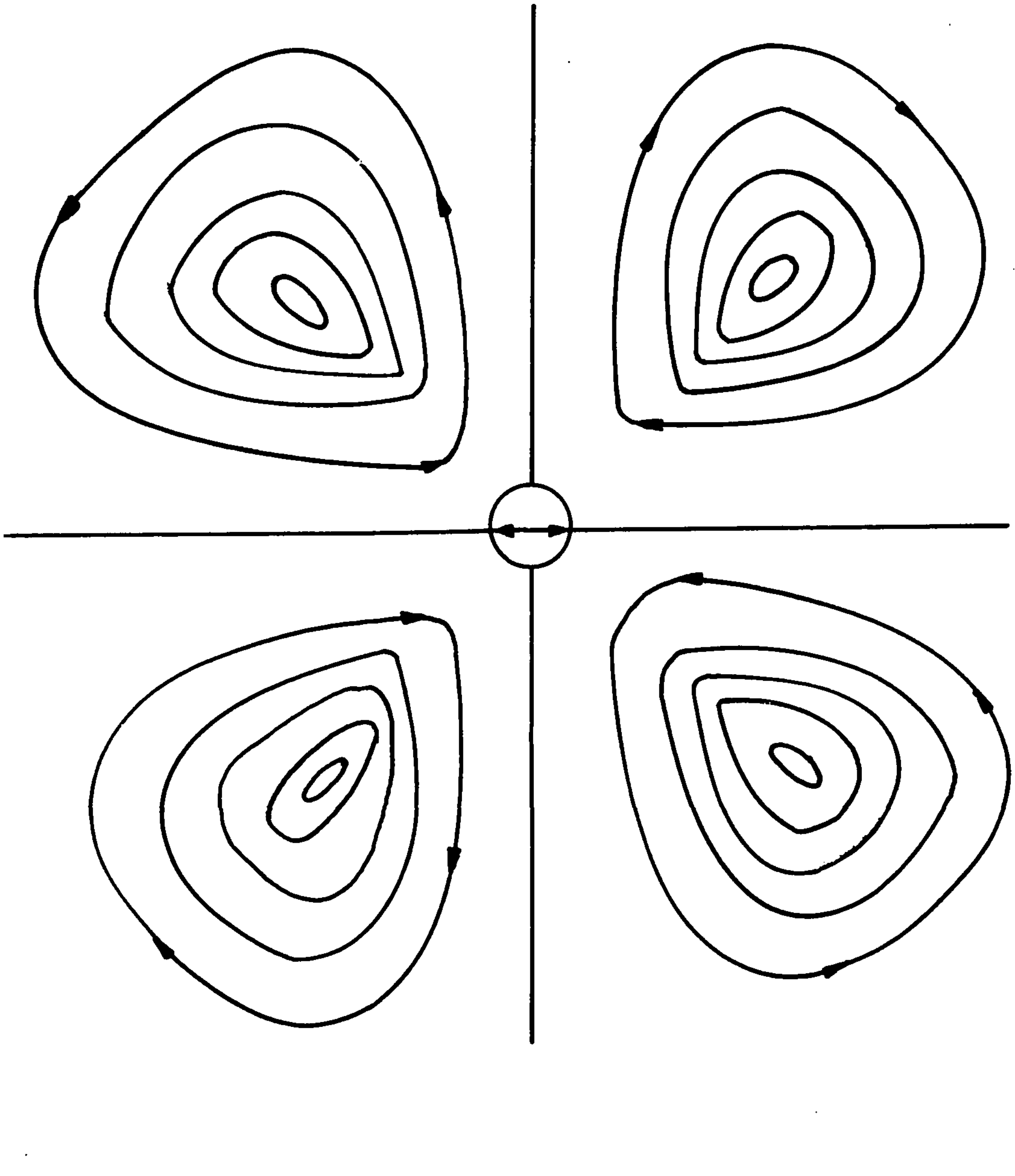

FIGURE 5

STREAMING AROUND A VIBRATING CYLINDER (AFTER WEST)

FREQUENCY = 550 CPS

AMPLITUDE > 0.04 CM

DIAMETER OF CYLINDER = 0.077 CM

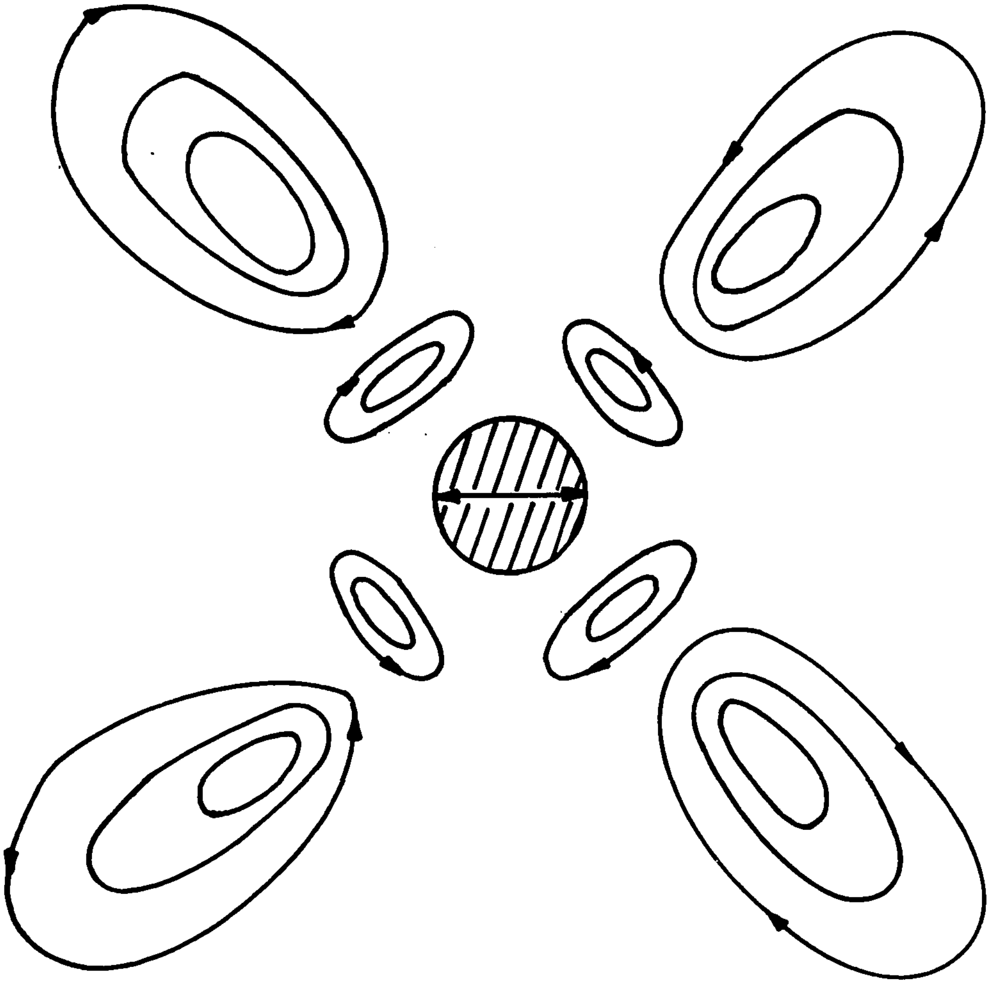

based on pin diameter, is more than 80.

An analysis of the flow similar to that of Schlichting was also presented by Holtsmark, Johnson, Sikkeland and Skavlem(11) who showed that the flow field was qualitatively similar to that obtained by boundary layer theory with the directions of streaming maintained in the same sense in each quadrant, but in which the inner streaming layer became larger than predicted by boundary layer theory in which the streaming velocities were also notably greater. For a cylinder of 0.22 cm in diameter and a Reynolds number of approximately 12, they observed the maximum radial component of the streaming velocity in the outer vortex to be equal to 0.06 cm/sec and the maximum tangential velocity in this vortex system to be equal to 0.15 cm/sec. The agreement observed by them between the theory and the experiment is excellent for the periodic flow and very good for streaming flow. Theoretical and experimental investigation by Raney, Corelli and Westervelt(12) showed that the size of the inner streaming layer departed systematically from the values predicted by laminar boundary layer theory as the ratio of the A.C. boundary layer thickness to the cylinder diameter was increased. They formulated a universal curve giving $(\frac{\delta_{D.C.}}{a})$ as a function of $(\frac{a}{\delta_{A.C.}})$. This curve was verified experimentally for the case of a right circular cylinder vibrating in solutions of water and glycerine with the kinematic viscosity range of up to 50 times that of water ove an octave of frequencies. Their experimental work also confirmed theoretical predictions that for small oscillation amplitudes the streaming patterns would be the same whether the cylinder oscillates in a quiescent fluid or is fixed in an oscillating fluid.

Streaming around a heated cylinder:

The study of the phenomenon of streaming in the presence of temperature gradients has received very limited attention. It is not yet known whether similar steady secondary motions can occur when the cylinder is heated and the amplitude of oscillation is large. Kubanskii(13), investigated the influence of stationary sound fields on free convection from an electrically heated horizontal cylinder in air. In Kubanskii's test arrangement, the direction of sound propagation was parallel to the axis of the cylinder. He deduced from shadowgraphs that a standing sound wave, directed parallel to the axis of a heated cylinder, produces cells of circulation near the hot surface. Near the wall of the heated cylinder the medium flows from the antinodes to the nodes; these mutually opposed streams meet at the nodes, merge into a single stream and move away perpendicular to the surface. The flow is asymmetrical with respect to the cylinder because of deformation by free convection.

Kubanskii(14), also made experimental studies of the influence of stationary sound waves on boundary layer flow in cross flow for cases (i) sound wave parallel to the axis of the cylinder (ii) sound wave perpendicular both to the axis of the cylinder and the direction of cross-flow. The observations were made for a cylinder 32.5 cm long, and 2.4 cm in diameter. The intensity at the centre of the collimated beam was from 0.03 to 0.34 watts/cm^2 and wave length, λ, was 2.8 cm at a cross flow Reynolds number of 2500. He observed marked changes in the boundary layer flows near the cylinder when the acoustic particle velocity was equal to or greater than the cross flow velocity. For case (i), the boundary layer was periodically distorted in space along the length of the cylinder and the period of distortion was $\lambda/2$; for case (ii), it was possible to move the point of separation either upstream or downstream depending upon the location of nodes and antinodes of stationary wave relative to the axis of the cylinder. He concluded that the flows of acoustic streaming could be superimposed on the convection flow field near the cylinder. Fand and Kaye$^{(15)}$, studied the boundary layer flow around a horizontally heated cylinder of $\frac{3}{4}$ in. in diameter. The cylinder was subjected to a transverse standing sound field where the vibration vector was perpendicular both to the axis of the cylinder and to the force of gravity. A system for generating and measuring stationary sound fields in the vicinity of the cylinder was also included. Sound pressure levels were measured by means of a calibrated high - intensity condenser microphone system with an accuracy of ± 1 db. They reported that they were unable to obtain pictures of isothermal acoustic streaming with a system for flow visualization using a set of smoke streams. This was attributed to the fact that the smoke streams which issued from the hypodermic needles had an initial velocity of from 20-40 cm/sec. which was large compared with the expected acoustic streaming velocities. The photographs taken with the heated cylinder located at the pressure antinodes in the stationary sound field of various frequencies and intensities revealed that at a definite sound pressure level the typical free convection boundary layer flow pattern around the heated cylinder is disrupted, and a fundamentally different type of boundary-layer flow called "thermoacoustic streaming" develops. This value of the sound pressure level (SPL) is referred to as the critical sound pressure level "critical SPL". This thermoacoustic streaming is characterised by a pair of oscillating vortices which begin to appear above the upper surface of the test cylinder when the sound pressure level reaches the critical value. The motion of these thermoacoustic vortices resembles the shedding of vortices behind a cylinder in forced flow normal to the axis of the cylinder. As the sound pressure level is increased beyond the critical value, the vortices eventually reach a fully developed stage and thereafter further increase in the sound pressure level increases the size of the vortices but does not alter their form. The data of Fand and Kaye(15) also showed that for $\frac{\ell}{D} \geq 6$, the sound intensity required for vortex development is 0.36 ft/sec., and the vibration intensity for fully developed thermoacoustic streaming is 0.71 ft/sec. Also they found that the sound intensity required for vortex development is independent of frequency and secondly the size of the vortices is independent of frequency at constant sound pressure level (SPL). For $\frac{\ell}{D} < 6$, the vortices became smaller as frequency was increased at constant SPL. It was concluded that thermoacoustic streaming is a much stronger phenomenon than isothermal streaming for the same geometry and sound intensity. The visual evidence of this phenomenon has been corroborated by quantitative heat transfer measurements where the effects of such streaming was to cause the convective rate of heat transfer from cylinder to increase by a factor of 3. Fand and Peebles(16) investigated the influence of horizontal transverse mechanical vibration upon the rate of convective heat transfer from horizontal cylinder. The frequency of vibration ranged up to 100 CPS. In their flow visualization study, employing smoke as the indicating medium, they reported that the flow resembled the thermoacoustic streaming observed previously by Fand and Kaye(15) with a stationary cylinder in a sound field. Their experimental results also proved that the physical mechanism of interaction between free convection from a heated horizontal cylinder and horizontal transverse vibrations is essentially the same whether the vibrations are acoustically ($\frac{\ell}{D} \geq 6$) or mechanically induced. Westervelt(17) suggested that the effect of sound waves in such cases is mainly a result of modification of the inner streaming boundary layer which is known to occur when the sound particle displacement, s, is greater than the acoustic boundary layer thickness $\delta_{A.C}$. For the case of heated horizontal cylinder, Lemlich(18) postulated that the vibrating cylinder does not carry the film back and forth with it but rather that the film surrounds the entire vibrating path, so that the body from which the heat transfer occurs is effectively larger than the actual size of the cylinder Lemlich also produced a correlation of his experimental data based on this concept to provide aducive support for it. Fand and Kaye(19) conducted flow visualization study with smoke for a heated cylinder undergoing vertical mechanically induced simple harmonic vibrations in still air. The photographs indicated that the fluid-dynamical mechanism which causes the observed increases in the heat transfer coefficient is vibrationally induced turbulence. This turbulent type of boundary-layer flow differs radically from the vortex type of flow which had been observed to develop near a heated horizontal cylinder in the presence of acoustically induced horizontal vibrations(15). Rao(20) in a review report mentioned that the interferograms for a heated cylinder vibrating with a high intensity were stated to show the boundary layer to be in a state of turbulence.

HEAT TRANSFER LITERATURE

Natural and Forced Convection-Air

Acoustically Vibrated Systems:

Kubanskii(21,22,23,24) conducted experimental and theoretical investigations of the influence of stationary sound fields on free convection from an electrically heated horizontal cylinder to air. The direction of the sound field was longitudinal, i.e. parallel to the axis of the cylinder. The cylinder, which consisted of a brass tube 2.4 cm in diameter and 32.5 cm long, contained thermocouples embedded in its surface. The sound field was generated by a vibrator, the radiations of which were focussed in a parallel beam with the aid of parabolic reflectors. As a result of collimation into a beam the sound wave had an uneven intensity along its front. The intensity of the radiated vibrations in the centre of the beam varied from 0.03 to 0.16 watt/cm^2 (approximately 145 to 152 db re 0.0002 microbar) and the range of frequency was from 8 to 30 KCPS. He observed an increase in heat transfer coefficient up to 75%. From his flow visualization techniques, it was concluded that acoustic streaming was responsible for the increase of heat transfer. Kubanskii's theoretical analysis was based on the assumption that the influence of sound and natural convection upon the Nusselt number is linearly additive. This particular assumption was based on his visual studies which showed clearly that the coupled flow corresponded to the pattern of superimposition of acoustic streaming upon natural convection. The results of his experimental data were correlated as

$$(Nu)_v = 10 K_c^{0.15} \tag{1}$$

where

$(Nu)_v$: Nusselt number in the presence of sound

K_c : $(P/\ell \rho a \beta g \Delta T)$, the ratio of the gradient of the mean acoustic radiation pressure P/ℓ, to the buoyant force per unit volume of the fluid, $\rho a \beta g \Delta T$. From Equation (1) it is evident that there is lower bound on K_c for which the equation is valid.

In deriving the above equation the lowest value of K_c used was 1.6. Fand and Kaye(25) investigated the influence of transverse sound fields upon free convection from a $\frac{3}{4}$ in. diameter horizontal cylinder to air. Experimental ranges of the primary variables were as follows:

frequency, f = 1100 - 6120 CPS

temperature difference, ΔT = 0 - 250°F

sound intensity = 0 - 151 db re 0.0002 microbar.

Results of their experiments demonstrated that intense transverse sound vibrations strongly influence the heat transfer. For the case of plane stationary sound waves, a critical sound pressure level exists between 136 and 140 db (re 0.0002 microbar) depending on the frequency, below which the heat transfer coefficient is unaffected, and above which the rate of heat transfer is increased rapidly. Eventually a stage is reached between 142 and 146 db, depending on frequency, beyond which the rate of increase of heat transfer becomes comparatively lower. Their data also indicated that for sound waves whose half wavelength was six or more times the diameter of the cylinder ($\frac{\ell}{D} \geq 6$), the coefficient of heat transfer is a function of only two variables; the temperature difference, ΔT, and the intensity of vibration (defined as the product of amplitude and frequency, af). For $\frac{\ell}{D} \geq 6$, and $f \leq 1496$, the data could be correlated in a simple form

$$h_v = 0.722 \left[\Delta T (af)^2 F \right]^{1/3}$$

$$(Nu)_v = 14.2 \left[(Gr.Pr) M_a^2 F \right]^{1/3} \quad .$$

The quantities $[(af)^2 F]$ and $[M_a^2 F]$ are proportional to the vibrational kinetic energy density averaged over the diameter of the test cylinder.

They also reported that for the same temperature difference, the superposition of a sound field increased the heat transfer coefficient by a factor of 3. Fand and Kaye explained the physical mechanism based on their earlier findings of the development of thermoacoustics- oscillating vortices on the upper part of the cylinder.

Richardson(26) performed experiments in which he measured the localised heat transfer effects of a standing sound wave which was propagated horizontally across a cylinder of $\frac{3}{4}$ in. diameter. The equipment for sound generation and measurement were identical with those used by Fand and Kaye(15). Schmidt's optical method was employed to measure the heat transfer coefficients. He observed that for sound pressure levels of about 130 db - a standing sound field induces local changes in heat transfer of the order of 5 - 10%. However, these local changes are in different directions at different locations around the cylinder and the net effect on average heat transfer is less than the experimental uncertainty of 2% or so to which average heat transfer can be measured. Thus a "critical sound pressure level" published by Fand and Kaye dos not correspond to a sudden change in fluid behaviour around the cylinder and has no intrinsic fluid mechanical significance. The above conclusions are drawn for situations where half wavelength of sound field exceeds 6 cylinder diameter.

Fand et al.(27) determined the local heat transfer coefficient around the circumference of a heated cylinder both in the presance and absence of a strong stationary sound field. A cylinder of $\frac{3}{4}$ in. diameter was suspended in an anechoic chamber equipped to create a horizontal plane stationary sound field. The sound field was oriented with respect to the cylinder so as to produce an antinode in the vertical plane passing through the longitudinal axis of the cylinder. The set up was such that average heat transfer coefficient for 15 degree increments of the base circle were obtained; this procedure provided heat transfer data at 24 circumferential positions. In the presence of sound field for which

SPL = 146 db (re 0.0002 microbar) and f = 1500 CPS, the maximum measured increases in the heat transfer coefficient on the lower and upper portions of the cylinder relative to the case of free convection at the same temperature potential were found to be approximately 250 and 1200 percent respectively. They concluded that the surface of a heated cylinder could be subdivided into two regions in each of which the character of the boundary layer flow is different. The bottom loop of the local heat transfer curve (0 - 97 degree, from the lower stagnation point) corresponds to a region of laminar boundary-layer flow; whereas the upper loop (97 to 180 degree from the lower stagnation point) corresponds to a region in which oscillating vortex flow occurs near the cylinder. The reason for the increase in heat transfer coefficient on the lower portion of the cylinder appeared to be due to the increase in the boundary-layer velocities and the modification of the temperature profile due to accoustically induced oscillations (unsteady components) within the laminar boundary layer.

An investigation of the quantitative influence of strong sound fields on free convective heat transfer from a $\frac{3}{4}$ in. diameter, electrically heated cylinder was undertaken by Holman and Mott-Smith(28). The cylinder was kept in a reverbrant chamber providing a constant sound-pressure field. Wall temperatures ranged from 208 to 270°F. An increase in heat transfer coefficient did not occur until the sound pressure level was greater than 135 db. The increase in heat transfer coefficient was attributed to a decrease in the D.C. boundary layer thickness with a corresponding increase in the acoustical streaming velocity in the boundary layer. The effect of frequency on D.C. boundary layer thickness was observed in the neighbourhood of the critical sound pressure level but at higher sound pressure levels the frequency effect was found to be very small in comparison to the amplitude effect.

Kubanskii(29) also studied the effect of sound on heat transfer from horizontal heated cylinder with a cross flow of air. The dimensions of the cylinder were 1.5 cm by 12 cm long. The studies were made for two separate cases; case (i) when the direction of the sound was parallel to the axis of the cylinder; case (ii) when the direction of sound was perpendicular both to the axis of the cylinder as well as to the crossflow. Wavelengths of sound were $\lambda = 2.0, 2.5$ cm with a restricted narrow range of cross flow Reynolds number, $(Re)_{cf}$, from 1450 to 1770 corresponding to a cross flow velocity from 1.45 to 1.77 meter/sec. For case (i) Kubanskii observed that the effect was always to increase the heat transfer rate whereas for case (ii) the heat transfer rate could either be increased or decreased by moving the cylinder relative to the nodes of the stationary sound waves. He correlated to data by

$$(Nu)_v = B(K_b)^n$$

where $$K_b = P/\rho a\ U^2$$

is the ratio of the mean acoustic radiation pressure to the dynamic head.

The values for B and n are as follows:

B = 28, $n = 0.08$ for $u < U$ - for case (i)
B = 23, $n \approx 0.06$ for $u < U$ - for case (ii)
B = 27, $n = 0.20$ for $u > U$ - for case (iii)

u - root mean square of vibrational velocity
U - cross flow velocity.

A maximum increase of about 50% was observed in the heat transfer rate. The primary basis of his correlation was the superposition of sound on free convection. Considerable scatter was observed in his experimental data for which no explanation was given. A similar study was also carried out by Fand and Cheng(30) with the same experimental set-up as that of Fand and Kaye(25,27) except for the introduction of the air stream (cross flow) cross flow velocity was controlled by a variable speed blower and measured with a thermal anemometer with calibration of ± 3%. The temperature of the air stream was kept at 70 ± 5°F. The ranges of the other experimental variables were as follows:

Cross flow velocity (U) = 1.5 - 30 ft/sec., $(Re)_{cf}$ = 590 - 10750,
Temperature difference = 50 - 360°F.
Sound Pressure Level = 130 - 150 db (u = 0.5 - 5.0 ft/sec.)
Sound frequency = 1100 and 1500 CPS.

The ratio $\epsilon = \frac{u}{U}$, called the "level of vibrations", varied between 1.6 and 250%. The setup also had the provision to measure the local heat transfer coefficient at 15 degree interval around the circumference of the cylinder. It was noticed that the heat transfer coefficient is increased in two regions. In one of the regions corresponding to $(Re)_{cf} \sim 1000$, the increase in the rate of heat transfer is the result of an interaction similar to thermoacoustic streaming. In the second region corresponding to $(Re)_{cf} \sim 10,000$, the increase was attributed to two different interactions; (a) a resonance interaction between the acoustic oscillations and the vortices shed from the cylinder and (b) modification of the flow in the laminar boundary layer on the upstream portion of the cylinder similar to the effect of free stream turbulence. However, the above explanations are highly suggestive and hence cannot be regarded as conclusive. Their results showed a maximum increase of 25% in heat transfer coefficient. An emperical equation was proposed to calculate the maximum increase in Nusselt number caused by a given sound wave in the region where $(Re)_{cf} \sim 10,000$.

Experimental studies of the influence of acoustic vibrations in flow field, on heat transfer to air with super-imposed forced and free convection were reported by Jackson et al.(31). The air flowed upward in a tube and was heated by saturated steam flowing in the annular space. The sound was generated by a speaker, located at the bottom of the tube, and energised by an audio amplifier. The sound intensity was measured simply as power input to the speaker by an audio wattmeter. Experiments were performed at 520 CPS. and a Graetz modulus of approximately 80 for variable tube lengths 6, 12, 18 in. and so forth. The results indicated that SPL below 118 db had little effect on the heat transfer coefficient. Above 118 db free convection forces were apparantly negligible, and the effect of sound appeared to be considerable. The paucity of data made it impossible to arrive at a conclusion on the effect of frequency. For the data above 118 db, two correlations were proposed.

$$\text{(i)} \qquad (Nu)_v = 2.52 \left[\frac{e^{\frac{SPL}{69.5}}}{(Re)^{0.25}} \right] \sqrt{Gz_x}$$

valid with ± 25%

$$\text{(ii)} \qquad (Nu)_v = 5.7 \left[\frac{e^{\frac{SPL}{69.5}}}{Re^{0.25} \quad f^{1/8}} \right] \sqrt{Gz_x}$$

valid with ± 16 % .

Mathewson and Smith$^{(32)}$ studied the effects of strong sonic pulsations on rates of heat transfer to air and on film condensation of Isopropanol. Pulses were generated in the flowing stream by a motor driven, flat-plate siren set in the exchanger inlet line. Pulse frequencies varied from 50 - 330 CPS and pulse amplitudes were between 10 and 250 lbs/ft^2. The amplitude and frequency were measured with a piezoelectric pickup connected to a piezocalibrator and an oscilloscope. Air, Isopropanol vapour or mixtures of air and Isopropanol vapour were passed downward at atmospheric pressure through a double pipe heat exchanger, consisting of $1\frac{1}{8}$ in. BWG copper tubing jacketed for 6 ft. with $1\frac{5}{8}$ in. copper tubing. In heat transfer to air the improvement in heat transfer coefficient increased with pulsed frequency and was a maximum of 44% at Re = 2300. The increase became negligible when Re exceeded 4,000. Variations in pulse amplitude had almost no effect. The effects of flow rate and pulse frequency were in accordance with a proposed correlation based on a surface renewal model. In condensing Isorproponal vapour in a vertical tube, in the presence of high vapour velocities, application of pulsation increased the heat transfer rate by 10 - 60%. The increase depended upon vapour flow rate but was almost independent of pulse frequency. For a given vapour rate there was a critical pulse amplitude below which pulse had no effect on heat transfer. At high pulse amplitudes the increase in heat transfer coefficient was independent of amplitude.

The condensate rate of isopropanol out of a highly turbulent stream of isopropanol vapour and air was increased by the application of pulsation but less so than in the condensation of isopropanol alone. Improvements in condensation rate appear to result from the effect of pulsation on the condensate film and not on the vapor stream.

Havemann et al.(33,34) carried out experiments in heat transfer to pulsating air flowing in a tube of 1 in. diameter by 7 ft. long. Pulsations were imposed on the flow by means of a poppet value operating in the path of flow. The wave form and amplitudes were also measrued. Reynolds number varied from 5,000 to 35,000 and frequency of pressure pulsations from 5 to 33 CPS. Wave form and amplitudes were also kept as variables. Nusselt number changed up to 30% in a rather uneven but defined manner under different conditions of frequency, amplitude, wave form and Reynolds number. In the range of the frequency investigated a critical frequency was observed above which an increase in heat transfer was noticed. This critical frequency was a function of the wave form and Reynolds number. It was concluded that not only the total magnitude of the pressure amplitude but also the steepness of the wave (or the rate of change of pressure in the wave) plays an important part in the mechanism of forced convective heat transfer under pulsating flow conditions.

Lemlich and Hwu(5) studied the effect of acoustic vibration on forced convection heat transfer. Sound at resonant frequencies of 198, 256 and 322 CPS as well as at nonresonant frequencies was imposed on air flowing at Reynolds number of 560 to 5900 in the core of a horizontal double pipe, stream to air, heat exchanger. Increases in Nusselt number of up to 51% in the nominally laminar region and up to 27% in the nominally turbulent region were obtained. The improvement peaked sharply at resonance and increased with both amplitude and resonant frequency. An attempt to develop an overall correlation applicable to the experimental results at all Reynolds number proved unsuccessful. The differences between laminar and turbulent flow, as well as the complicated nature of interaction among variables in the neighbourhood of Reynolds number of 2100 were too involved. However, they developed independent correlations for the two regimes as follows:

for $Re < 1500$

$$\frac{(Nu)_v}{Nu} - 1 = 1{\cdot}3 \times 10^{-6} (\bar{H}_p f)^2$$

for $Re > 2500$

$$\frac{(Nu)_v}{Nu} - 1 = 0.047 \left[\frac{\bar{H}_p f^3}{Re^2}\right]^{0.8}$$

where H_p - local pressure rise resulting from vibrations lb force/ft^2 .

$\bar{H}_p$ = root mean square (taken along the heated length) of H_p,lb force/ft^2 .

Mechanically Vibrated Systems:

The influence of vibrations on the rate of free convective heat transfer from horizontal heated wires has been investigated by Lemlich(36). In these experiments electrically heated wires of three different sizes (0.0253 in., 0.0396 in., and 0.0810 in),were vibrated with sinusoidal amplitudes upto 0.115 in. in the frequency range from 39 to 122 CPS. The temperature difference between the wires and ambient air was 7-365°F. The coefficient of heat transfer for vibrating wires was as much as four times the coefficient without vibration but with other conditions unaltered. An increase in heat transfer was observed for an increase in amplitude and/or frequency. For increases in heat transfer in excess of 10%, Lemlich correlated his experimental data by the following empirical equation

$$\frac{h_v}{h_o} = 0.75 + 0.0031 \frac{Re^{2.05} (\beta \Delta T)^{0.33}}{(Gr)^{0.41}}$$

Lemlich reported similar results for both vertical and horizontal vibrations. In order to account for this observation the concept of a stretched film surrounding the entire path of vibrations was proposed. An effort was made to observe the boundary layer flow using smoke by holding a lighted cigarette under the heated wires but these smoke observations were inconclusive.

Fand and Kaye(19) carried out an experimental investigation of the influence of vertical mechanically induced simple harmonic vibrations upon the rate of heat transfer by free convection from a heated cylinder to air. The diameter of the cylinder was $\frac{7}{8}$ in. and the ranges of the primary experimental variables were as follows: Temperature potential, ΔT - 25 to 180°F ; amplitude of vibration, a, 0 to 0.16 in ; frequency of vibration, f, 54 to 225 CPS; intensity of vibration, af, 0 to 1.22 ft/sec. Their data showed that the sole controlling vibrational variable was the intensity of vibration. For intensities of vibration less than 0.3 ft/sec., the influence of vibrations upon heat transfer was negligible, above this so called "critical intensity" the effect of vibrations was to increase the heat transfer significantly. A flow visualization study employing smoke as the indicating medium showed that the fluid-dynamical mechanism which caused the observed increases in the heat transfer coefficient is vibrationally induced turbulence. This turbulent boundary-layer flow differs radically from the vortex type of flow which has been observed to develop near a horizontal cylinder in the presence of acoustically induced transverse horizontal vibrations. A conclusion may be drawn that the direction of the vibration vector relative to the direction of the force of gravity controls the basic character of the boundary layer flow about a heated cylinder. It was found that in the experimental region defined by $\Delta T < 100^{o}F$ ($Gr.Pr < 3 \times 10^{4}$), the heat transfer coefficient is independent of ΔT for sufficiently high levels of vibration. In the region defined by $\Delta T \geq 100^{o}F$ and $af \geq 0.9$ ft/sec. ($Gr.Pr > 3 \times 10^{4}$ and $Re \geq 2200$), the following pair of empirical equations were derived:

$$h_v = 0.847 \left(\frac{\Delta T}{D}\right)^{0.2}$$

$$(Nu)_v = 8.5 \times 10^{-4} (Gr.Pr)^{0.2} Re .$$

The vibrational intensity $af = 0.9$ ft/sec corresponds to "fully developed turbulent flow" in the neighbourhood of the cylinder. This terminology is analogous to the descriptive phrase" fully developed vortex flow" which had been used to describe around a heated cylinder subjected to horizontally acoustically induced vibrations.

Anantanarayanan and Ramachandran(37) studied the effects of vibration on heat transfer from an electrically heated nichrome wire to parallel air streams. Air velocities ranged from 34 to 63 ft/sec. At each air velocity, frequencies ranging from 75 to 120 CPS and different amplitudes ranging from 3 mm to 20 mm were employed as vibrational variables. Both frequency and amplitude increased the heat transfer coefficient. Increases up to 130% were observed. The data showed that the increase in heat transfer was controlled by the ratio of the mean vibrational velocity to the air stream velocity. From the analysis of their data they proposed the following correlation

$$\frac{(Nu_v)}{(Nu)_s} - 1 = 4.25 \left[\frac{(Re)_v}{(Re)_f} \right]^{0.977}$$

where

$$(Nu)_s = 0.0522 \, (Re)_f^{0.729}$$

Sreenivasan and Ramachandran(38) investigated the effect of vibration on heat transfer from a cylinder in cross flow. The vibration vector was perpendicular both to the cylinder axis and to the direction of cross flow. The diameter of the cylinder was 0.344 in., the amplitude of vibration varied from 0.15 to 0.63 in., the cross flow velocity varied from 19 to 92 ft/sec. ($(Re)_{cf}$ 2500 - 15000), and frequency of vibration from 3 to 45 CPS. No appreciable change in the heat transfer coefficient was observed by imposing root mean-square vibrational velocities as high as 20 percent of the cross flow velocity. This insensitivity of the heat transfer coefficient to vibration was shown to agree with an analysis based on the resultant of the vibrational and cross flow velocities.

Natural and Forced Convection - Liquids

Acoustically Vibrated Systems:

An experimental investigation was conducted by Robinson et al.(39) to study the effect of 400 kilocycle sound waves on the temperature drop between heated oil and solid and between heated solid and water. They postulated that ultrasonic vibrations cause a decrease in temperature difference across a static laminar film only when the film has the ability to transmit the ultrasonics, and thus be disrupted to some extent by those vibrations. From their results of temperature difference versus electrical power input to the transducer, they found a marked reduction in ΔT when ultrasonic vibrations were applied. A reduction of 18% and 4% were obtained for transformer oil and water respectively. The amount of reduction is less in the later case primarily because the sound intensity reaching the interface is very much lower for the same oscillator power.

The effects of ultrasonics on this temperature difference are more radical at low values of sound power; beyond these values the change rapidly reaches a plateau where greater intensity values have little effect.

Larson and London(40) studied the effect of ultrasonic vibrations on natural and forced convection heat transfer from 1 in. electrically heated copper sphere to water and toluene. The sphere was located in the centre of 3 in. cross which had sound source located at the bottom. The experimental work, covering a range of 20 to 1000 KC, showed an increase of four-fold in heat transfer coefficeint in natural convection. At lower frequency this increase is attributed to ultrasonic cavitation as revealed by the shadowgraphs. For this range the data were correlated by the factor $I/I_C\ (C/C_S)^{1.5}$ which was interpreted as the ratio of the sound pressure to the cavitation threshold;

I - sound intensity at the transducer, watts/cm^2

I_C- cavitation threshold intensity

C - velocity of sound in fluid,ft/sec.

C_S- gas content of fluid under saturation conditions at prevailing temperature, ml/litre.

At the higher frequencies the quartz-wind streaming appeared to be an important contributor in increasing heat transfer. However, no concrete mechanism was proposed.

In forced convection the increase in film coefficient due to ultrasonic agitation became relatively smaller as the flow Reynolds number was increased.

Mechanically Vibrated Systems:

Davis(41) in 1924, published comprehensive data for heat transfer from single wires held in vertical positions in water and other fluids.

The wires were vibrated at velocities ranging from 0.33 to 2.3 ft/sec. These data were correlated as $(Nu)(Pr)^{-0.3}$ as a function of (Re). In 1938 Martinelli and Boelter(42) investigated the effect of mechanical vibrations upon the rate of heat transfer from a horizontal tube, $\frac{3}{4}$ in. in diameter, immersed in a tank of water. It was found that coefficient of heat transfer was unaffected by mechanical vibrations for low vibrational Reynolds numbers; and this result was attributed to the dominanc of free convection in this range. For sufficiently intense vibrations, however, the coefficient of heat transfer was observed to increase by as much as 400% of its value without vibrations. Unfortunately the accuracy of their data is in doubt, since in a later communication with Lemlich-Boelter(43) has reported that results obtained from a later experiment did not agree with the original data.

It has been shown by West and Taylor(44) that it is frequently possible to boost the capacity of existing heat exchangers operating with turbulent flow of liquid inside tubes without excessive increase in power consumption by switching to reciprocating pumps with a controlled degree of dampening of pulses. They obtained an increase of 60-70% in film coefficients of heat transfer inside tubes for heating and cooling at Reynolds numbers of 30,000 to 80,000 by the use of partially dampened pulsating flow from a reciprocating pump. There appears to be an optimum degree of dampening since severe pulsations were not as effecient and resulted in more vibrations than moderate pulsations

Shai and Rotem(45) reported the results of their study on heat transfer to water in turbulent pulsating flow in internally heated annuli. Based on 33 series of test runs no significant changes in heat transfer coefficients were obtained at Reynolds numbers of 30,000 to 65,000. Their results did not agree with those of West and Taylor(44), largely due to the fact that West et al.(44) did not calibrate the experimental unit for stationary flow, according to Shai.

Scanlan(46) studied the effects of normal surface pulsations on laminar forced convective heat transfer in a system where degassed water flowed under gravity effect to ensure freedom from spurious vibrations. The ranges of the experimental variables were frequency 0 to 600 CPS, amplitude 0 to 0.004 in. (corresponding to a Re from 360 to 2170). The data showed that the peak in $\frac{h_v}{h_o}$ occurs in the frequency range from 50-80 CPS with a tendency for the curves of greater amplitude to peak at the lower frequency. The increase almost became negligible at high frequencies when the amplitude of vibration was small. Scanlan described this decreasing effect as " the resulting blanketing effect would be expected to counteract the increase in coefficeint caused by mixing. Below a certain combination of amplitude and frequency, this blanketing effect will not occur. Above this point, the blanketing will increase with increased amplitude and frequency as that portion of a cycle during which the critical acceleration is exceeded becomes larger". Larson and London(47) have proposed that the maximum in the heat transfer coefficient observed by Scanlan(46) at about 70 CPS is probably due to the fact that the resonant frequency of the system is also at about 70 CPS. At higher frequencies and amplitudes, the cavitation which could occur can satisfactorily explain the increase in heat transfer rate reported by Scanlan(46).

Deaver, Penney and Jefferson(48) investigated the effect of low frequency oscillations of relatively large amplitude on the rate of heat transfer from a small horizontal wire to water. Platimum wires of 0.007 in. in diameter and about 6 in. long were mounted on a yoke and heated by passing a direct current through them. Harmonic motion in a vertical plane was imparted to the wire by a Scotch yoke driven by an electric motor and variable speed hydraulic transmission. Frequencies from 0 to 4.25 CPS and amplitude to 2.76 in. were employed. Temperature differences up to 140°F provided heat flux from 2000 to 300,000 $Btu/hr\text{-}ft^2$. It was shown that heat transfer rates may be predicted by either forced, free or mixed convection correlations depending on the relative magnitudes of Reynolds number, based on the mean velocity of the wire and Grashof number. They predicted that for the forced convection region and the free convection region, respectively, the following equations may be used.

$$\frac{Nu}{(Pr)^{0.3}} = 0.35 + 0.48\,(Re)^{0.52}$$

$$Nu = 1.15\,(Gr\ Pr)^{0.15} \quad .$$

However, for a mixed convection, a conservative approximation may be made by considering the equation

$$Re = 0.44 (Gr\ Pr)^{0.5}$$

to define a distinct dividing line between forced and free convection. In the above work it may be noted that there was a presence of extraneous agitation in the fluid even though the yoke legs were designed to present a minimum perpendicular cross section. There would still be drag at the sides of the legs, and this would definitely introduce extraneous agitation in the water. Also the validity of the above correlation is restricted to one fluid where there is little change in the value for Prandtl number. They made no attempt to study the flow problem around the oscillating wire which could have been of tremendous value in comparing the results with those already known for air. An extension of this work was carried out by Penney and Jefferson(49) who also conducted experiments on the effect of low frequency, large-amplitude horizontal oscillation from a horizontal wire to water and Ethylene glycol. Platinum wire of 0.008 in. diameter was oscillated in the horizontal plane 6 to 8 in. below the surface of the liquid in a 12 x 12 in. cylinderical glass container. The wire was oscillated by a Scotch yoke which was driven by an electric motor through a continuously variable speed transmission. The ranges of the primary experimental variables were as follows: Frequencies from 0 to 4.5 CPS, amplitude of oscillation 0 to 2.5 in., temperature differences between the wire and water from 5 to 140°F and between the wire and ethyleneglycol from 10 to 130°F; Reynolds number based on the time average wire velocity from 0.4 to 80 in water and 0.1 to 5 in ethylene glycol; Prandtl number from 2 to 120; (Gr Pr) from 1 to 10 in water and 0.5 to 45 in. ethylene glycol; and $\frac{a}{D}$ from 30 to 300. Comparison of the data with the previous investigation has shown that, in the range of this investigation, heat transfer for vertical oscillations is greater than for horizontal oscillations. In their words "For horizontal oscillations, the cylinder moves through a relatively constant temperature undisturbed fluid where the velocity of free convection is perpendicular to the cylinder motion. On the other hand, consider the environment of the cylinder in vertical oscillation. On the downstroke, the cylinder moves through cold fluid, and the velocity of the rising fluid adds to the velocity of oscillation; both of these effects increase heat transfer. On the upstroke the cylinder moves through the fluid which has been heated on the downstroke (if the velocity of the cylinder is greater than the velocity of convection currents; for high Reynolds number this was true). This fluid is hotter than the bulk temperature but it is also turbulent (the turbulence was obvious visually) which increases heat transfer. For the small cylinder oscillated at a large amplitude, it is proposed that these effects produce greater heat transfer for "vertical oscillations". They concluded that the previously accepted correlating methods ($\frac{Nu}{Pr^{0.3}} = \phi(Re)$ at constant (Gr.Pr), and Nu versus (Gr.Pr) at constant Re) would not correlate data of both water and ethylene glycol on a single plot. Plot of Nu versus ($Re.Pr^{0.8}$) at constant (Gr.Pr) did successfully correlate both water and ethylene glycol data for the range of their investigation. However, this method is not universal, probably because the grouping ($Re.Pr^{0.8}$) is not a "turbulence indicator". Concerning the effect of parameter $\frac{a}{D}$, it appeared that it did not have any measurable effect over the range of a single order of magnitude, as the present data and the data of Fand and Peebles(16) indicated. However, over three orders of magnitude it could have a pronounced effect.

Lemlich and Rao(50) vibrated vertically, an electrically heated horizontal cylinder of 0.049 in. diameter in free convection to water and aqueous glycerine. The ranges of the experimental variables were: frequency 17 to 37 CPS; displacement amplitude 0.023 to 0.086 in. with distilled water, and from 0.038 to 0.070 in. with 27.3 percent glycerine in water solution. The coefficient of heat transfer was found to increase with frequency and amplitude with some increases exceeding ten-fold. They proposed the following correlation

$$\frac{h_v}{h} = \phi \left[\frac{Re\ (\frac{a}{D})^{0.4}\ (Pr)^{0.6}}{(Gr.Pr)^{0.26}} \right]$$

Reynolds number is based on the mean vibration velocity of the cylinder. The form of their correlation supports the notion that increase in coefficient depends on the relative strength of the vibrational disturbance compared to that of ordinary free convection.

The effect of vibration on heat transfer under conditions of forced convection is perhaps a more important consideration, but the results are not as complete, nor in as good agreement as those for natural convection.

Ogle and Engel(51) studied the effect of vibrating the inner tube of a double pipe heat exchanger with water as the working fluid. The heat transfer area of this exchanger was 0.785 ft^2, based on the outside diameter of the tube. The inner tube was 8 ft. long by $\frac{3}{4}$ in. diameter stainless steel tubing. Vibration was transmitted to the tube through a $\frac{1}{2}$ in. stainless steel rod attached at the centre of the tube. The outside pipe of the exchanger was 4 ft. long by $1\frac{1}{2}$ in. pyrex pipe. The experimental variables were: frequency 5 to 45 CPS; amplitude 0.107 to 0.527 cm; tube Reynolds number 400 to 20,450 ; shell Reynolds number 629 to 9,560. They observed that at low flow rates, the coefficient was improved by as much as 66%, the predominant reasons being the disturbance induced in the laminar layer both inside and outside of the tube by the vibrating motion of the tube. Moreover the motion of the tube caused torroidal flow perpendicular to the natural flow direction in the shell(52) and thereby brings about disturbance eddies which aid in the heat transfer process. In the turbulent flow domain the improvement achieved was less. Similar successful results were obtained at Southwest Research Institute(53,54) where increases in heat transfer coefficients were observed when water flowed past an electrically heated, transversely vibrating tube.

Raben(55) determined the magnitude of improvement in water side film heat transfer coefficient using acoustical energy. His experimental unit utilized the transverse vibration of an electrically heated pipe, 1 in. O.D., with water flowing on the outside of the pipe in an annular space. The outer pipe was 3 in. I. D. pyrex glass pipe and the test section was 41 in. long. The 'Bozak' vibrator was mounted with a $\frac{1}{4}$ in. steel rod connecting it to the test section which ran through the glass opening and joined on the outside of the pipe. The experimental variables were: frequency 32 to 84 CPS, the natural frequency of the system being 42 CPS; amplitude from 0.025 to 0.150 in., water flow Reynolds number from 541 to 23,600. Improvements varied from 450% at a Reynolds number of 540 to 11% at a Reynolds number of 16,000. For (Re) greater than 5,000 he proposed the following correlation :

$$\frac{h_v}{h_o} - 1 = 0.115 \left[\frac{(Re)_v}{(Re)_f} \right]^{1.69}$$

The diameter used for calculating Reynolds number was the equivalent diameter. It was concluded that the most effective method of applying acoustic vibrations is the utilization of the transverse vibrations of a pipe with water flowing on the outside of the pipe in an annular system. Study of the effect of pulsations on forced convection has recently been done by Bergles(56) where degassed, deionised water was circulated in a loop. An electrodynamic vibrator installed at the downstream end produced flow pulsations. The experimental variables were: frequency: 80 CPS, amplitude:

0.08 in., and flow velocities: 7,11, and 18 ft/sec.

No influence of vibrations on forced convection heat transfer was noticed at low wall temperatures. Above a threshold wall temperature, however, a significant improvement in heat transfer was obtained. As the vibrational intensity was increased, this threshold wall temperature was reduced and a greater improvement in heat transfer was noticed.

Very recently Mori and Tokuda(57) conducted studies on the measurement of instantaneous local heat transfer from a horizontal cylinder oscillating in the direction of an oncoming flow of liquid. The amplitude of the vibrating velocity is small compared with the oncoming flow velocity. The ranges of the variables were: dimensionless amplitude of oscillating speed $\epsilon = \frac{\Delta U}{2U_\infty} = 0.05$ to 0.7; $Re = 500 - 1,800$; frequency $f = 1\text{-}25$ CPS. The heat transfer measurements were done by an optical method. The amplitude and phase angle of unsteady component by Nusselt number at the stagnation point are obtained from snap-shot photos and shown to be expressed by Strouhal number $\frac{\omega d}{U_\infty}$, where ω-angular velocity, d-diameter of the cylinder, U_∞-free stream velocity in X-direction i.e. along the length of the cylinder. The distribution of Nusselt number in the circumferential direction was shown to be almost similar to that in steady state for the forward part of the cylinder. These results were in good agreement with their theoretical predictions.

In the vicinity of the separation point, however, the discrepancy between theoretical and experimental results increased. This was attributed mainly to the change of flow pattern in the main stream which was caused by the oscillation of the wake.

Boiling Heat Transfer:

Acoustically vibrated system:

Isakoff(58) observed an increase of 60% in burnout heat flux for pool boiling of water when the ultrasonic vibrations at a frequency of 10 KCPS were introduced in the fluid media. However, no significant improvement was obtained in the region of nucleate boiling. It was seen that the film boiling could be made to revert to nucleate boiling by applying acoustic vibrations. The experimental set-up for the above work consisted of platinum wire of 0.008 in. diameter suspended horizontally in a tank measuring 6 in. x 10 in. x 3 in. deep. The sound intensity at the transducer surface, i.e., at the bottom of the tank was measured to be 2 watts/cm^2. No attempt was made to measure the sound intensity at the heat transfer surface.

Ornatskii and Shcherbakov(59) extended the above work to subcooled boiling. They used distilled water and a nichrome heater with a diameter of 0.4 mm suspended in a glass vessel. A quartz transducer was installed at the bottom of the vessel. The frequency of vibration and intensity of ultrasound at the heat transfer surface were 1000 KCPS and 1.5 to 2.0 watts/cm^2, respectively. Experiments were performed in water temperatures of 20°, 35°, 50°, 70° and 97°C. They found that the value of burnout heat flux increased with the increase of the degree of subcooling of the liquid.

The effect of acoustic vibrations on saturated pool boiling of Isopropanol was carried out by Markels, Durfee and Richardson(60) who introduced sound waves with frequencies varying from 20-3800 CPS along the length of the heat transfer surface. A horizontal, steam heated copper tube of $\frac{3}{8}$ in. diameter and $3\frac{1}{4}$ in. length was used as heater. A barium nitrate transducer was located in the bottom of the tank to generate sound waves. The sound pressure was measured by another transducer placed near the heating surface. Frequencies varied from 20 to 38,000 CPS. The acoustic energy did not have any effect either on burnout heat flux or on critical temperature difference. The effect of frequency in the above range also did not have any significant effect. It may be noted that the sound pressures measured by the second transducer located near the heating surface were very small except for a frequency of 38,000 CPS which was also the resonant frequency of the transducer. For example, the sound pressure was 7 psi when the frequency was 38,000 CPS, but it varied between 2.5×10^{-3} psi and 400×10^{-3} psi for frequencies from 200 to 18,000 CPS when the electrical power input to the transducer in each case was about the same. Probably one would not expect any effect on heat flux at such low sound pressures.

In the above setup, the exact position of the second transducer probe as well as its size were not given. Furthermore, there was no mention of the possible variation of sound pressure along the length of the copper tube.

Recently Wong and Chon(61) investigated the effects of ultrasonic vibrations on heat transfer to water and methanol by natural convection and by boiling. Experiments were conducted at three acoustic energy levels with frequency ranging from 20.6 to 306 KCPS, using electrically heated platinum wires of diameters 0.007 and 0.010 in. Up to an eight fold increase in heat transfer coefficient was obtained in natural convection, but the effects diminished with increased temperature difference and became negligible in the well-developed nucleate boiling region. High-speed photographs showed that the increase was due to the motion of cavitation bubbles on the wire surface. The heat transfer results were correlated as a function of local cavitation activity values measured by a technique developed for this work(62).

Ultrasonic vibrations at a frequency of 20.6 KCPS had a negligible effect on the burnout heat flux and the critical temperature difference(63) using methanol at 113°F and platinum wire of 0.007 in. diameter.

Romie and Aronson(64) made an experimental investigation of the effects of ultrasonic vibrations on the burnout heat flux for forced convection, subcooled boiling, In their experiment, water flowed at atmospheric pressure through an annulus formed by a $\frac{1}{4}$ in. diameter, electrically heated tube and a concentric glass tube of $\frac{3}{4}$ in. I.D. The length of the heating element was $5\frac{1}{2}$ in. The ultrasonic transducer, which was operated at 25 KCPS and an electrical power input of

300 watts, was located at the inlet end of the annulus. The ultrasonic waves were propagated in the same direction as the flow, and thus were parallel to the heating surface. The velocity of the water varied from 1.61 to 6.25 ft/sec and the degree of subcooling from 16° to 28°F. No measurement of acoustic power at the transducer surface or in the water was made. No appreciable effect of ultrasonic vibrations on burnout heat flux was noticed. They reported that at heat fluxes appreciably below the burnout level, the pressure of an ultrasonic field did have some effect on bubble activity surrounding the heating element, provided the flow velocities were low. The average bubble size appeared to have been decreased and the frequency of bubble generation increased. It was also noticed that the number of nucleation points for bubble generation did not appear to be influenced by the ultrasonic field. However, it is not clear whether there was cavitation in the water close to the heating element. No quantitative result in this range of heat flux was presented. As the flow velocity increased, the effect of ultrasonic vibrations decreased.

Mechanically Vibrated Systems:

Bergles(56) investigated the effects of flow vibration on heat transfer coefficient with forced convection boiling. The details of his experimental setup and ranges of variables have been discussed on page 45. The maximum pressure amplitude of 15 psi near the vibrator was attenuated to 2 psi at the upstream end. It was noticed that an increase in flow-stream velocity results in a decreased influence of the vibration on heat transfer. In the region of fully developed boiling, there is no noticable effect of vibration. No significant change in burnout heat flux was noticed. This confirms with the findings of Romie and Aronson(64). However, the burnout was reduced when the flow direction was reversed. They reported that it was probably due to the upstream compressibility produced by the action of the vibrator.

GENERAL COMMENTS:

Thus it is very obvious, from the published data, to conclude that under favourable combination of circumstances the presence of oscillations can cause significant increases in heat transfer coefficients. However, it is not yet possible to apply this fact in design. There is insufficient understanding of what constitute favourable combination of circumstances, although various suggestions and hypothesis have arisen as to the mechanism by which oscillations increase the heat transfer. The wide discrepancies, found in the published data, are usually due to the different experimental conditions and ranges of variables which have been used.

The influence of vibrations upon the rate of convective heat transfer becomes appreciable only under circumstances in which vibration is of sufficeint intensity to alter the character of the flow in the neighbourhood of the heat transfer surface. Thus, in order to understand the influence of vibrations upon heat transfer, it is necessary to inquire into the behaviour of fluids in the presence of vibrations of various amplitudes and frequencies. In all the works that have been reviewed, an emperical method was used to determine the governing parameters. The effects of vibrations on heat transfer by convection and by boiling have been studied experimentally either by vibrating the fluid or by vibrating the heating surface. The two methods are directly comparable if the wavelength of sound is large relative to the characteristic dimension of the heating surface.

The amount of data on nucleate boiling is very limited although many investigators have discussed the possible effects of vibrations on nucleate boiling. However, the mechanisms proposed by them cannot be taken as conclusive as they are based on visual observations.

NOMENCLATURE

ROMAN SYMBOLS

a	amplitude of vibration
c	gas content of liquid
CPS	cycles per second
C_p	specific heat at constant pressure
D	diameter
f	frequency of vibration
g	acceleration due to gravity
h	heat transfer coefficient
$\overline{H}_p$	root mean square pressure rise
I	sound intensity
k	thermal conductivity
L	length of the tube
ℓ	half wavelength of sound
P	acoustic pressure
P_p	peak acoustic pressure
SPL	sound pressure level
s	sound particle displacement
T	temperature
v	velocity
U	cross flow velocity
W	mass flow rate.

GREEK SYMBOLS

β	thermal coefficient of volumetric expansion
Δt	temperature difference
$\delta_{A.C}$	A-C boundary layer thickness
μ	viscosity
ν	kinematic viscosity
ρ	density
σ	surface tension
ω	angular frequency.

DIMENSIONLESS GROUPS

Gr	Grashof number, $g \beta \rho^2 D^3 \Delta t/\mu^2$
Gz	Graetz number, $W C_p/kL$
Nu	Nusselt number, $h D/k$
Pr	Prandtl number, $C_p \mu/k$
Re	Reynolds number, $D v \rho/\mu$.

SUBSCRIPTS

A	actual
ℓ	liquid
s	saturation conditions
v	with vibration
w	based on wall temperature
C_f	cross flow
f	air stream flow
0	without vibration.

REFERENCES

1. Nukiyama, S. J. Soc. Mech. Engrs. (Japan), 37 No. 206, 367 (1934)
2. Westwater, J.W. and J.G. Santagelo, Ind. Eng. Chem., 47, 1005 (1955).
3. Gunther, F.C. and F. Kreith. Heat Transfer and Fluid Mechanics Institute, p. 113-121, Berkeley, California (1949)
4. Rohsenow, W.M. and J.A. Clark. Trans. Am. Soc. Mech. Engrs., 73, 609 (1951).
5. Strenge, P.H., Aluforell, and J.W. Westwater, Am. I.Ch.E. J. 7, 578 (1961).
6. Schweppe, J.L. and A.S. Fourst, Chem. Eng. Progr. Symposium Ser. No. 5 49, 77 (1953).
7. Robinson, D.B. and D.L. Katz, Chem. Eng. Progr. 47, 317 (1951).
8. Andrade, E.N. Proc. Roy. Soc. (London) A 134, 445 (1931).
9. Schlichting, H. Physik Z. 61, 349 (1932).
10. West, G.D. Proc. Phy. Soc. (London) B 64, 483 (1951).
11. Holtsmark, J. Johnsen, I., Sikkeland, T. and S. Skavlem, J. Acoust Soc. Am., 26, 26 (1954).
12. Raney, W.P., J.C. Corelli and P.J. Westervelt. J. Acoust. Soc. Am., 26, 1006 (1954).
13. Kubanskii, P.N., Trans. USSR Academy of Science, 82, 585 (1952).
14. Kubanskii, P.N. J. Tech. Phys. USSR, 22, 593 (1952).
15. Fand, R.M. and J. Kaye. J. Acoust. Soc. Am., 32, 579 (1960).
16. Fand, R.M. and E.M. Peebles. J. Heat Transfer Trans. ASME, 84, 268 (1962).
17. Westervelt, P.J. J. Acoust. Soc. Am., 32, 337 (1960).

18. Lemlich, R. Ind. Eng. Chem. 47, 1175 (1955).

19. Fand, R.M. and J. Kaye. International Developments in Heat Transfer. Part 1. 490-498 (1961).

20. Rao, M.A. U.S. Air Force Office Aerosp. Res. ARL 65-215 (1965).

21. Kubanskii, P.N. J. Tech. Phys. USSR, 22, 593 (1952).

22. Kubanskii, P.N. Sov. Phys.- Acoustics, 5, No. 1, 49 (1959).

23. Kubanskii, P.N. Akoustichiskii Zhurnal, 6, No. 4, 464 (1960).

24. Kubanskii, P.N. Sov. Phys.- Acoustics, 7, No. 2, 165 (1961).

25. Fand, R.M. and J. Kaye. J. Heat Transfer, Trans. ASME, 83, 133 (1961).

26. Richardson, P.D. J. Acoust. Soc. Am., 36, 2323 (1964).

27. Fand et al. J. Heat Transfer, Trans. ASME, 84, 245 (1962).

28. Holman, J.P. and T.P. Mott-Smith, J. Aero/space Science, 26, 188 (1959)

29. Kubanskii, P.N. J. Tech. Phys. USSR, 22, 593 (1952).

30. Fand, R.M. and P. Cheng. Int. J. Heat Mass Transfer, 6, 571 (1963).

31. Jackson, T.W., W.B. Harrison and W.C. Boteler. J. Heat Transfer, Trans. ASME, 81, 68 (1959).

32. Mathewson, W.F. and J.C. Smith. Chem. Eng. Prog. Sym. Series, 59, No. 41, 173 (1963).

33. Havemann, H.A. and R.N.N. Narayan, Nature, 174, 41 (July 3, 1954).

34. Havemann, H.A., P. Jayo Chandra and G.C. Garg. J. Indian Institute Science, 38B, 172 (1956).

35. Lemlich, R. and C.K. Hwu. Am. I. Ch. E. J. 7, 102 (1961).

36. Lemlich, R. Ind. Eng. Chem. 47, 1175 (1955).

37. Anantanaryanan, R. and A. Ramachandran, Trans. ASME, 80, 1426 (1958).

38. Sreenivasan, K. and A. Ramachandran. Int. J. Heat Mass Transfer, 3, 60 (1961).

39. Robinson, G.C., C.M. McClure and R. Hendricks. Bull. Am. Ceramic Soc., 37, 399 (1958).

40. Larson, M.B. and A.L. London. ASME Paper 62-HT-44 (1962).

41. Davis, A.H. Phil. Mag. (6), 47, 1057 (1924).

42. Martinelli, T.C. and L.M.K. Boelter, Proceedings of the fifth International Congress of Applied Mechanics, p.578, Cambridge Massachusetts (1938).

43. Lemlich, R., Symposium on pulsatory and vibrational phenomenon, Ind. Eng. Chem. 47, No. 6, 1175-1180 (1955).

44. West, F. and A. Taylor. Chem. Eng. Progr. 48, 39 (1952).

45. Shai, I. and Z. Rotem. Am. Soc. Mech. Engrs. Pre-print 60-HT-21 (1960).

46. Scanlan, J.A. Ind. Eng. Chem., 50, 1565 (1958).

47. Larson, M.B. and A.L. London. ASME. Paper 62-HT-44 (1962).

48. Deaver, F.K., W.R.Penney and T.B. Jefferson. J. Heat Transfer, Trans. ASME, 84, 251 (1962).

49. Penney, W.R. and T.B. Jefferson. ASME Paper 63-WA/HT-14.

50. Lemlich, R. and M. Anandha Rao. Int. J. Heat Mass Transfer, 8, 27 (1965).

51 Ogle, J.W. and A.J. Engel Chem. Eng. Progr.Sym. Series, No. 57, 61 Heat Transfer Conference, Boston.

52. Schlichting, H., Boundary Layer Theory, Chapt. 11. Pergamon Press, New York (1955).

53. Anon. Chem. Eng. News, 92, 38, (May 30,1960).

54. Anon Saline Water Conversion Report, OSW, 17 (1961).

55. Raben, I. Proc. Heat Transfer and Fluid Mech. Institute, Stanford University, p.90 (1961).

56. Bergles, A.E. J. Heat Transfer, Trans. ASME, 86, 559 (1964).

57. Mori, Y. and S. Tokuda. Paper No. Am. I.Ch.E. 86, presented at the third international heat transfer conference, Chicago, (Aug.7-12, 1966).

58. Isakoff, S.E. Proc. Heat Transfer and Fluid Mech. Institute, Stanford University, p.15 (1956).

59. Ornatskii, A.P. and V.K. Shcherbakov, Teploenergetika, 6, 84 (1959). Translation appears in (65).

60. Markels, M., R.L. Durfee and R. Richardson. United States Atomic Energy Commission, NYO 9500, September, 1960.

61. Wong, S.W., Ph.D. Thesis, McGill University, Montreal, Que. (1967).

62. Wong, S.W., Ph.D. Thesis, McGill University, Montreal, Que. (1967).

63. Wong, S.W. and W.Y. Chon, Can. J. Chem. Eng., 45, No. 6, p.384 (1967).

64. Romie, F.E. and C.A. Aronson. Advanced Technology Laboratories, Report ATL-A-123, July, 1961.

PRESENT INVESTIGATION

PART 1

CONVECTIVE AND BOILING HEAT TRANSFER FROM OSCILLATING WIRE TO WATER AND METHANOL

INTRODUCTION

This part of the investigation is confined to the study of convective and boiling heat transfer from a single oscillating horizontal wire to subcooled water and methanol. Platinum wire which can be used as an accurate resistance thermometer was employed as the heating element. Vibrations of uniform amplitude were imposed on wire by an externally located electromagnetic device. This eliminates to a large extent the effect of any external agitation in the fluid system except in the boundary layer.

The heat transfer data for the complete heat flux versus ΔT curve are presented under various conditions of vibrations and the effect of each individual vibrational parameter is determined. A suitable criterion is used to estimate the incipient point for the subsequent development of heat transfer correlations in different regimes.

EXPERIMENTAL

Equipment:

The boiling apparatus consisted of a stainless steel vessel having two opposite walls of $\frac{1}{4}$ in. thick pyrex glass to permit visual observation and high-speed photographic work. The inside dimensions of the vessel were 9 in. x 6 in. x 11 in. high. Four electric strip heaters, each with a maximum capacity of 250 watts, were welded to the bottom and sides of the vessel. The power input to the heaters was controlled to maintain the bath at any desired temperature. The stainless steel vessel was insulated with 1 in. thick asbestos to minimise heat losses.

The heat transfer surface was a chemically pure grade platinum wire of 0.01 in. diameter. Platinum was selected for the combined heating element and resistance thermometer because of its resistance to corrosion and high temperature coefficient of electric resistance. In order to eliminate end effects and to have uniform amplitude of vibration, only a central part of the wire (approximately $\frac{3}{4}$ in.) was used as a test section with the help of platinum potential leads of 0.0045 in. diameter. A special assembly of Teflon,as shown in Figure 1 was designed to hold the heating element and the potential leads. This particular type of assembly kept the wire stretched in the horizontal position at all conditions of vibration. The heating element was 5 in. below the free surface of the liquid.

FIGURE 1

SKETCH OF AN ASSEMBLY TO HOLD

PLATINUM WIRE AND POTENTIAL LEADS

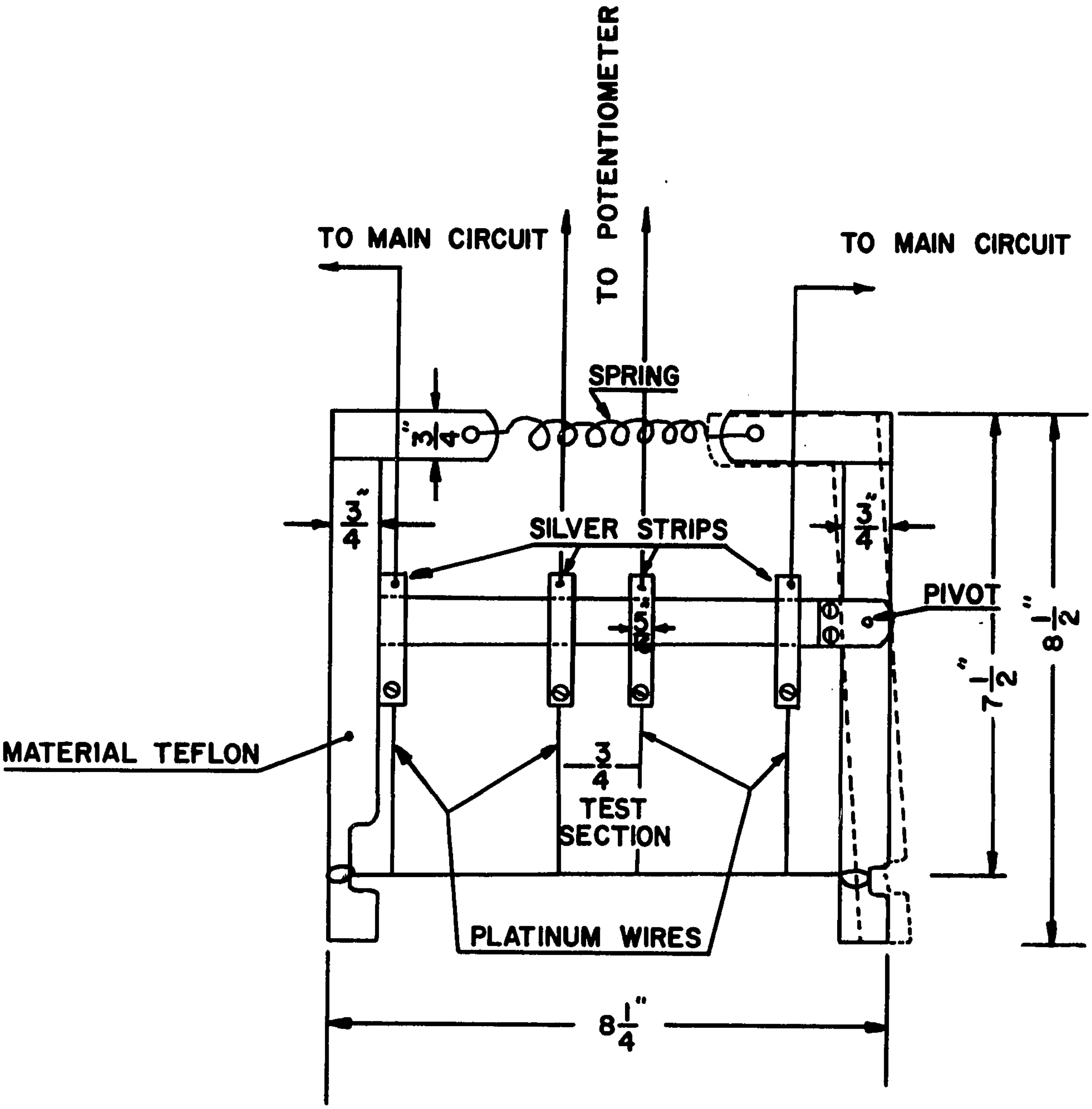
TO MAIN CIRCUIT
TO POTENTIOMETER
TO MAIN CIRCUIT
SPRING
3/4"
3/4"
SILVER STRIPS
3/4"
5/8"
PIVOT
7 1/2"
8 1/2"
MATERIAL TEFLON
3/4
TEST SECTION
PLATINUM WIRES
8 1/4"

At the level of the heat transfer surface there were two pockets (each $\frac{1}{2}$ in. x $\frac{1}{8}$ in. x 1 in. long) on opposite walls of the s.s. vessel through which the poles ($\frac{1}{2}$ in. x $\frac{1}{8}$ in. in cross section) of the D,C. electromagnets were inserted. The gap between the poles when fitted in position was $\frac{1}{2}$ in. The input to the electromagnet was fed from a custom made D.C. power supply (0-80V, 0-5A) which could produce a magnetic field with a maximum intensity of 10 k gauss. Platinum wire carried A.C.- superimposed D.C. current across a horizontal D.C. magnetic field produced by the electromagnets. As a result of interaction between the horizontal magnetic field and alternating current passing through the wire, the heating element was subjected to sinusoidal oscillations in the vertical plane. A thermometer located near the wire was used to measure the temperature of the liquid bath which was always controlled within ± 1°F.

The electrical circuit designed for this setup is shown in Figure 2. An A.C. signal of varying frequency supplied by an oscillator, Hewlett-Packard Model 204B, was amplified through a 75 watt Mozak audio amplifier. A special transformer with an impedance ratio of 8:0.5 ohm was connected to the output of the amplifier to match the output impedance of the amplifier with that of the external load. This helped in operating the amplifier at the maximum possible effeciency. The A.C. signal was superimposed with D.C. current through a regulated D.C. power supply, Model 520 A (0-36V, 0-25A) manufactured by Harrison Laboratories, which was connected in series with the A.C. circuit. A

FIGURE 2

SCHEMATIC DIAGRAM OF APPARATUS

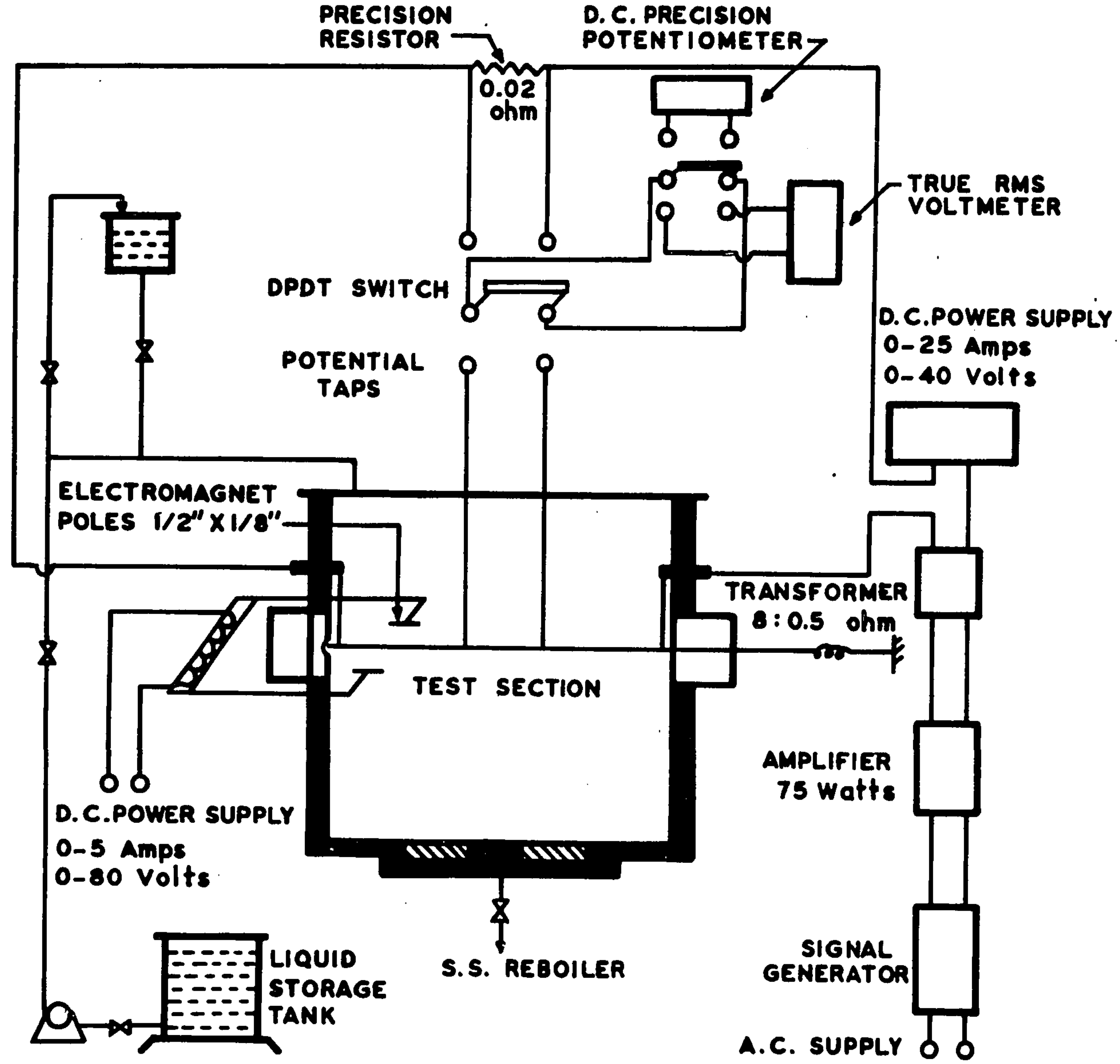
PRECISION RESISTOR
0.02 ohm
D. C. PRECISION POTENTIOMETER
TRUE RMS VOLTMETER
DPDT SWITCH
POTENTIAL TAPS
D.C.POWER SUPPLY
0-25 Amps
0-40 Volts
ELECTROMAGNET POLES 1/2" X 1/8"
TRANSFORMER 8:0.5 ohm
TEST SECTION
AMPLIFIER 75 Watts
D.C.POWER SUPPLY
0-5 Amps
0-80 Volts
LIQUID STORAGE TANK
S.S. REBOILER
SIGNAL GENERATOR
A.C. SUPPLY

precision resistor of 0.02 ohm, (Type 1682) manufactured by Guild Line Instruments Ltd., was also connected in series to measure the direct current in the circuit. A Tinsley precision potentiometer, Model 3184E and Tinsley galvanometer (Type SR-1) were used for recording potential drops across the test section and the precision resistor. The Tinsley potentiometer and galvanometer combination was capable of reading up to 0.05 millivolt. A true R.M.S. voltmeter, Model 400E, manufactured by Hewlett Packard, capable of reading up to 0.1 millivolt was used to measure the A.C. potential drop across the test section. For the measurment of amplitude of the oscillating wire, an optical system was designed. It consisted of a telephoto lens with an adjustable focal length up to 200 mm, which was attached on to an optical extension tube having ground glass screen at the other end. The whole unit was mounted on a cathetometer with an accuracy of 0.0004 in. A stroboscopic flashing light was used to project the image of the oscillating wire on to the screen. The frequency of vibration was measured by darkening the room and shining the stroboscopic light on the vibrating wire. The stroboscope used was the "Probostrobe, Model E 116A" manufactured by R.H. Nichols Co., with a measuring range of 600-15,000 R.P.M. The electrical components of the circuit were of such precision that readings were limited by the stability of the boiling phenomenon rather than the accuracy of the instruments. The photograph of the experimental setup is shown in Figure 3.

FIGURE 3

PHOTOGRAPH OF EXPERIMENTAL APPARATUS

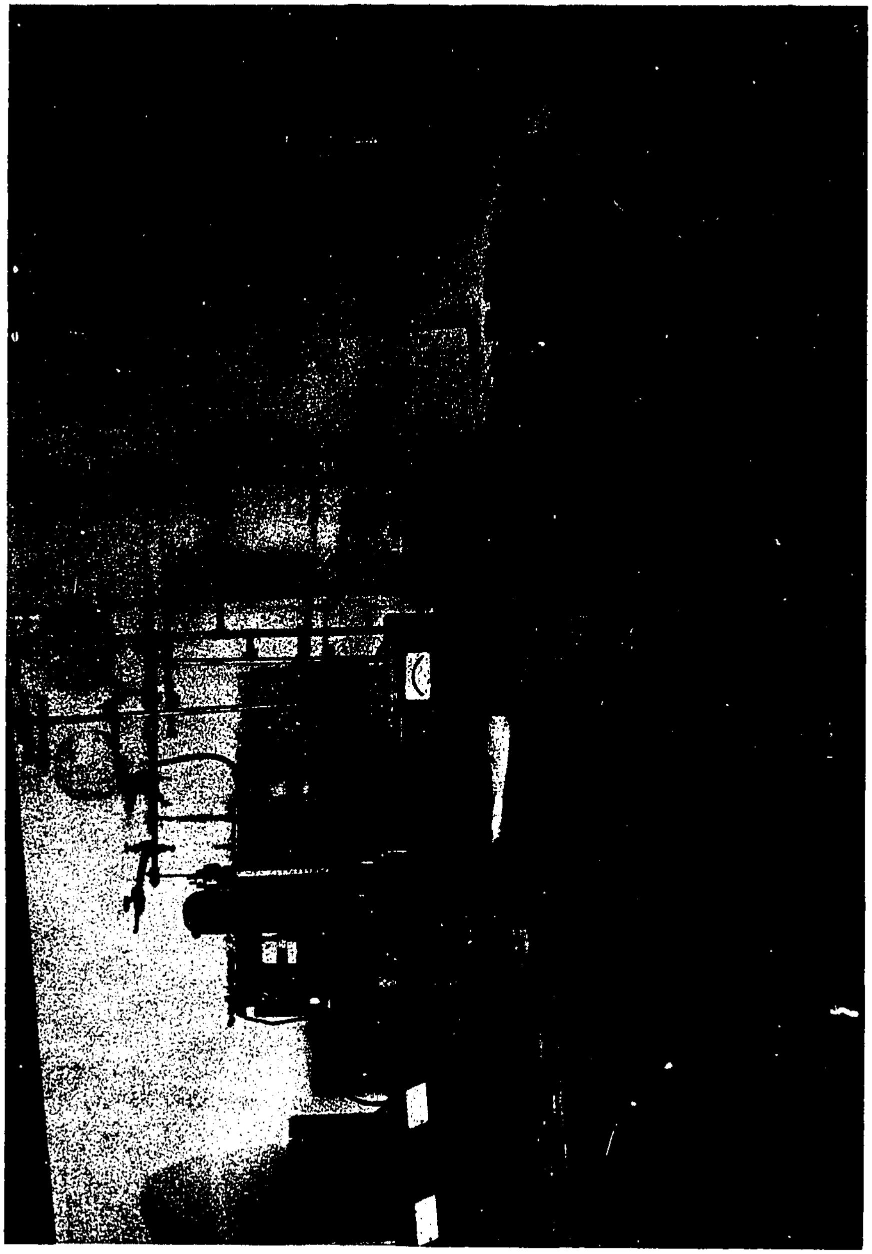

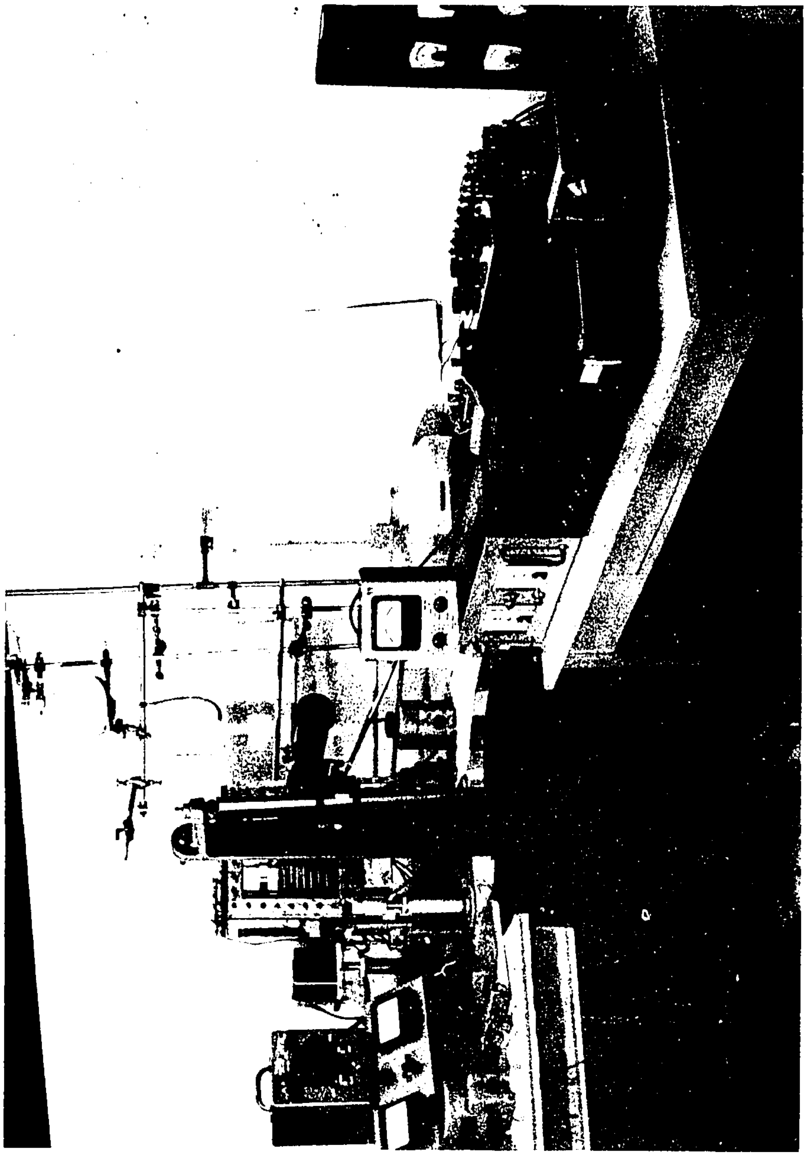

Materials used:

All platinum wires including the potential leads were of chemically pure grade manufactured by Englehard Industries. The liquids used were distilled water and reagent grade methanol supplied by Fisher scientific Co.

Procedure:

The platinum potential leads of 0.0045 in. diameter were spot-welded to the main heat transfer surface and then annealed for 15-20 minutes with alternating current. The test section of the wire was calibrated for its resistance at 32°F and 212°F by passing a very small D.C. current (0-50 milli amperes)using Kepko D.C. power supply (0-3A, 0-10 Volts).

Potential drops across the precision resistor (0.02 ohm) and the test section were measured to compute the resistance of the test section. The temperature coefficient of resistivity of platinum obtained from a series of calibrations performed both at 32°F and 212°F were found to be in good agreement with the known values. The length of the test section was measured by a scale capable of an accuracy of $\frac{1}{64}$ in. and the diameter of the wire was checked with a micrometer.

The calibrated platinum element and its mountings were then transferred into the bath of distilled water or methanol which was then maintained at the desired temperature. Before taking readings sufficient time was allowed for the bath to attain steady state such that the air content of the system reached its equilibrium value.

Since at given values of the frequency and tension on the wire, the amplitude of vibration of the wire is mainly controlled by A.C. current in the wire and D.C. current in the electromagnet, it was desirable to hold these two values constant for the entire duration of the experiment. However, even with this control the amplitude varied as the temperature difference was increased, most probably due to the interference of D.C. current through the wire with the magnetic field originally produced by the A.C. current. Therefore to maintain constant amplitude of vibration throughout the experimental run, the adjustment of D.C. magnet current was necessary from time to time.

For the measurement of the heat flux and temperature difference, the D.C. current was increased in steps and the D.C. potential drop across the test section and precision resistor, as well as the A.C. potential drop across the test section were measured as mentioned above. Temperature differences (ΔT) were calculated by using the relations for platinum resistance thermometry(1). Since surface condition changed after a few runs, it was necessary to use a new platinum wire after a reasonable number of experimental runs.

Heat Transfer From Stationary Wires:

The conventional plots, of heat flux versus temperature difference for stationary wires were established for distilled water at 118.4, and 170.6°F and for methanol at 95°F. As mentioned previously the methanol used was reagent grade supplied by Fisher Scientific Co. Before taking data the liquid was boiled for 20 minutes and sufficient time was provided for the system to attain equilibrium with the atmospheric conditions.

The input to the strip heaters was controlled so as to have minimum natural convection currents arising from the bottom of the vessel. For stationary wires, only D.C. part of the circuit was used. The current from the D.C. power supply was increased through the wire in very small steps such that the whole region of natural convection (low values of the temperature difference) and nucleate boiling (higher values of the surface temperature) were covered. The corresponding measurements of potential drops across the precision resistor and the test section were recorded to calculate heat flux and temperature difference.

Heat Transfer from Vibrating Wires:

Experiments were conducted to measure the effects of vertical sinusoidal oscillations of the heat transfer surface on natural convective and subcooled boiling heat transfer to water and methanol. The overall range for frequency varied from 20 to 80 CPS and amplitude of vibration from 0.035 to 0.08 in. The effects of these variables were studied starting from low temperature difference to the critical temperature difference.

The results of the heat transfer experiments with and without vibrations are presented in Figures 4 through 10.* In each of these figures, the heat flux versus ΔT curves are shown for different frequencies at a given particular amplitude. Similar results were obtained by cross-plotting the heat flux curves at a given frequency and varying amplitude. An increase in frequency or amplitude

---

* In Figures 4 through 10, lines AB represent the incipient boiling.

EFFECT OF VIBRATIONS ON

HEAT TRANSFER RATES IN

DISTILLED WATER AT 118.4°F.

FIGURE 4 AMPLITUDE = 0.0386 IN.

FIGURE 5 AMPLITUDE = 0.0673 IN.

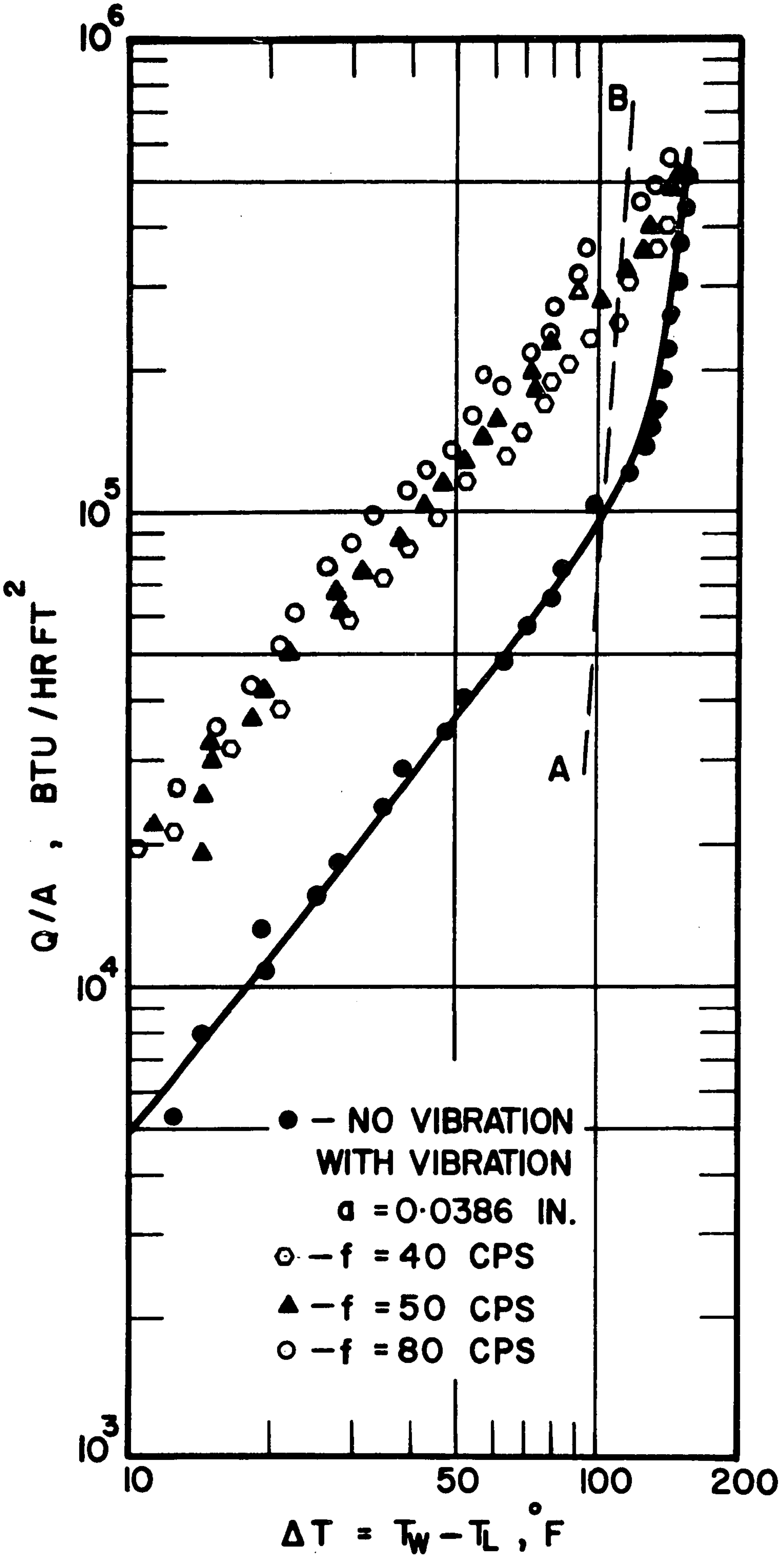

10^6
10^5
10^4
10^3
Q/A , BTU / HR FT^2
10
50
100
200
ΔT = T$_W$ − T$_L$, °F
A
B
● − NO VIBRATION
WITH VIBRATION
a = 0·0386 IN.
○ − f = 40 CPS
▲ − f = 50 CPS
○ − f = 80 CPS

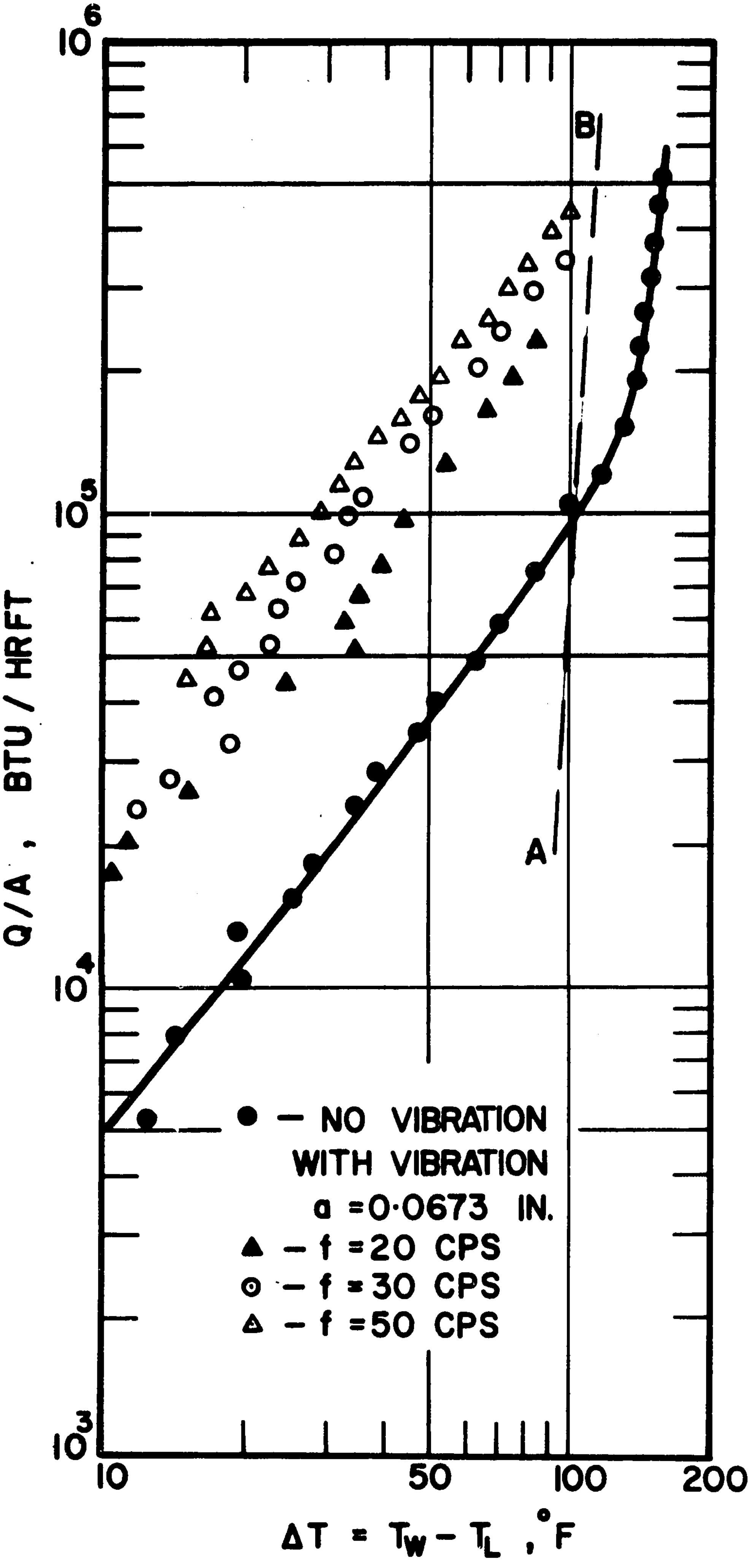

10^6
10^5
10^4
10^3
Q/A , BTU / HRFT²
10
50
100
200
ΔT = T_W − T_L , °F
B
A
● – NO VIBRATION
WITH VIBRATION
a = 0·0673 IN.
▲ – f = 20 CPS
○ – f = 30 CPS
△ – f = 50 CPS

EFFECT OF VIBRATIONS ON
HEAT TRANSFER RATES IN
DISTILLED WATER AT 170.6°F

FIGURE 6	AMPLITUDE	=	0.0386 IN.
FIGURE 7	AMPLITUDE	=	0.0673 IN.
FIGURE 8	AMPLITUDE	=	0.1070 IN.

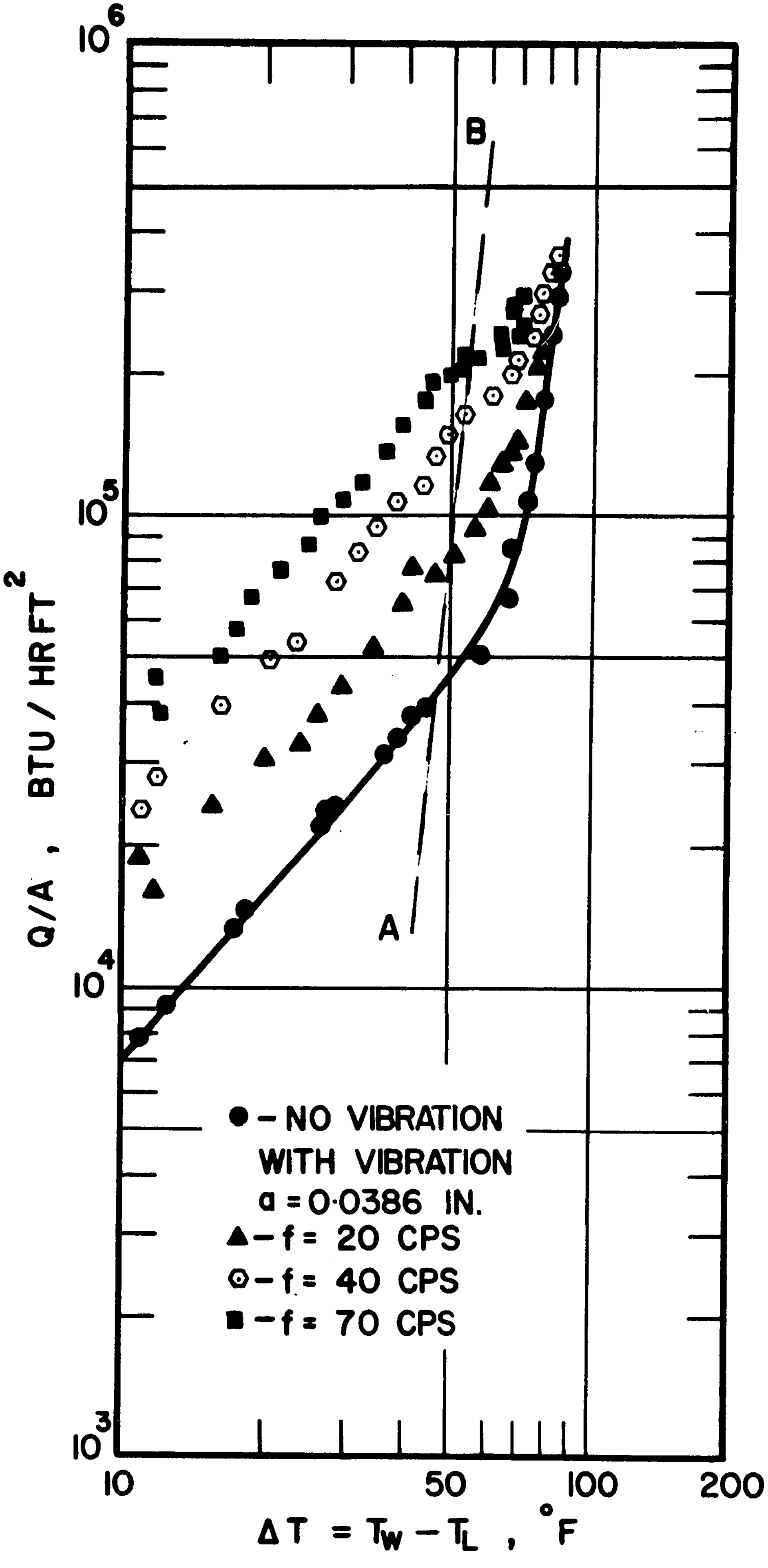

10^6
10^5
10^4
10^3
B
A
Q/A , BTU / HR FT^2
● – NO VIBRATION
WITH VIBRATION
a = 0·0386 IN.
▲ – f = 20 CPS
⊙ – f = 40 CPS
■ – f = 70 CPS
10
50
100
200
ΔT = $T_W - T_L$, °F

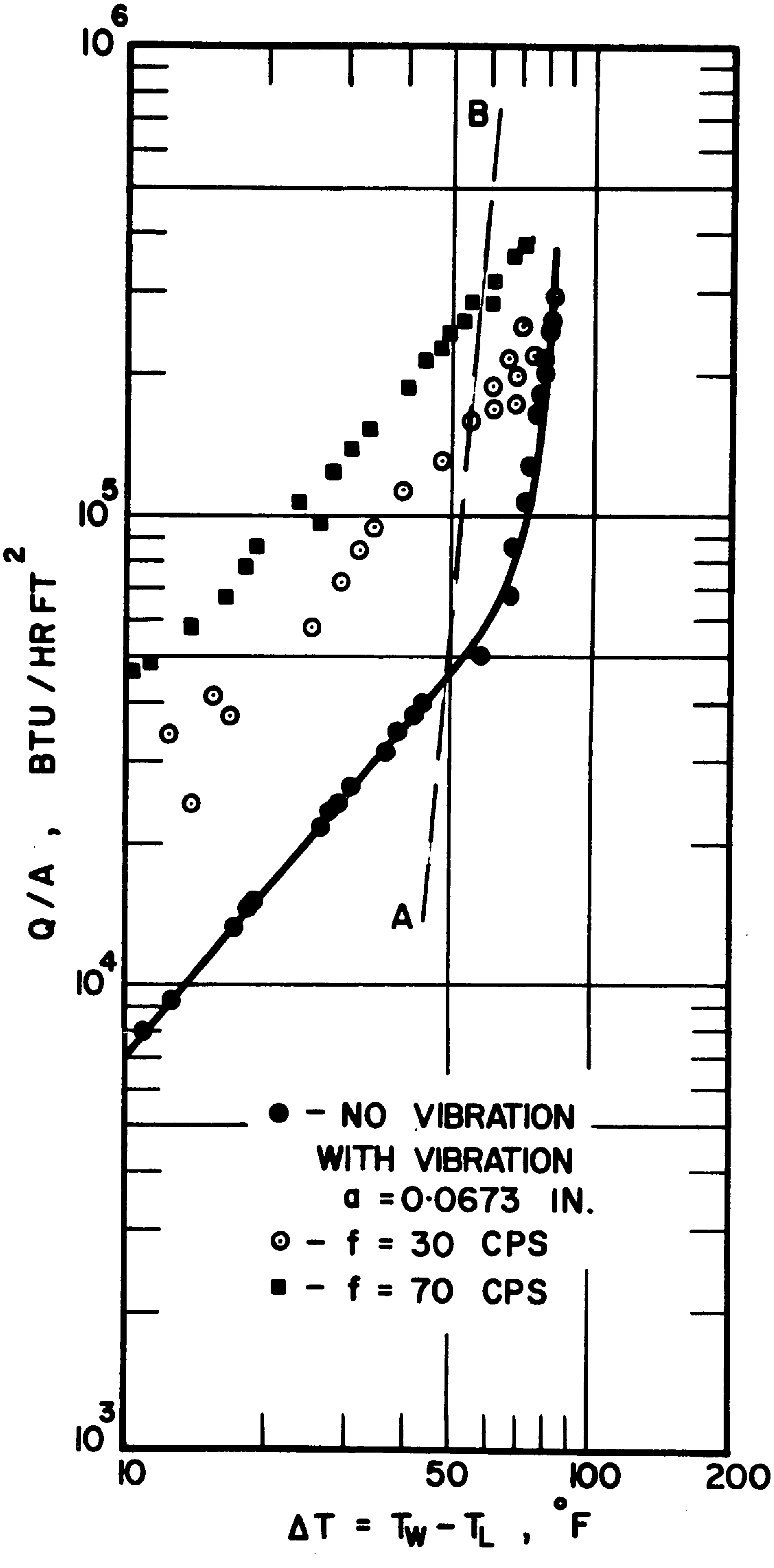

10^6
10^5
10^4
10^3
B
A
Q/A , BTU/HR FT²
10
50
100
200
ΔT = T_W − T_L , °F
● − NO VIBRATION
WITH VIBRATION
a = 0·0673 IN.
⊙ − f = 30 CPS
■ − f = 70 CPS

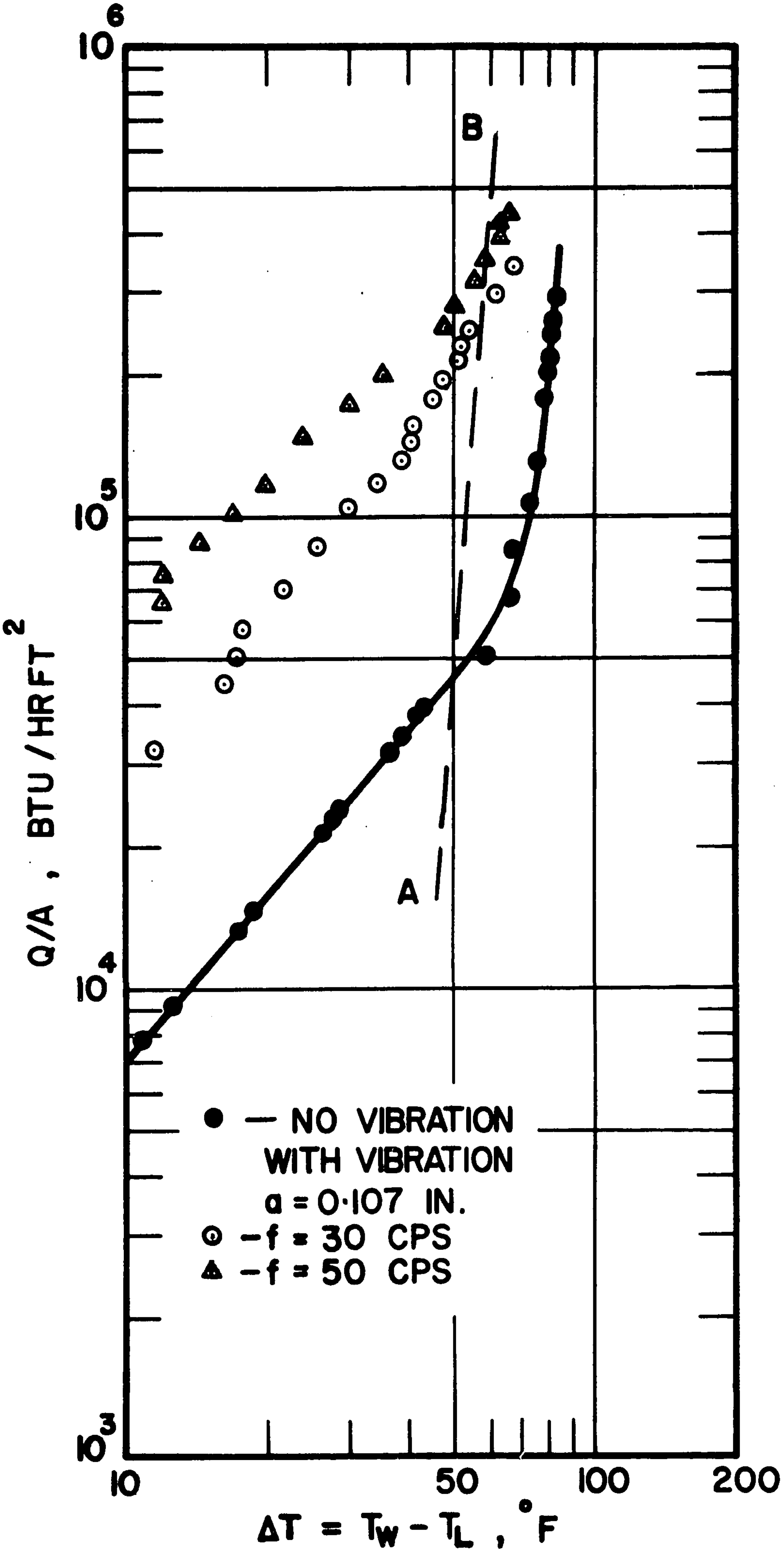

10^6
10^5
10^4
10^3
Q/A , BTU/HR FT^2
10
50
100
200
ΔT = T_W − T_L , °F
B
A
● — NO VIBRATION
WITH VIBRATION
a = 0·107 IN.
⊙ —f = 30 CPS
△ —f = 50 CPS

EFFECT OF VIBRATIONS ON
HEAT TRANSFER RATES IN METHANOL AT 95°F.

FIGURE 9 AMPLITUDE = 0.0386 IN.

FIGURE 10 AMPLITUDE = 0.0673 IN.

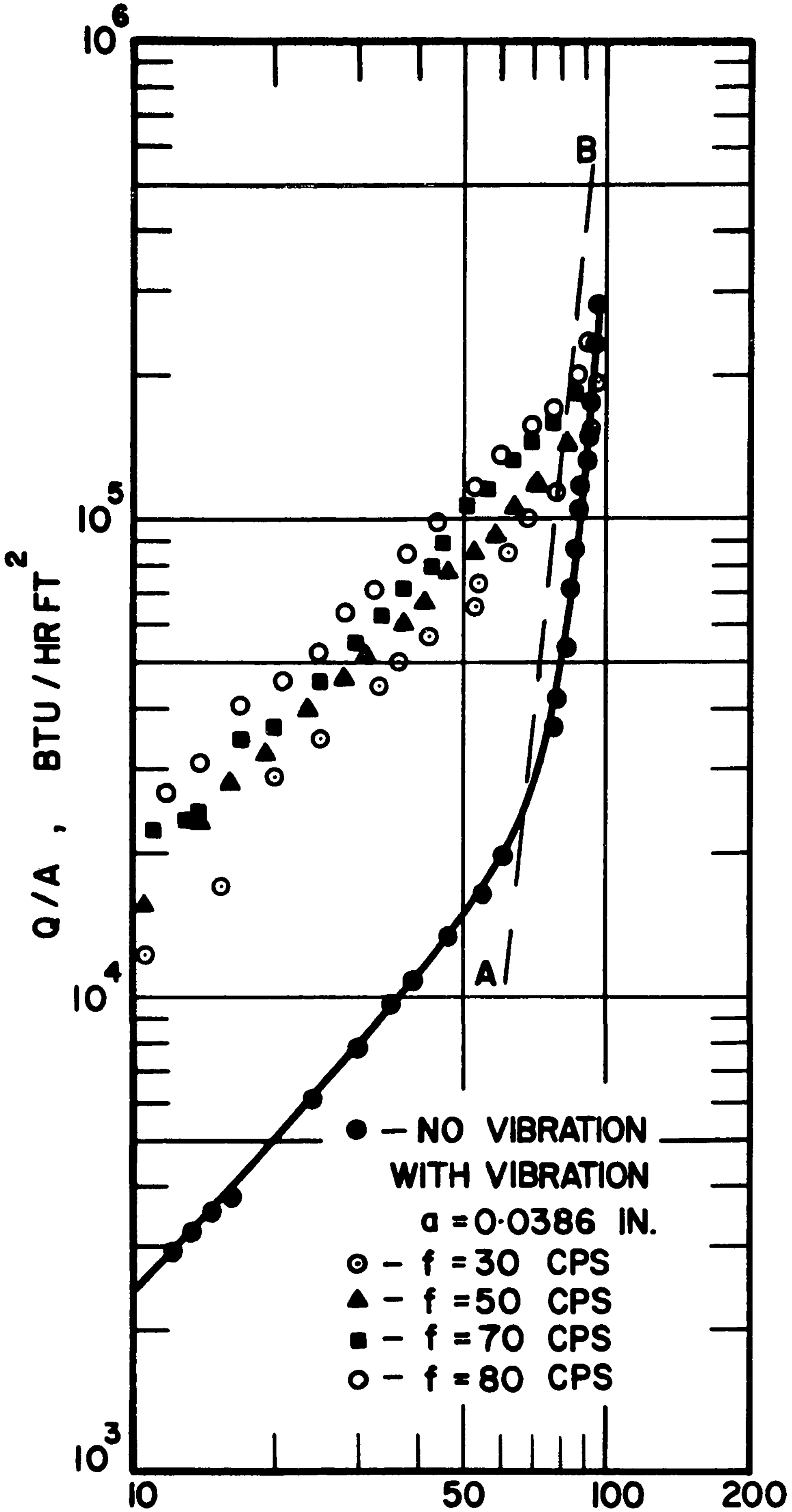

10^6
10^5
10^4
10^3
Q/A , BTU / HR FT^2
10
50
100
200
ΔT = $T_W - T_L$, °F
A
B
● – NO VIBRATION
WITH VIBRATION
a = 0·0386 IN.
⊙ – f = 30 CPS
▲ – f = 50 CPS
■ – f = 70 CPS
○ – f = 80 CPS

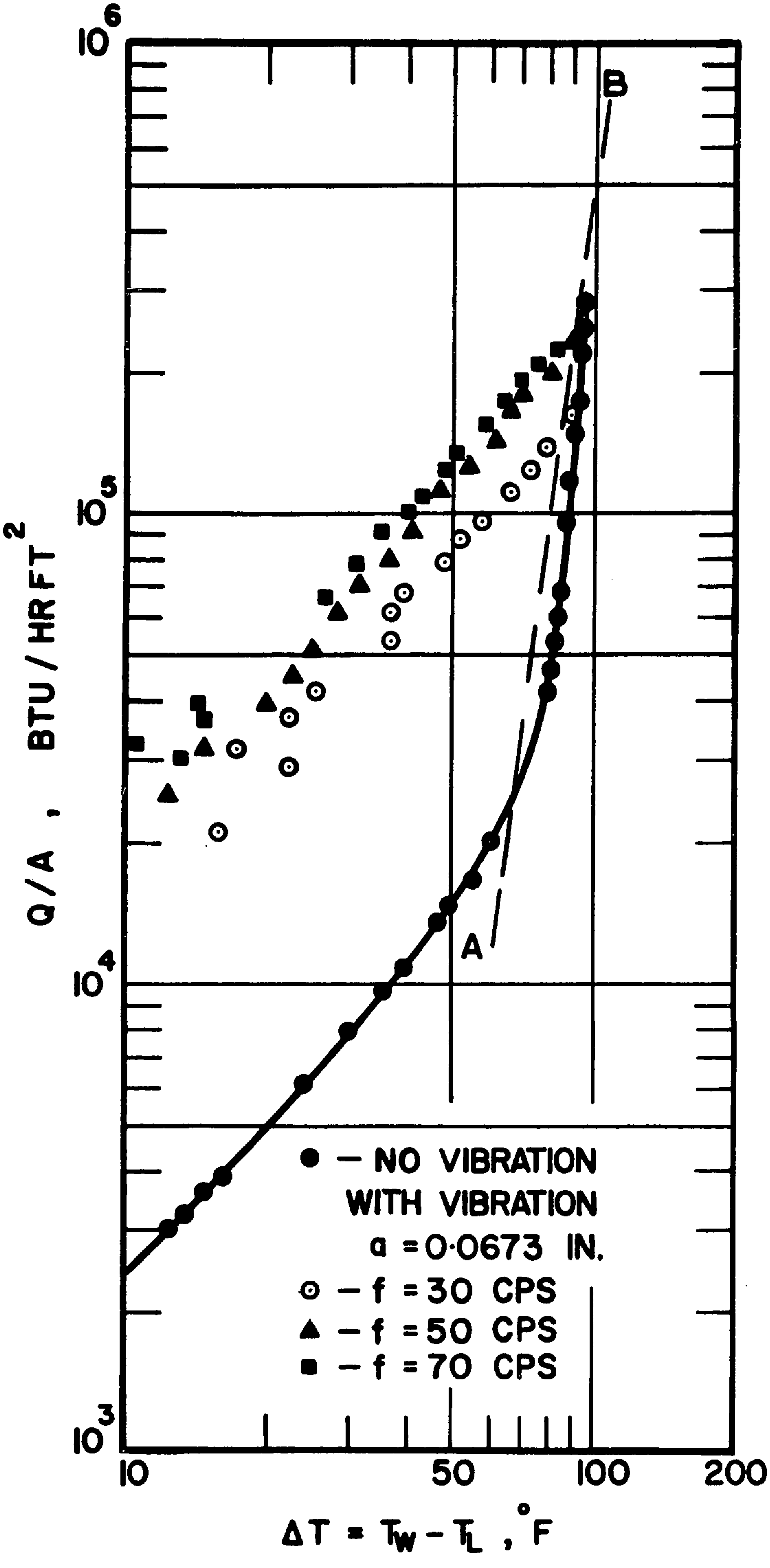
10^6
10^5
10^4
10^3
10
50
100
200
B
A
Q/A , BTU / HR FT^2
$\Delta T = T_W - T_L$, °F
● – NO VIBRATION
WITH VIBRATION
a = 0·0673 IN.
⊙ – f = 30 CPS
▲ – f = 50 CPS
■ – f = 70 CPS

enhances the heat flux at a given temperature difference. However, it may be noted that the increase in heat flux decreases with increasing ΔT. Three distinct regions are observed whenever vibrations are imposed on the heat transfer surface. At low surface superheat, the heat transfer is governed by natural convection superposed with oscillation induced forced convection. However, for the sake of convenience this region has been termed as forced convection region in this investigation. At moderate surface superheat, the bubbles start to form and the heat transfer is determined by the combined effects of forced convection and surface boiling. At higher surface superheat the effect of forced convection seems to disappear and there appears to be a single curve representative of fully developed boiling. The range of each region is dependent upon the vibrational parameters, the particular liquid used and its temperature. For the region of forced convection, depending upon the vibrational parameters as well as the temperature difference a maximum increase of heat transfer up to ten fold is observed for methanol and seven fold for distilled water.

Due to the complex phenomenon of boiling and vibrations the error in ΔT was calculated to be as large as 2°F. Subsequently, heat transfer data with ΔT smaller than 10°F were neglected and little emphasis was given on data with ΔT smaller than 20°F. The radial temperature gradient within the platinum wire was calculated according to an equation given by McAdams et al.(2). The correction was not necessary as the error involved was less than 2% of the measured mean temperature of the platinum wire. The heat transfer data for all regions are given in Appendix A and sample calculations for the heat transfer results are given in Appendix B.

Heat transfer experiments without vibration were analysed in order to check the experimental techniques. The data for natural convection were correlated as $Nu_o = \phi(Gr.Pr)$ and the best fitted line obtained with this relation was compared with the established correlation by McAdams(3). The range of (Gr.Pr) varried from 10 to 150. The agreement between the two is good as shown in Figure 11.

FIGURE 11

NATURAL CONVECTIVE HEAT TRANSFER FROM HORIZONTAL PLATINUM WIRES TO LIQUIDS .

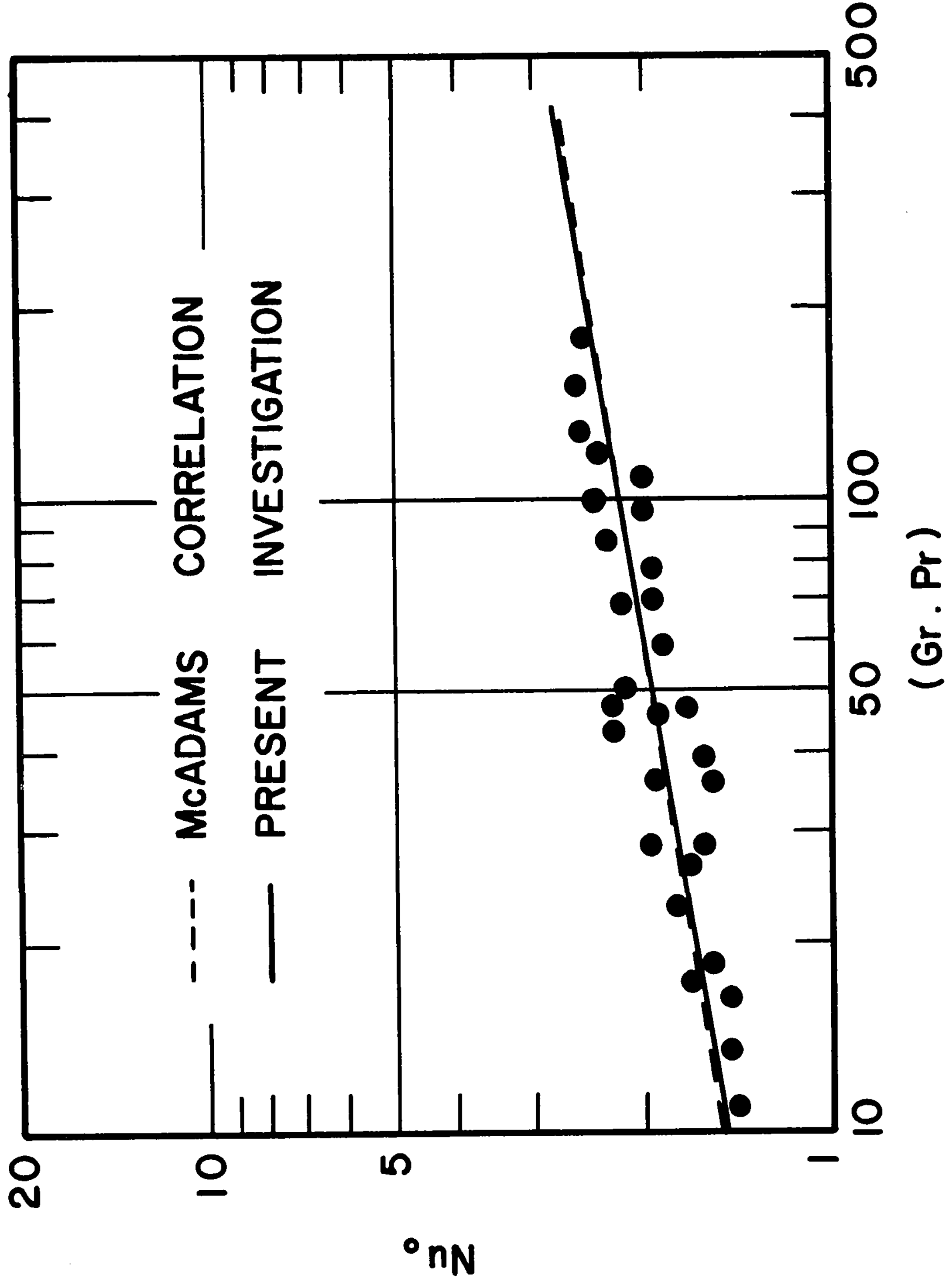
- - - - McADAMS CORRELATION
——— PRESENT INVESTIGATION
20
10
5
1
Nu_o
10
50
100
500
(Gr . Pr)

ANALYSIS OF HEAT TRANSFER DATA

The experimental results indicate that in the presence of surface vibrations, the heat flux curve consists of three distinct regimes. And hence, efforts have been made to locate the transition between these regions. Based on the theory of nucleation and bubble growth, a mathematical model has been proposed which determines quantitatively the incipient point under the conditions and thus enables the prediction of the boundaries between regions.

From the analysis of the forced convection data, dimensionless expression has been derived which correlates the data from vibrating heat transfer surfaces to various fluids. A Rohsenow-type correlation for fully developed nucleate boiling was then successfully combined with a correlation for oscillation-induced forced convection to interpret the heat flux for the transition region.

Forced Convection Correlation:

In the past, the knowledge of the mechanism of fluid fluctuations around a heated vertically oscillating cylinder or wire in liquids has been very much limited. The mathematical formulation of vibration and its effect on convective heat transfer has not been attempted even in a simpler case where the fluid is a gas. As mentioned in the literature review section the work carried out so far has been for the case of horizontal vibrations of the heat transfer surface in air where flow visualization techniques have shown the development of acoustic or thermoacoustic streaming depending upon the ratio of $\frac{\delta_{A.C.}}{D}$ employed. For heated cylinders undergoing vertical vibrations in air, Fand and Kaye(4) and Rao(5) have concluded from their interferogram studies that the boundary layer is in a state of turbulence which differs radically from the vortex type which is developed for horizontal vibrations. However, no quantitative work was reported.

Thus, in this investigation the problem is dealt with as that of unsteady forced convection. Following the conventional procedure for forced convection the representative data for water and methanol are first plotted in Figure 12 as $(Nu_v)(Pr)^{-0.3}$ against Re on a log-log scale with (Gr.Pr) as a parameter.

In Figure 12 each set of points represents the data from one run where the displacement amplitude and frequency of the wire were maintained constant and the change in Re was due to the change in the fluid properties because of increase in the surface temperature. Experimental conditions were such that for one set of data points, change in Gr was quite large, whereas there was not much change in the magnitude of Prandtl number. From Figure 12 it is then obvious that Grashof number has some influence throughout the range of the Reynolds number, particularly for water. This effect is indicated by the steep rise in Nu_v for each run. An approximate measure of the Grashof

FIGURE 12

RESULTS BASED ON CONVENTIONAL FORCED CONVECTION CORRELATION

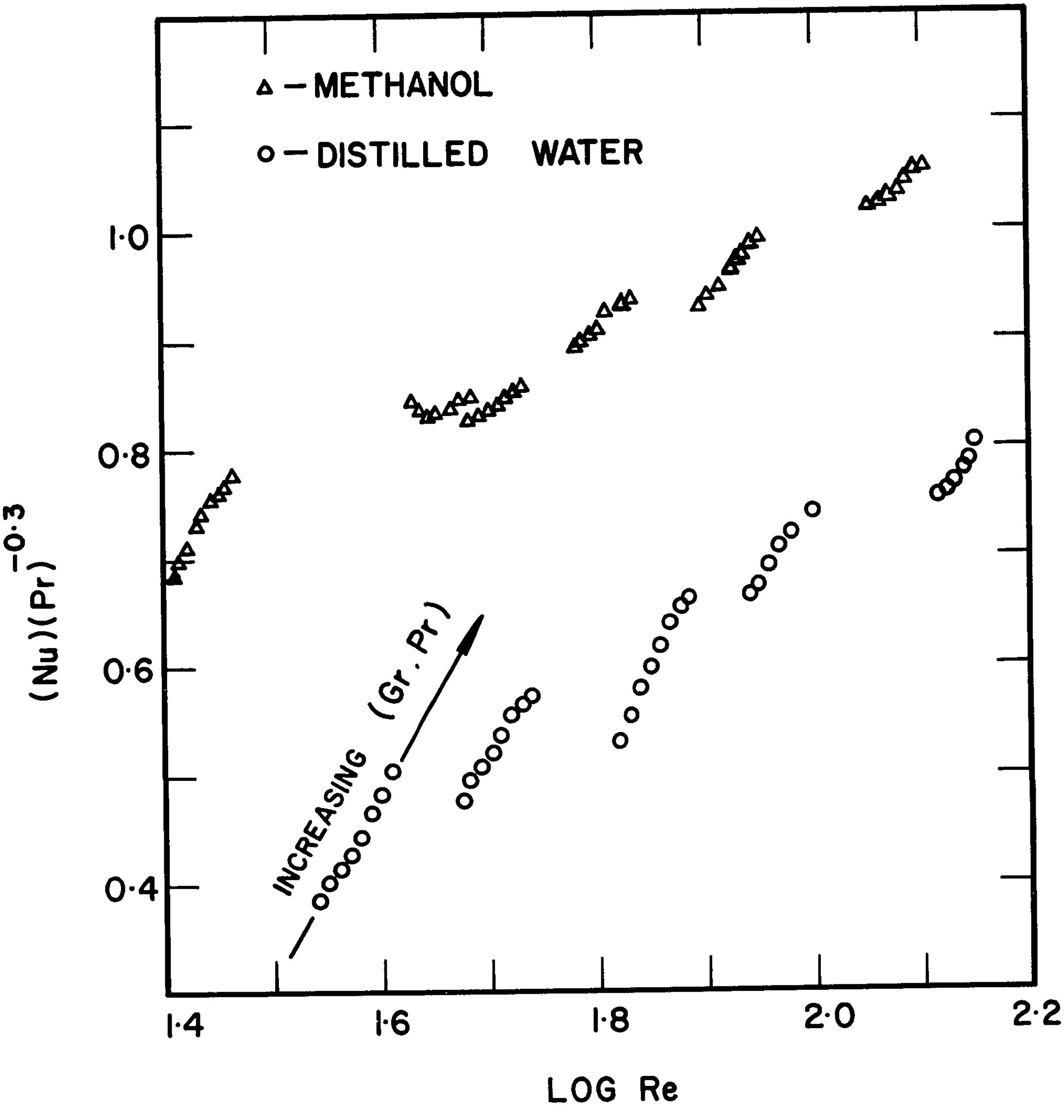
△ – METHANOL
○ – DISTILLED WATER
INCREASING (Gr . Pr)
1·0
0·8
0·6
0·4
(Nu)(Pr)$^{-0.3}$
1·4
1·6
1·8
2·0
2·2
LOG Re

effect is evaluated by plotting $(Nu_v)\ (Pr)^{-0.3}$ against Gr, assuming that Re does not vary during one run. The value thus evaluated for the exponent is around 0.08. When the data for water are plotted as $(Nu_v)\ (Pr)^{-0.3}\ (Gr)^{-0.08}$ against Re a good correlation was obtained as shown in Figure 13. It may be recalled that similar data for water were previously correlated by Deaver et al.(6) using $(Nu_v)\ (Pr)^{-0.3}$ as a function of Re. They limited the validity of their correlation for Reynolds number where the effect of buoyancy would be negligible.

As clearly seen in Figures 12 and 13, separate parallel lines are obtained for methanol and water with the line for the methanol lying higher. The comparison of data for methanol and water in Figure 12 also shows that with increasing Re the free convection effects diminish more rapidly for methanol than for water. In the present study, an attempt was made to define a dimensionless parameter which would determine the relative influence of free and forced convection but no successful results were obtained. The parameter, $\left(\frac{Gr}{Re^2}\right)$ derived theoretically by Gebhart(7), failed to work when extended to water and methanol simultaneously. The parameter, $(Re)\ (Pr)^{0.8}$, defined by Penny et al.(8) would not represent the real measure of turbulence in the thermal boundary layer and hence could not be used. Subsequently, correlations of the form

$$Nu_v = K(Pr)^x\ (Gr)^y\ (Re)^z$$

and

$$\frac{Nu_v}{Nu_o} - 1 = K_1\ (Pr)^{x_1}(Gr)^{y_1}\ (Re)^{z_1}$$

were tried but no satisfactory results were obtained.

FIGURE 13

RESULTS WITH GRASHOF NUMBER EFFECTS

INCLUDED IN FORCED CONVECTION CORRELATION

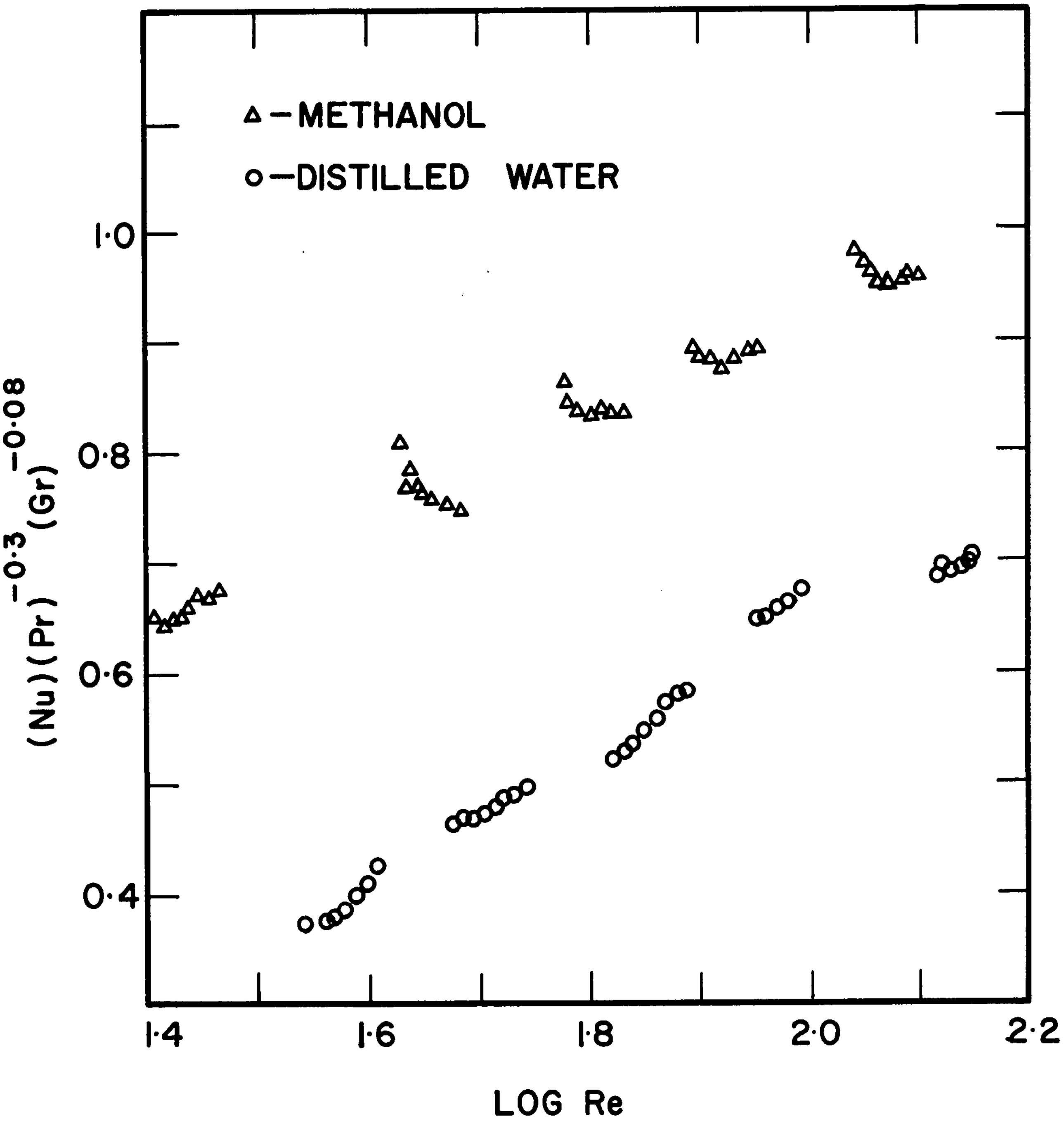
△ – METHANOL
○ – DISTILLED WATER
$(Nu)(Pr)^{-0.3}(Gr)^{-0.08}$
1·0
0·8
0·6
0·4
1·4
1·6
1·8
2·0
2·2
LOG Re

The analysis of the heat transfer data were further carried out to obtain a satisfactory correlations. Since Prandtl number dictates the temperature profiles in the thermal boundary layer, it may be presumed that the shift in the two lines of methanol and water would be due to Prandtl number effects. Thus accounting qualitatively for such an effect, one may write the correlation for the fluids as:

$$\frac{Nu_v}{(Pr)^{x_3}(Gr)^{y_3}} = K_2(Pr)^{l_3} + K_3(Re)^{z_3} \quad . \qquad (1)$$

Where the approximate values of x_3, y_3 and z_3 were obtained from Figures 12 and 13. Rewriting equation (1), one obtains:

$$\frac{Nu_v}{(Pr)^{x_3}\,(Gr)^{y_3}} - K_3(Re)^{z_3} = K_2(Pr)^{l_3} \qquad (2)$$

Assuming various values for K_3 and the above - mentioned approximate values of x_3, y_3, z_3 the L.H.S. of equation (2) was plotted against Pr on a log-log graph. This treatment evaluated various combinations of the values of K_2, K_3 and l_3. The particular combination which would represent the data of water and methanol on a single plot was selected. The values thus obtained were $K_2 = 0.50$, $K_3 = 0.1$ and $l_3 = 0.7$. To determine the exact values of the parameters x_3, y_3, z_3, l_3, K_2 and K_3, a method of least square fit was used. The function ϕ defined as :

$$\phi = \sum_{j=1}^{m} \left[(Nu_v)_j - K_2 (Pr)_j^{x_3} (Gr)_j^{y_3} (Pr)_j^{l_3} - K_3 (Pr)_j^{x_3} (Gr)_j^{y_3} (Re)_j^{z_3} \right]^2 \tag{3}$$

(m-number of data points.)

was subjected to minimization by iteration process on IBM 7044 computer. The technique uses varying step size and is a modification of the steepest descent method. The program has its unique feature of picking up the suitable criterion. During the process of minimisation the step size goes on decreasing from stage to stage and thus gives very accurate computation. The final values obtained were:

$x_3 = 0.72 \qquad y_3 = -0.06 \qquad z_3 = 0.86$

$l_3 = 1.08 \qquad K_2 = 0.32 \qquad K_3 = 0.06$.

The final correlation could then be written as:

$$\frac{Nu_v}{(Pr)^{0.72}(Gr)^{-0.06}} = 0.32(Pr)^{1.08} + 0.06\ (Re)^{0.86} \tag{4}$$

In the above correlations, data for water at 118.4, 170.6°F and methanol at 95°F were used for the whole range of vibrational parameters. The results based on the above correlation are plotted in Figures 14 through 17 Throughout the calculations the fluid properties were evaluated at the mean film temperature, defined as the arithmetic mean of temperature of wire and the bulk temperature of the liquid. Fluid property data were taken from the International Critical Tables.

FIGURES 14 - 17

CORRELATION OF HEAT TRANSFER DATA FOR FORCED CONVECTION REGION

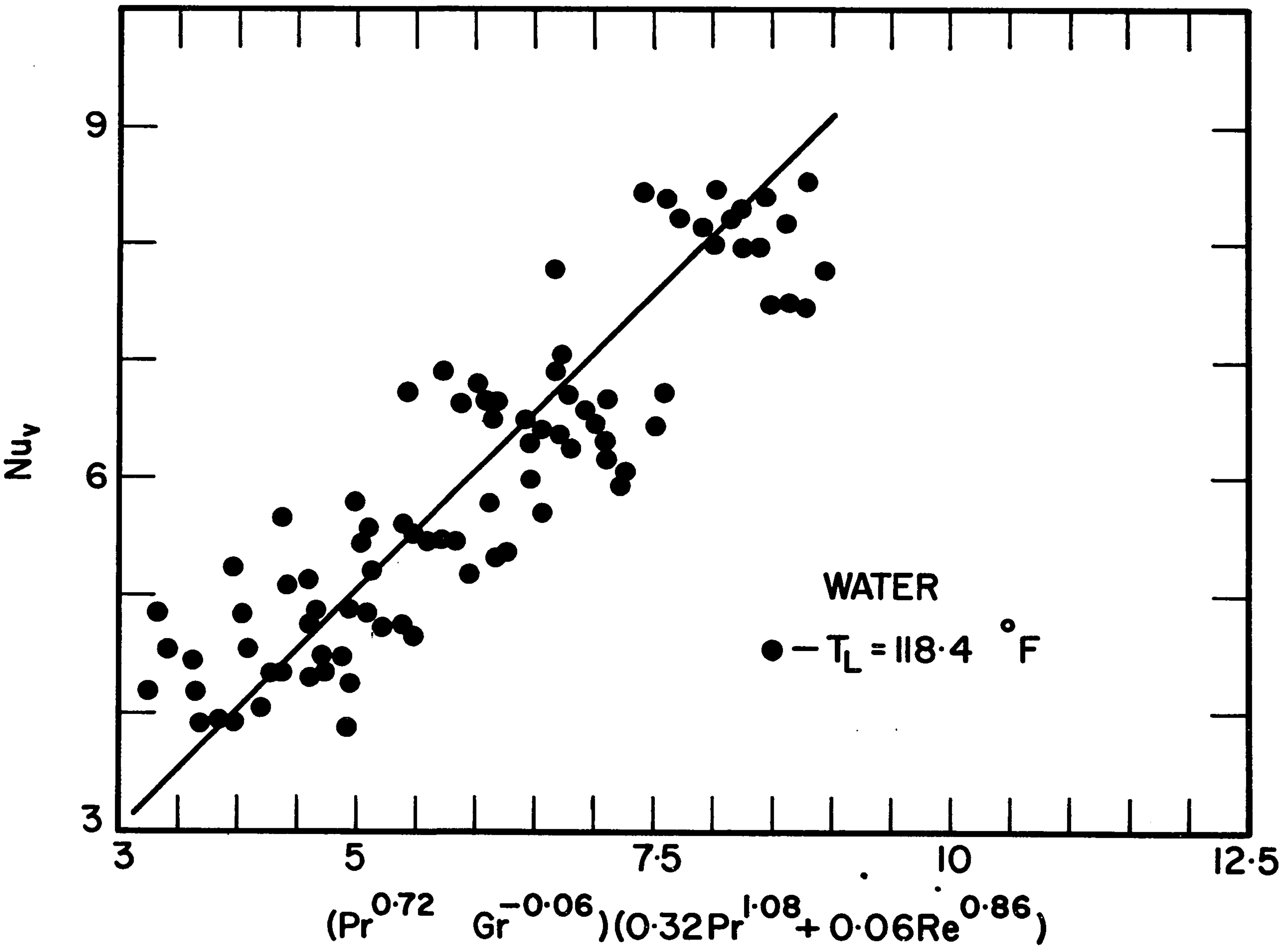
Nu_v
9
6
3
5
7·5
10
12·5
$(Pr^{0·72}\ Gr^{-0·06})(0·32Pr^{1·08}+0·06Re^{0·86})$
WATER
● — T_L = 118·4 °F

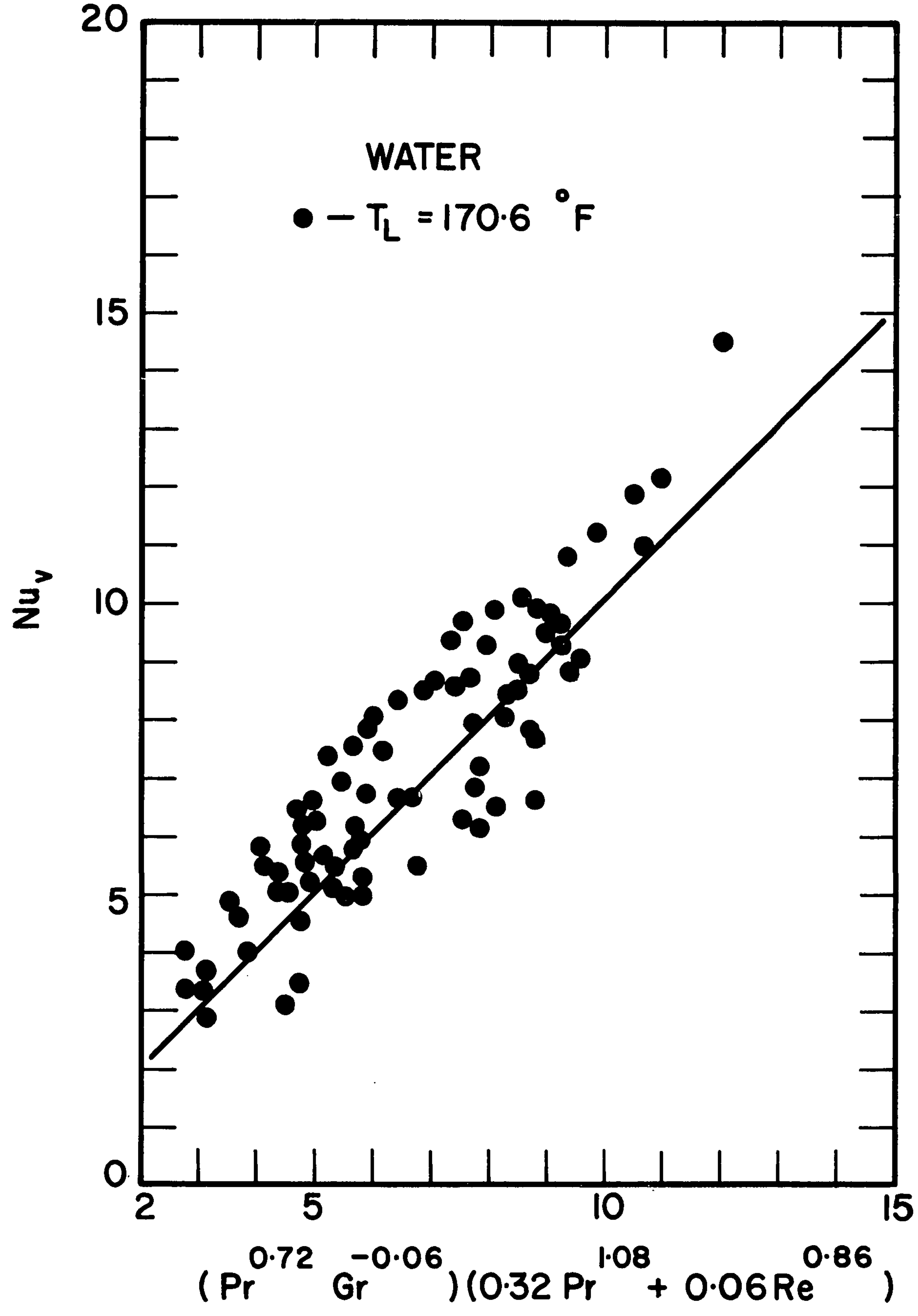
20
15
10
5
0
2
5
10
15
Nu$_v$
WATER
● — T_L = 170·6 °F
(Pr$^{0·72}$ Gr$^{-0·06}$)(0·32 Pr$^{1·08}$ + 0·06 Re$^{0·86}$)

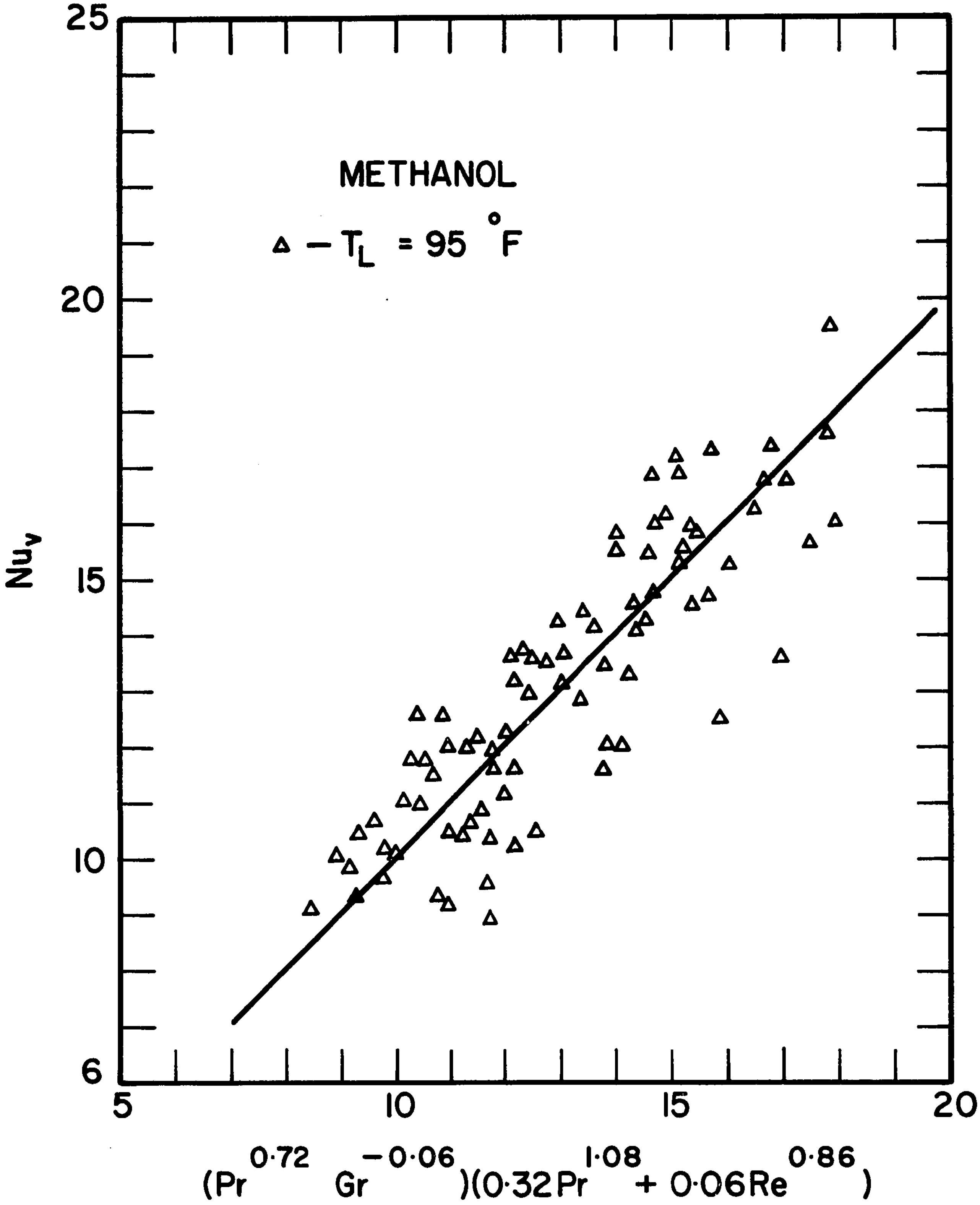
25
20
15
10
6
5
10
15
20
METHANOL
Δ — T_L = 95 °F
Nu_v
$(Pr^{0.72} Gr^{-0.06})(0.32 Pr^{1.08} + 0.06 Re^{0.86})$

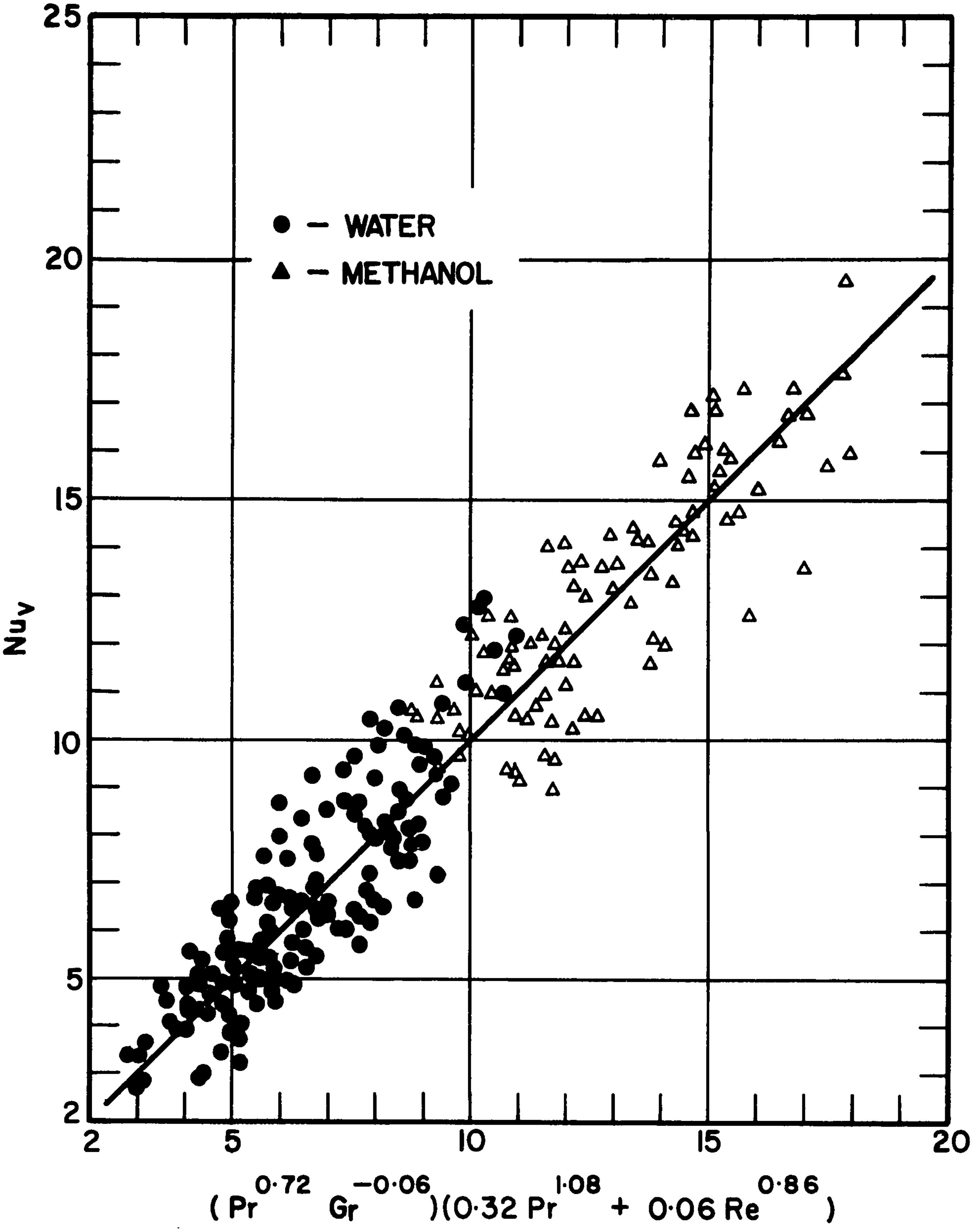
● – WATER
▲ – METHANOL
25
20
15
10
5
2
Nuv
2
5
10
15
20
(Pr$^{0.72}$ Gr$^{-0.06}$)(0·32 Pr$^{1.08}$ + 0·06 Re$^{0.86}$)

Determination of Incipience:

The word incipience can be defined in a number of ways when applied to boiling. The incipience corresponds to the surface-to-bulk temperature difference at which the curve heat flux versus ΔT begins to deviate from the free convection curve. It can also be defined as the condition when the waiting time between bubble departure and initiation of a new bubble is not infinitely long. However, for the present investigation the word incipience is defined as that temperature difference at which a given bubble nucleus begins to grow. The commonly accepted theory of nucleation in boiling systems, on the other hand, suggests that bubbles originate at small cavities in the heating surface.

Dengler(9), in an investigation of heat transfer to water in a vertical tube evaporator, attempted to correlate the minimum temperature difference required to initiate nucleate boiling with the average velocity of the liquid phase, but his correlation was not found to be valid. Hsu(10) developed a theory for the onset of nucleate boiling by using a model of Hsu and Graham(11) which related the size range of active nucleation sites on a heating surface to the superheat required to initiate nucleate boiling in the liquid. Application of Hsu's theory requires the knowledge of the limiting thermal layer thickness within which a bubble nucleus can develop, but it is not yet possible to predict this boundary-layer thickness from theory for the pool-boiling situation considered by Hsu(10).

Bergles and Rohsenow(12) proposed that a heated surface contains a wide range of cavities from which hemispherical vapour bubbles protrude. If such bubbles are to grow, the thermal layer surrounding them must attain a temperature such that there is net heat transfer from the liquid to the bubble. They also postulated that the bubble nucleus of hemispherical shape with radius r_c will grow if the liquid temperature at a distance $y = r_c$ from the surface is greater than the critical vapour temperature derived from bubble equilibrium. In the present solution of this problem, a similar model is postulated and is applied to all liquids unlike those of Bergles and Rohsenow(12) which was restricted to only water in forced flow.

Consider a bubble of radius r_c entrapped in a cavity as shown in Figure 18. A force balance on this bubble considered at equilibrium gives the relation:

$$p_V - p_L = \frac{2\sigma}{r_c} \tag{5}$$

since $p_L < p_V$ the liquid temperature must be superheated with respect to the liquid pressure.

The Clausius - Clapeyron equation:

$$\frac{dp_V}{dT} = \frac{h_{fg}}{v_{fg} T_S} \tag{6}$$

is integrated assuming that the slope of the vapour pressure curve

$\frac{h_{fg}}{v_{fg} T_S}$ is constant. From equation (6)

FIGURE 18

DIAGRAM OF A TYPICAL CAVITY
ON A HEAT TRANSFER SURFACE

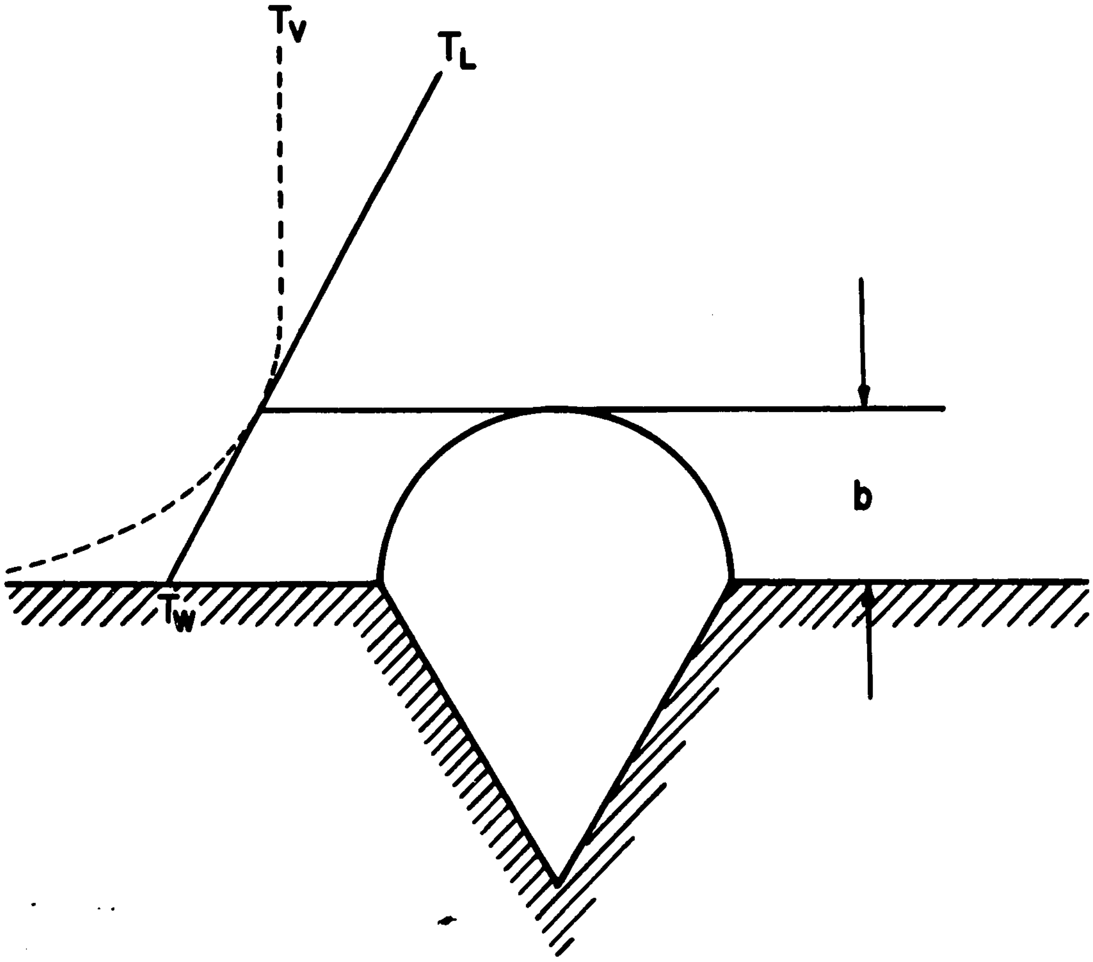

T_V
T_L
b
T_W

$$dp_V = \frac{h_{fg}}{v_{fg}\ T_S}\ dT \tag{7}$$

or
$$p_V - p_L = \frac{h_{fg}}{v_{fg}\ T_S}\ (T_V - T_S) \tag{8}$$

Equation (5) and (8) can be equated to give:

$$\frac{2\sigma}{r_c} = \frac{h_{fg}}{v_{fg}\ T_S}\ (T_V - T_S) \tag{9}$$

or
$$T_V = T_S + \frac{2\sigma\ v_{fg}\ T_S}{h_{fg}\ r_c} \tag{10}$$

The bubble and cavity sizes are generally smaller than the thickness of the laminar sublayer, therefore, the temperature distribution in the liquid near the wall can be approximated by a linear relation as follows:

$$T_L = T_W - (\frac{Q}{A})\ \frac{b}{k_L} \tag{11}$$

The boiling begins when the temperature profile in the thermal layer of liquid surrounding a bubble nucleus results in a net heat transfer to the bubble. Consequently it may be expected that the critical distance b, which is basically the depth of the liquid having a temperature in excess of the bubble vapour temperature, T_V, to be proportional to the Prandtl number and to the characteristic bubble dimension r_c. Thus a qualitative expression $b = (Pr)^n \cdot r_c$ is valid.

The emperical value $n = 2$ correlates the experimental data. The criterion for incipient boiling is:

$$T_L = T_V \quad \text{and} \quad \frac{dT_L}{dr_c} = \frac{dT_V}{dr_c} \quad \text{at} \quad b = (Pr)^2 \cdot r_c \tag{12}$$

Combining equations (10),(11) with equation (12) one obtins:

$$\frac{T_W - T_S}{\left[(Pr)^2 (\frac{Q}{A})_i\right]^{1/2}} = 2\sqrt{\frac{2\sigma\, v_{fg}\, T_S}{h_{fg}\, k_L}} \tag{13}$$

All the properties are evaluated at the saturation temperature. At a given pressure, $2\sqrt{\frac{2\sigma\, v_{fg}\, T_S}{h_{fg}\, k_L}} = N$ (constant). For calculating $(Q/A)_i$, the expression derived for forced convection region is used as follows:

$$(\frac{Q}{A}) = h(T_W - T_L) \tag{14}$$

where h is given by:

$$h = (Nu_v)\,\frac{k_L}{D} \tag{15}$$

and

$$Nu_v = \left[Pr^{0.72} Gr^{(-0.06)}\right]\left[0.32\ Pr^{1.08} + 0.06\ Re^{0.86}\right] \tag{16}$$

Substituting the value of (Q/A) obtained from equations (14), (15) and (16) into equation (13), one obtains :

$$(T_W - T_S)^2 - \left[(T_W - T_S) + (T_S - T_L)\right] (NPr)^2 \left[pr^{0.72} Gr^{(-0.06)}\right]$$

$$\left(\frac{k_L}{D}\right) \left[0.32\ Pr^{1.08} + 0.06\ Re^{0.86}\right] = 0 \qquad (17)$$

The quadratic equation (17) is solved to calculate values of $(T_W - T_S)$ under various conditions of vibrational parameters. The results obtained for water at 118.4 and 170.6°F and methanol at 95°F are shown in Table 1. This table represents the degree of superheat required for the onset of boiling corresponding to the given experimental conditions. These values are also represented by line AB in Figures 4 through 10 . The results are valid for several commercially finished surfaces which can be expected to have a wide range of cavity sizes available for nucleation.

Correlation for the Fully Developed Boiling Region:

As mentioned earlier, the heat flux curves for all wire vibrations are seen to merge into one curve when the boiling becomes more vigorous. The effect of the surface vibrations decreases and it seems quite appropriate to correlate the heat transfer data, for this region mostly by means of bubble Reynolds number based on bubble diameter and velocity. Gunther and Kreith(13) have shown quantitatively that only a small part of the total heat transferred from the heating surface is

TABLE 1

SUPERHEAT DATA FOR INCIPIENT BOILING

LIQUID : WATER TEMPERATURE = 118.4°F

$(T_W - T_S)$ °F

FREQUENCY CPS	AMPLITUDE = 0.0 in.	0.0386	0.0673
0	11.5	-	-
20	-	13.5	15.5
30	-	15.0	17.5
40	-	16.0	19.5
50	-	17.5	21.0
60	-	19.5	22.0
70	-	20.5	-
80	-	21.5	-

TABLE 1 (continued)

LIQUID : WATER TEMPERATURE = 170.6°F

$(T_W - T_S)^{o}F$

FREQUENCY CPS	AMPLITUDE = 0.0 in.	85 0.0386	0.0673	0.1070
0	8.0	-	-	-
20	-	9.0	-	-
30	-	10.0	12.0	14.5
40	-	11.0	13.5	16.5
50	-	12.0	15.0	-
60	-	13.0	16.0	-
70	-	13.5	17.0	-
80	-	-	-	-

TABLE 1 (continued)

LIQUID : METHANOL TEMPERATURE = 95°F

FREQUENCY CPS	$(T_W - T_S)^oF$ AMPLITUDE = 0.0 in.	0.0386	0.0673
0	14.0	-	-
20	-	-	28.5
30	-	27.5	31.0
40	-	29.5	33.5
50	-	30.5	35.5
60	-	32.0	38.0
70	-	33.5	40.0
80	-	34.5	-

directly from the surface to the liquid, and the bubbles provide the agitation of the liquid by their motion. Since the Prandtl number is significant in relation for heat transfer to non-boiling fluid, the suggested expression may be written as:

$$Nu_b = \emptyset (Re_b, Pr_L)$$

The Reynolds number Re_b in this relationship represents the local agitation of the fluid caused by bubble motion. Rohsenow(14) assumed that the movement of bubbles at the instant of breaking away from the heating surface is of prime importance. The agitation caused by bubble release breaks the stagnant liquid film and thus provides an excellent convective heat transfer. From this concept Rohsenow developed a correlation for the nucleate pool boiling heat transfer coefficient by using non-dimensional groups. Rohsenow's final correlation is written as:

$$\frac{C_{pL} T_x}{h_{fg}} = C_{sf} \left[\frac{(Q/A)}{\mu_L h_{fg}} \sqrt{\frac{\sigma g_o}{(\rho_L - \rho_v) g}} \right]^r \left(\frac{C_{pL} \mu_L}{k_L} \right)^s \tag{18}$$

Foster and Zuber(15) derived another correlation based on the assumption that the movement of the bubble boundary layer, while bubbles are still attached to the surface, is of prime importance. The linear velocity of the bubble boundary motion at the early stage of growth is of the order of 10 ft/sec. The product of characteristic length and significant velocity is taken as $R\dot{R}$ and the Reynolds number becomes $(R\dot{R}\ \rho_L/\mu_L)$. Using the solution for isobaric bubble growth equation, they derived the final correlation as

$$Nu = 0.0015 \ Re_b^{0.62} \ Pr_L^{1/3} \tag{19}$$

The exponent on the Reynolds and Prandtl numbers in Equation (19) are roughly the same as those used for ordinary forced convection heat transfer. On the other hand this equation predicts the same heat transfer coefficient for a liquid boiling on any hot surface (all heterogeneous cases)or boiling in the bulk (all homogeneous cases). The validity of the same equation for all hot solids as well as for no hot bounding surface is open to serious question. Rohsenow's equation was developed, and is applied to the heterogeneous case only.

Thus the Rohsenhow's Equation (18) appears to be most noted method of correlating heat transfer data in the régime of nucleate pool boiling. The equation accounts for the pool boiling phenomenon in terms of fluid properties, the coefficient c_{sf} and the exponents r and s. The coefficient c_{sf} accounts for the surface-liquid combination, the exponent s accounts for surface cleanliness, and r represents the reciprocal of the least squares slope for the heat flux-superheat data in question. The Prandtl number exponent, s, varies from 0.8 to 2.0.

Rohsenow initially recommended a value of 1.7 for clean surface for all liquid-surface combinations, although he(16) has recently recommended that this value be changed to 1.0 for water. In order to develop a correlation in the present investigation, experimental data for water at 118.4°F, 170.6°F and for methanol at 95.0, 120.2, 149°F for non vibrating conditions, were first used. Figures 19 and 20, represent heat flux versus superheat (T_x) for different degrees of subcooling for water and methanol. The exponent for Prandtl number is taken as 1.0 for water and 1.7 for methanol. In order to evaluate the values for C_{sf} and r, functions

$$\phi_2 = \sum_{j=1}^{m} \left[\frac{C_{pL}(T_x)_j}{h_{fg}} - C_{sf} \left[\frac{(Q/A)_j}{\mu_L \, h_{fg}} \sqrt{\frac{\sigma \, g_o}{(\rho_L - \rho_V) g}} \right]^r (Pr_L)^{1.0} \right]^2 \quad \text{for water} \qquad (20)$$

$$\phi_3 = \sum_{j=1}^{m} \left[\frac{C_{pL}(T_x)_j}{h_{fg}} - C_{sf} \left[\frac{(Q/A)_j}{\mu_L \, h_{fg}} \sqrt{\frac{\sigma \, g_o}{g(\rho_L - \rho_V) g}} \right]^r (Pr_L)^{1.7} \right]^2$$

(m-number of data points.) for methanol (21)

were subjected to minimization. The values obtained are:

For water: $c_{sf} = 0.016$; $r = 0.30$

For Methanol: $c_{sf} = 0.0031$; $r = 0.147$

HEAT FLUX VERSUS SUPERHEAT

FOR NUCLEATE BOILING REGION

FIGURE 19 WATER

FIGURE 20 METHANOL

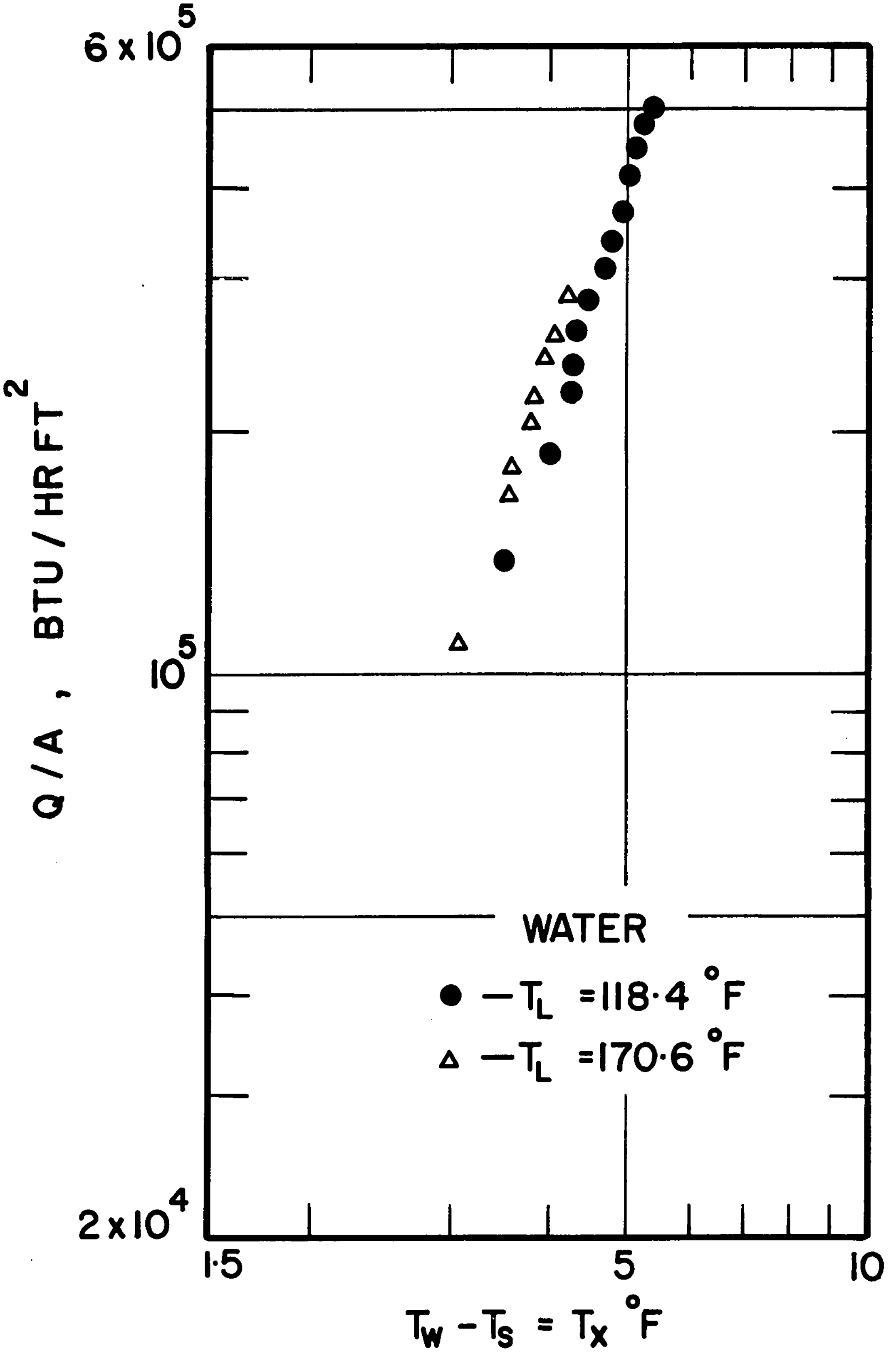
6 x 10^5
10^5
2 x 10^4
Q / A , BTU / HR FT^2
1·5
5
10
T_W − T_S = T_X °F
WATER
● — T_L = 118·4 °F
△ — T_L = 170·6 °F

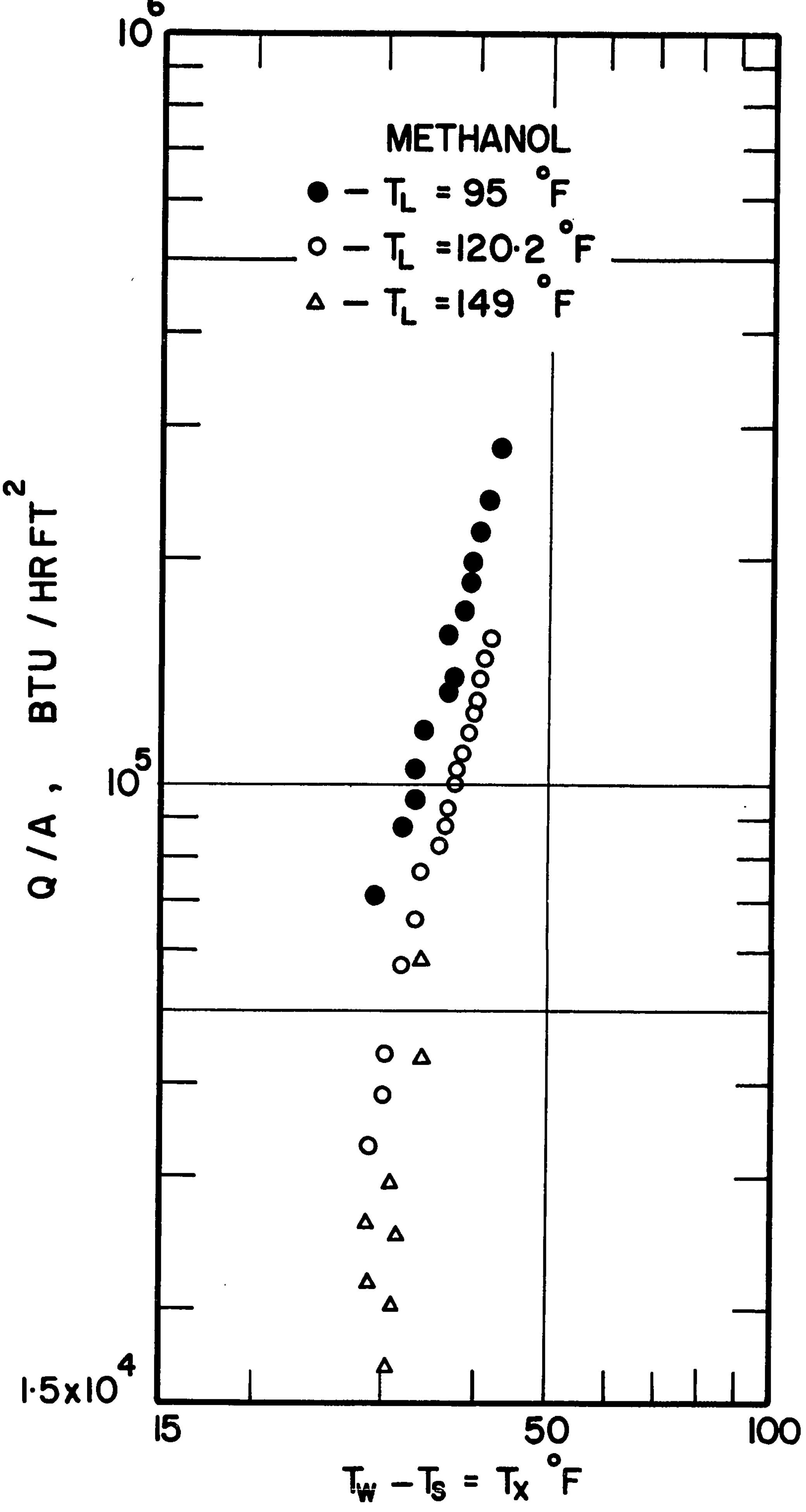
METHANOL
● – T_L = 95 °F
○ – T_L = 120·2 °F
△ – T_L = 149 °F
Q / A , BTU / HR FT²
10⁶
10⁵
1·5x10⁴
15
50
100
T_W – T_S = T_X °F

The final correlations for water and methanol are written as:

$$\frac{C_{pL}\,T_x}{h_{fg}} = 0.016\left[\frac{(Q/A)}{\mu_L h_{fg}}\sqrt{\frac{\sigma\, g_o}{(\rho_L-\rho_V)g}}\right]^{0.30}(Pr_L)^{1.0} \qquad (22)$$

$$\frac{C_{pL}\,T_x}{h_{fg}} = 0.0031\left[\frac{(Q/A)}{\mu_L\, h_{fg}}\sqrt{\frac{\sigma\, g_o}{(\rho_L-\rho_V)g}}\right]^{0.147}(Pr_L)^{1.7} \qquad (23)$$

The final results are plotted and shown in Figures 21 and 22. The values of C_{sf} agree very closely with the ones quoted in the literature. Equations (22) and (23) would correlate the data only for the fully developed boiling where the surface vibrations have negligible effect. Also they play a great role in explaining the heat transfer data for the transition region as would be shown later.

Correlation for the Transition Region:

When predicting the complete boiling curve for a particular system it is important to cover the transition region which is always present between incipient boiling and fully developed boiling. The range of this transition region with respect to vibrations has been discussed earlier. In the present investigation an attempt was made to include the combined effects of forced convection and nucleate boiling. The total heat flux is assumed to be given by a superposition of the heat flux due to bubble motion and oscillation-induced forced convection i.e.

CORRELATION OF HEAT TRANSFER DATA FOR FULLY DEVELOPED BOILING REGION

FIGURE 21 WATER

FIGURE 22 METHANOL

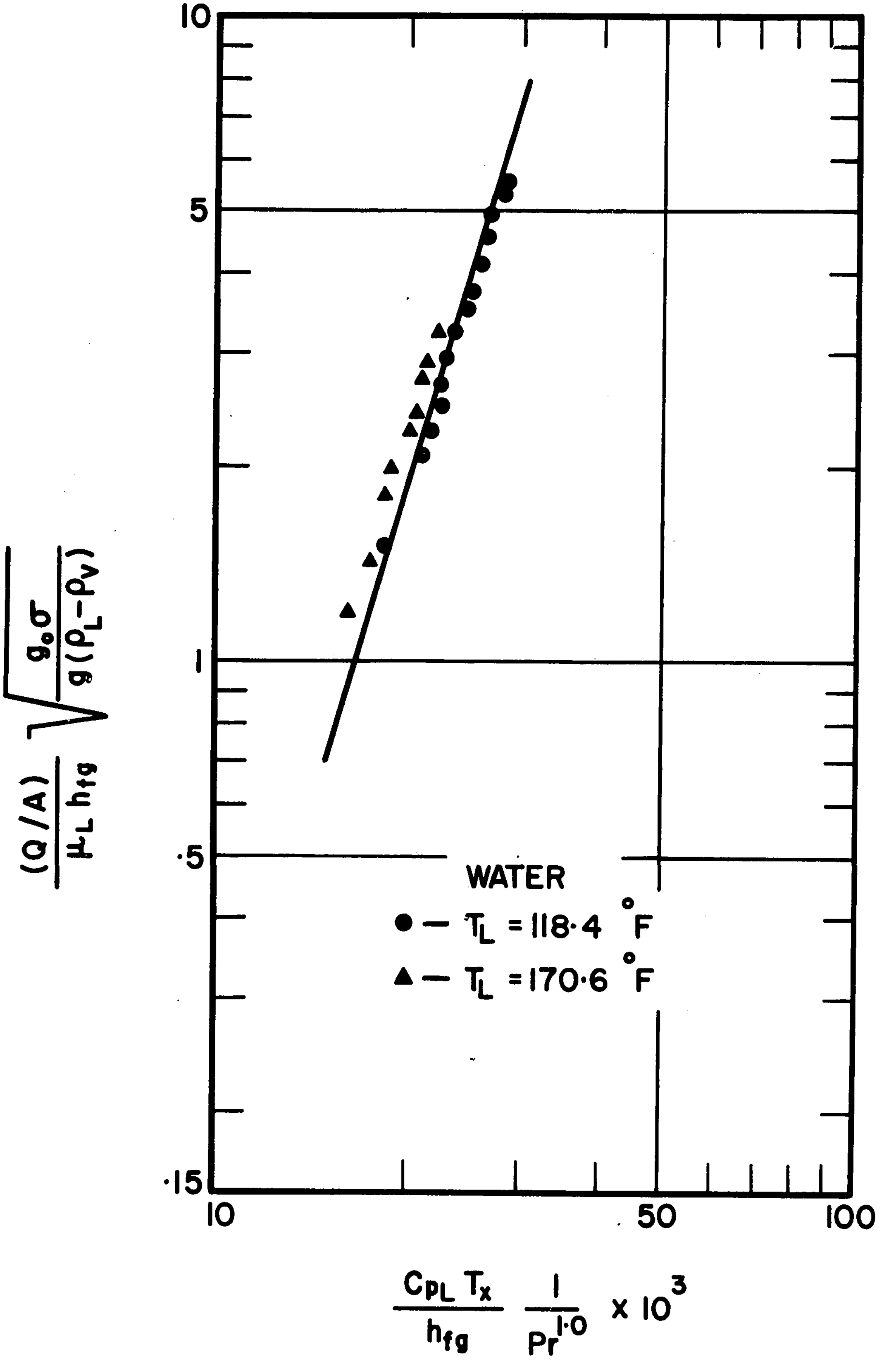

10
5
1
·5
·15
10
50
100
WATER
● — T_L = 118·4 °F
▲ — T_L = 170·6 °F
$\frac{(Q/A)}{\mu_L h_{fg}} \sqrt{\frac{g_o \sigma}{g(\rho_L - \rho_V)}}$
$\frac{C_{pL} T_x}{h_{fg}} \frac{1}{Pr^{1\cdot0}} \times 10^3$

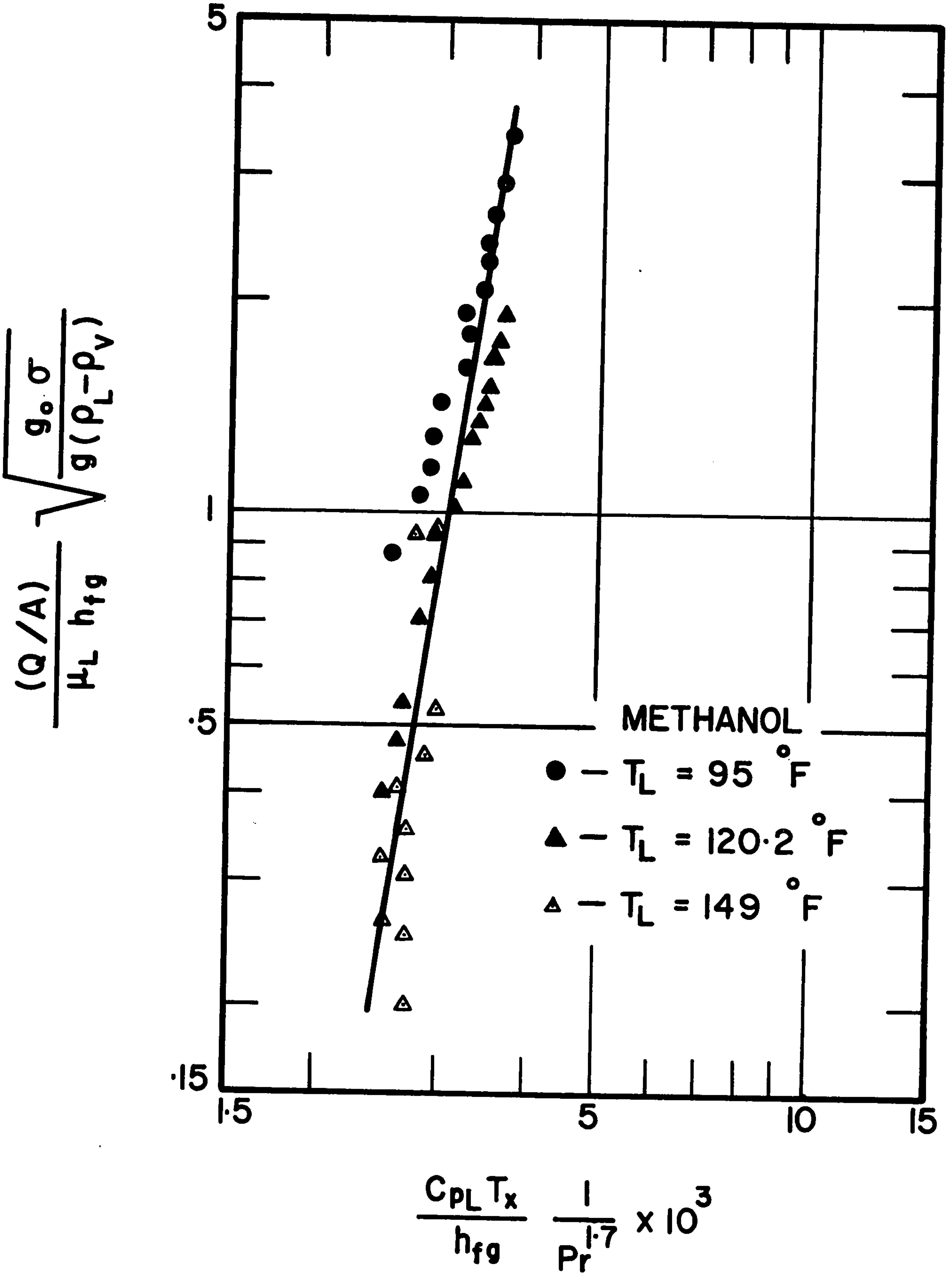
5
1
·5
·15
1·5
5
10
15
METHANOL
● — T_L = 95 °F
▲ — T_L = 120·2 °F
△ — T_L = 149 °F
$\frac{(Q/A)}{\mu_L h_{fg}}\sqrt{\frac{g_o \sigma}{g(\rho_L-\rho_V)}}$
$\frac{C_{pL} T_x}{h_{fg}} \frac{1}{Pr^{1\cdot7}} \times 10^3$

$$(Q/A) = (Q/A)_{boil} + (Q/A)_{FC} \tag{24}$$

The forced convection term $(Q/A)_{FC}$ is the heat flux predicted by the earlier developed forced convection correlation as represented by Equation (4). The effect of the bubble motion is given by the correlation developed for fully developed boiling, i.e. Equations (22) and (23). From Equation (24) it is apparant that at low superheat (T_x) the boiling curve will merge with forced convection curve and at higher wall superheat the curve will join with the pool boiling curve.

The values of $(Q/A)_{boil}$ for water and methanol are evaluated for the transition region covering the whole range of vibrational parameters. Correlating this $(Q/A)_{boil}$ data using the equations for fully developed boiling results in Figures(23) and (24). Although, the data points deviate from the curves computed from Equation (24) the agreements appear still fairly good, considering the extremely complicated physical picture involved.

CORRELATION OF HEAT TRANSFER DATA FOR TRANSITION REGION

FIGURE	23	WATER
FIGURE	24	METHANOL

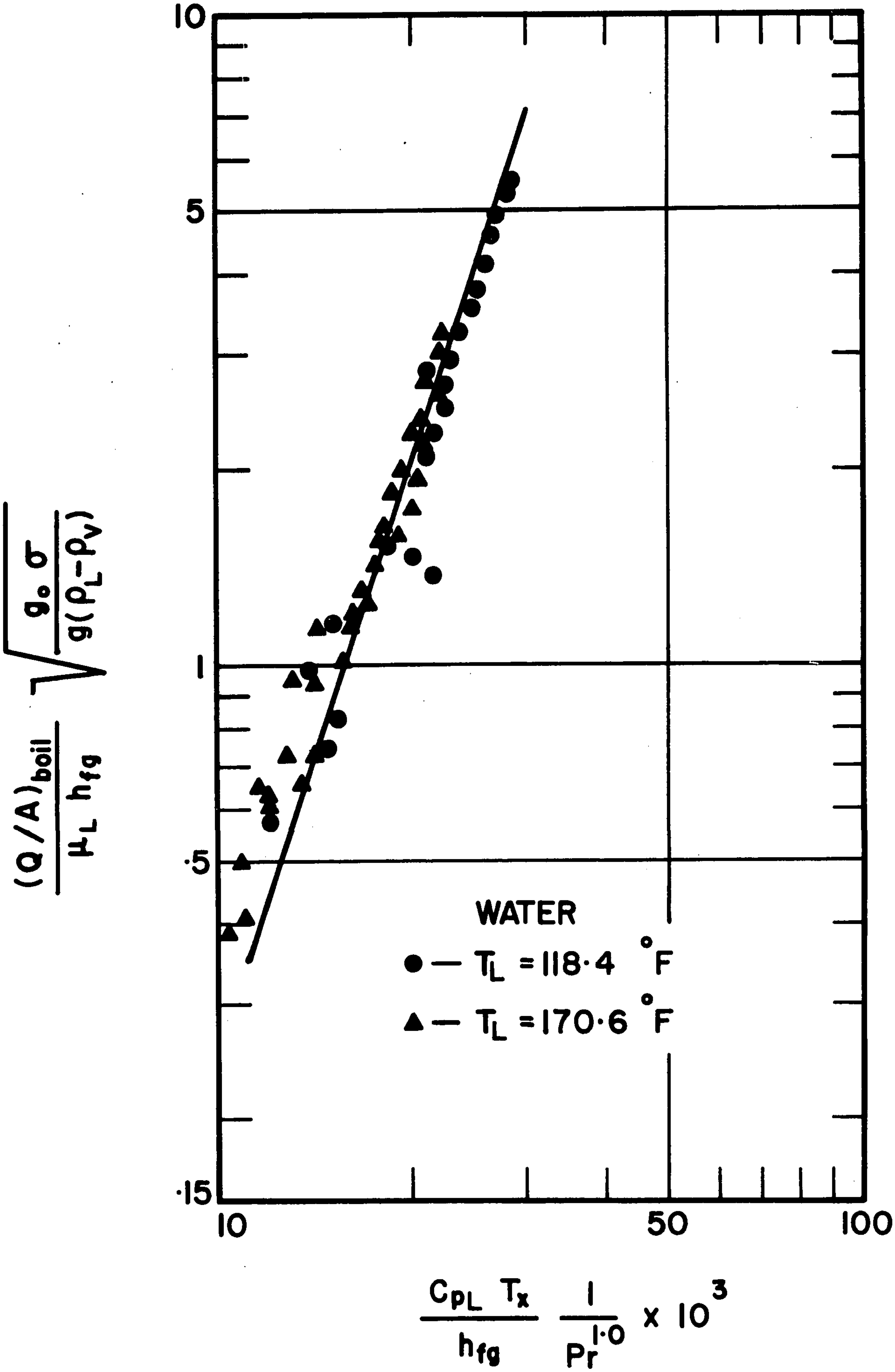
10
5
1
·5
·15
10
50
100
WATER
● — T_L = 118·4 °F
▲ — T_L = 170·6 °F
$\frac{(Q/A)_{boil}}{\mu_L h_{fg}} \sqrt{\frac{g_o \sigma}{g(\rho_L - \rho_v)}}$
$\frac{C_{pL} T_x}{h_{fg}} \frac{1}{Pr^{1\cdot0}} \times 10^3$

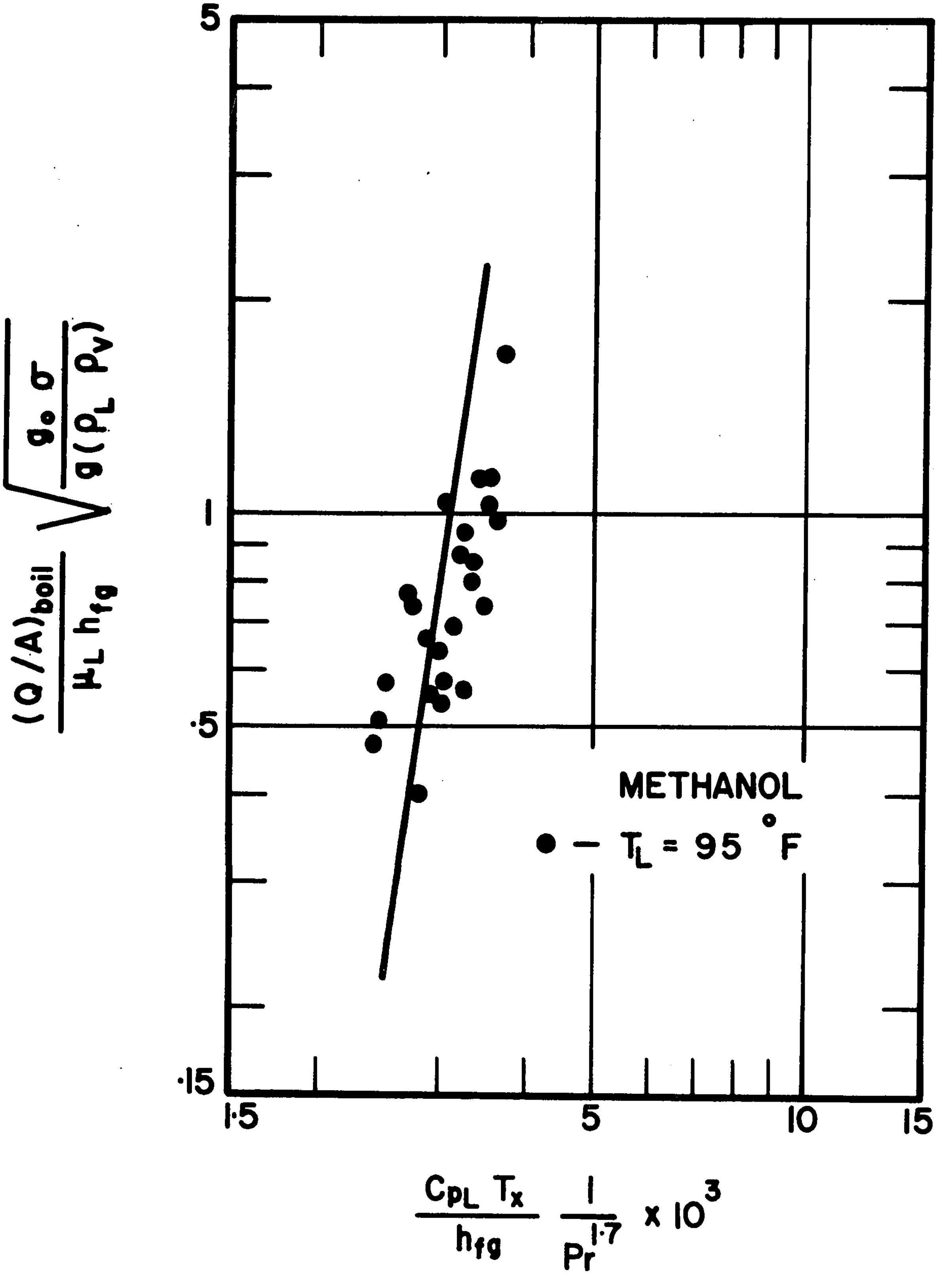
5
1
·5
·15
1·5
5
10
15
$\frac{(Q/A)_{boil}}{\mu_L h_{fg}} \sqrt{\frac{g_o \sigma}{g(\rho_L - \rho_v)}}$
$\frac{C_{pL} T_x}{h_{fg}} \frac{1}{Pr^{1.7}} \times 10^3$
METHANOL
● – T_L = 95 °F

CONCLUSIONS

1. With the introduction of vertical oscillations on horizontal wire three distinct regions were noticed; forced convection, transition and fully developed boiling. Experimental data obtained show the increase of heat flux as frequency and amplitude are increased, although the effect diminishes as the boiling becomes vigorous.

2. An equation was solved which predicts quantitatively the incipient point in natural and forced flow of various fluids. This solution helped in defining the range of each regime for known conditions of vibrational parameters. The value of n agrees with other investigations(17

3. For the region of forced convection, an increase in heat flux upto a maximum of ten fold for methanol and seven fold for distilled water were observed. The conventional correlation using $(Nu_v)(Pr)^{-0.3} = \phi(Re)$ is valid only for one particular fluid and completely fails when extended to other liquids. On the other hand, the parameter $\frac{Gr}{Re^2}$ does not measure the relative influence of free and forced convection in various fluids. It is postulated that the imposed vibrations result in a decrease in effective thickness of the boundary layer and a flatter temperature profile across it. A general correlation which correlates the heat transfer data in the present work is given by :

$$\frac{Nu_v}{(Pr)^{0.72}(Gr)^{-0.06}} = 0.32\ (Pr)^{1.08} + 0.06\ (Re)^{0.86} \qquad (4)$$

4. Modification for the evaluation of constants for the Rohsenow pool boiling correlation was attempted. The data for water and methanol with different degrees of subcooling are correlated as:

$$\frac{C_{pL}\,T_x}{h_{fg}} = 0.016\left[\frac{(q/A)}{\mu_L\,h_{fg}}\sqrt{\frac{\sigma\,g_o}{(\rho_L-\rho_V)g}}\right]^{0.3}(Pr_L)^{1.0}$$

for water (23)

$$\frac{C_{pL}\,T_x}{h_{fg}} = 0.00307\left[\frac{(q/A)}{\mu_L\,h_{fg}}\sqrt{\frac{\sigma\,g_o}{(\rho_L-\rho_V)g}}\right]^{0.147}(Pr_L)^{1.7}$$

for methanol (24)

Equations (23) and (24) correlate the heat transfer data for fully developed boiling regions for oscillating wires.

5. A Rohsenow type correlation for fully developed nucleate boiling was successfully combined with a correlation for an oscillation - induced forced convection to interpret the heat flux for the transition region.

NOMENCLATURE

ROMAN SYMBOLS:

a - amplitude of vibration of wire (peak to peak), in.

b - distance measured perpendicular from the top of the wire, ft

C_{pL} - specific heat of the liquid at constant pressure, Btu/lb°F

D - diameter of platinum heating wire, ft

d - diameter of the bubble as it leaves the surface, ft

f - frequency of vibration of the wire, CPS

g - accelaration due to gravity ft/hr^2

g_o - gravitational constant lb$_m$- ft/lb$_f$ hr^2

h - convective heat transfer coefficient Btu/hr ft^2 °F.

h_{fg} - latent heat of vaporisation Btu/lb$_m$

k - thermal conductivity, Btu/hr ft°F

K - constant,

l - constant, exponent

n - constant, exponent

N - $2\sqrt{\dfrac{2\sigma\, v_{fg}\, T_S}{h_{fg}\, k_L}}$ (constant)

p - pressure, lb/ft^2

(Q/A) - heat transfer rate per unit area, Btu/hr ft^2

$(Q/A)_{boil}$ - heat transfer rate per unit area due to bubble motion Btu/hr f

$(Q/A)_{FC}$ - heat transfer rate per unit area due to forced convection, Btu/hr ft^2

$(Q/A)_i$ - heat transfer rate per unit area at the incipient boiling Btu/hr ft^2

r_c - radius of bubble nucleus, ft
r - constant in Rohsenow equation, exponent
R - bubble radius, ft
$\dot{R}$ - rate of bubble growth, ft/hr
s - constant in Rohsenow equation, exponent
T - temperature, ^{o}F
T_L - temperature of the liquid bath, ^{o}F
T_S - saturation temperature of the liquid, ^{o}F
T_W - wire temperature, ^{o}F
T_x - $(T_W - T_S)$, ^{o}F
v_{fg} - difference in specific volume between saturated vapour and liquid, ft^3/lb_m
x - constant, exponent
y - constant, exponent
z - constant, exponent .

GREEK SYMBOLS:

β - coefficient of thermal expansion of fluid, $^{o}F^{-1}$
ΔT - temperature difference between the wire and the liquid, ^{o}F
μ - viscosity, lb/ft hr
ρ - density, lb/ft^3
σ - surface tension lb_f/ft
ϕ - function .
ν - kinematic viscosity, ft^2/hr

DIMENSIONLESS GROUPS :

Gr - Grashof number $\left(g \frac{\beta \rho_L^2 D^3 \Delta T}{\mu_L^2} \right)$

Nu - Nusselt number

Nu_v - Nusselt number, for a vibrating wire $\left(\frac{hD}{k_L} \right)$

Nu_b - bubble Nusselt number, $\left(\frac{h_x d}{k_L} \right)$,where $h_x = \frac{(Q/A)}{T_x}$

Nu_o - Nusselt number without vibration

Pr - Prandtl number, $\left(\frac{C_{pL} \mu_L}{k_L} \right)$

Re - Reynolds number based on mean wire velocity,

$$\left(D \cdot \frac{2af}{12} \frac{\rho_L}{\mu_L} \times 3600 \right)$$

Re_b - Reynolds number based on bubble motion, $\left(\frac{G_b d}{\mu_L} \right)$

SUBSCRIPTS:

FC - forced convection

i - incipience

L - liquid

V - vapour

W - wire

REFERENCES

1. Burgess, G.K. and H. Lechatelier. "The Measurement of High Temperature", 3rd. Ed., p.194-237, 493-495, John Wiley and Sons Inc., New York (1912).

2. McAdams, W.H., J.N. Addoms, R.M. Rinaldo and R.S. Day, Chem.Eng. Progr. 44, 639 (1948).

3. McAdams, W.H. "Heat Transmission", Third Edition McGraw Hill, p. 176, (1954).

4. Fand, R.M. and J. Kaye. International Developments in Heat Transfer, Part 1, 490-498 (1961).

5. Rao, M.A., U.S. Air Force office Aerosp. Res. ARL 65-215 (1965).

6. Deaver, F.K. et al. Journal of Heat Transfer, Trans. ASME Series C, 84, 251 (1962).

7. Gebhart, B. Heat Transfer, McGraw-Hill Book Co. Inc., New York 273 (1961).

8. Penny, W.R. et al. ASME Paper 63-WA/HT-14.

9. Dengler, C.E. Ph.D. Thesis, M.I.T. Cambridge (1952).

10. Hsu, Y.Y. Journal of Heat Transfer 84,207 (1962).

11. Hsu, Y.Y. and R.M. Graham. NASA TN-D594 (1961).

12. Bergles, A.E. and W.M. Rohsenow, ASME Trans. Series C, Vol. 86 365 (1964).

13. Gunther, F.C. and F. Kreith, Jet Propulsion Laboratory Progress Report 4-120, C.I.T. (1950).

14. Rohsenow, W.M. and J.A. Clark, Heat Transfer and Fluid Mechanics Institute, p.193-207, Stanford University Press (1951).

15. Foster, H.K. and N. Zuber, J. Appl. Phys. 25, 474-488 (1954).

16. Rohsenow, W.M. Personal Communication (1966).

17. Frost, W. Personal Communication, Tennessee Space Institute, Tullahoma, Tenn. (1968).

PART II

EXPERIMENTAL STUDY OF EBULLITION CYCLE FROM A PULSATING HEAT TRANSFER SURFACE IN SATURATED NUCLEATE BOILING OF WATER

INTRODUCTION

The theories postulated for nucleate boiling heat transfer are based upon the information derived from single isolated bubbles where the effects of interaction between two consecutive bubbles or between the neighbouring bubbles have not been taken into consideration. Recently it has become more and more clear that there actually exist several subdivisions in nucleate boiling, namely, a discrete bubble regime, a merging bubble regime and also a vapour patch regime(1,2,3,4). Thus, in order to describe the complete nucleate boiling curve of heat flux versus temperature difference, it is evident that studies of each regime should be made individually.

This investigation section presents the results of a study of the statistical behaviour of ebullition cycles of bubbles growing from a natural active site on a vibrating heat transfer surface. The heat flux was maintained at a value of 1×10^5 Btu/hr ft^2. According to the terminology used in boiling heat transfer, it could be described as a bubble merging regime.

EXPERIMENTAL

The same apparatus and experimental procedure were used as described in Part I except that a 16 mm Fastax camera with its accessories was included for high speed photographic work. The heat transfer surface consisted of 0.01 in. diameter platinum wire which was heated electrically and vibrated electromagnetically at a frequency of 45 CPS and an amplitude of 0.0492 in. The liquid used was water at its saturation temperature.

At a constant heat flux of 1×10^5 Btu/hr ft^2 high speed movies were taken at 4800 frames/sec to photograph the vapour columns originating from the natural active sites for both stationary and vibrating wires.

The temperature difference for the stationary wire was 38°F, and for the vibrating wire, 35°F. The decrease in temperature difference for the latter case was attributed to the extra turbulence created in the boundary layer. The films were analysed frame by frame and the bubble characteristics computed as a function of time throughout the ebullition cycle. The data from these films are summarised in Appendix C.

STATISTICAL BEHAVIOUR OF BUBBLES

The evolution of a bubble is believed to take place in three distinct stages. The first stage is marked by the development of the boundary layer when a superheated liquid layer is formed and a bubble starts growing on a potential active site. In the second stage the boundary layer is disturbed considerably by the further growth of the bubble. The interfering action of a bubble extends to as far as one bubble diameter away from the nucleation site(5). The third stage can be characterised by the destruction of the boundary layer. After the bubble leaves the surface, relatively cold liquid flows towards the nucleation site and a finite time is required for the cooler liquid to warm up to the proper superheat before the cycle repeats itself. In studying the mechanisms of boiling heat transfer, a statistical analysis of the bubbles is of great assistance, since the bubble behaviour involved is inherently random.

Bubble Growth Rate

Bubble growth takes place as a result of evaporation at the bubble wall, the heat for this evaporation being transferred by conduction from the surrounding fluid. The bubble growth rate is thus governed by the temperature distribution in the boundary layer as well as its thickness. Since these two factors would be affected by the onset of vibration, it may therefore be expected that the bubble growth rate would be different from that without vibration. In the present investigation it was not feasible to determine the actual localised values for the temperature distribution and thickness of the thermal boundary layer and hence no theoretical model was attempted. However, an equation similar to the one proposed for stationary surfaces has been evaluated.

The equations proposed to date for stationary surfaces(6,7) have the following form:

$$R = k(\tau)^n \tag{1}$$

In order to develop a corresponding equation for a pulsating heat transfer surface, the film was analysed frame by frame with a magnification of 1:44. About 50 values of R, the mean bubble radius, against time were read from the film for various bubbles growing on one particular natural active site. The best fit line was drawn for the above data by the least square method as shown in Figure 1. The values of n and k are thus evaluated as:

$$n = 0.32$$
$$k = 0.16$$

A comparison of the growth rate of bubbles under conditions of pulsating and stationary wires was then made. In both the cases, the heat flux density was maintained at the same value. Since the surface temperature was higher in the case of a stationary wire, the number of active sites was also greater. The values of mean bubble radii against time, are plotted in Figure 1 for stationary and pulsating

FIGURE 1

BUBBLE GROWTH RATE FROM

STATIONARY AND VIBRATING WIRES

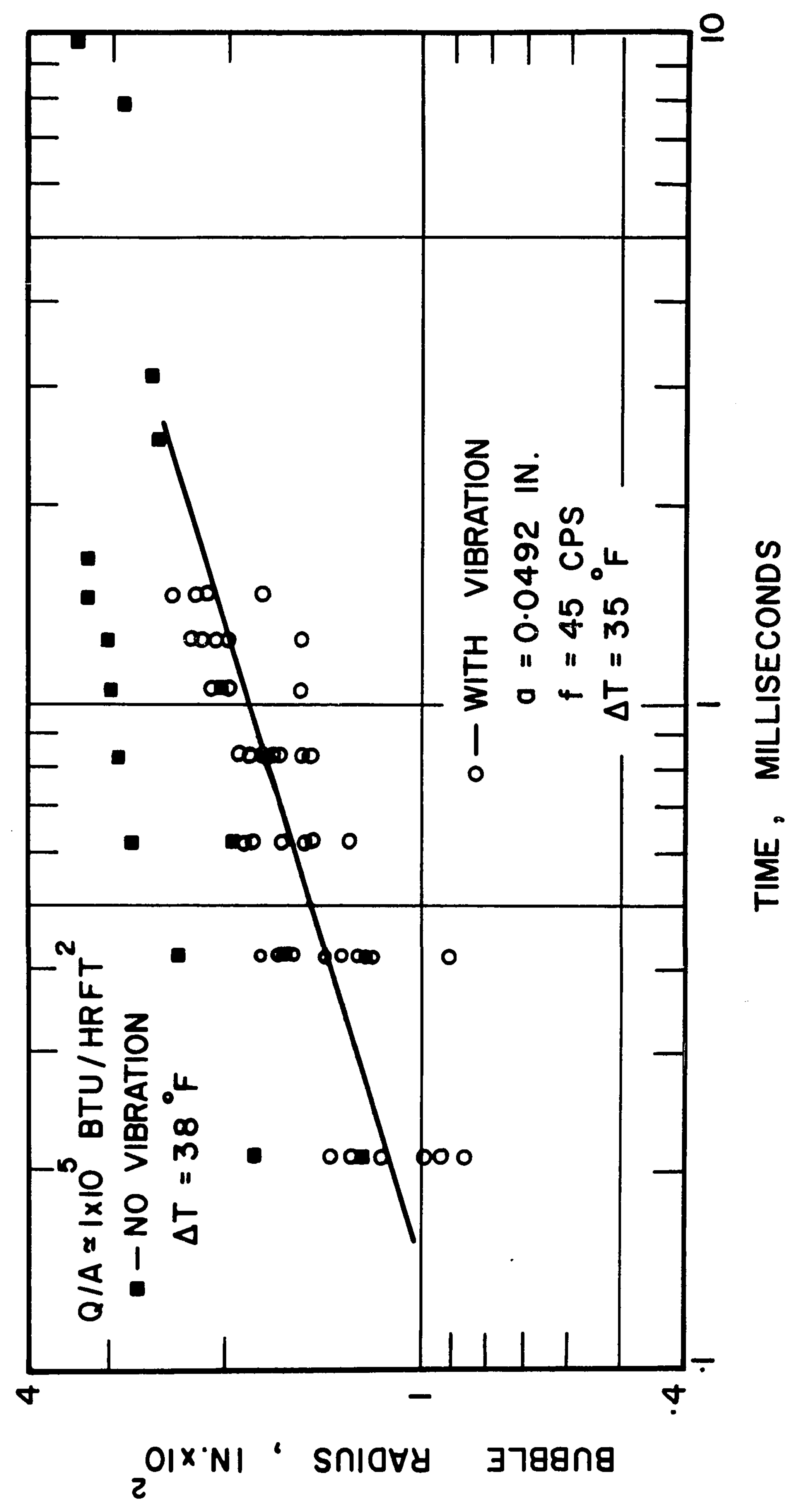
Q/A ≈ 1x10^5 BTU/HRFT^2
■ — NO VIBRATION
ΔT = 38 °F
○ — WITH VIBRATION
a = 0·0492 IN.
f = 45 CPS
ΔT = 35 °F
BUBBLE RADIUS , IN.x10^2
4
1
.4
.1
1
10
TIME , MILLISECONDS

surfaces. The experimental results show that for a stationary surface, bubbles start to grow at a very high speed, which decreases sharply and becomes negligible before departure. However, the bubble growth data from vibrating wire could be represented by one single line on a log-log plot. At time = 1.5 milliseconds most of the bubbles in the case of a vibrating wire break off the surface, whereas for stationary wires they remain attached to the surface and continue to grow, but at a very slow rate. The overall time a bubble needs to grow and leave the surface is much shorter for vibrating wires. However, as may be expected, the diameter at break-off is smaller. The generating period, defined as the time a bubble needs to grow and leave the surface, was also smaller for a vibrating wire. The maximum value for the generating period of a bubble growing on the pulsating wire was 2.5 milliseconds, whereas for a stationary wire it was often 3 to 4 times this value.

Waiting Period

By waiting period, also called the delay time, is meant the time between the departure of a bubble and the first appearance of a new one at the same nucleation site. As reported by many investigators(8,9) and also found in this investigation, the waiting period is not equal to the bubble growth period. For stationary surface delay time is also one of the important factors which determines the shape of the bubbles. Spherical bubbles were only observed for very small delay times whereas for relatively large delay times only oblate or hemispherical bubbles were photographed. The observations agree with those reported by other workers(10,11).

The waiting period in the case of oscillating surface was studied on the same individual natural active site where it varied from 0.2 to 18 milliseconds. It appears that the nucleation of bubbles is also affected by the oscillation of the heat transfer surface. An oscillating wire surface experiences a decrease in pressure and thus creates a larger pressure differential between the vapour inside the surface of the bubble and the superheated liquid next to the surface. Since the pressure differential would increase with increasing vibrational parameters it may be expected that the corresponding waiting period would be lower. In the present investigation the time between changes is $\frac{1000}{90} \simeq 11$ milliseconds which is a good average for the longer waiting times as shown in Figure 2. However, several times the departed bubble was immediately followed by the nucleation of the new bubble. This resulted in very short waiting periods for some bubbles. The waiting period for bubbles which are generated in succession on the same nucleation site of an oscillating heat transfer surface, is shown in Figure 2. The above results represent very qualitative analysis of the waiting period.

FIGURE 2

WAITING PERIOD OF BUBBLES

GROWING ON A VIBRATING WIRE

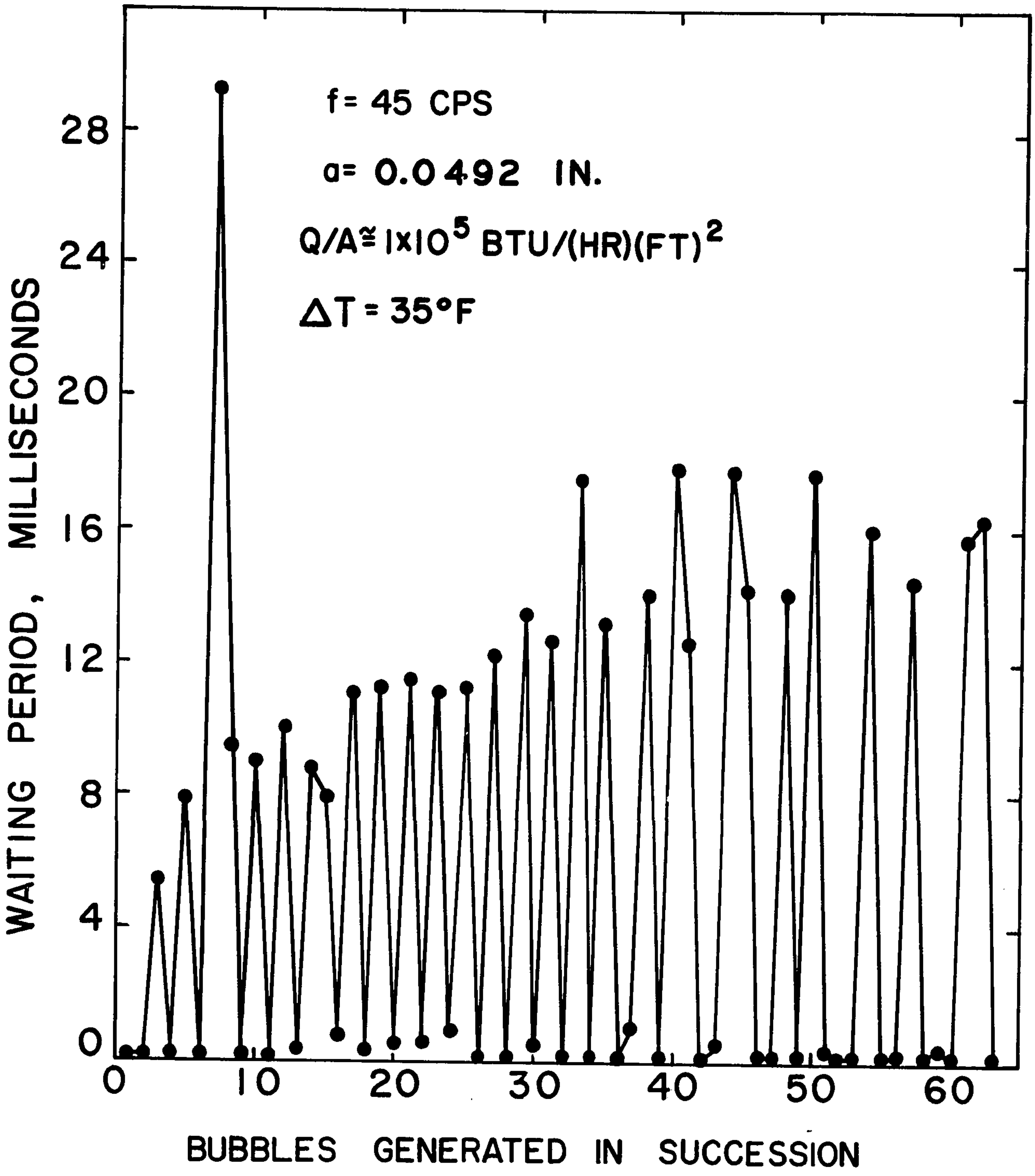
f= 45 CPS
a= 0.0492 IN.
Q/A≅ 1×10^5 BTU/(HR)(FT)^2
ΔT = 35°F
WAITING PERIOD, MILLISECONDS
0
4
8
12
16
20
24
28
0
10
20
30
40
50
60
BUBBLES GENERATED IN SUCCESSION

Generating Period and Diameter at Break-Off

As predicted by Zuber(12) and others, there is an inflection point for the bubble diameter at break-off when the bubble population density attains a value such that the interfering action of one bubble overlaps the interfering action of the neighbouring bubble and hence the bubble experiences an additional pressure to leave off from the surface. It may be expected that bubbles would experience the similar situation for a vibrating wire even though the bubble population density has not reached a value as mentioned above. The equations such as proposed by Fritz(13) will not be valid in estimating the diameter at break-off, The relative velocity between the fluid and the wire surface tends to shear off the bubble from the surface. This resulted in smaller sizes of the bubbles at departure.

From the film analysis it was found that the diameters at break-off and their generating periods follow normal patterns of distribution. Theoretical normal curves were fitted to these properties as shown in Figures 3 and 4. The normal distribution curves could be represented by

$$N = \frac{1}{0.0048\sqrt{2\pi}}\, e^{-1/2\left(\frac{d-0.0334}{0.0048}\right)^{2}} \quad \text{- for diameter at break-of}$$

$$N = \frac{1}{0.4997\,\sqrt{2\pi}}\, e^{-1/2\left(\frac{\tau_g x10^{-3} - 1.7123}{0.4997}\right)^{2}} \quad \text{- for generatin period .}$$

The frequency of bubble emission defind as $\frac{1}{(\tau_w + \tau_g)}$, was found to be slightly higher for a vibrating wire.

FIGURE 3

VARIATIONS IN BUBBLE DIAMETER AT

BREAK-OFF FOR A VIBRATING WIRE

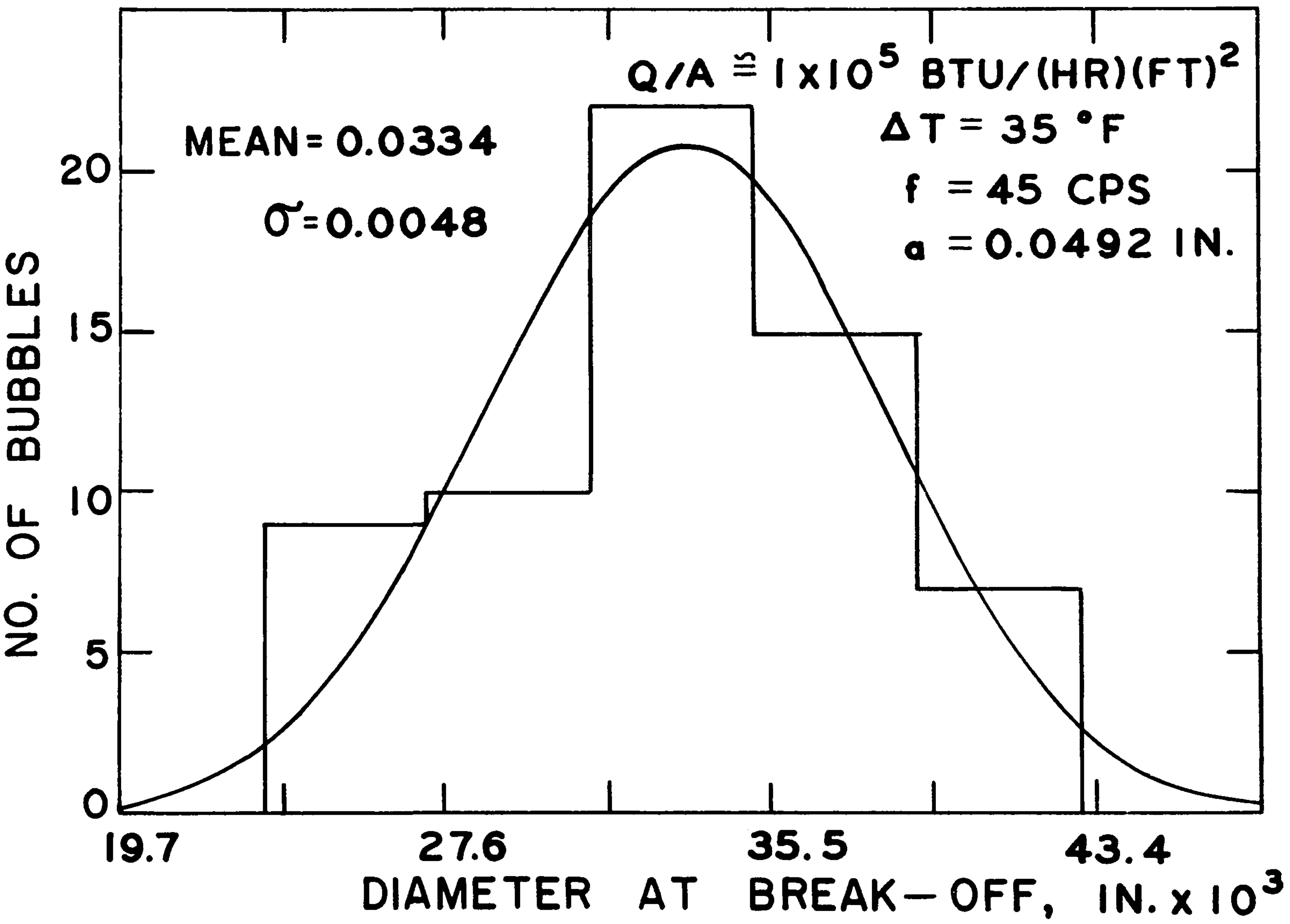
MEAN = 0.0334
σ = 0.0048
Q/A ≅ 1 x 10⁵ BTU/(HR)(FT)²
ΔT = 35 °F
f = 45 CPS
a = 0.0492 IN.
NO. OF BUBBLES
0
5
10
15
20
19.7
27.6
35.5
43.4
DIAMETER AT BREAK-OFF, IN. x 10³

FIGURE 4

VARIATIONS IN GENERATING PERIOD OF

BUBBLES GROWING ON A VIBRATING WIRE

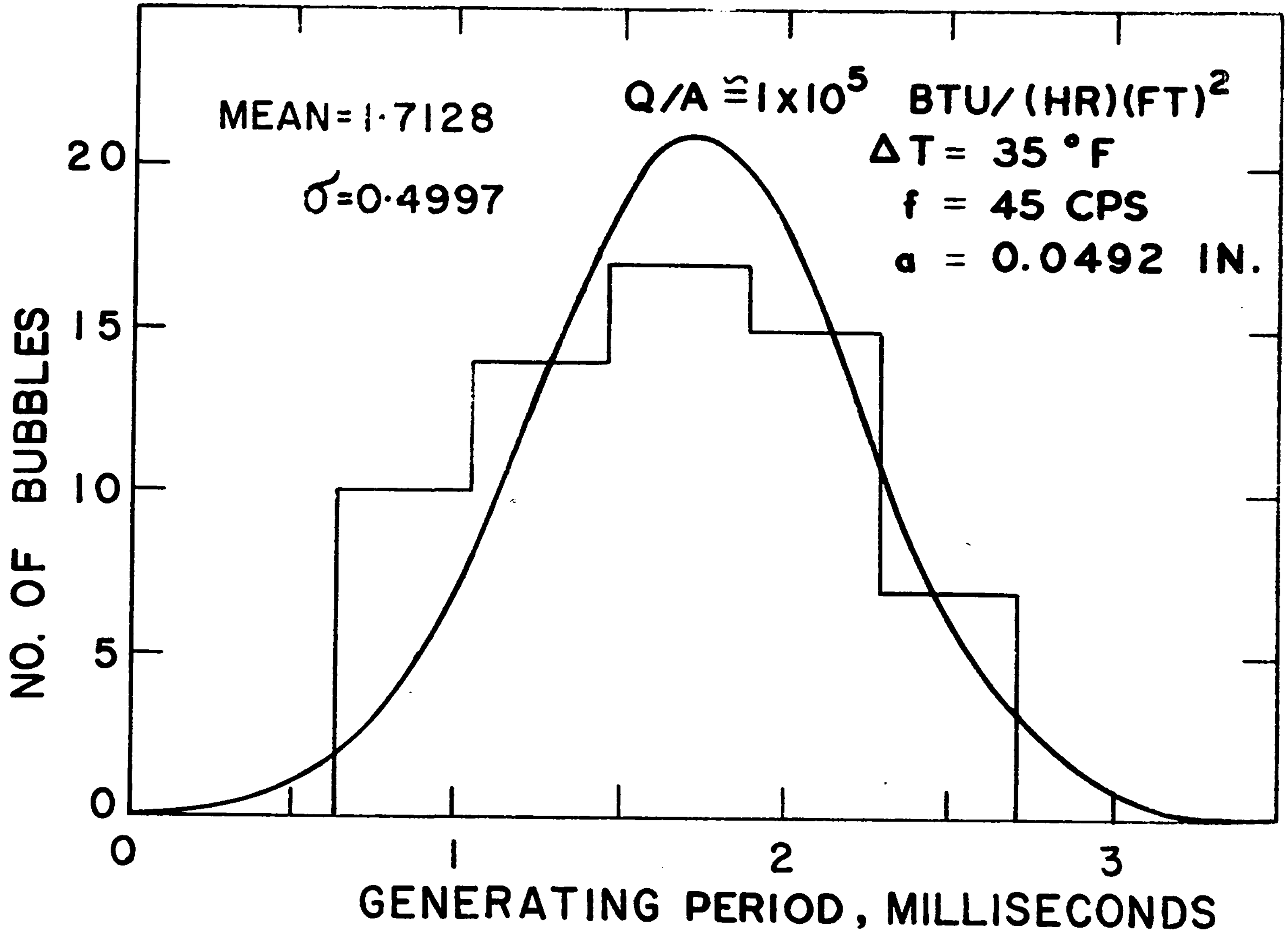
MEAN=1·7128
σ=0·4997
Q/A ≅ 1x10^5 BTU/(HR)(FT)^2
ΔT = 35 °F
f = 45 CPS
a = 0.0492 IN.
NO. OF BUBBLES
0
5
10
15
20
0
1
2
3
GENERATING PERIOD, MILLISECONDS

CONCLUSIONS

(1) Imposed vibrations induce extra agitation which results in a decrease in effective thickness of the thermal boundary layer.

(2) The oscillations of the heat transfer surface control the start of the nulceation and hence the waiting period. The waiting period decreases with increase in the vibrational parameters.

(3) In general, vibration of the heater surface results in a larger number of smaller bubbles covering the surface of the heater.

(4) The generating period for bubbles and their diameters at break-off are less for a vibrating wire. The distribution of these variables can be represented by normal distribution curves.

(5) A slight increase in bubble emission frequency is noticed for a pulsating wire.

NOMENCLATURE

ROMAN SYMBOLS

a - total displacement of amplitude of vibration of wire (peak to peak), in.

D - diameter of platinum heating wire, in.

d - diameter of bubble at break-off, in.

f - frequency of vibration of the wire, CPS

h - heat transfer coefficient at bubble wall, Btu/hr ft^2 ^oF

k - constant

N - number of bubbles

n - constant

Q/A - heat flux from test section to water Btu/hr ft^2

R - mean radius of the bubbles, in.

T - temperature, ^oF

GREEK SYMBOLS

ΔT - temperature difference between the wire and bulk water, $(T_W - T_S)$, ^{o}

σ - standard deviation of the distribution

τ - time, seconds

SUBSCRIPTS

g - generating period a bubble needs to grow and leave the surface

S - saturation condition

W - wire

w - waiting period

REFERENCES

1. Gaertner, R.F.,Am. Soc. Mech. Engrs. Paper 63-WA-76 (1963) .
2. Zuber, Novak. Int. J. Heat Mass Transfer, 6 No.1, 53-78 (1963).
3. Yamagata et al., Kyushu Imperial University, Faculty Eng. Memoirs, 15, No. 1, 97-163 (1955).
4. Kirby, D.B., and J.W. Westwater, Chem. Eng. Sci., 18, No. 7, 469 (July 1963).
5. Gaertner, R.F., and J.W. Westwater, Chem. Eng. Progr. Symposium Ser. No.30, 56, 39 (1960).
6. Plesset, M.S., and S.A.Zwick, A.I.Ch.E..Journal, 25,493 (1954).
7. Foster, H.K., and Novak Zuber, J. Appl. Phys., 25, 474 (1954).
8. Strenge, P.H. et al. A.I.Ch.E. Journal, 7, p.578 (1961).
9. Westwater, J.W., and D.B. Kirby, "Sixth National Heat Transfer Conference A.I.Ch.E. - A.S.M.E., Boston, Mass. (1963).
10. Roll, J.B. "The effect of Surface Tension on Boiling Heat Transfer" Ph.D. Thesis, Purdue Univ. (1962).
11. Griffith, P. Tech. Report No. 8, M.I.T. Cambridge, Mass. (June,1956).
12. Zuber, Novak, AECU 4439, AEC (1959).
13. Jakob Max, Heat Transfer, Vol. 1, John Wiley and Sons Inc., 614 (1949).

PART III

DYNAMICS OF BOILING BUBBLES FROM VIBRATING SURFACES IN SATURATED NUCLEATE BOILING OF WATER

INTRODUCTION

Heat transfer to boiling liquids is a complex phenomenon which requires an understanding of the local thermal process at the surface, the local hydrodynamic flow regimes induced by bubbles and the nucleation characteristics of the surface. Various investigations indicate that the large heat transfer rates associated with nucleate boiling are a consequence of microconvection in the superheated sublayer. In order to arrive at a quantitative understanding of the process and to formulate an analysis, the dynamics of vapour bubbles must be taken into account.

Many aspects of bubble behaviour such as rate of growth, the maximum size, the frequency of formation, and bubble shape, have been investigated to some extent for a stationary surface. However, no work has been carried out, to the best knowledge of the author, to study the bubble dynamics in nucleate boiling on a vibrating heat transfer surface.

With a view to achieve a quantitative conception of bubble dynamics from a vibrating surface, attempts are made in this investigation toward very basic studies of the boiling process, starting with the formation of individual bubbles, their growth and departure. However, it may be pointed out that the statistical nature of bubble behaviour, as well as the complicated flow regimes encountered in boiling, should also be taken into account when trying to apply the results obtained for a single bubble to boiling heat transfer.

In the present study, detailed photographs of individual bubbles in nucleate boiling, for different vibrational conditions, were obtained. Pertinent bubble dimensions were measured throughout the growth period to compute the magnitude of the forces that significantly influence the bubble behaviour.

EXPERIMENTAL

Heated Test Section:

The test specimens were made from 304 stainless steel strips, $2\frac{3}{4}$ in. long, $\frac{1}{2}$ in. wide and $\frac{1}{16}$ in. thick. Each strip was first mounted using Quickmount, a self setting resin supplied by Fulton Metallurgical Products. A smooth surface was then obtained by a series of metallurgical processes. The polishing technique developed for the present work is described in a flow diagram in Figure 1. This procedure was followed rigorously each time a smooth edge of surface was desired. The stainless steel piece was pressed in a die to form a channel shape having a polished surface inside with an overall length of $1\frac{1}{4}$ in. The top surface and the edges were polished to a roughness less than one microinch. The top surface of the strip was checked on a Vicker M55 Metallograph to ensure that the surface was free of pits and scratches other than those left by the $\frac{1}{4}$ micron diamond paste. Some inclusions were observed that were inherent in the steel matrix and could not be removed. However, these did not seriously influence the surface roughness. The artificial nucleation site was then drilled in the centre of the surface.

Artificial Sites:

Hummel(1,2) has suggested that a heterogeneous surface possessing poorly wetted spots (contact angle between 90° and 180°) on a well wetted

FIGURE 1

FLOW DIAGRAM OF THE
POLISHING PROCEDURE

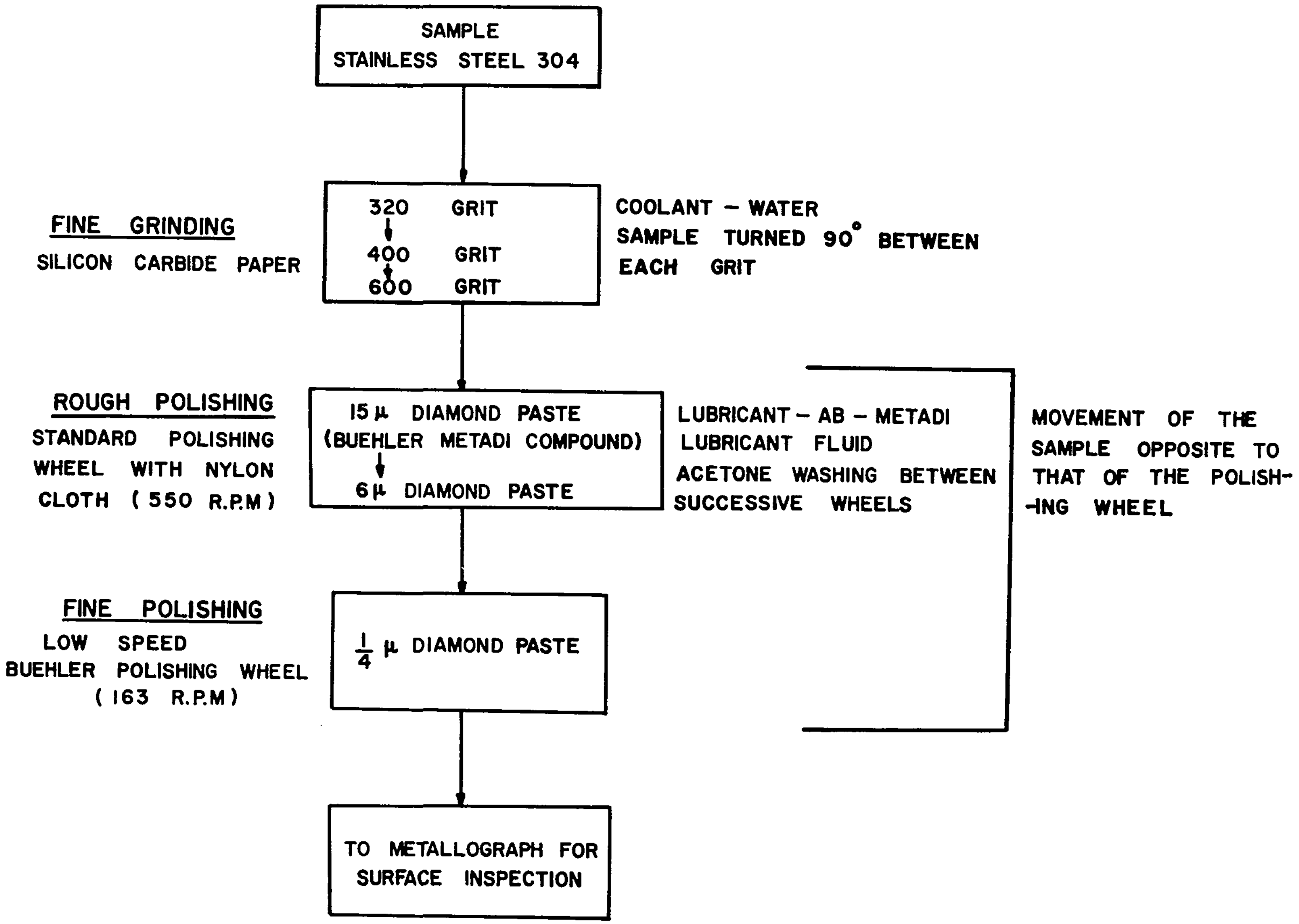

FLOW DIAGRAM OF THE POLISHING PROCEDURE

solid surface would be effective in providing stable sites for vapour growth. The contact angle is defined as the angle through the liquid from the solid surface to the tangent of the vapour liquid interface at the point of contact of the solid, liquid and vapour under equilibrium conditions. Because tetra-flouroethylene resin (Teflon) is poorly wetted by water and is commercially available in a form that will adhere to metals, it has been used in the present study to provide the poorly wetted spots on a stainless steel surface for boiling of water.

Sphinx micro-drills of 0.0059 in. nominal diameter, manufactured by Swiss Instruments Limited, were used on a precision Dumore drill press to drill a cavity. The cavity depth was controlled during drilling by a depth gauge installed on the precision drill press. To obtain better accuracy the drilling operation was carried out through a stereomicroscope with a magnification of 12.5 x as shown in Figure 2. This produced a hole that was quite round at the surface with no cratering evident. The mouth diameter and depth of the cavity were measured using a Reichert optical microscope with a calibrated eye-piece to an accuracy estimated as ± 1 micron. A micrograph picture of the cavity mouth is shown in Figure 3.

Coating the Cavity with Teflon:

A cavity of 0.007 in. diameter and 0.003 in. deep was drilled. Since it was important that Teflon occupied only the cavity dimensions

FIGURE 2

EXPERIMENTAL SETUP FOR DRILLING
CAVITIES ON A HEAT TRANSFER SURFACE

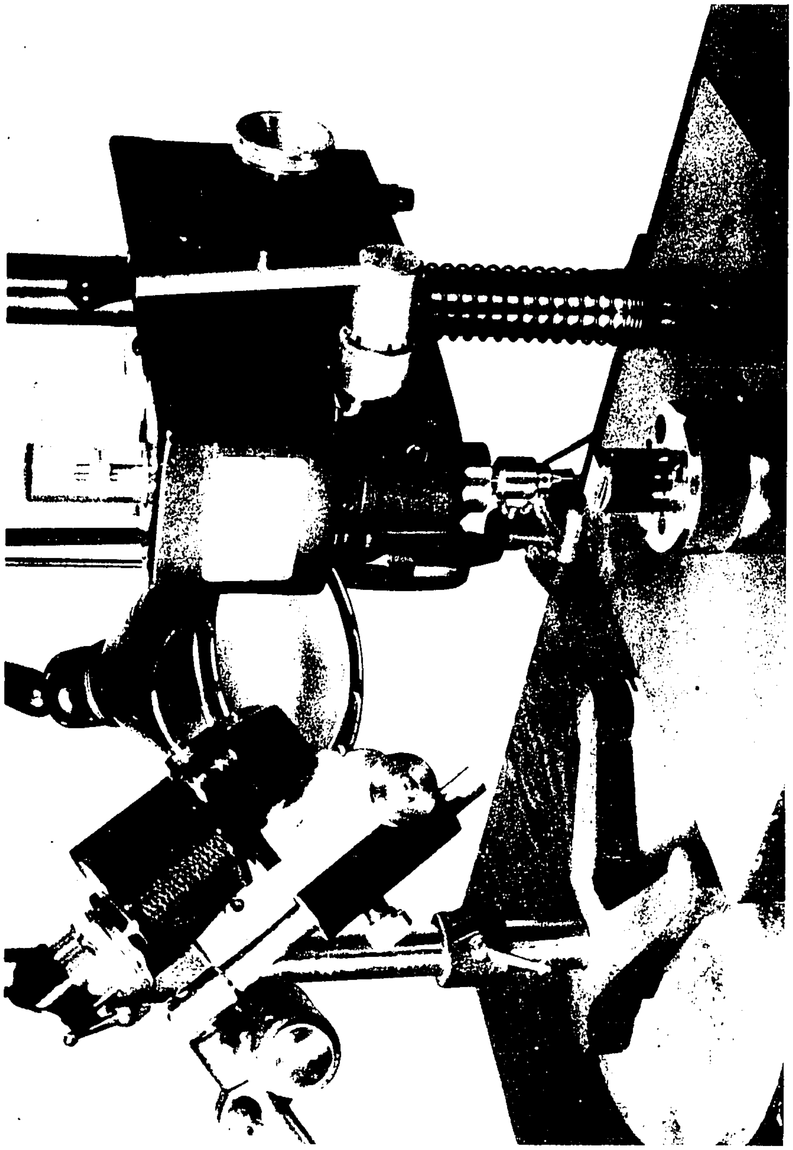

FIGURE 3

MICROGRAPH PICTURE OF THE CAVITY

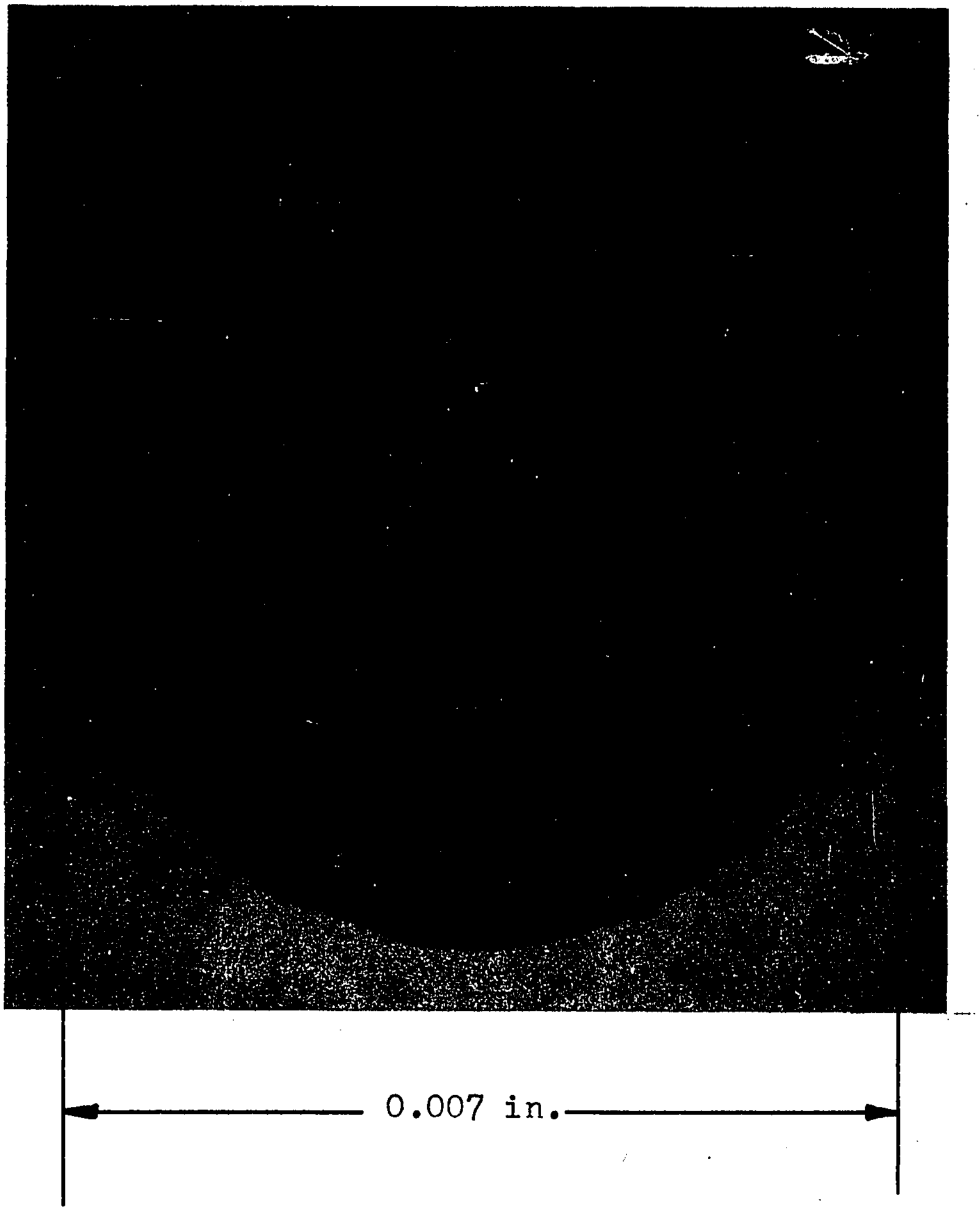
0.007 in.

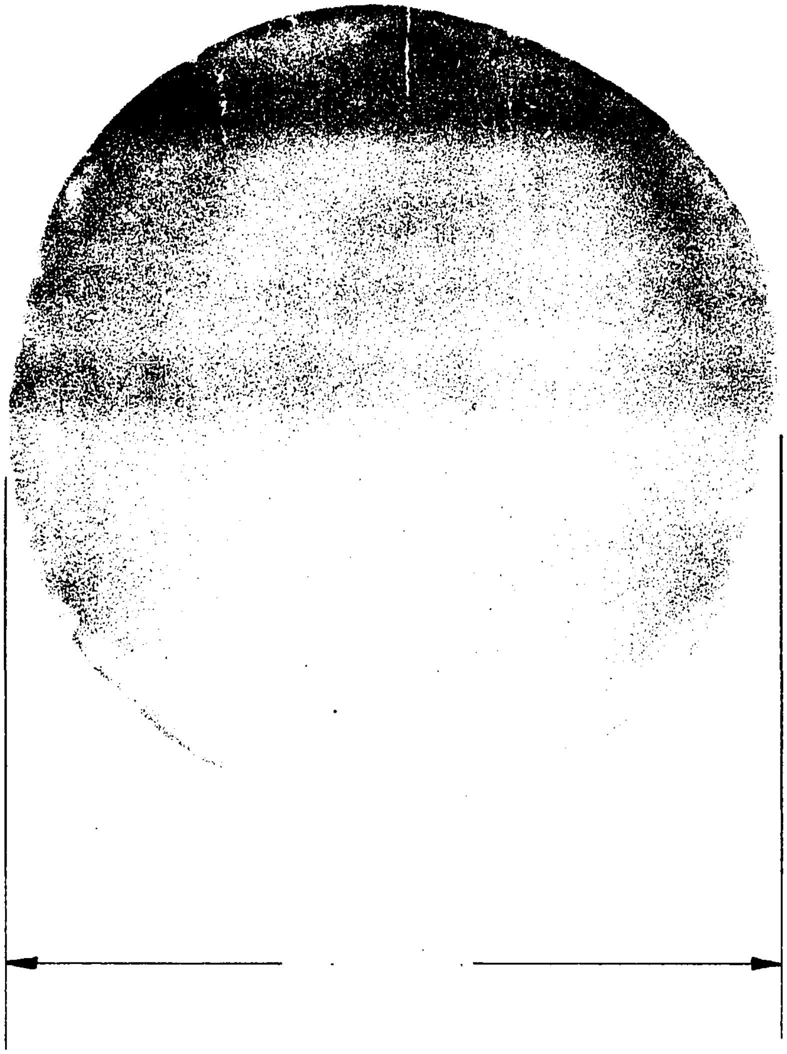

care was taken to ensure that the cavity had a sharp edge at the mouth diameter. A coat of Teflon emulsion (Dupont Teflon TFE tetra flouroethylene resin, Green primer, No. 851-204) was applied in the vicinity of the cavity and excess Teflon was wiped off the surface. Frequent passes were made on the surface, using a water-damp piece of filter paper against the straight end of a putty knife, until no colour appeared on the filter papers. The straight edge was used to prevent the paper from entering the pit and removing Teflon from it. The Teflon was allowed to dry for about 20 minutes at room temperature, and the strip was then sintered at 700°F for about 10 minutes in the nitrogen atmosphere so that Teflon woudd fuse and bond properly to the metal inside the cavity. Thorough inspection of the cavity and the overall surface smoothness were made before mounting the strip on the support; which consisted of a Bakelite Cylinder $1\frac{1}{4}$ in. diameter, which had a raised platform to conform to the dimensions of the specimen as shown in Figure 4. A piece of Vitron was placed between the Bakelite and the strip to avoid the formation of bubbles from the underside of the strip.

Vibration Device:

The vibrations were induced by means of cams connected to a rod which passed through the Bakelite block and supported the heating strip. A uniformly accelerated motion cam was designed to produce a fixed displacement amplitude of $\frac{1}{8}$ in. The plate was vibrated in a direction transverse to its length through a range of frequencies which was controlled

FIGURE 4

HEAT TRANSFER SURFACE MOUNTED
ON A BAKELITE CYLINDER

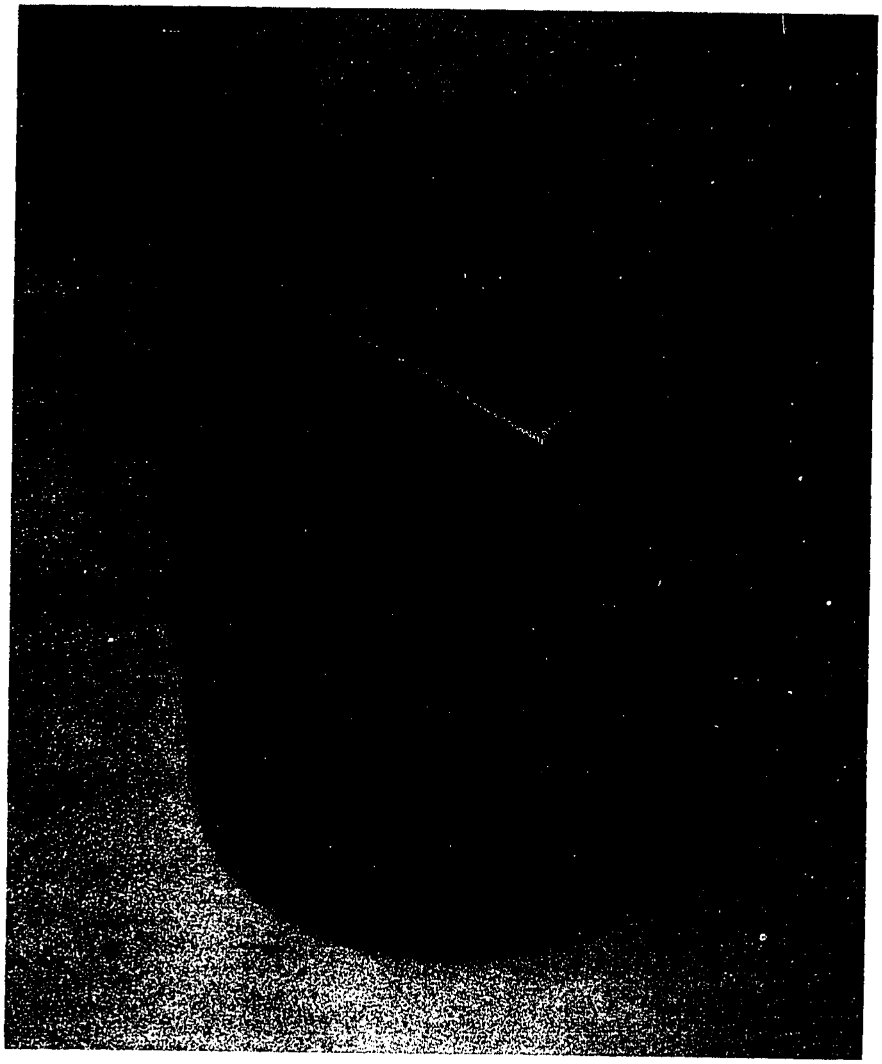

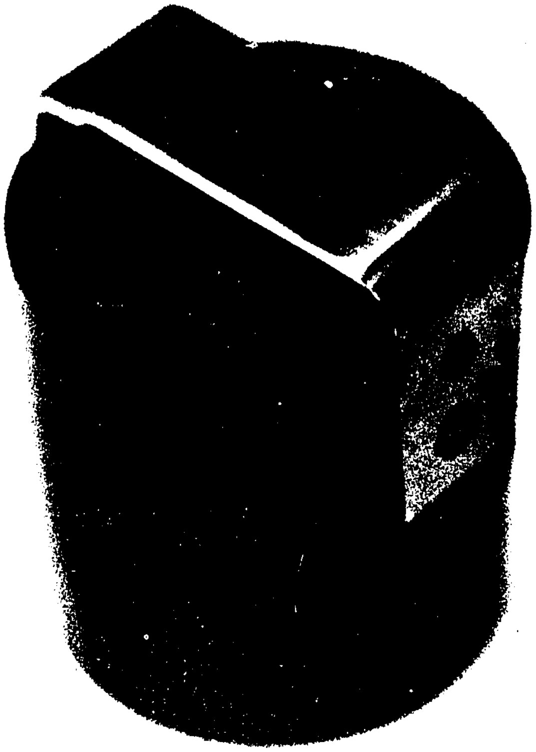

by the speed of the varidrive motor. This variable speed motor was used to power the vibrating device. The details of this arrangement are shown in Figure 5. The reboiler consisted of a stainless steel vessel used for Part 1 of this thesis. A photograph of the reboiler and vibrating device is shown in Figure 6. Auxiliary heaters were welded to the reboiler to provide saturation conditions. Power was supplied to the heat transfer surface through a regulated D.C. power supply,(0-40V, 0-250A) manufactured by Stoney Creek Co., and a Leeds and Northrup precision resistor (0.001 ohm, 300A) was connected in series to measure the current. To calculate power input a Tinsely potentiometer, Model 3184E, and a Tinsley galvanometer (Type SR-1) were used for measuring the potential drops across the specimen and the standard resistor. The complete experimental setup is shown in Figure 7.

Procedure:

The test specimen was clamped to the vibrating device and the reboiler was charged with distilled water. The auxiliary heaters were activated until saturation was reached. To reduce convective currents in the tank the power to the auxiliary heaters was decreased to a level just sufficient to maintain saturation. Power at a low level was then applied to the specimen and the water bulk temperature, and voltage drops across the specimen and standard resistor were recorded. Note was made as to the level of bubble production at the artificial site. The power was increased and new set of readings recorded. This process was continued until the artificial site was producing bubbles continuously.

FIGURE 5

DIAGRAMATIC SKETCH OF THE

VIBRATION DEVICE

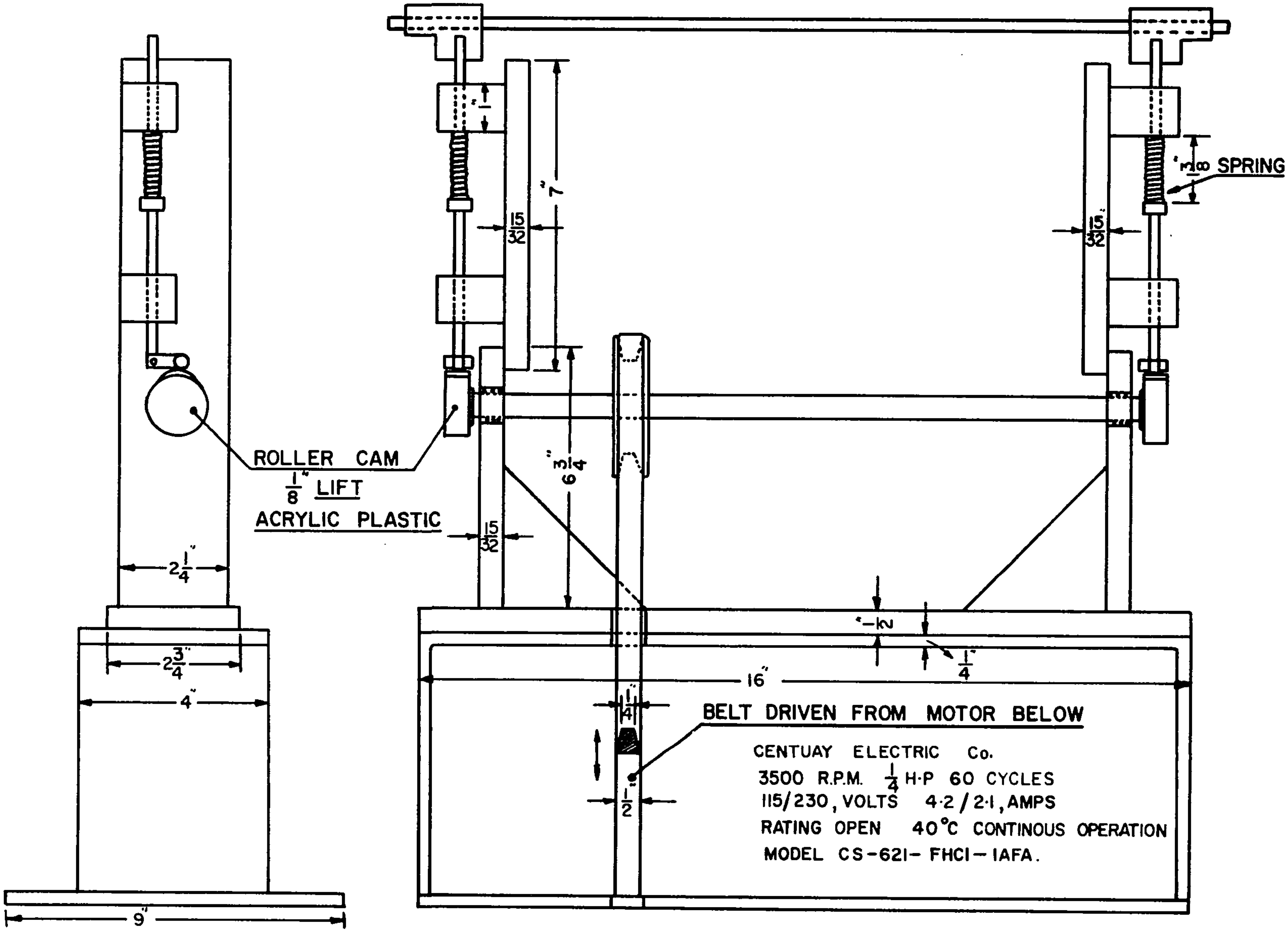

SIDE VIEW

FRONT VIEW

FIGURE 6

PHOTOGRAPH OF THE

REBOILER WITH VIBRATING DEVICE

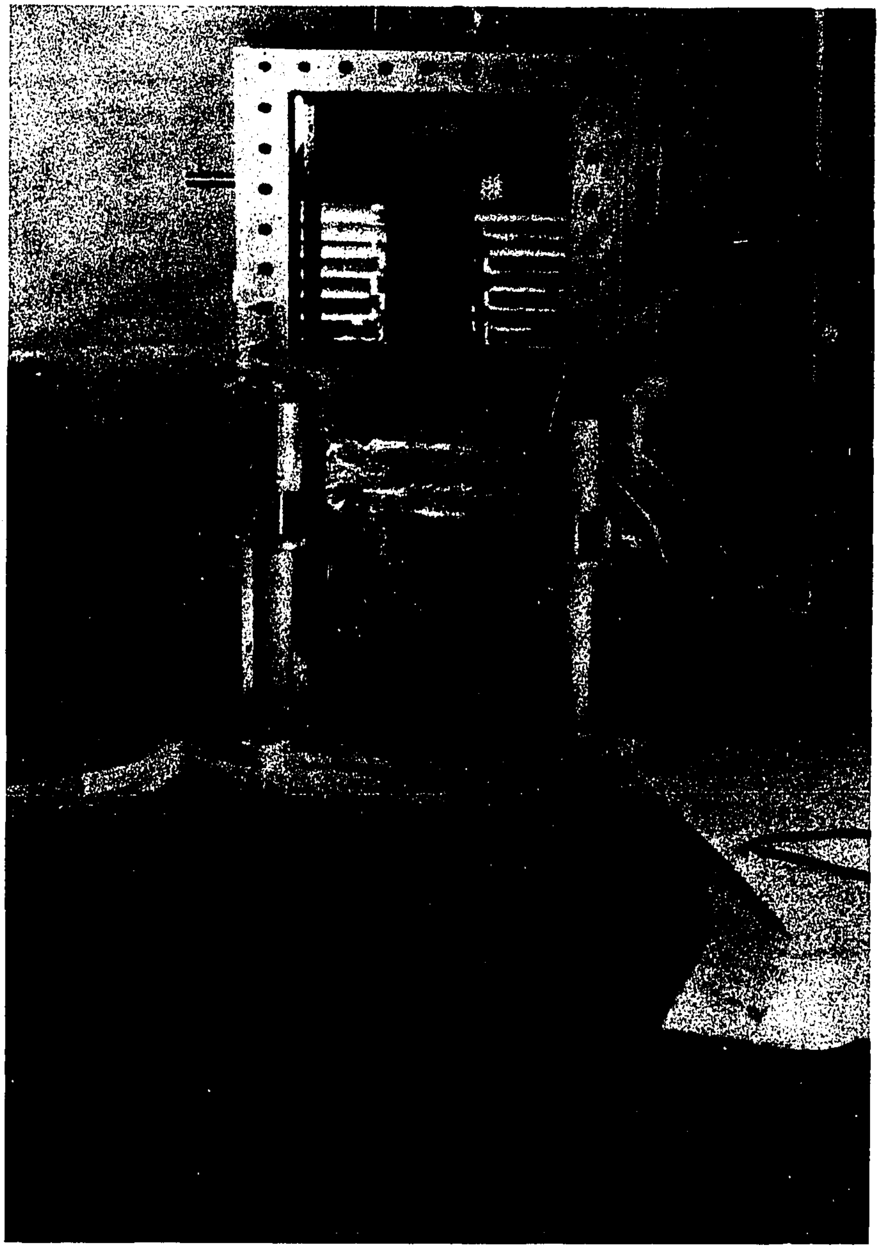

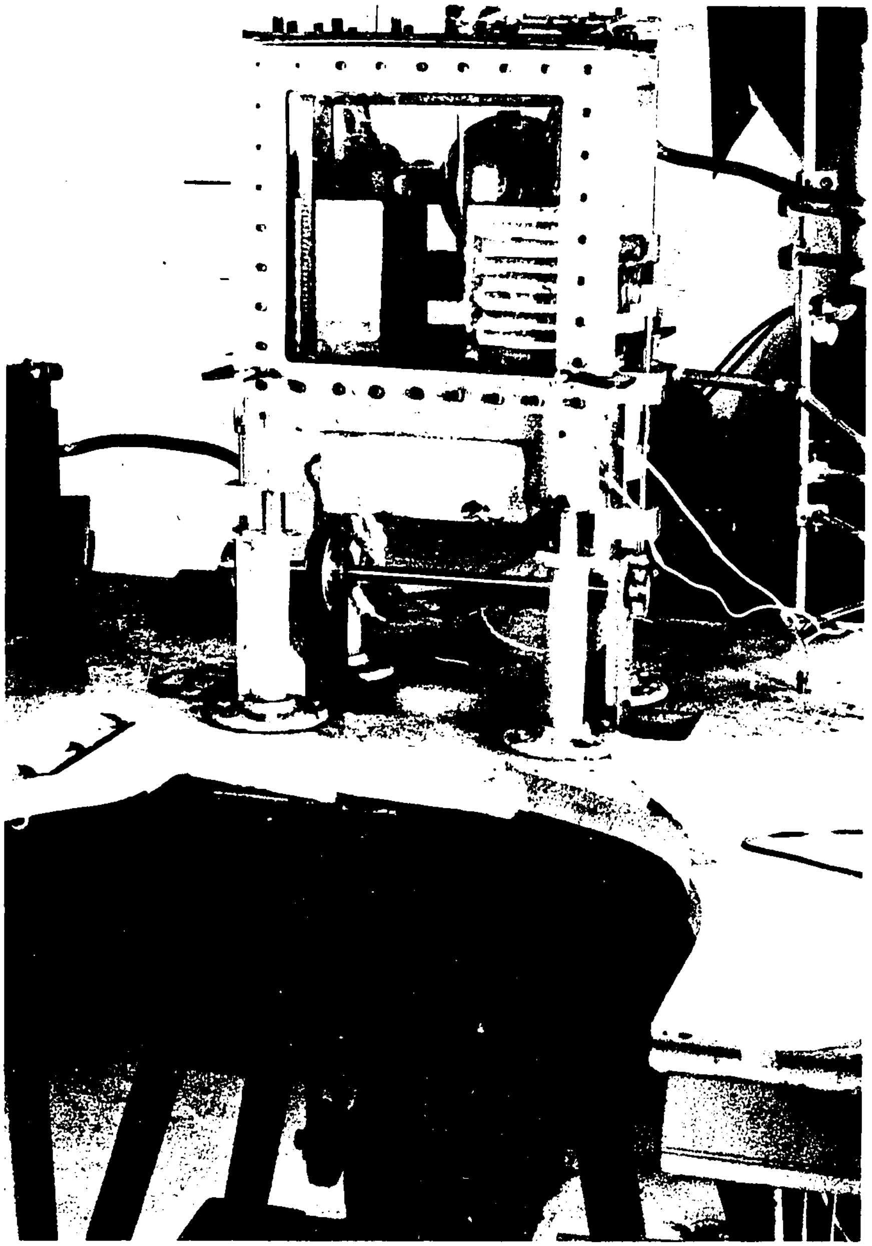

FIGURE 7

PHOTOGRAPH OF THE COMPLETE
EXPERIMENTAL SETUP

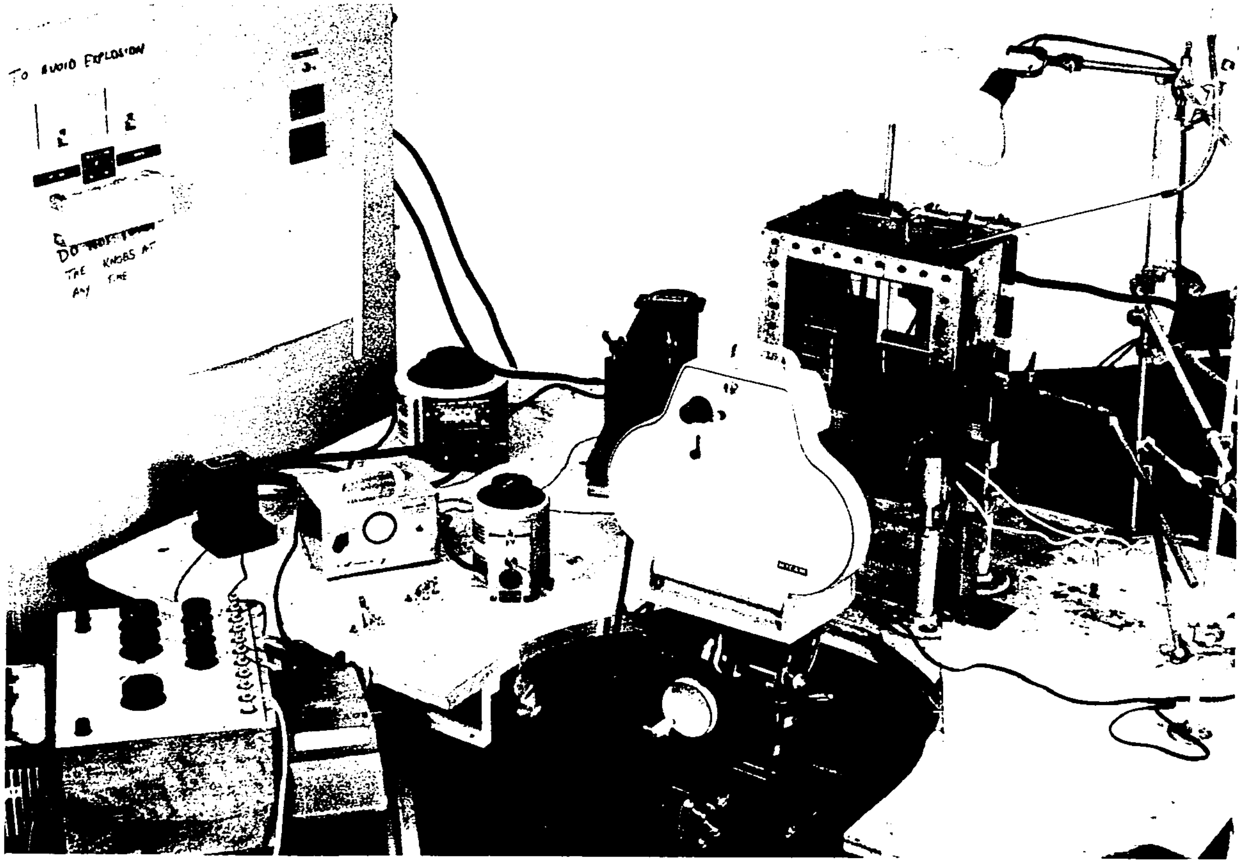
TO AVOID EXPLOSION
DO
THE KNOBS AT
ANY TIME

Under these sets of conditions high speed motion pictures were taken with a Hycam Camera at a speed of 5000 frames/second. The camera was equipped with a timing device which was set at 1000 pipps per second to confirm the actual camera speed. A lens of focal length 75 mm was arranged with the extension tubes so that the individual bubbles were magnified to practically fill the frame of the camera.

Maintaining a constant heat flux of 7×10^3 Btu/hr ft^2, the surface was subjected to vibrations of 10 CPS, 20 CPS, and high speed motion picures were taken of the bubbles growing from that artificial site. The amplitude of vibration for each case was $\frac{1}{8}$ in. For every experimental run a 16 mm Reversal film roll of 200 ft length was used. However, the first 100 ft were discarded to compensate for the acceleration period of the camera. A rod of 0.1265 in. diameter located near the cavity mouth was photographed for use as a reference length.

EXPERIMENTAL RESULTS

The artificial nucleation site produced rather spherical, surface tension-dominated bubbles, as opposed to the oblate or hemispherical, liquid inertia-dominated bubbles generally characteristic of a polished surface. An idealized representation of a bubble growing at a poorly wetted site on a well wetted surface is shown in Figure 8a. High speed films taken for surface vibrations of 0,600 and 1200 RPM were analysed frame by frame with a magnification of 33x approximately. The bubble dimensions a,b,c,θ defined in Figure 8b were measured for all frames to compute their variations with time throughout the growth period of a bubble. Despite the fact that the data were for bubbles from one single cavity and taken from one single experimental run, the physical dimensions of the bubbles varied considerably. This was true for stationary and pulsating surfaces. Each departing bubble left a vapour nucleus behind and hence the waiting time was always zero.

Because of the continuous formation of bubbles, the phenomenon of coalescence was observed on a stationary surface. The bubbles which were free from the coalescence effect and had the most rapid initial growth rate were selected for the analysis of force balance. The growth rate of such bubbles should correspond most closely to the conditions where the theoretical equations would apply(3).

For a pulsating surface the merging between the preceding bubbles decreased with the increase in the vibrational parameters. Occasionally the following phenomena were noticed:

FIGURE 8

BUBBLE GROWING ON A
POORLY WETTED CAVITY

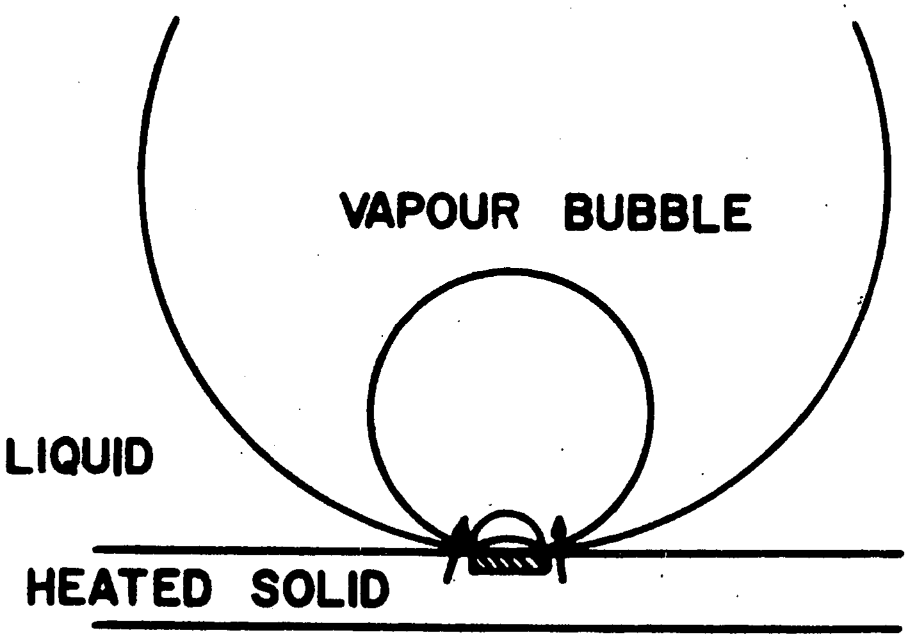

(8a)

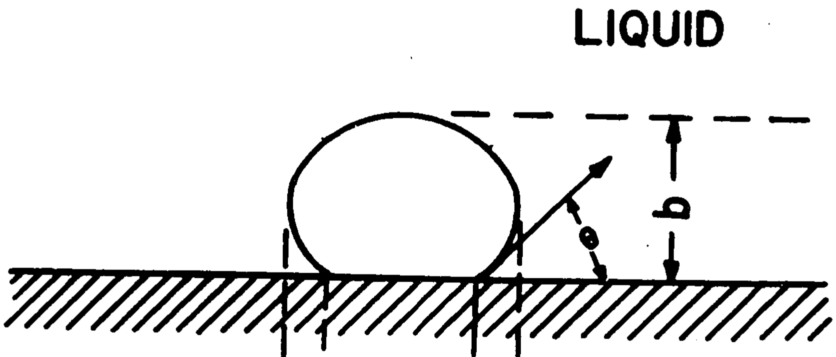

(8b)

During the downward movement of the surface the immediately departed bubble had a tendency to move downward and join with the newly formed bubble. It became a big vapour mass and thus left the surface comparatively earlier. The bubbles which left the surface during the upward movement of the surface had a rising velocity lower than the speed of the surface and would again merge with the newly created bubble.

The growth rates for bubbles which grew till departure without merging with other bubbles were the same as those measured before coalescence for bubbles which merged on the heating surface as described above.

In order to obtain a consistent comparison between vibrating and stationary surfaces, the statistical randomness was minimised by selecting the bubbles which were least affected by the preceding bubbles. The bubbles thus selected for the present work were as follows:

Stationary Surface:	bubble no. 25
Vibrating Surface :	
RPM = 600	bubble no. 8
RPM = 1200	bubble no. 4

The data for these bubbles are summarised in Appendix D.

<u>Growth Rate:</u>

The bubbles were assumed as spheres symmetric about their vertical axis, although in reality they were slightly tear-shaped. The diameter at any instant was taken as the arithmetic mean of horizontal diameter, a, and the vertical distance, b, between the bubble top and the heating surface. The variations of bubble diameters with time for bubbles no. 25, 8,4 (corresponding to 0,600 and 1200 RPM) are presented on log-log plots in Figures 9 through 12. For bubble no. 25 growing on a stationary surface, it was observed that growth rate is a continuously decreasing function of time. Even though the continuous variation of growth rate with time is always the case, for spherical bubbles two consecutive periods of growth may be separated: a first period of very fast growth followed by a second period of a much slower growth rate. The analytic equations of the form

$$D = k\,\tau^{n}$$

were obtained separately for the two regions. The equations obtained from least squares analysis are:

$$D = 0.61\,(\tau)^{0.87} \tag{2}$$

$$0 < \tau < 0.003 \text{ seconds.}$$

$$D = 0.017\,(\tau)^{0.25} \tag{3}$$

$$0.003 < \tau < 0.063 \text{ seconds.}$$

However, the bubble growth data from oscillating surface could be represented by one single line as shown in Figures 10 and 11.

BUBBLE GROWTH RATES

FIGURE 9	STATIONARY SURFACE BUBBLE No: 25
FIGURE 10	VIBRATING SURFACE RPM = 600, BUBBLE No: 8
FIGURE 11	VIBRATING SURFACE RPM = 1200, BUBBLE No: 4
FIGURE 12	COMPARISON BETWEEN BUBBLES No: 25, 8, 4.

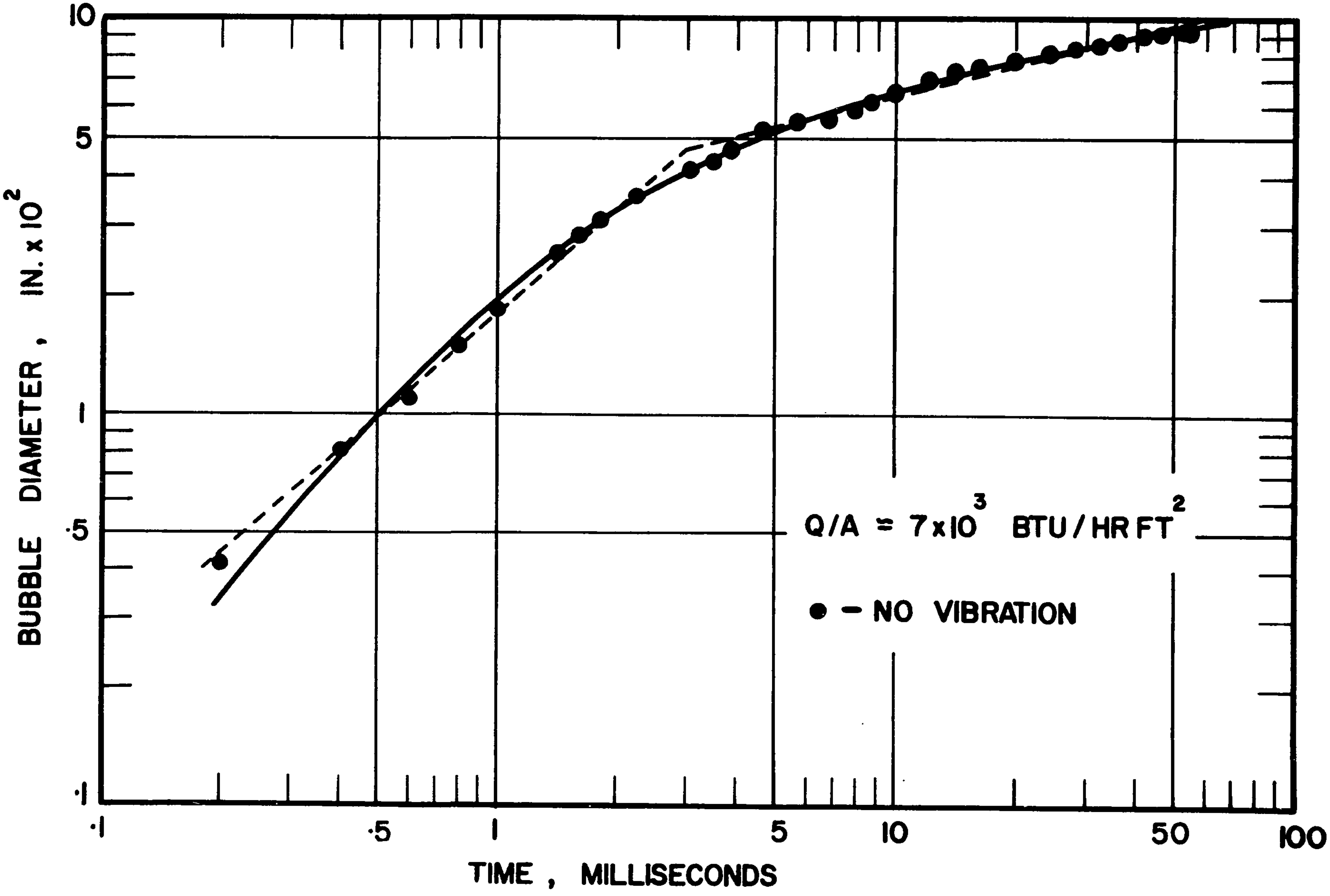
10
5
1
·5
·1
BUBBLE DIAMETER , IN. x 10^2
·1
·5
1
5
10
50
100
TIME , MILLISECONDS
Q/A ≈ 7 x 10^3 BTU / HR FT^2
● – NO VIBRATION

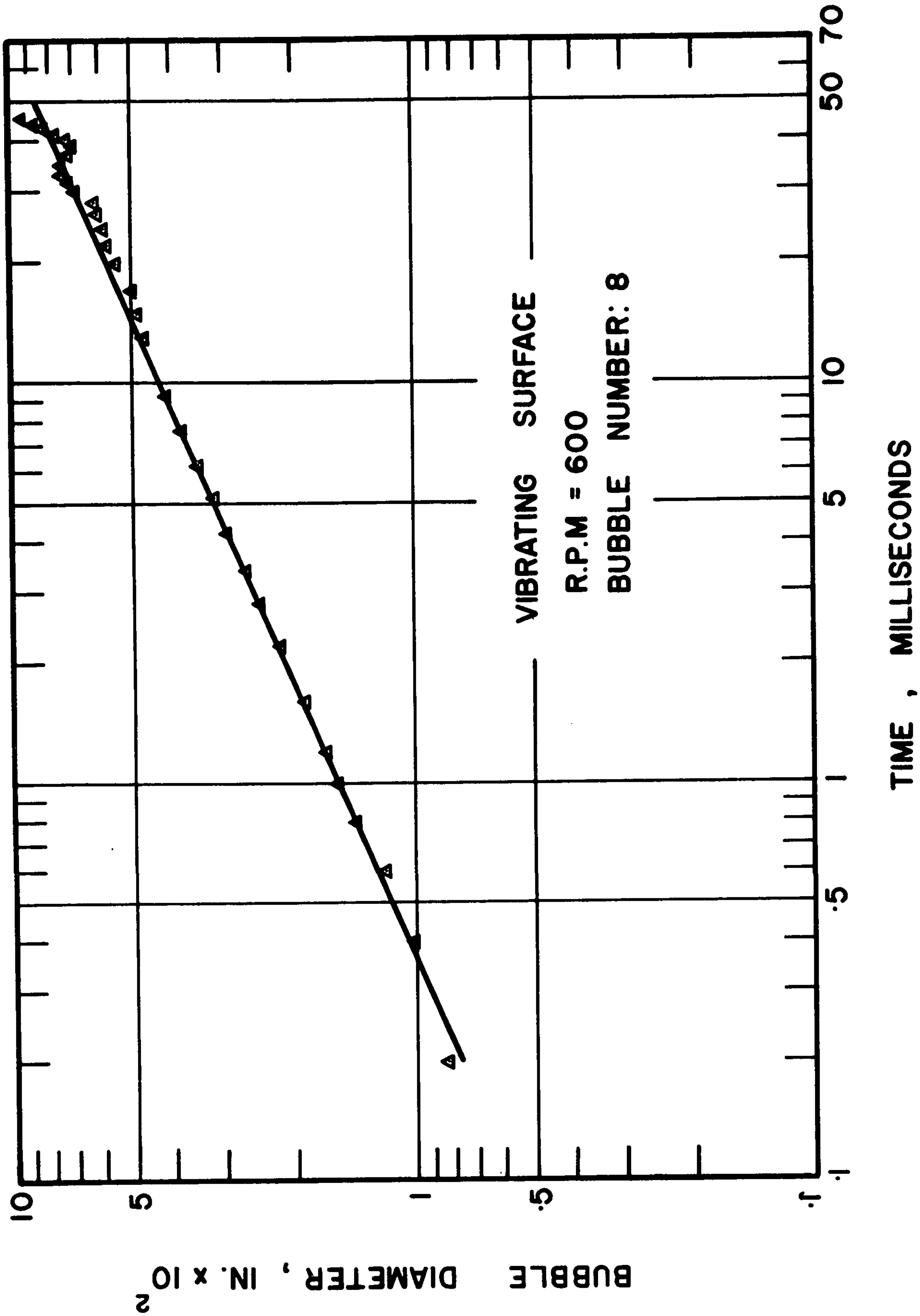
VIBRATING SURFACE
R.P.M = 600
BUBBLE NUMBER: 8
TIME , MILLISECONDS
.1
.5
1
5
10
50
70
BUBBLE DIAMETER , IN. x 10^2
10
5
1
.5
.1

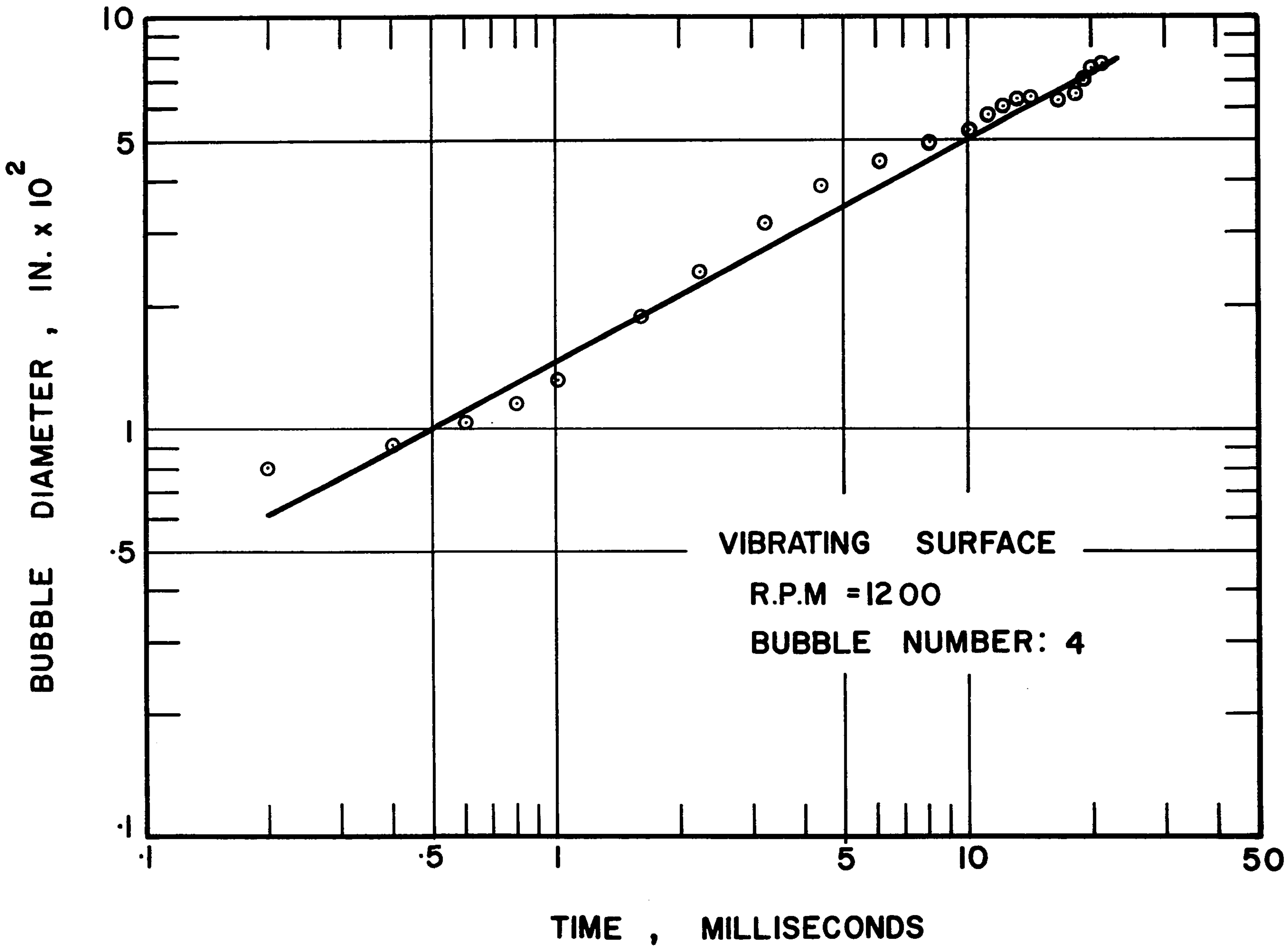
10
5
1
·5
·1
·1
·5
1
5
10
50
BUBBLE DIAMETER , IN. x 10^2
TIME , MILLISECONDS
VIBRATING SURFACE
R.P.M =1200
BUBBLE NUMBER: 4

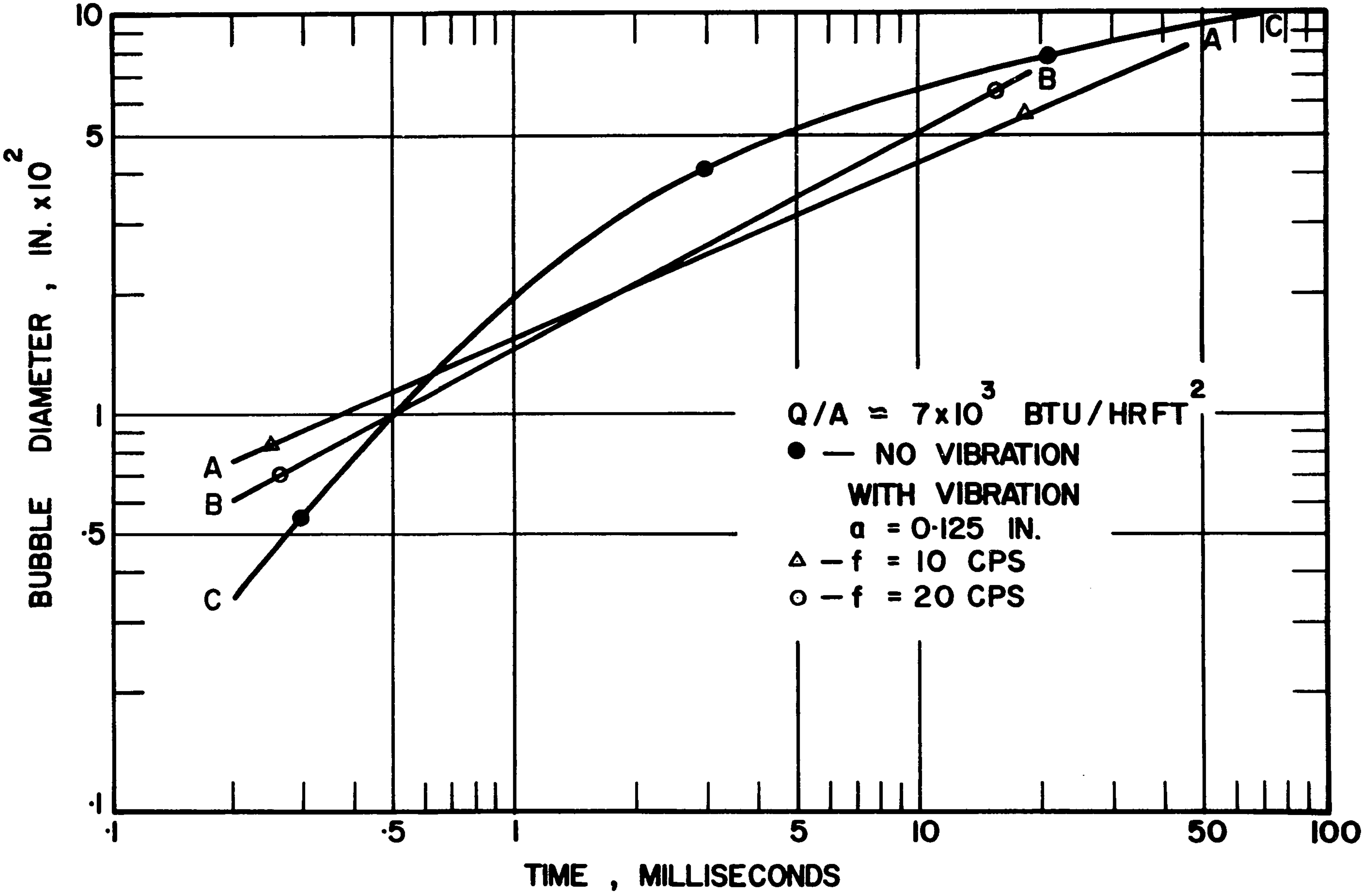
BUBBLE DIAMETER, IN. x 10^2
TIME, MILLISECONDS
10
5
1
·5
·1
·1
·5
1
5
10
50
100
A
B
C
A
B
C
Q/A ≃ 7 x 10^3 BTU/HRFT^2
● — NO VIBRATION
WITH VIBRATION
a = 0·125 IN.
△ — f = 10 CPS
○ — f = 20 CPS

The corresponding equations for bubbles no: 8 and 4 are:

$$D = 0.027\ (\tau)^{0.44} \quad (\text{RPM} = 600) \tag{4}$$

$$D = 0.052\ (\tau)^{0.54} \quad (\text{RPM} = 1200) \tag{5}$$

Variation of Bubble Base Diameter (D_b) and Contact Angle (θ)

The bubble base diameter is a measure of the area of the bubble which is in contact with the hot surface. Its variation with time for bubble No. 25 on the stationary surface is shown in Figure 13. It increased rapidly during the early stages of growth, went through a maximum, and then started to decrease slowly with time until the bubble departed from the surface. The following polynomials were found to describe the data.

$$D_b = \frac{1}{2.54 \times 12}\left(0.00213 + 67.1\ \tau - 47.54 \times 10^3\ \tau^2 + 14.54 \times 10^6\ \tau^3 - 1.545 \times 10^9\ \tau^4 \right) \tag{6}$$

$$0 < \tau < 0.0040 \text{ seconds.}$$

$$D_b = \frac{1}{2.54 \times 12}\left(0.037 + 0.3972\ \tau - 9.4\ \tau^2\right) \tag{7}$$

$$4.0 < \tau < 0.063 \text{ seconds.}$$

These analytical expressions were used for the calculation of forces for a bubble growing on a stationary surface.

The contact angle for this bubble remained essentially constant

STATIONARY SURFACE

BUBBLE No: 25

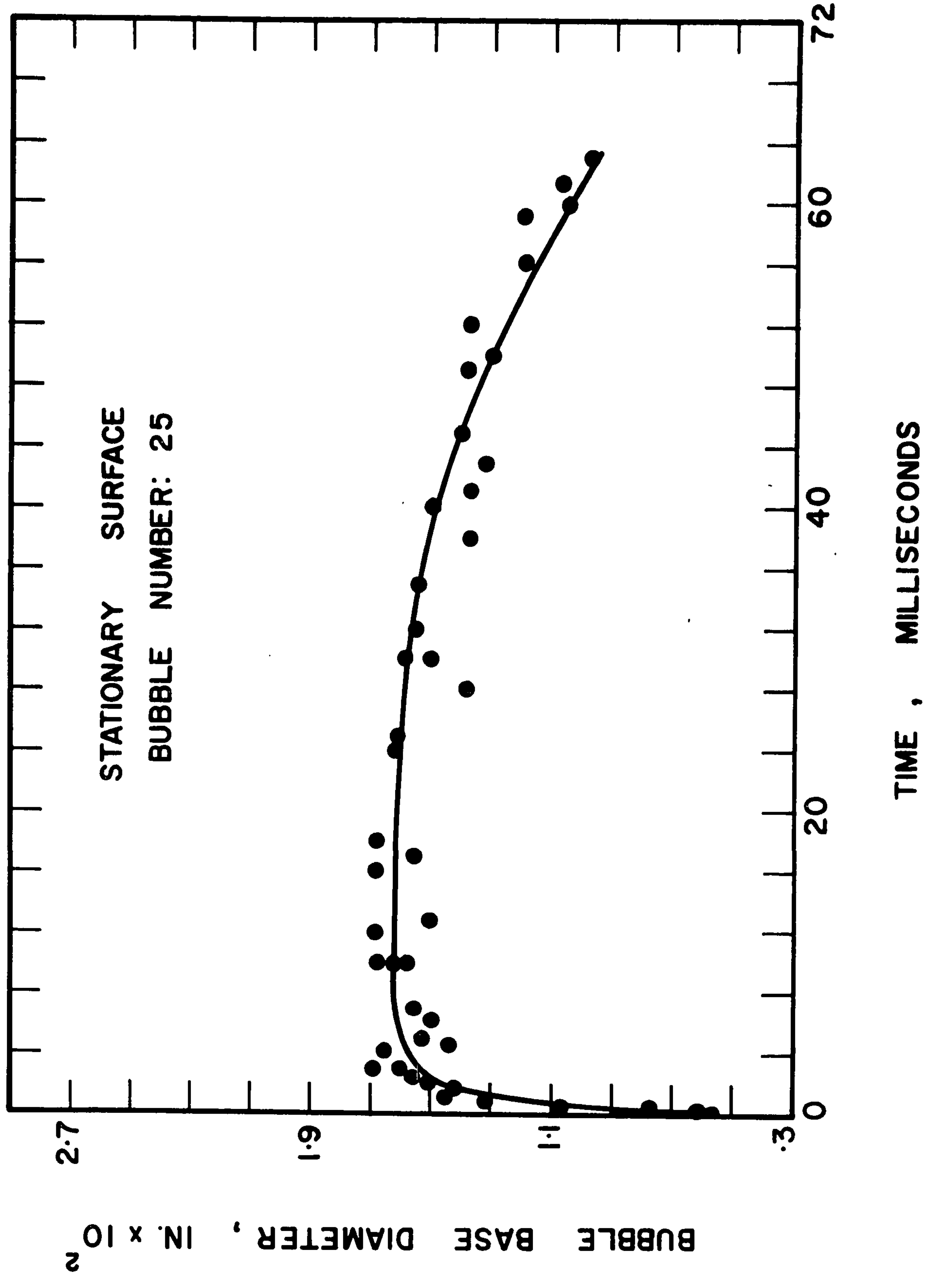
STATIONARY SURFACE
BUBBLE NUMBER: 25
TIME , MILLISECONDS
0
20
40
60
72
BUBBLE BASE DIAMETER , IN. x 10^2
·3
1·1
1·9
2·7

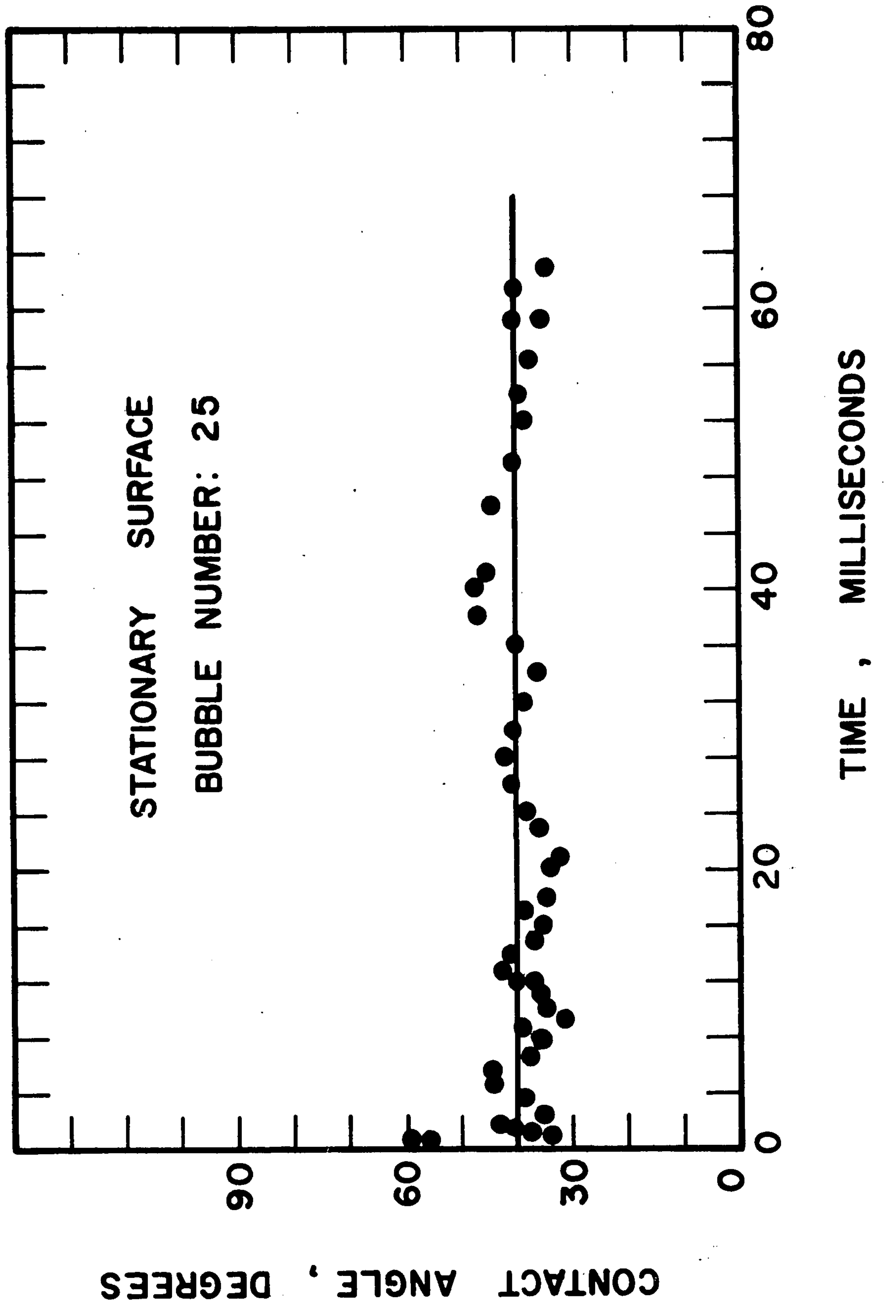
STATIONARY SURFACE
BUBBLE NUMBER: 25
TIME , MILLISECONDS
0
20
40
60
80
CONTACT ANGLE , DEGREES
0
30
60
90

during growth and fluctuated between 34-46 degrees as shown in Figure 14(p.159). An average value of 40.19 degrees was used for the calculation of forces.

$$\theta = 40.19^{\circ} \tag{8}$$

Oscillations of the surface caused considerable change in the behaviour of the base diameter and contact angle as shown in Figures 15, 16, 17 and 18. These oscillations start to predominate after the bubble has grown to about half of its full growth. The cyclic variation in D_b (and correspondingly in θ) continued to increase in magnitude until the bubble broke off and this bubble release was usually preceded by a peak in base diameter. Moreover, it was also evident that such oscillations were much lower in amplitude and frequency when the RPM was increased from 600 to 1200. The close observation of the high speed films suggests that these oscillations are due to the interaction of heat transfer surface, vibration and the bubble whose behaviour follows the latter. Due to these drastic oscillations in D_b and θ, no attempt was made to fit any order of polynomials. Instead, the actual experimental values obtained for D_b and θ were substituted directly in the analysis of the force balances in order to obtain a more accurate time-dependent force balance. Because of the uncertainty in real mechanism, this procedure would definitely be more accurate than using any mathematical functions for D_b and θ.

VIBRATING SURFACE

RPM = 600

BUBBLE No: 8

FIGURE 15 BUBBLE BASE DIAMETER VERSUS TIME

FIGURE 16 CONTACT ANGLE VERSUS TIME

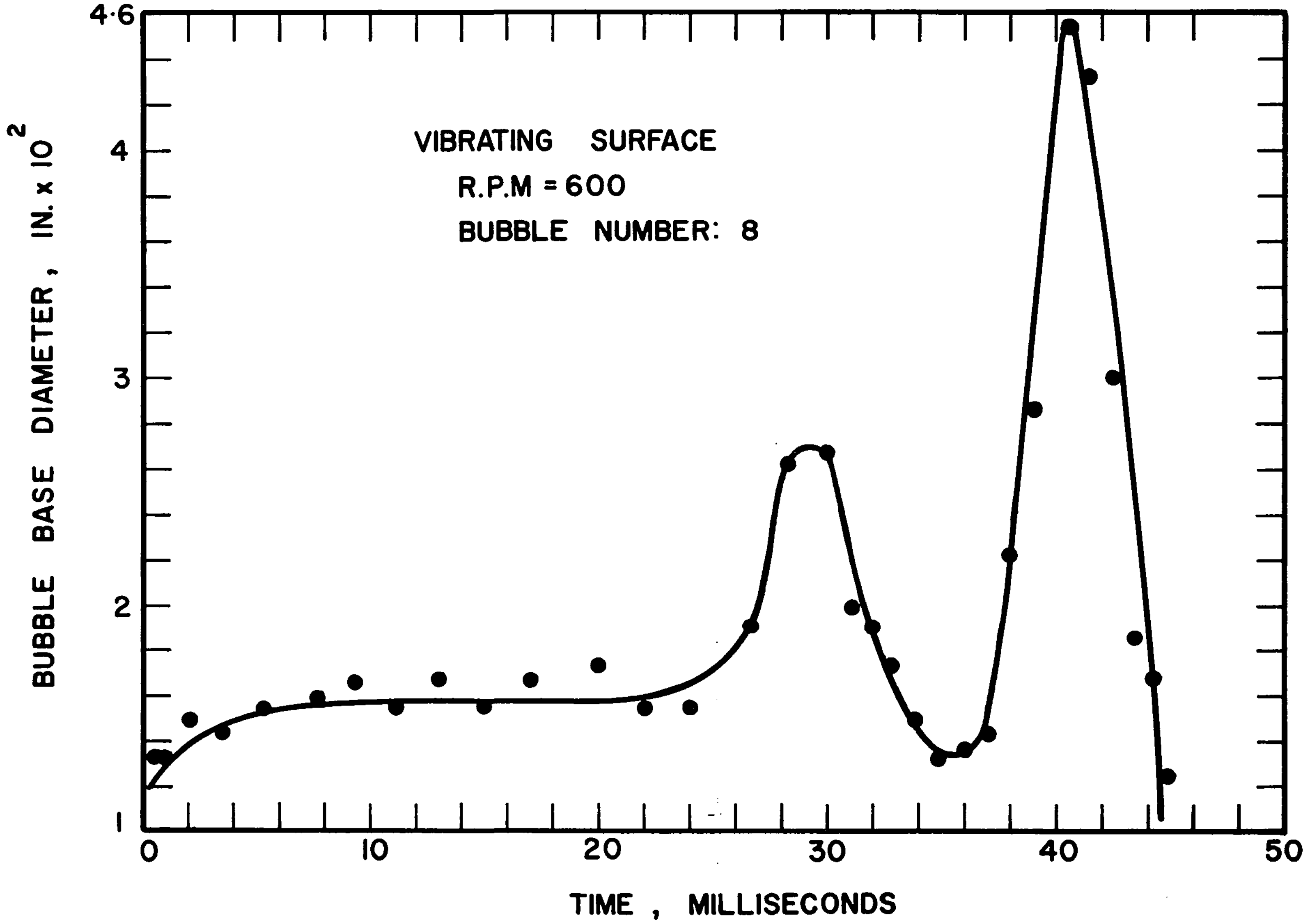
VIBRATING SURFACE
R.P.M = 600
BUBBLE NUMBER: 8
BUBBLE BASE DIAMETER, IN. x 10^2
4·6
4
3
2
1
0
10
20
30
40
50
TIME, MILLISECONDS

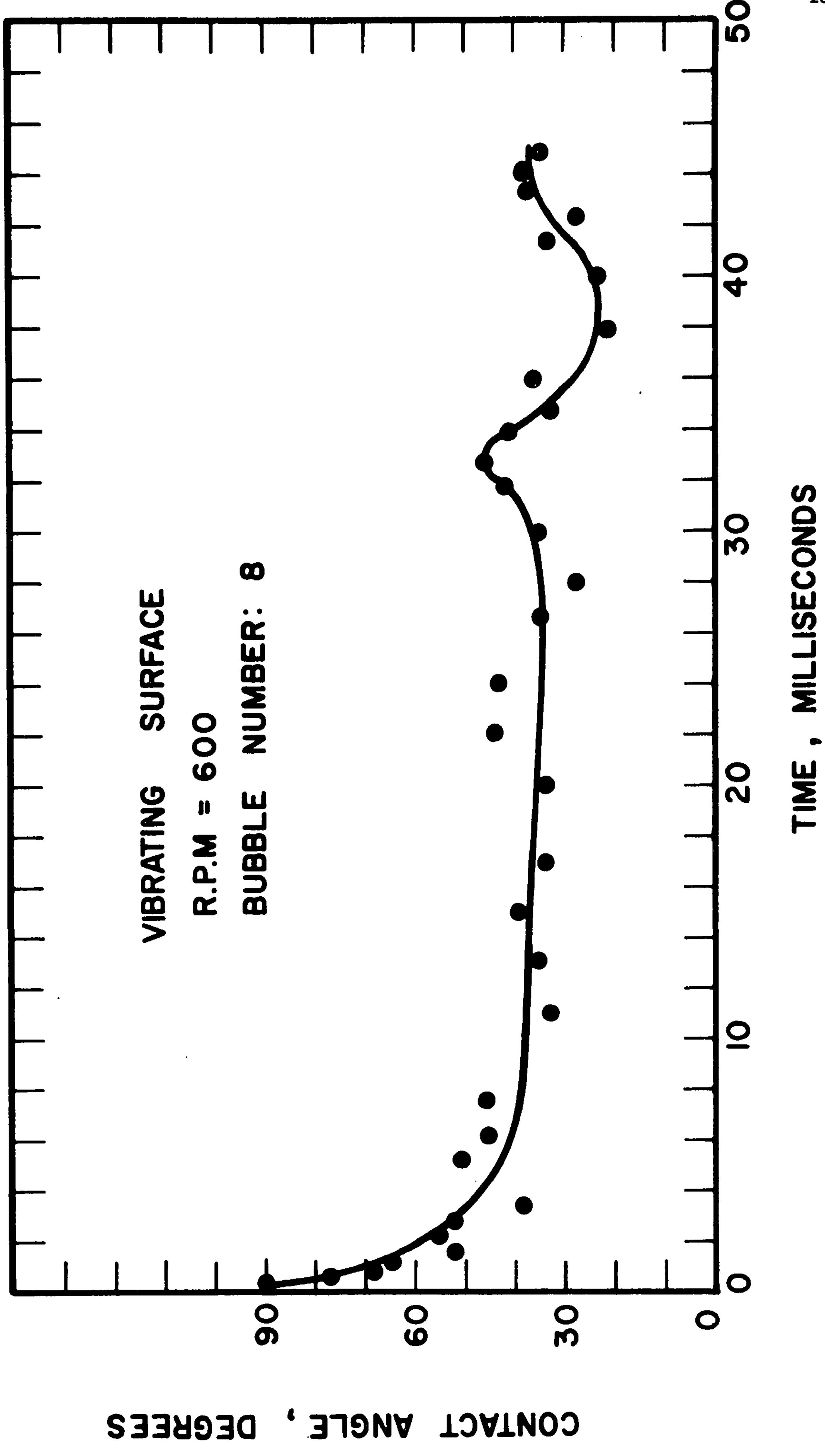
VIBRATING SURFACE
R.P.M = 600
BUBBLE NUMBER: 8
TIME , MILLISECONDS
0
10
20
30
40
50
CONTACT ANGLE , DEGREES
90
60
30
0

VIBRATING SURFACE

RPM = 1200

BUBBLE No: 4

FIGURE 17 BUBBLE BASE DIAMETER VERSUS TIME

FIGURE 18 CONTACT ANGLE VERSUS TIME

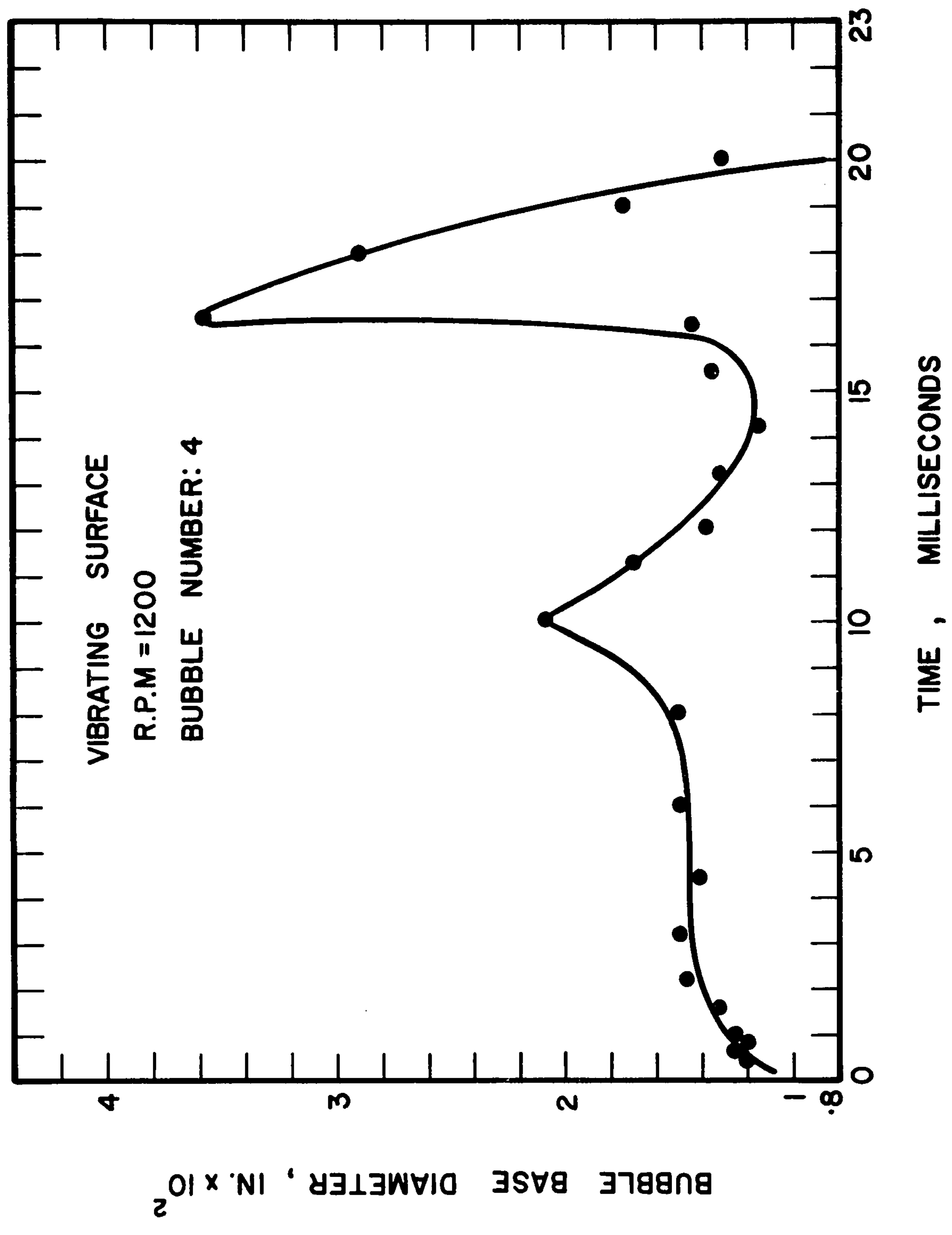
VIBRATING SURFACE
R.P.M = 1200
BUBBLE NUMBER: 4
TIME , MILLISECONDS
0
5
10
15
20
23
BUBBLE BASE DIAMETER , IN. x 10^2
.8
1
2
3
4

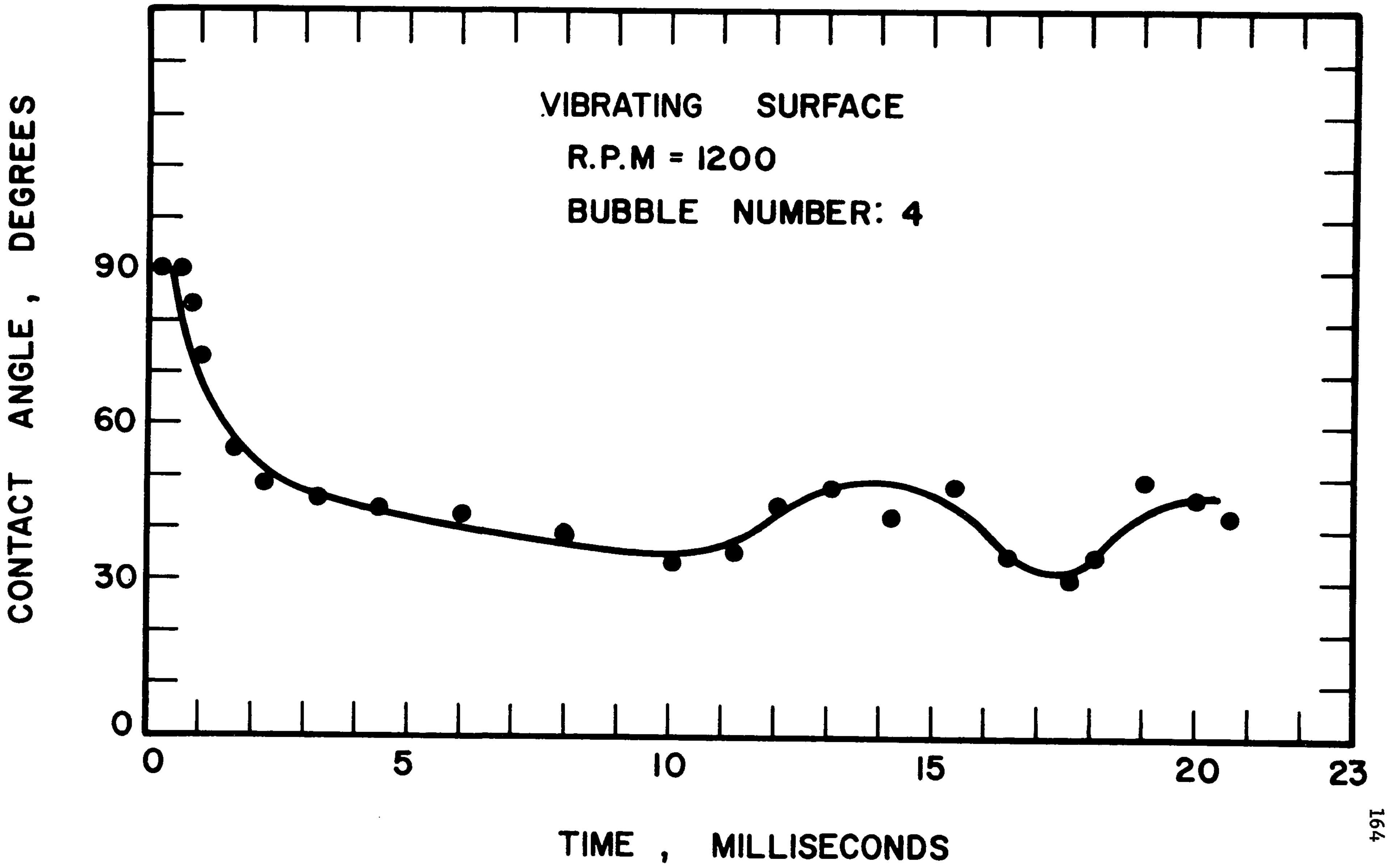
VIBRATING SURFACE
R.P.M = 1200
BUBBLE NUMBER: 4
CONTACT ANGLE , DEGREES
90
60
30
0
0
5
10
15
20
23
TIME , MILLISECONDS

FORCES ACTING ON A BUBBLE

1. Inertia

During the growth of a bubble the inertia force pushes the surrounding liquid outwards. Han and Griffith(4) have shown that the apparent mass of the affected liquid is $\frac{11}{16}$ of the total volume a bubble would occupy. And hence,

$$F_{\text{INERTIAL}} = \frac{d}{d\tau}(mu) = \frac{d}{d\tau}\left[\left(\frac{11}{16}\frac{\rho_L}{g_n}\frac{\pi D^3}{6}\right)\frac{1}{2}\left(\frac{dD}{d\tau}\right)\right]$$

$$= \frac{11}{192}\frac{\pi\,\rho_L}{g_n}\left[D^3\frac{d^2D}{d\tau^2} + 3D^2\left(\frac{dD}{d\tau}\right)^2\right] \qquad (9)$$

2. Buoyancy

Wark, I.W.(5) and Sullivan, S.L., Jr.et al.(6) have derived an equation for the buoyancy force acting on a spherical bubble attached to a surface. This is expressed as:

$$F_{\text{BUOYANCY}} = \frac{\pi D^3}{6}(\rho_L - \rho_V)\frac{g}{g_n} + (p_b - P_b)\frac{\pi D_b^2}{4} \qquad (10)$$

Keshock and Siegel(7) subsequently suggested that the radius of curvature at the bubble base is significantly larger than the bubble radius, and thus deduced a simplified form of Equation (10) which is given by:

$$F_{BUOYANCY} = \frac{\pi D^3}{6}(\rho_L - \rho_V) \frac{g}{g_n} + \frac{\pi D_b}{2} \sigma \sin \theta \qquad (11)$$

3. Surface Tension

The surface tension force which holds the bubble base to the surface is given by

$$F_{SURFACE\ TENSION} = \pi D_b \sigma \sin \theta \qquad (12)$$

4. Drag

Only a very rough estimate of the drag force for a growing bubble could be made. A bubble growing on the surface was assumed to behave as a spherical vapour bubble rising through the liquid with a velocity equal to its change of radius with time. This assumption is only approximate since the top of the bubble has an upward velocity closer to $(\frac{dD}{d\tau})$, while the remaining portions of the bubble have upward velocities ranging between $(\frac{dD}{d\tau})$ and zero. Also, a bubble freely rising through a liquid has a wake associated with it, and hence the use in the present case of a drag coefficient obtained from a freely rising bubble will tend to make the computed drag larger than that actually present. The drag coeffecient for a freely rising bubble has the form $C_d = \frac{a}{Re}$ where $a = 45$. The Reynolds number for the growing bubble is computed as a function of time from:

$$Re = \frac{\rho_L \; D}{2 \; \mu_L} \left(\frac{dD}{d\tau}\right) \tag{13}$$

$$F_{DRAG} = \frac{1}{2} \frac{\rho_L}{g_n} C_d \frac{\pi D^2}{4} \left(\frac{1}{2} \frac{dD}{d\tau}\right)^2$$

$$= \frac{\pi}{16} \frac{a}{g_n} \mu_L D\left(\frac{dD}{d\tau}\right) \tag{14}$$

When the vibration is imposed on the heat transfer surface, additional inertia and drag forces must be taken into account. An additional drag is caused due to the vibration induced bulk movement of the bubble in the liquid. This force $F_{DRAG\ VIB.}$ takes the form of

$$F_{DRAG\ VIB.} = \frac{1}{2} \frac{\rho_L}{g_n} C_d \frac{\pi D^2}{4} v_s \tag{15}$$

where v_s is the slip velocity between the bubble and the surrounding liquid caused by the motion of the heat transfer surface. As before

$$C_d = \frac{45}{Re}$$

where

$$Re = \frac{D \; v_s \; \rho_L}{\mu_L} \tag{16}$$

Hence,

$$F_{DRAG} = \frac{45}{2} \left[\mu_L \left(\frac{\pi D}{4}\right) v_s \right] \tag{17}$$

Assuming that the slip velocity v_s is related to the traversing velocity of the heat transfer surfaces V_s, by the factor of ℓ, one obtains:

$$\frac{F_{DRAG\ VIB.}}{F_{DRAG}} = 2\,\ell\,\frac{V_s}{\left(\frac{dD}{d\tau}\right)} \tag{18}$$

The value of ℓ's for each condition of vibration is not known, although they are assumed to be much smaller than unity, due to the relatively large projected area of the heat transfer surface compared to that of the bubble; the vertical component of local velocity on and at the centre of a large flat surface which is moving vertically could be safely estimated to be negligible. The calculations made with $\ell = 1$ also show that $F_{DRAG\ VIB.}$ is very small in magnitude.

The inertia force due to vibration, which really is the initial cause for the above mentioned drag force and hence the balancing force for the latter, is again believed to be small. Altogether, the contribution of these forces to the overall force balance is virtually nil. However, the slight compression and stretching experienced by the bubble during the upward and downward motion of the surface respectively, would contribute significantly to the oscillation of base diameter D_b and contact angle Θ. Surface tension-controlled elastic rebounding of the bubble takes place upon the initial deformation of the bubble and due to this vibration-induced inertia and drag forces, and the cyclic oscillation of bubble dimensions is thus triggered. No further mathematical treatment of the oscillation phenomenon will be attempted in the present case.

FORCE BALANCES

Substituting the emperical equations for $\dot{D}$ and D_b, i.e., Equations (2), (3), (6), (7) and the value $\theta = 40.19$ degrees into Equations (9), (11), (12) and (14), the forces acting on a growing bubble from the stationary surface were first calculated. The results obtained are shown in Figure 19.

As may be seen from the figures, the initial rapid rate of bubble growth causes a maximum in the inertia force which is balanced by the interfacial tensions and the drag forces. The interfacial tension is increased through the increase in the bubble base area. As the bubble diameter increases, however, the buoyancy force will grow correspondingly which eventually approach the value of surface tension, since the inertia force and drag force effects become minimal by this time. The bubble diameter is now described by Equations (3); past its fast period of growth. Since the bubble has become quite large, and the centre of the bubble, has accordingly moved further upward, neck formation is initiated.

In Figure 19, it appears that the upward total force as dominated by the buoyancy force, far surpasses the downward force which consists mostly of interfacial tension, but the fact that this picture is in error is obvious from the force balance considerations. The increasing disparity between the buoyancy and interfacial tension forces is attributed to the initial assumption of the sphericity of the bubble. In reality , the

FIGURE 19

FORCES ACTING ON A BUBBLE

STATIONARY SURFACE

BUBBLE No: 25

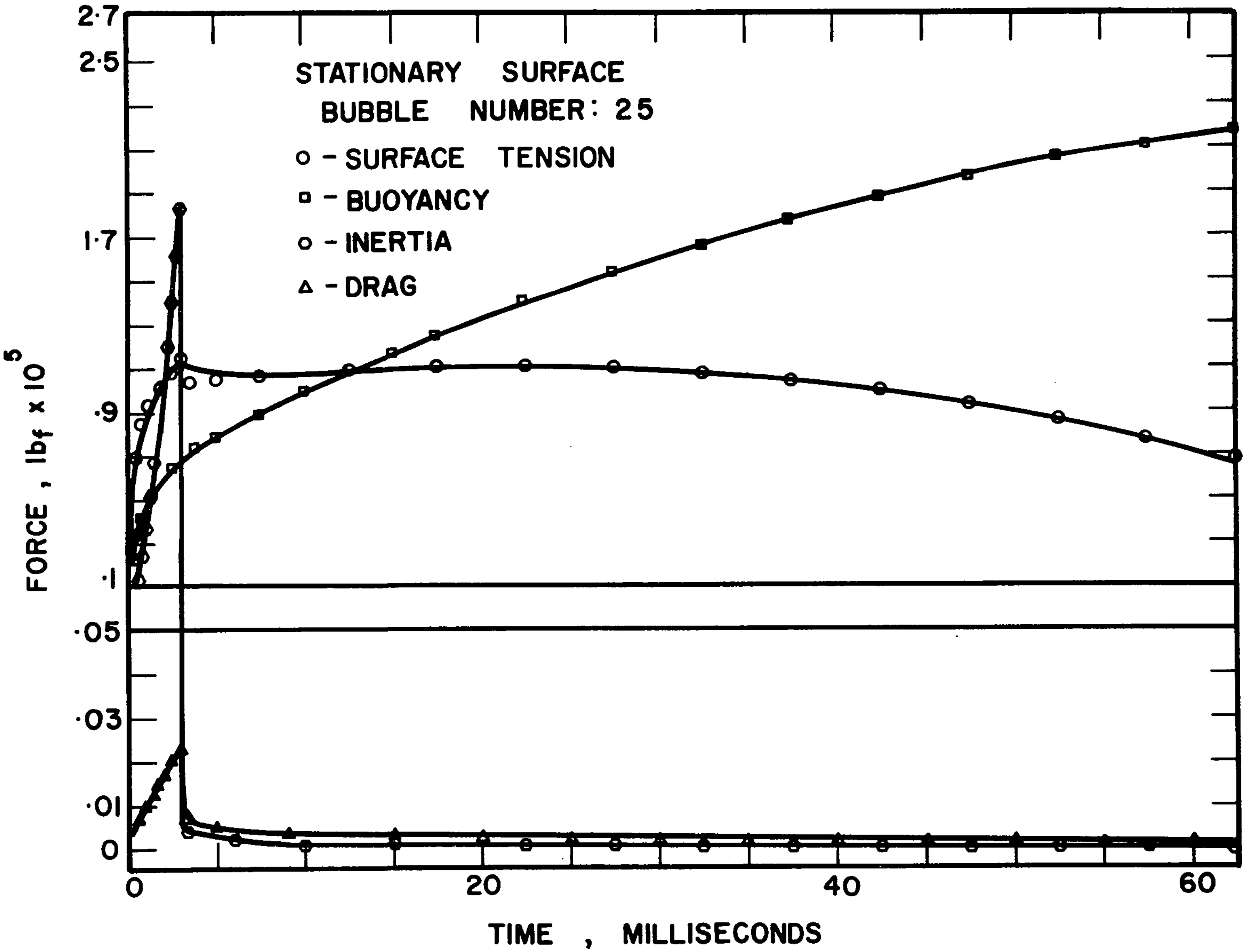
STATIONARY SURFACE
BUBBLE NUMBER: 25
○ - SURFACE TENSION
□ - BUOYANCY
○ - INERTIA
△ - DRAG
FORCE, $lb_f \times 10^5$
TIME, MILLISECONDS
2·7
2·5
1·7
·9
·1
·05
·03
·01
0
0
20
40
60

bubble is far from a sphere. The inertia and drag forces are negligible except during the initial growth period of the bubble.

In order to establish the force balance on a bubble growing from a vibrating heat transfer surface, the empirical equations for D i.e. Equations (4), (5) and the instantaneous values of D_b and Θ were substituted into Equations (9), (11), (12) and (14) as previously mentioned. Thus the trend shown in Figures 20 and 21 for 600 and 1200 RPM respectively, should be considered to be merely indicative of what is happening in the physical picutre. Contrary to the case of stationary surfaces, the early growth rate is not very rapid and hence the initial surge of inertia force and the drag force are non-existent. The cyclic oscillation of the bubble is initiated earlier for the case of 1200 RPM then for 600 RPM, due to the increased vibration-induced inertia and subsequent elastic rebounding of the bubble. As mentioned earlier, the magnitude of such an inertia (second kind of inertia due to vibration) is small, but its influence in triggering the oscillation of the bubble shape as exemplified by the variations of D, D_b and Θ, is striking. The increased oscillation subsequently contributes to earlier detachment of the bubble from the surface. The observed discrepancies in the overall force balance as seen in Figures 20 and 21 are comparatively less than for a stationary surface. The discrepancies observed in Figures 20 and 21 are again due to be the oversimplified assumption made on the bubble shape.

FIGURE 20

FORCES ACTING ON A BUBBLE

VIBRATING SURFACE
RPM = 600

BUBBLE No: 8

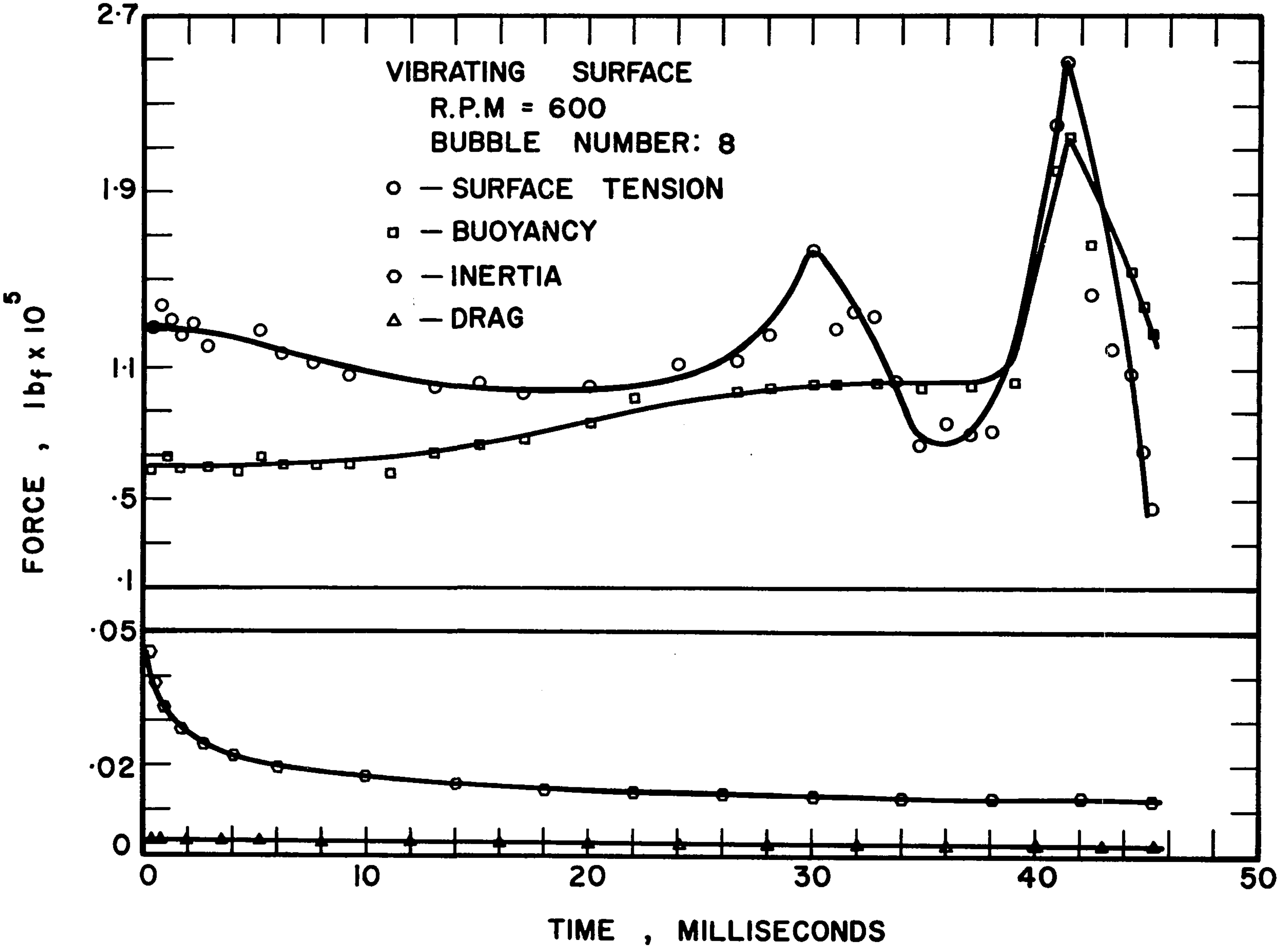
VIBRATING SURFACE
R.P.M = 600
BUBBLE NUMBER: 8
○ — SURFACE TENSION
□ — BUOYANCY
○ — INERTIA
△ — DRAG
FORCE , $lb_f \times 10^5$
TIME , MILLISECONDS
2·7
1·9
1·1
·5
·1
·05
·02
0
0
10
20
30
40
50

FIGURE 21

FORCES ACTING ON A BUBBLE

VIBRATING SURFACE

RPM = 1200

BUBBLE No: 4

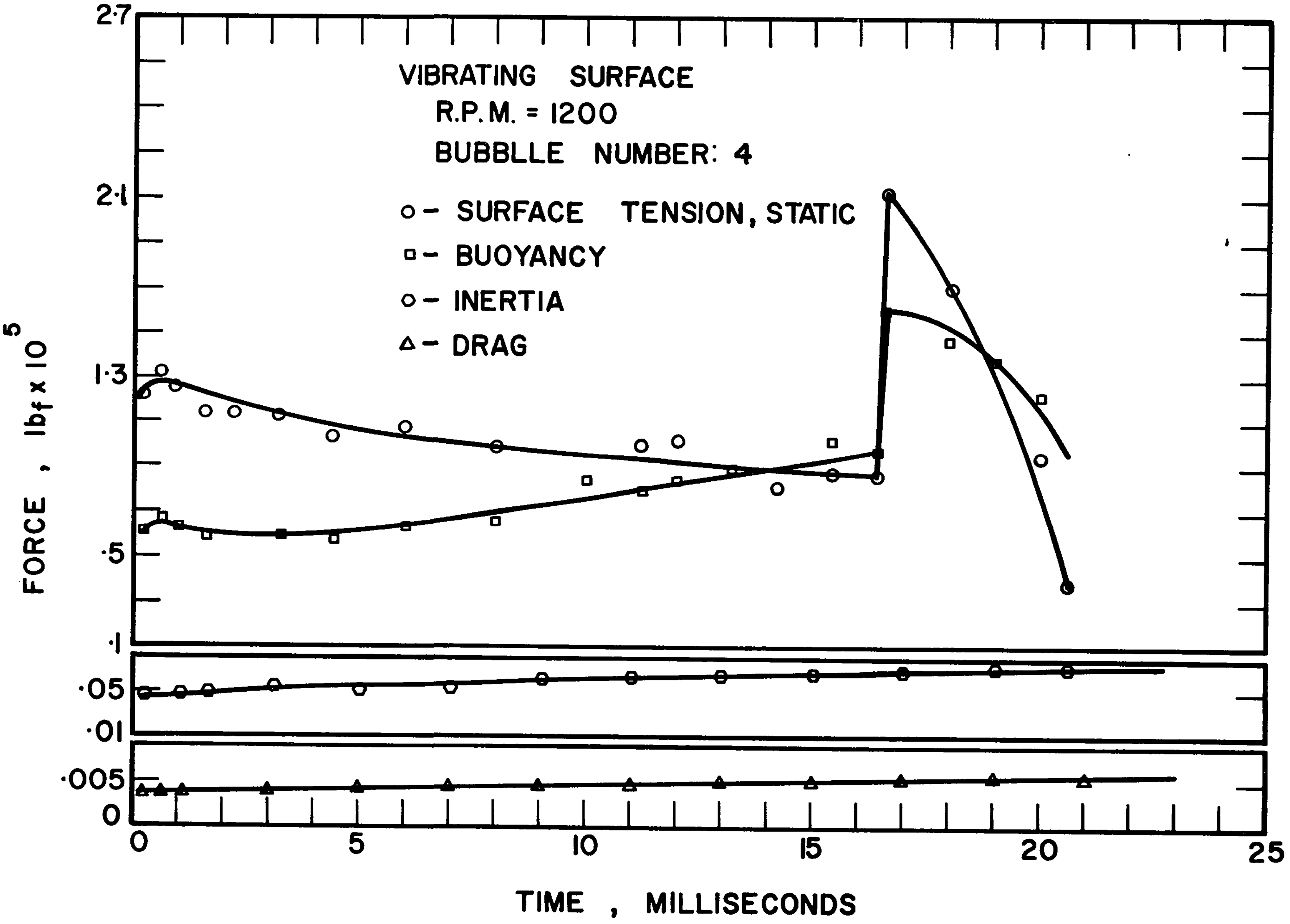
VIBRATING SURFACE
R.P.M. = 1200
BUBBLLE NUMBER: 4
○ – SURFACE TENSION, STATIC
□ – BUOYANCY
○ – INERTIA
△ – DRAG
2·7
2·1
1·3
·5
·1
·05
·01
·005
0
0
5
10
15
20
25
FORCE , $lb_f \times 10^5$
TIME , MILLISECONDS

CONCLUSIONS

The general observations as well as the frame to frame analysis of high speed pictures, show some insight into the behaviour of a single bubble formed on a stationary and vibrating heat transfer suface.

1. In the case of a stationary surface, the inertia and the drag force reach a peak in the early stages of bubble growth. Henceforth, these forces decrease and the buoyancy and interfacial tension forces dominate the force balance. There are two distinctive stages of bubble growth rate as formulated by Equations (2) and (3). A relatively slow process of neck formation immediately precedes the detachment of the bubble from the surface.

2. When the heat transfer surface is vibrated, there are developed additional drag and inertia forces due to the acceleration of the surface. Compared to the inertia and drag forces caused by the radial expansion of the bubble, the relative magnitudes of the forces of the second kind (due to vibration) are estimated to be small. However, they contribute significantly to the early initiation of the cyclic fluctuations in bubble dimensions and thus the associated forces. Contrary to the case of a stationary surface, no early upsurge of inertia and drag of the first kind (radial expansion-induced) is observed. The growth rate can be represented by a single curve, i.e., Equation (4) for 600 RPM and Equation (5) for 1200 RPM. The overall growth is faster and bubble detachment comes earlier for vibrating surfaces, and these trends are enhanced with increasing frequency and amplitude.

3. The spherical model of the bubble is a gross distortion of the real picture, and contributes further to the apparent discrepancies observed in the overall force balance for both stationary and vibrating surfaces.

4. Finally, the surface temperature at which the interfacial tension is computed, is expected to vary during the bubble growth period, and this also is believed to contribute to the discrepancies.

NOMENCLATURE

ROMAN SYMBOLS

a - horizontal diameter of the bubble on a projection screen, cm

b - vertical distance between the top of the bubble to the heat transfer surface, on a projection screen, cm

c - bubble base diameter on a projection screen, cm

CPS - cycles per sec

C_d - drag coefficient, dimensionless

D - actual mean diameter of bubble, ft

D_b - actual bubble base diameter, ft

F - force, lb_f .

f - gravitational constant, ft/sec^2

g_n - conversion constant, $lb_m\ ft/lb_f\ sec^2$

k - constant

ℓ - factor, dimensionless

m - apparent mass of the bubble, lb_m

n - constant, exponent

p_b - pressure inside bubble at its base lb_f/ft^2

P_b - pressure outside bubble at its base lb_f/ft^2

RPM - revolutions per minute

u - rate of increase of bubble radius, ft/sec

v_s - slip velocity between bubble and liquid due to surface vibration, ft/sec

V_s - traverse velocity of heat transfer surface, ft/sec.

GREEK SYMBOLS

θ - contact angle, degrees

ρ - density, lb_m/ft^3

σ - surface tension, lb_f/ft

μ - viscosity, lb_m/ft sec

τ - time, sec

SUBSCRIPTS

L - liquid

V - vapour

REFERENCES

1. Hummel, R.L., U.S. Patent Application 247; 975 (1962)
2. Hummel, R.L., Paper presented at Chem. Inst. Canada Conf. Sarnia, Canada (1962)
3. Staniszewski, B.E., TR 16 Mass. Inst. Tech., Aug. 1959.
4. Han, C.Y. and P. Griffith. TR 19 Mass. Inst. Tech; Feb. 1962.
5. Wark, I.W., J. Phys. Chem; 37; 623 (1933).
6. Sullivan, S.L. Jr., B.W. Hardy, and C.D. Holland, A.I.Ch.E. paper 31E, Dec. 1963.
7. Keshock, E.G., and R. Siegel. NASA - TN - D 2299, 1964.

SUMMARY AND CONTRIBUTION TO KNOWLEDGE

The effect of surface vibrations on convective and nucleate boiling heat transfer from electrically heated, horizontal, platinum wires (diameter = 0.010 in.) were investigated. The overall range of frequency was from 20 to 80 CPS and amplitude of vibration from 0.035 to 0.08 in. Data were taken using distilled water at 118.4°F and 170.6°F and methanol at 95°F.

1. With the imposition of vertical oscillations on horizontal wires three distinct regions were noticed; forced convection, transition and fully developed boiling. For the region of forced convection an increase in heat flux of up to ten fold was observed. This effect diminished with the increase in temperature difference. In the fully developed boiling region, the oscillations had no effect.

2. A mathematical model, based on the theory of nucleation and bubble growth, was solved which determined successfully the incipient point under a given set of conditions. This was then used to predict the boundaries between convective and boiling heat transfer regions.

3. The correlations of the heat transfer data for each individual region are as follow :

(i) Forced Convection Region:

The conventional correlation using $(Nu)\ (Pr)^{-0.3} = \phi(Re)$ was found to be valid only for one particular fluid and completely failed when extended to another fluid. On the other hand, the parameter, $\frac{Gr}{Re^2}$, did not measure the relative influence of free and forced convection in the various fluids. A dimensionless expression

$$\frac{Nu_V}{(Pr)^{0.72}(Gr)^{-0.06}} = 0.32\,(Pr)^{1.08} + 0.06\,(Re)^{0.86}$$

correlated the data.

(ii) Fully Developed Boiling Region:

Values of the constants for the Rohsenow-type pool boiling correlations were determined for the present system. The data for water and methanol with different degrees of sub-cooling were correlated as:

$$\frac{C_{pL}\,T_x}{h_{fg}} = 0.016\left[\frac{(Q/A)}{\mu_L\,h_{fg}}\sqrt{\frac{\sigma\quad g_o}{(\rho_L-\rho_V)g}}\right]^{0.3}(Pr_L)^{1.0}$$

for water,

and

$$\frac{C_{pL}\,T_x}{h_{fg}} = 0.00307\left[\frac{(Q/A)}{\mu_L\,h_{fg}}\sqrt{\frac{\sigma\quad g_o}{(\rho_L-\rho_V)g}}\right]^{0.147}(Pr_L)^{1.7}$$

for methanol.

(iii) Transition Region:

A Rohsenow-type expression for fully developed nucleate boiling was successfully combined with an expression for the oscillation-induced forced convection to interpret the heat flux for the transition region. Considering the complexity of the problem the agreement is good.

4. The statistical behaviour of ebullition cycles of bubbles growing on a vibrating wire was studied. The experimental conditions for water at 100°C were; wire frequency = 45 CPS, amplitude = 0.0492 in., and heat flux = 1×10^5 Btu/hr ft^2 .

The vibration of the wire resulted in a larger number of smaller bubbles covering the surface of the heater. The distribution of generating period and bubble diameter at break-off could be represented by normal distributions:

$$N = \frac{1}{0.4997\sqrt{2\pi}} e^{-\frac{1}{2}\left(\frac{\tau_g \times 10^{-3} - 1.7123}{0.4997}\right)^2}$$

for generating time,

and

$$N = \frac{1}{0.0048\,\sqrt{2\pi}} e^{-\frac{1}{2}\left(\frac{d - 0.0334}{0.0048}\right)^2}$$

for diameter at break-off.

A slight increase in bubble emission frequency was noticed. It appeared that the oscillations of the wire controlled the start of nucleation and hence the waiting period.

5. The study of the dynamics of boiling bubbles from vibrating surfaces was carried out for water at 212°F. The amplitude of vibration was 0.125 in. and the frequencies were 10 and 20 CPS. At a heat flux of 3×10^7 Btu/hr ft^2, high speed photographs were taken of bubbles generated from an artificial active site on the heat transfer surface. Pertinent

bubble dimensions were measured during their growth to compute the magnitude of the forces that would significantly influence their behaviour.

(i) For a stationary surface, the inertia and drag forces were found to be important in the early stages and henceforth became negligible. The buoyancy and interfacial tension forces dominated the force balance. A slow process of neck formation precedes the detachment of the bubble from the surface.

(ii) When the surface was vibrated, additional drag and inertia forces were developed. The relative magnitudes of these forces were estimated to be small. However,they contributed significantly to the early initiation of a cyclic fluctuation in bubble dimensions and thus, the associated forces. The overall growth was faster and bubble detachment came earlier. These trends are enhanced with increasing frequency and amplitude.

SUGGESTIONS FOR FUTURE WORK

1. Although it has been established that the increase in heat transfer rate is due to the change in the character of flow in the neighbourhood of the heat transfer surface, no mechanism through which vibrations interact with the fluid has been proposed. Any attempt to formulate the complete analysis of the flow problem will be of great assistance in establishing the theoretical equations for heat transfer from vibrating surfaces to fluids.

2. As pointed out in the analysis of the forced convection data that Prandtl number dictates the thickness and the temperature profile of the boundary layer. It is therefore suggested that a theoretical analysis to determine quantitatively the Prandtl number effects on thermal boundary layer be investigated to improve upon the empirical correlation proposed for vibration-induced forced convection correlation.

3. There exist several subdivisions in nucleate boiling. Thus in order to describe the complete nucleate boiling curve of heat flux versus temperature difference, it is evident that studies of each regime should be made individually.

4. The study of Bubble Dynamics from vibrating surfaces should be extended especially to study the problems pertaining to the hydrodynamic phenomenon induced by bubbles and the vibrating surfaces.

5. A regulated D.C. power supply with increased amperage output could be used so that more data can be obtained for distilled water in the high

heat flux regions. With a large D.C. power supply, larger platinum wire diameters can be used as heating elements in measuring the heat transfer effects.

6. It is suggested that heat transfer data should be obtained using a forced convection system as it may have more industrial significance.

APPENDIX A

HEAT TRANSFER DATA

TABLE A-1

LIQUID: METHANOL

TEMPERATURE: 95.0°F

AMPLITUDE: 0

WIRE DIA: 0.010 in.

$L = 1\frac{1}{32}$ in.

$R_{100} = 0.0705$ Ohm

FREQUENCY: 0 CPS

V Volts	EDC Volts	EAC Volts	ΔT °F	(Q/A) Btu/(hr)(ft^2)	$(Q/A)_{NC}$ Btu/(hr)(ft^2)	Nu_o	X	$(Q/A)_{boil}$ Btu/(hr)(ft^2)	Y_1	X_1
0.0330	0.0978	-	15.67	3,647	-	1.662	-	-	-	-
0.0342	0.1017	-	16.69	3,909	-	1.673	-	-	-	-
0.0375	0.1120	-	19.91	4,757	-	2.408	-	-	-	-
0.0411	0.1233	-	23.56	5,703	-	1.230	-	-	-	-
0.0492	0.1505	-	32.48	8,353	-	1.854	-	-	-	-
0.0657	0.2085	-	53.31	15,511	-	2.129	-	-	-	-
0.0712	0.2288	-	60.31	18,402	-	2.218	-	-	-	-
0.0789	0.2565	-	67.54	22,800	-	2.485	-	-	-	-
0.1377	0.4062	-	83.85	71,314	-	-	-	71,314	0.8681	0.002550
0.1522	0.5102	-	85.68	87,388	-	-	-	87,388	1.0638	0.002776
0.1588	0.5335	-	87.03	95,341	-	-	-	95,341	1.1606	0.002894
0.1667	0.5600	-	86.98	105,056	-	-	-	105,056	1.2789	0.002890
0.1765	0.5937	-	87.83	117,935	-	-	-	117,935	1.4357	0.002965
0.1863	0.6295	-	90.54	131,979	-	-	-	131,979	1.6066	0.003202
0.1965	0.6645	-	91.03	146,945	-	-	-	146,945	1.7888	0.003245
0.2043	0.6900	-	90.25	158,640	-	-	-	158,640	1.9312	0.003177
0.2112	0.7158	-	92.39	170,130	-	-	-	170,130	2.0711	0.003364
0.2210	0.7498	-	93.03	186,481	-	-	-	186,481	2.2701	0.003420
0.2283	0.7746	-	93.06	199,012	-	-	-	199,012	2.4227	0.003423
0.2384	0.8100	-	93.92	217,319	-	-	-	217,319	2.6455	0.003498
0.2505	0.8530	-	95.28	240,465	-	-	-	240,465	2.9273	0.003618
0.2702	0.9216	-	96.30	280,236	-	-	-	280,236	3.4110	0.003710

TABLE A-1 (continued)

FREQUENCY: 30 CPS

AMPLITUDE: 0.0386 in.

V Volts	EDC Volts	EAC Volts	ΔT ^oF	(Q/A) Btu/(hr)(ft^2)	$(Q/A)_{FC}$ Btu/(hr)(ft^2)	Nu_V	X^*	$(Q/A)_{boil}$ Btu/(hr)(ft^2)	Y_1^*	X_1^*
0.0231	0.0680	0.1450	11.68	9,805.5	9,805.5	5.968	10.670	-	-	-
0.0324	0.0950	0.1460	11.26	11,630.4	11,630.4	7.340	10.710	-	-	-
0.0420	0.1234	0.1400	10.67	13,339.9	13,339.9	8.880	10.770	-	-	-
0.0524	0.1554	0.1430	15.66	16,923.6	16,923.6	7.710	10.338	-	-	-
0.0606	0.1780	0.1450	10.50	20,194.5	20,194.5	13.640	10.780	-	-	-
0.0680	0.2007	0.1450	13.10	23,375.3	23,375.3	12.710	10.540	-	-	-
0.0774	0.2315	0.1470	20.24	28,295.1	28,295.1	9.990	10.010	-	-	-
0.0873	0.2635	0.1460	25.20	33,835.14	33,835.14	9.630	9.710	-	-	-
0.1010	0.3095	0.1490	33.54	43,331.8	43,331.8	9.320	9.266	-	-	-
0.1088	0.3350	0.1490	36.20	49,135.9	49,135.9	9.807	9.140	-	-	-
0.1184	0.3680	0.1520	41.47	57,399.2	57,399.2	10.030	8.903	-	-	-
0.1260	0.3992	0.1530	52.36	64,920.25	64,920.25	9.050	8.480	-	-	-
0.1352	0.4291	0.1540	53.37	73,696.9	73,696.9	10.080	8.420	-	-	-
0.1450	0.4672	0.1540	62.11	84,520.5	84,520.5	10.000	9.750	-	-	-
0.1564	0.5088	0.1770	67.75	100,390.5	100,390.5	10.930	10.820	-	-	-
0.1673	0.5530	0.1780	77.22	114,903.0	79,373.4	7.6292		35,529.6	0.4325	0.00203
0.1795	0.6073	0.1850	91.32	134,061.3	88,017.97	7.220		46,043.5	0.5605	0.00327
0.1890	0.6498	0.2090	101.25	152,507.0	93,310.0	6.950		59,197.0	0.7206	0.00414
0.2012	0.6901	0.2080	99.77	170,451.0	92,561.0	6.990		77,890.0	0.9482	0.00401
0.2132	0.7328	0.2110	101.10	190,397.0	93,224.0	6.950		97,173.0	1.1800	0.00412

$$X = Pr^{0.72}\ Gr^{-0.06}\ \ 0.32\ Pr^{1.08} + 0.06\ Re^{0.86}$$

$$Y_1 = \frac{(Q/A)_{boil}}{\mu_L\ h_{fg}} \sqrt{\frac{\sigma \quad g_o}{(\rho_L - \rho_V)g}} \qquad X_1 = \frac{c_{pL}\ \ T_x}{h_{fg}}\ \frac{1}{Pr^{1.7}}$$

TABLE A-1 (continued)

FREQUENCY: 40 CPS

V Volts	EDC Volts	EAC Volts	ΔT ^oF	(Q/A) Btu/(hr)(ft^2)	$(Q/A)_{FC}$ Btu/(hr)(ft^2)	Nu_v	X	$(Q/A)_{boil}$ Btu/(hr)(ft^2)	Y_1	X_1
0.0060	0.0175	0.158	6.78	9,750	9,750	10.19	12.13	-	-	-
0.0253	0.0739	0.159	7.60	11,844	11,844	11.11	12.02	-	-	-
0.0496	0.1460	0.159	11.65	17,815	17,815	10.87	11.55	-	-	-
0.0596	0.1763	0.159	14.29	21,443	21,443	10.69	11.32	-	-	-
0.0743	0.2232	0.159	22.60	28,134	28,134	9.60	10.50	-	-	-
0.0825	0.2493	0.175	25.84	34,551	34,551	10.21	10.39	-	-	-
0.0922	0.2798	0.172	28.17	40,002	40,002	9.24	9.95	-	-	-
0.1022	0.3150	0.172	36.77	47,031	47,031	9.34	9.78	-	-	-
0.1094	0.3394	0.169	40.40	52,146	52,146	10.64	9.65	-	-	-
0.1195	0.3728	0.195	43.56	63,851	63,851	10.40	9.41	-	-	-
0.1267	0.3994	0.196	49.48	70,663	70,663	11.20	9.30	-	-	-
0.1343	0.4254	0.211	52.23	80,111	80,111	11.70	9.10	-	-	-
0.1444	0.4610	0.212	56.76	90,757	90,757	11.73	10.32	-	-	-
0.1518	0.4888	0.217	61.74	99,960	99,960	11.82	10.53	-	-	-
0.1740	0.5790	0.218	81.23	129,449	129,449	12.30	11.70	-	-	-
0.1906	0.6434	0.217	89.94	153,705	96,949	8.06		56,756	0.6909	0.00315
0.2005	0.6795	0.220	92.40	169,392	98,556	7.99		70,836	0.8623	0.00336
0.2078	0.7067	0.219	94.50	181,134	99,945	7.94		81,189	0.9883	0.00355

TABLE A-1 (continued)

FREQUENCY: 50 CPS

V Volts	EDC Volts	EAC Volts	ΔT ^oF	(Q/A) Btu/(hr)(ft^2)	$(Q/A)_{FC}$ Btu/(hr)(ft^2)	Nu_V	X	$(Q/A)_{boil}$ Btu/(hr)(ft^2)	Y_1	X_1
0.0597	0.1750	0.134	9.44	18,651	18,651	14.03	12.66	-	-	-
0.0695	0.2055	0.134	14.06	22,907	22,907	11.60	12.19	-	-	-
0.0793	0.2354	0.134	16.17	27,815	27,815	12.27	12.02	-	-	-
0.0865	0.2584	0.134	19.58	31,918	31,918	11.65	11.76	-	-	-
0.0970	0.2918	0.145	23.38	39,718	39,718	12.17	11.50	-	-	-
0.1058	0.3208	0.146	27.70	46,107	46,107	11.96	11.24	-	-	-
0.1134	0.3458	0.142	30.83	51,572	51,572	12.04	11.07	-	-	-
0.1235	0.3815	0.142	38.02	60,368	60,368	11.48	10.70	-	-	-
0.1308	0.4065	0.141	41.41	67,035	67,035	11.74	10.55	-	-	-
0.1402	0.4404	0.142	47.47	76,709	76,709	11.76	10.28	-	-	-
0.1475	0.4677	0.142	52.83	84,791	84,791	11.72	10.07	-	-	-
0.1550	0.4964	0.142	58.58	93,673	93,673	11.72	9.85	-	-	-
0.1650	0.5338	0.143	64.48	106,233	106,233	13.28	12.65	-	-	-
0.1840	0.6107	0.146	78.70	133,902	133,902	16.71	15.65	-	-	-
0.1895	0.6314	0.146	82.01	141,850	100,042	9.08		41,808	0.509	0.00245
0.1989	0.6693	0.147	88.01	157,041	104,837	8.90		52,204	0.635	0.00298
0.2088	0.7070	0.148	91.81	173,409	107,749	8.79		65,660	0.799	0.00331
0.2186	0.7446	0.149	95.47	190,511	110,454	8.69		80,057	0.974	0.00363

TABLE A-1 (continued)

FREQUENCY: 70 CPS

V Volts	EDC Volts	EAC Volts	ΔT ^oF	(Q/A) Btu/(hr)(ft^2)	$(Q/A)_{FC}$ Btu/(hr)(ft^2)	Nu_v	X	$(Q/A)_{boil}$ Btu/(hr)(ft^2)	Y_1	X_1
0.0385	0.1130	0.174	10.12	16,504	16,504	11.59	13.24	-	-	-
0.0505	0.1485	0.188	11.12	21,966	21,966	14.04	14.13	-	-	-
0.0558	0.1650	0.188	14.09	23,812	23,812	12.04	13.80	-	-	-
0.0776	0.2308	0.192	17.22	34,104	34,104	14.14	13.55	-	-	-
0.0825	0.2467	0.187	20.13	36,065	36,065	12.81	13.32	-	-	-
0.0925	0.2790	0.210	24.82	45,497	45,497	13.15	13.00	-	-	-
0.1019	0.3100	0.231	29.53	55,289	55,289	13.47	12.71	-	-	-
0.1180	0.3425	0.232	33.39	62,864	62,864	13.58	12.50	-	-	-
0.1216	0.3754	0.233	37.68	71,162	71,162	13.66	12.28	-	-	-
0.1298	0.4040	0.235	42.26	78,981	78,981	13.55	12.06	-	-	-
0.1392	0.4354	0.235	45.04	88,076	88,076	14.21	11.95	-	-	-
0.1490	0.4714	0.276	51.55	106,141	106,141	15.02	11.85	-	-	-
0.1588	0.5055	0.278	55.08	117,660	117,660	15.62	11.52	-	-	-
0.1710	0.5517	0.278	62.88	133,125	133,125	15.43	11.41	-	-	-
0.1810	0.5898	0.281	68.73	147,408	147,408	15.51	11.37	-	-	-
0.1905	0.6286	0.283	76.18	162,076	162,076	15.01	11.41	-	-	-
0.2029	0.6793	0.286	84.91	182,605	119,502	10.49		63,103	0.768	0.00271
0.2103	0.7107	0.288	90.62	195,819	124,985	10.32		70,834	0.862	0.00321

TABLE A-1 (continued)

FREQUENCY: 20 CPS AMPLITUDE: 0.0673 in.

V Volts	EDC Volts	EAC Volts	ΔT ^oF	(Q/A) Btu/(hr)(ft^2)	$(Q/A)_{FC}$ Btu/(hr)(ft^2)	Nu_v	X	$(Q/A)_{boil}$ Btu/(hr)(ft^2)	Y_1	X_1
0.0564	0.1664	0.125	12.90	16,521	16,521	9.12	11.00	-	-	-
0.0736	0.2180	0.137	15.00	25,188	25,188	11.97	10.83	-	-	-
0.0838	0.2506	0.138	20.15	30,800	30,800	10.93	10.45	-	-	-
0.0930	0.2805	0.153	24.81	38,091	38,091	11.01	10.15	-	-	-
0.1017	0.3104	0.153	31.32	44,213	44,213	10.16	9.80	-	-	-
0.1145	0.3528	0.151	36.59	53,788	53,788	10.60	9.54	-	-	-
0.1248	0.3894	0.152	43.65	63,078	63,078	10.49	9.22	-	-	-
0.1320	0.4180	0.187	52.08	74,521	74,521	10.44	8.90	-	-	-
0.1380	0.4400	0.191	56.01	81,209	81,209	10.60	8.70	-	-	-
0.1478	0.4769	0.194	62.94	92,449	92,449	10.80	8.65	-	-	-
0.1578	0.5150	0.218	69.64	107,843	107,843	10.95	8.43	-	-	-
0.1676	0.5622	0.222	86.10	122,572	89,594	7.76		32,978	0.401	0.002812
0.1773	0.5978	0.224	89.22	136,026	91,591	7.68		44,434	0.541	0.003086
0.1924	0.6525	0.227	92.78	158,380	93,786	7.58		64,594	0.786	0.003399
0.1992	0.0735	0.242	90.91	174,474	92,643	7.63		77,831	0.947	0.003235
0.2085	0.7072	0.244	92.87	185,691	93,838	7.57		91,853	1.118	0.003406
0.2192	0.7516	0.247	99.57	205,430	97,729	7.39		107,701	1.311	0.003990

TABLE A-1 (continued)

FREQUENCY: 30 CPS

V Volts	EDC Volts	EAC Volts	ΔT ^oF	(Q/A) Btu/(hr)(ft^2)	$(Q/A)_{FC}$ Btu/(hr)(ft^2)	Nu_V	X	$(Q/A)_{boil}$ Btu/(hr)(ft^2)	Y_1	X_1
0.0296	0.0878	0.216	15.76	20,626	20,626			-	-	-
0.0395	0.1185	0.252	21.88	29,089	29,089	9.52	11.51	-	-	-
0.0475	0.1412	0.250	16.92	31,209	31,209	13.16	12.15	-	-	-
0.0574	0.1726	0.244	23.14	33,431	33,431	10.35	11.70	-	-	-
0.0650	0.1950	0.244	21.89	36,597	36,597	11.97	11.79	-	-	-
0.0726	0.2192	0.249	25.38	41,019	41,019	11.60	11.57	-	-	-
0.0796	0.2421	0.272	29.39	49,062	49,062	12.00	11.35	-	-	-
0.0868	0.2675	0.272	36.70	53,146	53,146	10.46	10.95	-	-	-
0.0966	0.2978	0.283	36.89	61,610	61,610	12.07	10.98	-	-	-
0.1046	0.3236	0.283	38.86	67,226	67,226	12.52	11.05	-	-	-
0.1134	0.3560	0.315	47.12	81,001	81,001	12.50	10.84	-	-	-
0.1232	0.3894	0.310	51.00	88,205	88,205	12.61	10.52	-	-	-
0.1309	0.4182	0.306	57.17	94,589	94,589	12.11	10.38	-	-	-
0.1376	0.4435	0.311	62.30	102,447	102,447	12.04	10.15	-	-	-
0.1452	0.4710	0.313	66.05	110,951	110,951	12.30	10.05	-	-	-
0.1556	0.5109	0.315	73.23	123,471	123,471	12.70	10.01	-	-	-
0.1653	0.5477	0.325	78.05	137,760	137,760	12.83	9.99	-	-	-
0.1774	0.5975	0.326	88.57	154,795	107,403	9.07		47,392	0.576	0.00303
0.1898	0.6497	0.330	98.53	174,575	114,985	8.78		59,590	0.725	0.00350
0.2020	0.6932	0.345	100.10	196,614	116,108	8.74		80,506	0.980	0.00400

TABLE A-1 (continued)

FREQUENCY: 50 CPS

V Volts	EDC Volts	EAC Volts	ΔT ^{o}F	(Q/A) Btu/(hr)(ft^2)	$(Q/A)_{FC}$ Btu/(hr)(ft^2)	Nu_v	X	$(Q/A)_{boil}$ Btu/(hr)(ft^2)	Y_1	X_1
0.0774	0.2281	0.117	12.29	25,096	25,096	14.53	15.37	-	-	-
0.0894	0.2647	0.116	14.80	31,745	31,745	15.29	15.11	-	-	-
0.1015	0.3034	0.115	19.92	39,635	39,635	14.23	14.67	-	-	-
0.1090	0.3274	0.115	22.54	45,116	45,116	14.33	14.47	-	-	-
0.1165	0.3516	0.115	25.15	51,028	51,028	14.55	14.29	-	-	-
0.1293	0.3924	0.114	28.19	61,918	61,918	15.79	14.10	-	-	-
0.1391	0.4248	0.113	31.65	71,203	71,203	16.21	13.90	-	-	-
0.1466	0.4516	0.114	36.46	79,252	79,252	15.70	13.73	-	-	-
0.1583	0.4912	0.110	40.54	91,894	91,894	16.42	13.42	-	-	-
0.1656	0.5174	0.116	44.42	101,270	101,270	16.56	13.24	-	-	-
0.1730	0.5434	0.138	47.43	112,617	112,617	17.28	13.10	-	-	-
0.1832	0.5820	0.137	53.92	126,639	126,639	17.10	13.80	-	-	-
0.1940	0.6234	0.138	60.54	142,772	142,772	17.20	13.70	-	-	-
0.2068	0.6704	0.167	65.69	165,702	165,702	18.50	13.65	-	-	-
0.2164	0.7064	0.168	69.77	181,760	181,760	18.60	13.53	-	-	-
0.2247	0.7464	0.170	80.17	198,534	198,534	17.80	13.41	-	-	-
0.2372	0.7994	0.172	88.94	223,269	223,269	11.62		85,087	0.855	0.00230
0.2488	0.8485	0.173	96.23	247,450	145,997	11.40		101,453	1.035	0.00306
0.2436	0.8284	0.173	94.47	237,002	144,149	11.45		92,853	1.130	0.00354

TABLE A-1 (continued)

FREQUENCY: 70 CPS

V Volts	EDC Volts	EAC Volts	ΔT $^{\circ}F$	(Q/A) Btu/(hr)(ft^2)	$(Q/A)_{FC}$ Btu/(hr)(ft^2)	Nu_v	X	$(Q/A)_{boil}$ Btu/(hr)(ft^2)	Y_1	X_1
0.0495	0.1454	0.252	10.54	32,430	32,430	21.80	18.37	-	-	-
0.0598	0.1770	0.252	14.61	36,056	36,056	17.58	17.75	-	-	-
0.0665	0.1967	0.253	14.25	39,074	39,074	19.53	17.81	-	-	-
0.0845	0.2538	0.276	22.53	52,676	52,676	16.75	17.04	-	-	-
0.1034	0.3130	0.276	26.79	64,742	64,742	17.35	16.73	-	-	-
0.1108	0.3367	0.276	28.91	70,194	70,194	17.43	16.59	-	-	-
0.1183	0.3608	0.283	30.92	77,586	77,586	18.00	16.76	-	-	-
0.1254	0.3843	0.285	33.58	84,060	84,060	18.05	16.61	-	-	-
0.1338	0.4106	0.283	34.34	91,196	91,196	19.16	16.56	-	-	-
0.1430	0.4431	0.283	39.75	100,394	100,394	18.20	15.98	-	-	-
0.1503	0.4682	0.285	42.73	108,537	108,537	18.43	15.85	-	-	-
0.1629	0.5121	0.288	47.91	123,572	123,572	18.78	15.59	-	-	-
0.1700	0.5370	0.290	50.65	132,697	132,697	19.10	15.40	-	-	-
0.1788	0.5718	0.330	57.75	153,378	153,378	19.40	15.10	-	-	-
0.1915	0.6193	0.330	64.26	171,361	171,361	19.60	15.04	-	-	-
0.2034	0.6638	0.330	69.62	189,497	189,497	19.75	14.92	-	-	-
0.2128	0.7020	0.330	76.03	205,264	205,264	19.81	14.85	-	-	-
0.2224	0.7420	0.330	82.81	222,443	158,251	14.23		64,192	0.781	0.00253

TABLE A-2

LIQUID: WATER

TEMPERATURE: 118.4°F

AMPLITUDE: 0.0

WIRE DIA: 0.010 in.

$L = \frac{53}{64}$ in.

$R_{100} = 0.050706$ Ohm

FREQUENCY: 0 CPS

V Volts	EDC Volts	EAC Volts	ΔT °F	(Q/A) Btu/(hr)(ft^2)	$(Q/A)_{FC}$ Btu/(hr)(ft^2)	Nu_o	X^*	$(Q/A)_{boil}$ Btu/(hr)(ft^2)	Y_1^*	X_1^*
0.0505	0.1118	-	12.69	5,334	-	0.9377	-	-	-	-
0.0610	0.1355	-	14.56	7,808	-	1.195	-	-	-	-
0.0705	0.1582	-	20.27	10,537	-	1.155	-	-	-	-
0.0790	0.1769	-	19.08	13,202	-	1.539	-	-	-	-
0.0850	0.1926	-	25.79	15,466	-	1.329	-	-	-	-
0.0927	0.2111	-	28.65	18,487	-	1.428	-	-	-	-
0.1053	0.2425	-	35.12	24,124	-	1.515	-	-	-	-
0.1144	0.2650	-	38.52	28,640	-	1.638	-	-	-	-
0.1248	0.2938	-	48.03	34,640	-	1.582	-	-	-	-
0.1347	0.3192	-	51.94	40,626	-	1.713	-	-	-	-
0.1463	0.3535	-	63.67	48,859	-	1.673	-	-	-	-
0.1590	0.3888	-	70.98	58,402	-	1.789	-	-	-	-
0.1682	0.4172	-	79.82	66,294	-	1.800	-	-	-	-
0.1790	0.4477	-	85.04	75,709	-	-	-	-	-	-
0.1883	0.4795	-	96.46	85,299	-	-	-	-	-	-
0.1960	0.4989	-	96.19	92,380	-	-	-	-	-	-
0.2083	0.5337	-	100.42	105,025	-	-	-	-	-	-
0.2215	0.5828	-	117.79	121,954	-	-	-	121,954	1.3410	0.01275

* $X = Pr^{0.72}\ Gr^{-0.06}\quad 0.32\ Pr^{1.08} + 0.06\ Re^{0.86}$;

$$Y_1 = \frac{(Q/A)_{boil} \sqrt{\dfrac{\sigma \quad g_o}{(\rho_L - \rho_V) g}}}{\mu_L \times h_{fg}} ;$$

$$X_1 = \frac{C_{pL}\ T_x}{\bar{h}_{fg}} \times \frac{1}{Pr^{1.0}} .$$

TABLE A-2 (continued)

FREQUENCY: 0 CPS

V Volts	EDC Volts	EAC Volts	ΔT ^oF	(Q/A) Btu/(hr)(ft^2)	$(Q/A)_{FC}$ Btu/(hr)(ft^2)	Nu_o	X	$(Q/A)_{boil}$ Btu/(hr)(ft^2)	Y_1	X_1
0.2340	0.6257	-	128.57	138,321	-	-	-	138,321	1.5950	0.018450
0.2442	0.6567	-	130.60	151,502	-	-	-	151,502	1.6610	0.019540
0.2565	0.6943	-	132.60	168,245	-	-	-	168,245	1.8500	0.020590
0.2714	0.7368	-	133.80	188,915	-	-	-	188,915	2.0790	0.021010
0.2836	0.7122	-	134.60	206,891	-	-	-	206,891	2.2790	0.021640
0.2953	0.8055	-	136.10	224,717	-	-	-	224,717	2.4780	0.022450
0.3078	0.8372	-	136.35	243,447	-	-	-	243,447	2.6750	0.022585
0.3235	0.8735	-	136.75	266,640	-	-	-	266,640	2.9315	0.022774
0.3375	0.9150	-	138.75	292,796	-	-	-	292,796	3.2191	0.023671
0.3520	0.9580	-	140.50	318,503	-	-	-	318,503	3.5017	0.024753
0.3640	0.9920	-	141.40	341,702	-	-	-	341,702	3.7568	0.025239
0.3830	1.0370	-	142.72	373,750	-	-	-	373,750	4.1092	0.025931
0.4015	1.0470	-	143.68	415,569	-	-	-	415,569	4.5689	0.026432
0.4160	1.1390	-	144.80	447,553	-	-	-	447,553	4.9063	0.027007
0.4185	1.1780	-	146.10	479,444	-	-	-	479,444	5.2712	0.027693
0.4400	1.2100	-	147.30	503,655	-	-	-	503,655	5.5370	0.028364

TABLE A-2 (continued)

FREQUENCY: 20 CPS AMPLITUDE: 0.386 in.

V Volts	EDC Volts	EAC Volts	ΔT ^oF	(Q/A) Btu/(hr)(ft^2)	$(Q/A)_{FC}$ Btu/(hr)(ft^2)	Nu_V	X	$(Q/A)_{boil}$ Btu/(hr)(ft^2)	Y_1	X_1
0.0877	0.1936	0.085	11.10	19,132	19,132	3.85	4.90	-	-	-
0.1004	0.2220	0.085	12.00	24,144	24,144	4.48	4.88	-	-	-
0.1634	0.3775	0.134	36.97	65,617	65,617	3.91	3.98	-	-	-
0.1778	0.4148	0.135	42.68	77,055	77,055	3.96	3.84	-	-	-
0.1904	0.4492	0.135	49.30	88,098	88,098	3.92	3.69	-	-	-
0.2020	0.4785	0.134	51.71	98,475	98,475	4.10	3.74	-	-	-
0.2050	0.4880	0.144	54.68	103,000	103,000	3.37	3.58	-	-	-
0.2070	0.4960	0.142	59.10	105,120	105,120	3.93	3.49	-	-	-
0.2090	0.5080	0.123	66.93	106,230	106,230	3.95	3.35	-	-	-
0.2105	0.5135	0.142	69.18	116,878	116,878	3.68	3.31	-	-	-
0.2200	0.5400	0.223	73.79	131,188	131,188	3.87	3.24	-	-	-
0.2320	0.5740	0.234	77.57	145,488	145,488	4.05	3.20	-	-	-
0.2402	0.5975	0.252	81.74	160,005	160,005	4.20	3.30	-	-	-
0.2600	0.6530	0.231	87.85	180,490	180,490	4.44		-	-	-
0.2801	0.7050	0.162	88.58	196,788	196,788	4.81		-	-	-
0.2900	0.7450	0.172	99.53	214,783	214,783	4.64		-	-	-
0.3001	0.7745	0.230	104.56	239,593	239,593	4.91		-	-	-
0.3102	0.8200	0.205	120.47	255,978	150,654			105,324	1.540	0.01422
0.3200	0.8550	0.321	126.78	295,767	155,449			140,318	1.158	0.01758
0.3972	1.0690	0.222	133.34	418,652	160,303			258,349	2.840	0.02100

TABLE A-2 (continued)

FREQUENCY: 40 CPS

V Volts	EDC Volts	EAC Volts	ΔT ^{o}F	(Q/A) Btu/(hr)(ft^2)	$(Q/A)_{FC}$ Btu/(hr)(ft^2)	Nu_v	X	$(Q/A)_{boil}$ Btu/(hr)(ft^2)	Y_1	X_1
0.0590	0.1297	0.147	8.77	16,516	16,516	4.21	6.10	-	-	-
0.0690	0.1539	0.165	13.62	21,689	21,689	3.55	5.75	-	-	-
0.0769	0.1698	0.165	11.23	23,984	23,984	4.77	6.17	-	-	-
0.1090	0.2428	0.163	16.13	36,271	36,271	5.01	6.10	-	-	-
0.1212	0.2723	0.164	20.96	42,488	42,488	4.51	5.78	-	-	-
0.1313	0.2960	0.164	22.89	47,988	47,988	4.65	5.80	-	-	-
0.1503	0.3430	0.164	29.88	59,838	59,838	4.43	5.50	-	-	-
0.1607	0.3679	0.164	31.71	66,953	66,953	4.67	5.41	-	-	-
0.1702	0.3915	0.165	34.45	74,132	74,132	4.75	5.41	-	-	-
0.1828	0.4239	0.165	39.15	84,365	84,365	4.74	5.27	-	-	-
0.1975	0.4625	0.175	44.91	98,721	98,721	4.83	5.11	-	-	-
0.2070	0.4875	0.175	42.86	107,690	107,690	4.90	5.03	-	-	-
0.2167	0.5144	0.177	52.97	117,778	117,778	4.87	4.92	-	-	-
0.2280	0.5503	0.174	62.99	130,384	130,384	4.51	4.71	-	-	-
0.2432	0.5933	0.201	69.54	151,961	151,961	4.75	4.59	-	-	-
0.2554	0.6316	0.204	77.95	168,293	168,293	4.68	4.45	-	-	-
0.2697	0.6695	0.214	80.32	188,013	188,013	5.07	4.41	-	-	-
0.2807	0.7057	0.214	88.31	204,350	204,350	5.10	4.40	-	-	-
0.2966	0.7563	0.253	97.33	235,635	235,635	5.36	3.95	-	-	-
0.3035	0.7936	0.256	113.68	251,223	211,055	3.98	-	40,168	0.442	0.0106
0.3374	0.8900	0.256	119.48	307,160	218,767	3.91	-	88,393	0.972	0.0136
0.3642	0.9825	0.266	134.56	362,827	238,320	3.78	-	124,507	1.369	0.0216

TABLE A-2 (continued)

FREQUENCY: 50 CPS

V Volts	EDC Volts	EAC Volts	ΔT ^oF	(Q/A) Btu/(hr)(ft^2)	$(Q/A)_{FC}$ Btu/(hr)(ft^2)	Nu_v	X	$(Q/A)_{boil}$ Btu/(hr)(ft^2)	Y_1	X_1
0.0630	0.1378	0.1180	6.00	14,216	14,216	5.30	6.61	-	-	-
0.0874	0.1930	0.1170	11.27	21,792	21,792	4.30	6.60	-	-	-
0.1117	0.2483	0.1240	14.97	32,737	32,737	4.88	6.55	-	-	-
0.1290	0.2891	0.1300	19.54	42,357	42,357	4.82	6.52	-	-	-
0.1388	0.3120	0.1480	21.24	50,118	50,118	5.24	6.50	-	-	-
0.1572	0.3577	0.1480	28.19	62,217	62,217	4.89	6.21	-	-	-
0.1655	0.3764	0.1470	27.91	67,827	67,827	5.37	6.21	-	-	-
0.1754	0.4012	0.1470	31.19	75,406	75,406	5.35	6.15	-	-	-
0.1917	0.4436	0.1480	37.92	89,280	89,280	5.19	5.92	-	-	-
0.2090	0.4872	0.1470	42.22	104,954	104,954	5.46	5.81	-	-	-
0.2191	0.5143	0.1480	46.30	115,271	115,271	5.46	5.71	-	-	-
0.2308	0.5464	0.1480	51.36	127,880	127,880	5.45	5.58	-	-	-
0.2430	0.5796	0.1475	55.84	141,675	141,675	5.54	5.48	-	-	-
0.2528	0.6077	0.1550	60.60	154,588	154,588	5.56	5.38	-	-	-
0.2690	0.6607	0.1550	73.70	177,146	177,146	5.22	5.13	-	-	-
0.2781	0.6832	0.1540	73.85	188,616	188,616	5.54	5.12	-	-	-
0.2853	0.7077	0.1530	79.86	199,662	199,662	5.41	5.02	-	-	-
0.2975	0.7403	0.1670	81.84	218,654	218,654	5.78	5.00	-	-	-
0.3115	0.7866	0.1670	91.11	241,916	241,916	5.72	4.98	-	-	-
0.3278	0.8288	0.1780	91.91	268,503	268,503	6.30	4.96	-	-	-
0.3354	0.8604	0.1790	101.21	284,428	284,428	6.04	5.01	-	-	-
0.3475	0.9000	0.1800	117.41	307,282	307,282	6.13	4.97	-	-	-
0.3595	0.9458	0.1800	117.73	332,856	248,422	4.52		84,434	0.3545	0.01271
0.3714	0.9834	0.2070	121.99	360,330	255,157	4.47		105,179	1.1560	0.01498
0.3813	1.0115	0.2050	123.24	379,333	257,111	4.46		122,222	1.3440	0.01564
0.3910	1.0494	0.2050	131.10	402,429	269,285	4.38		133,144	1.4640	0.01978

TABLE A-2 (continued)

FREQUENCY: 70 CPS

V Volts	EDC Volts	EAC Volts	ΔT ^{o}F	(Q/A) Btu/(hr)(ft^2)	$(Q/A)_{FC}$ Btu/(hr)(ft^2)	Nu_v	X	$(Q/A)_{boil}$ Btu/(hr)(ft^2)	Y_1	X_1
0.1124	0.2494	0.1120	13.95	31,824	31,824	5.28	8.11	-	-	-
0.1362	0.3038	0.1125	16.89	44,451	44,451	5.86	8.01	-	-	-
0.1484	0.3335	0.1130	21.11	52,124	52,124	5.50	7.80	-	-	-
0.1640	0.3703	0.1130	23.79	62,715	62,715	5.85	7.63	-	-	-
0.1785	0.4085	0.1120	31.49	74,065	74,065	5.20	7.31	-	-	-
0.1908	0.4370	0.1110	31.95	83,853	83,853	5.80	7.35	-	-	-
0.2052	0.4733	0.1120	36.03	96,891	96,891	5.93	7.20	-	-	-
0.2170	0.5027	0.1120	38.56	108,172	108,172	6.20	7.13	-	-	-
0.2325	0.5417	0.1125	41.91	124,116	124,116	6.52	7.03	-	-	-
0.2472	0.5805	0.1125	46.55	140,660	140,660	6.63	8.87	-	-	-
0.2606	0.6195	0.1100	53.83	157,327	157,327	6.40	6.71	-	-	-
0.2755	0.6508	0.1120	55.55	175,918	175,918	6.92	6.67	-	-	-
0.2898	0.7028	0.1120	65.90	197,300	197,300	6.52	6.41	-	-	-
0.3044	0.7478	0.1120	73.84	219,872	219,872	6.47	6.28	-	-	-
0.3217	0.8068	0.1125	86.76	249,969	249,969	6.51	6.21	-	-	-
0.3315	0.8355	0.1125	89.89	266,403	266,403	6.51	6.15	-	-	-
0.3432	0.8733	0.1130	96.00	287,891	287,891	6.46	6.05	-	-	-
0.3554	0.9142	0.1140	102.98	311,721	311,721	6.39	5.95	-	-	-
0.3665	0.9535	0.1150	110.36	334,944	334,944	6.23	5.93	-	-	-
0.3780	0.9925	0.1160	116.41	359,270	307,093	5.65		52,178	0.5737	0.01204
0.3926	1.0440	0.1170	121.76	392,082	324,587	5.55		67,496	0.7421	0.01481
0.4075	1.0727	0.1170	120.11	417,877	310,626	5.70		107,251	1.1780	0.01398

TABLE A-2 (continued)

FREQUENCY: 80 CPS

V Volts	EDC Volts	EAC Volts	ΔT ^oF	(Q/A) Btu/(hr)(ft^2)	$(Q/A)_{FC}$ Btu/(hr)(ft^2)	Nu_V	X	$(Q/A)_{boil}$ Btu/(hr)(ft^2)	Y_1	X_1
0.1067	0.2374	0.165	15.50	35,491	35,491	5.11	8.70	-	-	-
0.1215	0.2719	0.165	18.73	42,703	42,703	5.17	8.50	-	-	-
0.1335	0.3000	0.182	21.10	51,762	51,762	5.50	8.40	-	-	-
0.1487	0.3350	0.182	22.50	60,952	60,952	6.10	8.30	-	-	-
0.1664	0.3775	0.205	26.48	76,845	76,845	6.43	8.16	-	-	-
0.1787	0.4075	0.205	29.43	86,205	86,205	6.48	8.04	-	-	-
0.1935	0.4439	0.205	32.89	98,454	98,454	6.61	7.91	-	-	-
0.2072	0.4803	0.206	38.93	111,312	111,312	6.30	7.70	-	-	-
0.2194	0.5125	0.206	43.43	123,390	123,390	6.24	7.50	-	-	-
0.2335	0.5498	0.210	48.14	138,976	138,976	6.40	7.43	-	-	-
0.2503	0.5950	0.238	53.81	163,208	163,208	6.64	7.28	-	-	-
0.2698	0.6495	0.240	61.42	188,154	188,154	6.68	7.10	-	-	-
0.2767	0.6725	0.242	67.24	198,579	198,579	6.42	6.97	-	-	-
0.2911	0.7135	0.242	72.43	218,792	218,792	6.56	6.86	-	-	-
0.3057	0.7556	0.242	77.63	240,604	240,604	6.72	6.77	-	-	-
0.3175	0.7870	0.242	79.40	258,382	258,382	7.05	6.73	-	-	-
0.3322	0.8246	0.242	80.29	281,081	281,081	7.58	6.70	-	-	-
0.3444	0.8596	0.242	83.74	301,850	301,850	7.80	6.66	-	-	-
0.3558	0.8963	0.242	89.57	323,240	323,240	7.78	6.53	-	-	-
0.3685	0.9305	0.243	91.10	346,029	346,029	8.20	6.44	-	-	-
0.3780	0.9610	0.243	95.43	365,122	365,122	8.22	6.37	-	-	-

TABLE A-2 (continued)

TABLE

LIQUID: WATER

WIRE DIA: 0.010 in.

FREQUENCY: 20 CPS

TEMPERATURE: 118.4°F

$L = \frac{53}{64}$ in.

AMPLITUDE: 0.0673 in.

R_{100} = 0.050706 Ohm

V Volts	EDC Volts	EAC Volts	ΔT °F	(Q/A) Btu/(hr)(ft^2)	$(Q/A)_{FC}$ Btu/(hr)(ft^2)	Nu_v	X	$(Q/A)_{boil}$ Btu/(hr)(ft^2)	Y_1	X_1
0.0866	0.1926	0.1535	15.24	25,766	25,766	3.76	5.79	-	-	-
0.1018	0.2274	0.2070	17.70	39,992	39,992	5.02	5.55	-	-	-
0.1098	0.2482	0.2065	24.43	43,568	43,568	3.95	5.40	-	-	-
0.1250	0.2878	0.2050	34.98	51,230	51,230	3.23	5.20	-	-	-
0.1378	0.3160	0.2040	32.67	58,283	58,283	3.94	5.10	-	-	-
0.1504	0.3465	0.2050	35.35	66,466	66,466	4.14	5.04	-	-	-
0.1644	0.3812	0.2050	39.10	76,328	76,328	4.29	4.94	-	-	-
0.1826	0.4268	0.2440	43.79	97,690	97,690	4.90	4.82	-	-	-
0.1984	0.4690	0.2450	50.48	111,895	111,895	4.86	4.66	-	-	-
0.2130	0.5061	0.2450	53.54	125,707	125,707	4.85	4.65	-	-	-
0.2345	0.5660	0.1770	64.12	138,342	138,342	4.70	4.35	-	-	-
0.2419	0.6080	0.1900	68.94	148,387	148,387	4.68	4.29	-	-	-
0.2540	0.6170	0.2010	73.29	170,631	170,631	4.81	4.21	-	-	-
0.2670	0.6570	0.2050	76.14	181,351	181,351	5.18	4.16	-	-	-
0.2785	0.6940	0.2100	81.59	190,166	190,166	5.25	4.08	-	-	-
0.2942	0.7360	0.2134	84.80	222,349	222,349	5.65	4.03	-	-	-
0.3350	0.8310	0.2189	90.89	230,057	230,057	6.51	4.02	-	-	-
0.3384	0.8710	0.2230	101.90	310,361	310,361	5.75	4.02	-	-	-

TABLE A-2 (continued)

FREQUENCY: 30 CPS

V Volts	EDC Volts	EAC Volts	ΔT ^{o}F	(Q/A) Btu/(hr)(ft^2)	$(Q/A)_{FC}$ Btu/(hr)(ft^2)	Nu_v	X	$(Q/A)_{boil}$ Btu/(hr)(ft^2)	Y_1	X_1
0.0778	0.1720	0.162	11.92	23,857	23,857	5.20	7.20	-	-	-
0.1134	0.2532	0.177	17.45	40,382	40,382	5.15	6.86	-	-	-
0.1255	0.2813	0.176	19.63	46,408	46,408	5.30	6.70	-	-	-
0.1374	0.3097	0.177	22.89	53,336	53,336	5.26	6.61	-	-	-
0.1518	0.3430	0.176	24.19	62,141	62,141	5.69	6.56	-	-	-
0.1643	0.3726	0.178	26.27	71,034	71,034	5.99	6.47	-	-	-
0.1785	0.4086	0.182	31.63	82,575	82,575	5.77	6.28	-	-	-
0.1914	0.4395	0.213	33.43	98,137	98,137	6.48	6.22	-	-	-
0.2032	0.4685	0.210	35.79	108,007	108,007	6.65	6.15	-	-	-
0.2183	0.5068	0.214	39.82	123,155	123,155	6.80	6.03	-	-	-
0.2327	0.5458	0.215	45.85	138,606	138,606	6.63	5.86	-	-	-
0.2523	0.5967	0.215	50.77	160,691	160,691	6.93	5.74	-	-	-
0.2621	0.6225	0.246	53.29	178,211	178,211	7.32	5.68	-	-	-
0.2763	0.6680	0.246	64.02	198,014	198,014	6.74	5.45	-	-	-
0.2900	0.7062	0.247	68.43	217,147	217,147	6.90	5.37	-	-	-
0.3046	0.7455	0.247	71.53	238,077	238,077	7.23	5.30	-	-	-
0.3170	0.7804	0.274	75.15	262,523	262,523	7.58	5.24	-	-	-
0.3364	0.8382	0.275	82.66	295,059	295,059	7.27	5.21	-	-	-
0.3578	0.9128	0.298	97.64	341,433	341,433	7.51	5.19	-	-	-

TABLE A-2 (continued)

FREQUENCY: 50 CPS

V Volts	EDC Volts	EAC Volts	ΔT °F	(Q/A) Btu/(hr)(ft^2)	$(Q/A)_{FC}$ Btu/(hr)(ft^2)	Nu_v	X	$(Q/A)_{boil}$ Btu/(hr)(ft^2)	Y_1	X_1
0.1370	0.3046	0.107	15.08	44,288	44,288	6.54	9.10	-	-	-
0.1495	0.3334	0.107	16.78	51,938	51,938	6.89	9.01	-	-	-
0.1622	0.3619	0.106	17.05	60,213	60,213	7.85	8.88	-	-	-
0.1715	0.3848	0.106	20.21	67,076	67,076	7.37	8.89	-	-	-
0.1836	0.4138	0.106	22.75	76,484	76,484	7.46	8.76	-	-	-
0.1962	0.4445	0.106	25.70	87,076	87,076	7.51	8.63	-	-	-
0.2086	0.4754	0.105	29.09	98,257	98,257	7.47	8.48	-	-	-
0.2242	0.5130	0.105	31.39	113,209	113,209	7.97	8.39	-	-	-
0.2368	0.5452	0.105	34.98	126,491	126,491	7.98	8.26	-	-	-
0.2508	0.5810	0.126	38.56	144,135	144,135	8.23	8.54	-	-	-
0.2602	0.6012	0.126	42.84	155,688	155,688	7.99	8.00	-	-	-
0.2742	0.6445	0.137	47.09	174,498	174,498	8.13	7.88	-	-	-
0.2893	0.6859	0.152	52.24	196,670	196,670	8.24	7.74	-	-	-
0.3082	0.7392	0.165	58.78	226,099	226,099	8.42	7.57	-	-	-
0.3258	0.7894	0.165	65.35	253,586	253,586	8.45	7.42	-	-	-
0.3360	0.8178	0.202	68.11	275,430	275,430	8.80	7.36	-	-	-
0.3475	0.8525	0.202	72.98	295,583	295,583	8.79	7.26	-	-	-
0.3657	0.9091	0.202	81.21	329,665	329,665	8.79	7.12	-	-	-
0.3800	0.9605	0.204	91.72	360,370	360,370	8.45	7.09	-	-	-
0.3962	1.0174	0.208	101.86	396,730	396,730	8.38	7.07	-	-	-

TABLE A-3

LIQUID: WATER

TEMPERATURE: 170.6°F

AMPLITUDE: 0.0 in.

WIRE DIA: 0.010 in.

$L = \frac{41}{64}$ in.

R_{100} = 0.044133 Ohm

FREQUENCY: 0 CPS

V Volts	EDC Volts	EAC Volts	ΔT °F	(Q/A) Btu/(hr)(ft^2)	$(Q/A)_{FC}$ Btu/(hr)(ft^2)	Nu_o	X	$(Q/A)_{boil}$ Btu/(hr)(ft^2)	Y_1	X_1
0.0550	0.1158	-	11.00	7,802	-	1.520	-	-	-	-
0.0595	0.1252	-	12.61	9,116	-	1.550	-	-	-	-
0.0712	0.1510	-	17.21	13,174	-	1.640	-	-	-	-
0.0741	0.1577	-	18.59	14,458	-	1.660	-	-	-	-
0.0754	0.1606	-	18.95	14,819	-	1.670	-	-	-	-
0.0900	0.1955	-	25.89	21,512	-	1.766	-	-	-	-
0.0940	0.2025	-	27.80	23,271	-	1.786	-	-	-	-
0.0955	0.2068	-	28.58	24,098	-	1.797	-	-	-	-
0.1100	0.2408	-	36.55	32,384	-	1.884	-	-	-	-
0.1142	0.2510	-	38.58	34,485	-	1.902	-	-	-	-
0.1182	0.2604	-	41.60	37,723	-	1.929	-	-	-	-
0.1197	0.2648	-	43.60	39,943	-	1.948	-	-	-	-
0.1959	0.4529	-	71.88	108,350	-	-	-	108,350	1.1912	0.016092
0.2135	0.4954	-	74.34	129,165	-	-	-	129,165	1.4201	0.017385
0.2403	0.5594	-	76.52	164,160	-	-	-	164,160	1.8049	0.018536
0.2514	0.5855	-	76.82	179,756	-	-	-	179,756	1.9763	0.018694
0.2676	0.6255	-	79.28	204,411	-	-	-	204,411	2.2474	0.019993
0.2770	0.6476	-	79.41	219,068	-	-	-	219,068	2.4085	0.020060
0.2928	0.6860	-	80.86	245,294	-	-	-	245,294	2.6969	0.020827
0.3014	0.7069	-	81.58	260,191	-	-	-	260,191	2.8607	0.021207
0.3187	0.7493	-	83.23	291,628	-	-	-	291,628	3.2063	0.022083

TABLE A-3 (continued)

FREQUENCY: 20 CPS

AMPLITUDE: 0.0386 in.

V Volts	EDC Volts	EAC Volts	ΔT ^{o}F	(Q/A) Btu/(hr)(ft^2)	$(Q/A)_{FC}$ Btu/(hr)(ft^2)	Nu_v	X	$(Q/A)_{boil}$ Btu/(hr)(ft^2)	Y_1	X_1
0.0479	0.1008	0.132	11.83	16,008	16,008	2.890	3.10	-	-	-
0.0582	0.1223	0.132	10.96	18,818	18,818	3.670	3.12	-	-	-
0.7060	0.1495	0.142	15.65	24,518	24,518	3.350	3.01	-	-	-
0.0831	0.1784	0.162	24.11	33,033	33,033	2.920	2.87	-	-	-
0.0947	0.2039	0.162	25.93	38,466	38,466	3.170	2.84	-	-	-
0.1052	0.2276	0.164	28.94	44,422	44,422	3.270	2.81	-	-	-
0.1198	0.2610	0.164	33.32	53,261	53,261	3.400	2.84	-	-	-
0.1352	0.3119	0.156	38.45	62,503	62,503	3.455	2.83	-	-	-
0.1495	0.3295	0.183	40.67	78,713	78,713	4.110	2.81	-	-	-
0.1520	0.3225	0.138	46.22	73,560	73,560	3.390	2.79	-	-	-
0.1600	0.3580	0.176	50.32	89,486	89,486	3.295	2.78	-	-	-
0.1662	0.3650	0.188	54.22	93,113	93,113	3.495	2.77	-	-	-
0.1650	0.3748	0.229	59.22	104,537	69,640	2.490	-	28,897	0.31771	0.00940
0.1750	0.3990	0.293	64.15	131,374	74,338	2.450	-	57,036	0.62708	0.01201
0.1800	0.4130	0.292	67.08	136,872	77,071	2.430	-	59,811	0.65748	0.01355
0.1840	0.4230	0.302	67.84	143,757	77,777	2.430	-	65,895	0.72448	0.01395
0.2010	0.4645	0.335	70.85	172,447	80,548	2.410	-	91,899	1.01040	0.01554
0.3178	0.7360	0.210	82.90	308,612	81,884	2.390	-	226,728	2.49270	0.02190
0.3398	0.7908	0.212	83.60	350,971	83,965	2.380	-	267,006	2.93560	0.02238

TABLE A-3 (continued)

FREQUENCY: 40 CPS

V Volts	EDC Volts	EAC Volts	ΔT ^{o}F	(Q/A) Btu/(hr)(ft^2)	$(Q/A)_{FC}$ Btu/(hr)(ft^2)	Nu_v	X	$(Q/A)_{boil}$ Btu/(hr)(ft^2)	Y_1	X_1
0.0800	0.1682	0.112	11.29	16,433	16,433	3.12	4.50	-	-	-
0.0800	0.1681	0.112	10.92	23,713	23,713	4.65	4.54	-	-	-
0.0899	0.1892	0.110	11.88	27,793	27,793	5.01	4.51	-	-	-
0.1045	0.2215	0.147	16.24	40,717	40,717	5.36	4.38	-	-	-
0.1190	0.2540	0.147	20.53	49,276	49,276	5.12	4.31	-	-	-
0.1269	0.2721	0.147	23.35	54,475	54,475	4.98	4.23	-	-	-
0.1513	0.3271	0.148	28.48	72,811	72,811	5.45	4.15	-	-	-
0.1618	0.3513	0.159	31.17	83,634	83,634	5.72	4.11	-	-	-
0.1738	0.3794	0.162	34.57	95,208	95,208	5.86	4.15	-	-	-
0.1875	0.4115	0.162	37.96	108,828	108,828	6.08	4.12	-	-	-
0.2084	0.4634	0.162	46.33	132,349	132,349	6.06	4.09	-	-	-
0.2210	0.4933	0.177	48.80	152,276	152,276	6.54	4.09	-	-	-
0.2555	0.5857	0.190	66.23	201,982	115,904	4.32	-	86,077	0.9464	0.01311
0.2655	0.6102	0.192	67.95	217,434	118,468	4.28	-	98,966	1.0115	0.01401
0.2796	0.6474	0.207	72.91	243,655	125,797	4.23	-	117,858	1.2958	0.01663
0.2933	0.6812	0.222	74.96	269,907	128,795	4.22	-	141,112	1.5514	0.01771
0.3059	0.7124	0.254	76.69	299,962	131,453	4.21	-	168,504	1.8526	0.01868
0.3153	0.7361	0.252	78.46	316,653	133,859	4.19	-	182,793	2.0097	0.01956
0.3250	0.7608	0.252	80.29	335,086	136,492	4.18	-	198,593	2.1834	0.02052
0.3325	0.7794	0.263	81.19	352,514	137,794	4.17	-	214,719	2.3607	0.02100
0.3393	0.7975	0.263	83.04	366,388	140,427	4.16	-	225,961	2.4843	0.02197
0.3452	0.8110	0.263	82.73	377,842	139,988	4.16	-	237,854	2.6151	0.02181

TABLE A-3 (continued)

FREQUENCY: 50 CPS

V Volts	EDC Volts	EAC Volts	ΔT °F	(Q/A) Btu/(hr)(ft^2)	$(Q/A)_{FC}$ Btu/(hr)(ft^2)	Nu_v	X	$(Q/A)_{boil}$ Btu/(hr)(ft^2)	Y_1	X_1
0.0919	0.1928	0.094	9.96	26,781	26,781	5.76	5.23	-	-	-
0.1064	0.2243	0.094	12.90	34,263	34,263	5.68	5.14	-	-	-
0.1237	0.2618	0.094	15.31	44,647	44,647	6.24	5.07	-	-	-
0.1385	0.2944	0.094	17.98	54,871	54,871	6.52	5.00	-	-	-
0.1534	0.3278	0.090	21.24	66,068	66,068	6.64	4.92	-	-	-
0.1804	0.3911	0.090	29.90	90,816	90,816	6.48	4.82	-	-	-
0.1928	0.4208	0.090	34.46	103,650	103,650	6.40	4.75	-	-	-
0.2084	0.4575	0.090	38.14	120,980	120,980	6.62	4.72	-	-	-
0.2225	0.4925	0.116	43.40	141,246	141,246	6.89	4.69	-	-	-
0.2493	0.5614	0.126	54.52	179,527	-	-	-	-	-	-
0.2666	0.6066	0.128	61.30	206,288	-	-	-	-	-	-
0.2763	0.6315	0.128	64.26	221,836	-	-	-	-	-	-
0.2884	0.6634	0.128	68.52	242,346	138,573	4.28	-	103,773	1.1410	0.01431
0.2977	0.6904	0.135	73.97	260,595	148,047	4.23	-	112,548	1.2374	0.01719
0.3171	0.7390	0.144	77.27	297,041	153,707	4.21	-	143,334	1.5759	0.01893
0.3268	0.7638	0.144	79.21	315,662	157,024	4.19	-	158,638	1.7441	0.01995
0.3368	0.7884	0.144	80.27	335,090	158,818	4.18	-	176,272	1.9380	0.02050
0.3465	0.8125	0.157	81.43	356,647	160,793	4.17	-	195,854	2.1533	0.02110
0.3800	0.8930	0.204	83.46	437,515	164,218	4.16	-	273,297	3.0050	0.02220

TABLE A-3 (continued)

FREQUENCY: 70 CPS

V Volts	EDC Volts	EAC Volts	ΔT ^oF	(Q/A) Btu/(hr)(ft^2)	$(Q/A)_{FC}$ Btu/(hr)(ft^2)	Nu_v	X	$(Q/A)_{boil}$ Btu/(hr)(ft^2)	Y_1	X_1
0.0832	0.1752	0.187	12.23	38,081	38,081	6.67	6.44	-	-	-
0.0983	0.2068	0.186	11.65	44,908	44,908	8.26	6.46	-	-	-
0.1088	0.2306	0.186	16.20	50,573	50,573	6.68	6.30	-	-	-
0.1205	0.2555	0.186	16.45	57,524	57,524	7.48	6.29	-	-	-
0.1350	0.2874	0.186	18.92	67,227	67,227	7.58	6.22	-	-	-
0.1482	0.3170	0.186	21.85	77,124	77,124	7.54	6.14	-	-	-
0.1602	0.3444	0.186	24.98	87,030	87,030	7.44	6.10	-	-	-
0.1701	0.3665	0.204	26.37	99,720	99,720	8.07	6.05	-	-	-
0.1794	0.3883	0.204	29.21	108,551	108,551	7.92	6.00	-	-	-
0.1892	0.4115	0.208	32.25	119,371	119,371	7.88	5.98	-	-	-
0.2040	0.4464	0.220	36.09	138,222	138,222	8.11	5.95	-	-	-
0.2282	0.5052	0.268	43.51	180,410	180,410	8.59	5.91	-	-	-
0.2400	0.5350	0.279	48.69	200,823	200,823	8.72	5.84	-	-	-
0.2420	0.5435	0.280	52.47	205,270	205,270	-	-	-	-	-
0.2470	0.5585	0.280	57.62	210,410	150,598	5.54	-	59,812	-	-
0.2500	0.5735	0.322	65.03	230,187	167,644	5.46	-	62,543	0.702	0.01248
0.2560	0.5860	0.336	66.31	243,421	170,539	5.44	-	72,882	0.814	0.01315
0.2850	0.6850	0.256	68.18	263,092	174,793	5.43	-	88,299	0.988	0.01412
0.2880	0.6645	0.276	70.06	274,520	179,038	5.41	-	95,982	1.069	0.01515
0.3000	0.6920	0.228	70.54	281,397	180,102	5.40	-	101,295	1.135	0.01538

TABLE A-3 (continued)

TABLE

LIQUID: WATER

TEMPERATURE: 170.6^{o}F

AMPLITUDE: 0.0687 in.

WIRE DIA: 0.010 in.

L = $\frac{41}{64}$ in.

R_{100} = 0.044133 Ohm

FREQUENCY: 30 CPS

V Volts	EDC Volts	EAC Volts	ΔT ^{o}F	(Q/A) Btu/(hr)(ft^2)	$(Q/A)_{FC}$ Btu/(hr)(ft^2)	Nu_v	X	$(Q/A)_{boil}$ Btu/(hr)(ft^2)	Y_1	X_1
0.0585	0.1228	0.163	10.31	24,230	24,230	5.04	5.38	-	-	-
0.0794	0.1685	0.187	16.97	36,461	36,461	4.59	5.36	-	-	-
0.1120	0.2370	0.186	15.21	52,382	52,382	7.36	5.23	-	-	-
0.1123	0.2416	0.208	25.43	57,692	57,692	4.84	4.98	-	-	-
0.1298	0.2810	0.220	29.36	71,845	71,845	5.22	4.90	-	-	-
0.1450	0.3152	0.221	31.92	83,253	83,253	5.56	4.86	-	-	-
0.1574	0.3432	0.221	33.84	93,324	93,324	5.87	4.84	-	-	-
0.1770	0.3894	0.221	39.50	111,282	111,282	5.88	4.82	-	-	-
0.1944	0.4332	0.221	47.72	129,609	129,609	5.73	4.79	-	-	-
0.2040	0.4590	0.272	54.74	154,700	-	4.55	-	-	-	-
0.2120	0.4815	0.276	60.17	165,809	136,954	4.50	-	28,855	0.323	0.00988
0.2380	0.5451	0.317	65.19	212,220	127,700	4.45	-	84,520	0.947	0.01251

TABLE A-3 (continued)

FREQUENCY: 70 CPS

V Volts	EDC Volts	EAC Volts	ΔT ^oF	(Q/A) Btu/(hr)(ft^2)	$(Q/A)_{FC}$ Btu/(hr)(ft^2)	Nu_v	X	$(Q/A)_{boil}$ Btu/(hr)(ft^2)	Y_1	X_1
0.0525	0.1952	0.415	8.70	38,275	38,275	9.45	9.78	-	-	-
0.0678	0.2518	0.406	8.00	41,582	41,582	11.15	9.84	-	-	-
0.0857	0.3201	0.406	11.46	48,421	48,421	9.05	9.59	-	-	-
0.1032	0.3870	0.408	13.88	57,058	57,058	8.80	9.46	-	-	-
0.1208	0.4548	0.408	16.31	67,090	67,090	8.80	9.35	-	-	-
0.1384	0.5225	0.402	18.00	77,892	77,892	9.25	9.28	-	-	-
0.1485	0.5615	0.402	18.95	85,337	85,337	9.62	9.24	-	-	-
0.1610	0.6160	0.404	26.28	95,968	95,968	7.80	9.12	-	-	-
0.1759	0.6702	0.405	23.68	108,894	108,894	9.82	9.08	-	-	-
0.1911	0.7330	0.405	27.84	123,713	123,713	9.48	8.96	-	-	-
0.2067	0.7958	0.407	30.18	140,410	140,410	9.92	8.90	-	-	-
0.2190	0.8473	0.407	33.26	154,522	154,522	9.89	8.82	-	-	-
0.2314	0.9000	0.435	36.59	173,832	173,832	10.01	8.81	-	-	-
0.2412	0.9440	0.440	40.57	187,531	187,531	9.85	8.81	-	-	-
0.2543	0.9995	0.486	43.28	212,640	212,640	10.20	8.80	-	-	-
0.2665	1.0532	0.486	46.79	230,351	230,351	10.20	8.78	-	-	-
0.2763	1.0961	0.486	49.25	245,201	245,201	10.28	8.75	-	-	-
0.2860	1.1415	0.486	53.20	260,937	260,937	10.30	8.72	-	-	-
0.2984	1.1945	0.495	55.12	282,590	282,590	10.35	8.70	-	-	-
0.3085	1.2398	0.500	57.69	300,883	300,883	10.50	8.67	-	-	-
0.3086	1.2490	0.743	61.02	285,123	239,391	8.32	-	75,732	0.502	0.01032
0.3384	1.3817	0.510	68.15	359,468	264,578	8.22	-	94,890	1.042	0.01412
0.3482	1.4285	0.510	71.33	379,451	275,681	8.18	-	103,770	1.141	0.01579
0.3557	1.4632	0.510	73.13	394,936	281,949	8.16	-	112,987	1.242	0.01675

APPENDIX B

SAMPLE CALCULATIONS OF HEAT TRANSFER RESULTS

CALCULATION FOR THE HEAT TRANSFER RESULTS

1. Calculation of (ΔT) and (Q/A)

The formulae used are as follows:

$$I = \frac{V}{0.02}$$

$$R_T = \left(\frac{EDC}{I} \right)$$

$$Q = 3.415 \left[(EDC) \left(\frac{V}{0.02} \right) + \frac{(EAC)^2}{R_T} \right]$$

$$(Q/A) = 3.415 \left[(EDC) \left(\frac{V}{0.02} \right) + \frac{(EAC)^2}{R_T} \right] / (\pi D \ell)$$

$$T_W = \left(\frac{R_T - R_o}{R_{100} - R_o} \right) 100$$

Taking $\frac{R_{100}}{R_o} = 1.3925$

$$T_W = \left(\frac{354.777}{R_{100}} \right) \frac{(EDC)}{I} - 254.777$$

$$\Delta T = T_W - T_L$$

where

D - diameter of the platinum wire, ft

EAC - R.M.S. value for the A.C. voltage drop across the test section of the platinum wire, volts

EDC - D.C. potential drop across test section of the platinum wire, volts

I - D.C. current flowing through the wire, amperes

ℓ - length of the test section, ft

P - total electrical power dissipated from the test section to the surrounding liquid, watts

Q - rate of heat transfer from the wire to the liquid, Btu/hr

(Q/A) - heat flux, Btu/hr ft^2

R_o - electrical resistance of the test section at 0^oC, ohm

R_{100} - electrical resistance of the test section at 100^oC, ohm

R_T - resistance of the test section at T_W, ohm

T_W - temperature of the platinum wire, ^oC

T_L - temperature of the liquid, ^oC

ΔT - $(T_W - T_L)$, ^oC

Using data from Table A-2, p A-13

$T_L = 48^oC\ (118.4^oF)$

frequency of vibration of the wire = 40 CPS

amplitude of vibration of the wire = 0.0386 in.

V = 0.1975 volts EDC = 0.4625 volts EAC = 0.1755 volts

$D = \frac{0.01}{12}$ ft $\ell = \frac{53}{64} \times \frac{1}{12}$ ft $R_{100} = 0.0507$ ohm

substitution of these values in the above mentioned formulae gives:

$(Q/A) = 98{,}721$ Btu/hr ft^2

$\Delta T = 44.9^oF$.

2. Calculations of Re, Gr, Pr, Nu_v, X, X_1, Y_1

The following analytical expressions were used to calculate the physical properties of the fluid at any desired temperature, T, °F (TC, °C) .

For Water:

$$C_{pL} = [0.88616 + 1.4075 \left(\frac{T}{10^3}\right) - 2.3372 \left(\frac{T}{10^3}\right)^2], \text{ Btu/lb}^\circ\text{F}$$

$$h_{fg} = 10^4 [0.11594 + 0.0711 \left(\frac{T}{10^3}\right) - 1.0978 \left(\frac{T}{10^3}\right)^2$$

$$+ 4.1048 \left(\frac{T}{10^3}\right)^3 - 6.0493 \left(\frac{T}{10^3}\right)^4], \text{ Btu/lb} .$$

$$k_L = [0.2109 + 3.583 \left(\frac{T}{10^3}\right) - 35.935 \left(\frac{T}{10^3}\right)^2$$

$$+ 207.6 \left(\frac{T}{10^3}\right)^3 - 619.4 \left(\frac{T}{10^3}\right)^4 + 728.3 \left(\frac{T}{10^3}\right)^5], \text{Btu/hr ft } {}^\circ\text{F}$$

$$\beta = \frac{1}{1.8} [-0.06427 (10)^{-3} + 8.5053 (10)^{-6} (TC) - (6.79)(10)^{-8}$$

$$(TC)^2], \quad {}^\circ\text{F}^{-1}$$

$$\mu_L = 10 [0.7644 - 15.171 \left(\frac{T}{10^3}\right) + 171.16 \left(\frac{T}{10^3}\right)^2 - 1179.7 \left(\frac{T}{10^3}\right)^3$$

$$+ 4854.6 \left(\frac{T}{10^3}\right)^4 - 10901.0 \left(\frac{T}{10^3}\right)^5 + 10248.5 \left(\frac{T}{10^3}\right)^6], \text{ lb/ft h}$$

$$\rho_L = 100\ [\ 0.62284 + 0.07584\ (\frac{T}{10^3}) - 1.1890\ (\frac{T}{10^3})^2 + 1.3417\ (\frac{T}{10^3})^3],\ \text{lb}/\text{ft}^3$$

$$\sigma = \frac{1}{100}\ [0.53467 - 0.50921\ (\frac{T}{10^3}) - 0.52466\ (\frac{T}{10^3})^2],\ \text{lb/ft}$$

For Methanol:

$$C_{pL} = [\ 0.52223 + 1.5339\ (\frac{T}{10^3}) - 6.1728\ (\frac{T}{10^3})^2],\ \text{Btu/lb}\ ^\circ\text{F}$$

$$h_{fg} = 10^3\ [0.56558 + 0.16213\ (\frac{T}{10^3}) - 3.32646\ (\frac{T}{10^3})^2 + 3.64578\ (\frac{T}{10^3})^3],\ \text{Btu/lb}\ .$$

$$k_L = [\ 0.132074 - 0.00014815\ (T)],\ \text{Btu/hr ft}^\circ\text{F}$$

$$\beta = \frac{1}{1.8}\ [1.1342\ (10)^{-3} + 1.3635\ (10)^{-6}\ (TC) + 0.8741\ (10)^{-8}\ (TC)^2],\quad {}^\circ\text{F}^{-1}$$

$$\mu_L = [-0.4816 + 104.06\ (\frac{T}{10^3}) - 1942.9\ (\frac{T}{10^3})^2 + 15988.0\ (\frac{T}{10^3})^3 - 62994.0\ (\frac{T}{10^3})^4 + 96551.0\ (\frac{T}{10^3})^5],\ \text{lb/ft hr}$$

$$\rho_L = \frac{(2.54 \times 12)^3}{453.6} [\, 0.80999 - 0.0009253\ (TC) - 0.00000041\ (TC)^2], \ \ lb/ft^3$$

$$\sigma = \frac{1}{100} [\, 0.171386 - 0.232415\ (\frac{T}{10^3}) - 0.325992\ (\frac{T}{10^3})^2], \ lb/ft.$$

For forced convection region the fluid properties are used at the mean film temperature i.e. $T_{FIL} = \frac{T_W + T_L}{2}$, using the same data from Table A-2, p A - 13

$$Re = (\frac{2\ a\ f\ D}{12} \frac{\rho_L}{\mu_L}) \times 3600 = 41.862$$

$$Pr = \frac{C_{pL} \quad \mu_L}{k_L} = 3.095$$

$$Gr = \frac{g\ \beta\ \rho_L^2\ D^3\ \Delta T}{\mu_L^2} = 9.28$$

$$Nu_v = \frac{(Q/A)\ D}{\Delta T \quad k_L} = 4.83$$

$$X = (Pr^{0.72}\ Gr^{-0.06})\ (0.32\ Pr^{1.08} + 0.06\ Re^{0.86})$$

$$= 5.11$$

For pool boiling correlation the fluid properties are calculated at the saturation temperature of the fluid:

Using data from table A-2, p-A-11

$T_L = 48^oC(118.4^oF)$ Liquid: Water

$(Q/A) = 373{,}750$ Btu/hr ft^2

$\Delta T = 142.72^oF$

$T_W = 142.72 + 118.4 = 261.12\ ^oF$

$T_x = T_W - T_S = 261.12 - 212.0$

$= 49.12\ ^oF$

$$X_1 = \frac{C_{pL}\ T_x}{h_{fg}} \quad \frac{1}{Pr^{1.0}} = 0.02593$$

$$Y_1 = \frac{(Q/A)}{\mu_L\ h_{fg}} \sqrt{\frac{\sigma\ \ g_o}{(\rho_L - \rho_V)g}} = 4.11$$

For Methanol:

$$X_1 = \frac{C_{pL}\ T_x}{h_{fg}} \quad \frac{1}{Pr^{1.7}}$$

$$Y_1 = \frac{(Q/A)}{\mu_L\ h_{fg}} \sqrt{\frac{\sigma\ \ g_o}{(\rho_L - \rho_V)g}}$$

3. Calculation of Radial Gradient in Temperature within the Wire

Assuming that the thermal conductivity is constant and the electric heat is uniformly generated, McAdams et al.* derived the following equation:

$$T_{SW} = T_W - \frac{(Q/A)\ D}{8k}$$

where T_{SW} = surface temperature of the wire, °F

T_W = measured mean temperature of the wire, °F

(Q/A) = heat flux, Btu/hr ft^2

D = diameter of the wire, ft

k = thermal conductivity of the wire, Btu/hr ft °F

using data from Table A-2, p A-11

where $D = \frac{0.01}{12}$ ft

(Q/A) = 503,655 Btu/hr ft^2

ΔT = 147.3 °F

T_L = 118.4 °F

T_W = 147.3 + 118.4 = 265.7 °F

---

* McAdams, W.H., J.N. Addams, R.M. Rinaldo and R.S. Day, Chem.Eng.Prog.44 639 (1948)

$$\frac{(Q/A)\ D}{8k} = \frac{503{,}655 \times 0.01}{8 \times 42 \times 12} = 1.25\ ^{\circ}F$$

$$T_{SW} = T_W - 1.25 = 264.45\ ^{\circ}F$$

It can be seen that the error involved in neglecting the radial temperature gradient of the wire is less than 0.5%. At lower heat flux values the error is even smaller.

APPENDIX C

BUBBLE DYNAMICS DATA FROM NATURAL ACTIVE SITE

TABLE C-1

STATIONARY WIRE

ΔT = $38^{\circ}F$

Q/A = 10^5 Btu/(hr)(ft^2) approx.

Camera speed = 4800 frames/sec.

Bubble No.	Frame No.	Time Milli-seconds	Actual Bubble radius r, in. x 2.54
1	1	0.2083	0.03025
	2	0.4166	0.04100
	3	0.6249	0.04850
	4	0.8332	0.04960
	5	1.0420	0.05020
	8	1.6670	0.05190
	12	2.4990	0.06350
	15	3.1240	0.06460
	38	7.9150	0.07270
2	1	0.2083	0.04510
	2	0.4166	0.05888
	3	0.6249	0.06927
	4	0.8332	0.07331
	5	1.0420	0.07390
	6	1.2500	0.07562
	7	1.4580	0.07970
	8	1.6770	0.08080
	48	9.9980	0.08312

TABLE C-2

VIBRATING WIRE

f = 45 CPS

a = 0.0492 in.

ΔT = $35^{\circ}F$

Q/A = 10^5 Btu./(hr)(ft^2) approx.

Camera speed = 4800 frames/sec

Bubble No.	Frame No.	Time Milli-seconds	Actual Bubble radius r, in. x 2.54
1	1	0.2083	0.03233
	2	0.4166	0.03325
	4	0.8332	0.04468
	5	1.0420	0.05161
	6	1.2500	0.05599
	10	2.0830	0.05773
Waiting period = 44 frams = 9.165 Milli-seconds			
2	1	0.2083	0.02898
	2	0.4166	0.03117
	4	0.8332	0.03810
	5	1.0420	0.05311
	6	1.2500	0.05484
	7	1.4580	0.05542

Waiting period = 1 frame = 0.2083 Milli-seconds

TABLE C-2 (continued)

Bubble No.	Frame No.	Time Milli-seconds	Actual Bubble radius r, in. x 2.54
3	1	0.2083	0.02330
	2	0.4166	0.03060
	3	0.6249	0.03233
	4	0.8332	0.03694
	6	1.2500	0.03810
	7	1.4580	0.04387
Waiting period = 42 frames = 8.748 Milli-seconds.			
4	1	0.2083	0.02090
	2	0.4166	0.02252
	3	0.6249	0.03694
	4	0.8332	0.04156
	5	1.0420	0.04907
Waiting period = 1 frame = 0.2083 Milli-seconds .			
5	1	0.2083	0.03175
	2	0.4166	0.03579
	3	0.6249	0.03752
	5	1.0420	0.03810
Waiting period = 49 frames = 10.207 Milli-seconds.			
6	1	0.2083	0.02471
	2	0.4166	0.02967
	3	0.6249	0.03983
	4	0.8333	0.04156
Waiting period = 1 frame = 0.2083 Milli-seconds .			
7	1	0.2083	0.03117
	3	0.6249	0.04618
	4	0.8332	0.04733
	5	1.0420	0.05079
	6	1.2500	0.05195
	7	1.4580	0.05426
Waiting period = 2 frames = 0.4166 Milli-seconds .			

TALBE C-2 (continued)

Bubble No.	Frame No.	Time Milli-seconds	Actual Bubble radius r, in. x 2.54
8	1	0.2083	0.03475
	2	0.4166	0.04387
	3	0.6249	0.04618
	4	0.8332	0.04791
	5	1.0420	0.04964
	6	1.2500	0.05079
	7	1.4580	0.06003
Waiting period = 42 frames = 8.748 Milli-seconds .			
9	1	0.2083	0.03059
	2	0.4166	0.03925
	3	0.6249	0.04618
	4	0.8332	0.04733
Waiting period = 1 frame 0.2083 Milli-seconds.			
10	1	0.2083	0.03579
	2	0.4166	0.03925
	3	0.6249	0.04098
	4	0.8332	0.04214

TABLE C-3

VIBRATING WIRE

f = 45 CPS

a = 0.0492 in.

ΔT = 35°F

Q/A = 10^5 Btu/(hr)(ft^2) approx.

Camera speed = 4800 frames/sec

Bubble No.	Frame No. when bubble appears	Frame No. when bubble breaks off	Generating period $\tau_g \times 10^3$ secs	Waiting period $\tau_w \times 10^3$ secs	Bubble diameter at break-off d in. x 2.54
1	1	5	1.0420	0.2083	0.09513
2	6	9	0.8332	0.2083	0.09295
3	10	21	2.4996	5.4158	0.06670
4	48	52	1.0420	0.2083	0.08420
5	53	56	0.8332	7.9154	0.07983
6	95	103	1.8747	0.2083	0.11040
7	104	108	1.0420	28.7450	0.09295
8	247	256	2.0830	9.3735	0.10900
9	302	309	1.6670	0.2083	0.09513
10	310	315	1.2500	8.9569	0.06890
11	359	365	1.4580	0.2083	0.08857
12	366	369	0.8332	9.9984	0.07326
13	418	426	1.8747	0.4166	0.09076
14	429	435	1.4580	8.7486	0.09513
15	478	487	2.0830	7.9154	0.08857

TABLE C-3 (continued)

Bubble No.	Frame No. when bubble appears	Frame No. when bubble breaks off	Generating period $\tau_g \times 10^3$ secs	Waiting period $\tau_w \times 10^3$ secs	Bubble diameter at break-off d in. x 2.54
16	526	535	2.0830	0.8332	0.07764
17	540	544	1.0420	11.0400	0.06452
18	598	604	1.4580	0.4166	0.09951
19	607	610	0.8332	11.2480	0.06670
20	665	674	2.0830	0.6250	0.08420
21	678	683	1.2500	11.4560	0.07545
22	739	748	2.0830	0.6250	0.08857
23	752	761	2.0830	11.0400	0.10800
24	814	825	2.4996	1.0420	0.08200
25	831	836	1.2500	11.2480	0.08857
26	891	900	2.0830	0.2083	0.08638
27	901	906	1.2500	12.0814	0.10900
28	965	972	1.6670	0.2083	0.08200
29	973	980	1.6670	13.3300	0.09295
30	1045	1057	2.7079	0.6250	0.08420
31	1061	1070	2.0830	12.5000	0.07110
32	1131	1139	1.8747	0.2083	0.07982
33	1140	1146	1.4580	17.2900	0.08420
34	1230	1239	2.0830	0.2083	0.09295
35	1240	1250	2.2913	13.1230	0.10900
36	1314	1321	1.6670	0.2083	0.08420
37	1322	1327	1.2500	1.0420	0.06890
38	1333	1336	0.8330	13.9560	0.05796
39	1404	1415	2.4996	0.2083	0.09076
40	1416	1423	1.6670	17.7050	0.09732
41	1509	1519	2.2913	12.5000	0.06890
42	1580	1586	1.4580	0.2083	0.07764
43	1587	1594	1.6670	0.6250	0.08857
44	1598	1602	1.0420	17.7050	0.07764
45	1688	1694	1.4580	14.1640	0.07110
46	1763	1771	1.8747	0.2083	0.07764
47	1772	1779	1.6670	0.4166	0.08201
48	1782	1788	1.4580	13.9560	0.06670
49	1856	1863	1.6670	0.2083	0.07326
50	1864	1872	1.8747	17.4970	0.09295
51	1957	1968	2.4996	0.4166	0.09010
52	1971	1977	1.4580	0.2083	0.07982
53	1978	1985	1.6670	0.2083	0.08200

TABLE C-3 (continued)

Bubble No.	Frame No. when bubble appears	Frame No. when bubble breaks off	Generating period $\tau_g \times 10^3$ secs	Waiting period $\tau_w \times 10^3$ secs	Bubble diameter at break-off d in. x 2.54
54	1986	1993	1.6670	15.8310	0.09510
55	2070	2077	1.6670	0.2083	0.07110
56	2078	2085	1.6670	0.2083	0.08201
57	2086	2097	2.4996	14.3730	0.09076
58	2167	2173	1.4580	0.2083	0.06452
59	2174	2184	2.2913	0.4166	0.08640
60	2287	2297	2.2913	0.2083	0.08860
61	2298	2309	2.4996	15.6220	0.09951
62	2385	2394	2.0830	16.2470	0.09294
63	2473	2482	2.0830	0.2083	0.08201

APPENDIX D

BUBBLE DYNAMICS DATA
FROM ARTIFICIAL ACTIVE SITE

TABLE D-1

STATIONARY SURFACE

Q/A = 7×10^3 Btu/(hr)(ft^2) approx.

Camera speed = 500 frames/sec

Magnification on the projection table = 32.834X

Bubble No.	Frame No.	a cm	b cm	c cm	Contact Angle θ Deg-Min	Actual Bubble Diameter D in.	Actual Base Diameter D_b in.	Time Milli-Second
25	1	0.20	0.50	0.50	90-00	0.00417	0.00598	0.2
	2	0.55	0.80	0.65	56-00	0.00807	0.00775	0.4
	3	0.80	1.00	0.90	59-30	0.01080	0.01078	0.6
	4	1.20	1.30	1.10	54-15	0.01496	0.01318	0.8
	5	1.45	1.65	1.20	33-00	0.01858	0.01437	1.0
	6	1.90	1.95	1.20	37-00	0.02307	0.01437	1.2
	7	2.20	2.10	1.20	40-00	0.02574	0.01437	1.4
	8	2.50	2.30	1.15	43-30	0.02874	0.01377	1.6
	9	2.70	2.50	1.25	37-30	0.03114	0.01496	1.9
	11	3.02	2.85	1.27	34-30	0.03515	0.01519	2.2
	13	3.25	3.15	1.30	26-30	0.03834	0.01555	2.6
	15	3.45	3.35	1.45	34-45	0.04074	0.01736	3.0
	17	3.60	3.70	1.50	27-45	0.04370	0.01795	3.4
	19	3.90	3.80	1.50	38-30	0.04614	0.01795	3.8
	21	4.35	3.85	1.38	28-30	0.04913	0.01653	4.2
	23	4.65	4.00	1.20	44-45	0.05185	0.01437	4.6
	25	4.75	4.20	1.17	-	0.05362	0.01401	5.0
	28	4.95	4.20	1.15	-	0.05480	0.01377	5.6
	31	5.05	4.25	1.25	37-00	0.05574	0.01496	6.2

TABLE D-1 (continuoud)

Bubble No.	Frame No.	a cm	b cm	c cm	Contact Angle θ Deg-Min	Actual Bubble Diameter D in.	Actual Base Diameter D_b in.	Time Milli-seconds
25	34	4.80	4.55	1.30	38-00	0.05602	0.01555	6.8
	36	4.70	4.80	1.30	37-00	0.05692	0.01555	7.2
	39	4.80	5.00	1.50	34-30	0.05874	0.01795	7.8
	41	5.00	4.95	1.80	36-00	0.05964	-	8.2
	43	5.15	5.05	2.25	39-00	0.06114	-	8.6
	46	5.30	5.30	1.90	30-45	0.06354	-	9.2
	50	5.45	5.55	1.40	34-30	0.06594	0.01677	10.0
	55	5.85	5.55	1.50	35-00	0.06830	0.01795	11.0
	60	6.30	5.55	1.40	36-30	0.07102	0.01677	12.0
	64	6.35	5.70	1.25	42-30	0.07220	0.01496	12.8
	70	6.50	5.75	1.25	41-30	0.07342	0.01496	14.0
	75	6.70	5.70	1.35	36-45	0.07433	0.01618	15.0
	80	6.55	5.85	1.40	35-00	0.07433	0.01677	16.0
	85	6.40	6.05	1.30	38-30	0.07460	0.01555	17.0
	90	6.45	6.05	1.40	34-30	0.07492	0.01677	18.0
	100	6.48	6.40	1.15	33-15	0.07720	0.01377	20.0
	105	6.52	6.50	1.60	32-00	0.07803	0.01917	21.0
	115	7.05	6.45	1.45	35-30	0.08090	0.01736	23.0
	120	7.20	6.55	1.35	38-00	0.08240	0.01618	24.0
	130	7.65	6.50	1.25	41-00	0.08480	0.01496	26.0
	140	7.60	6.55	1.15	42-30	0.08480	0.01377	28.0
	150	7.55	6.60	1.25	40-15	0.08480	0.01496	30.0
	160	7.30	6.80	1.30	38-30	0.08452	0.01555	32.0
	170	7.35	6.90	1.45	35-45	0.08539	0.01736	34.0
	180	7.50	7.00	1.50	40-00	0.08692	0.01795	36.0
	190	7.85	7.05	1.20	46-30	0.09000	0.01370	38.0
	200	8.20	7.00	1.25	47-30	0.09110	0.01496	40.0
	205	8.30	7.00	1.15	45-30	0.09169	0.01377	41.0
	215	8.30	7.05	1.10	51-30	0.09200	0.01318	43.0
	230	8.05	7.10	0.95	44-15	0.09082	0.01137	46.0
	245	8.10	7.10	1.15	40-15	0.09110	0.01377	49.0
	260	8.03	7.35	1.15	38-30	0.09220	0.01377	52.0
	270	8.25	7.30	1.15	39-30	0.09318	0.01377	54.0
	281	8.45	7.45	1.00	37-30	0.09531	0.01196	56.2
	296	8.70	7.45	1.00	41-45	0.09681	0.01196	59.2
	307	8.80	7.45	0.90	40-30	0.09740	0.01078	61.4
	313	8.85	7.45	0.65	35-00	0.09771	0.00775	62.6
	315	8.25	7.50	-	34-00	0.09440	-	Departed

TABLE D-2

VIBRATING SURFACE

Amplitude = 0.125 in.

RPM = 600.00

(Q/A) = 7×10^3 Btu/(hr)(ft^2) approx.

Camera speed = 5000 frames/sec

Magnification on the projection table = 32.834X

Bubble No.	Frame No.	a cm	b cm	c cm	Contact Angle Θ Deg-Min	Actual Bubble Diameter D in.	Actual Base Diameter D_b in.	Time Milli-seconds
8	1	0.40	1.00	1.00	90-00	0.00838	0.01196	0.2
	2	0.60	1.10	1.10	90-00	0.01015	0.01318	0.4
	3	0.85	1.15	1.05	76-30	0.01196	0.01255	0.6
	4	1.15	1.20	1.10	67-45	0.01405	0.01318	0.8
	5	1.30	1.30	1.15	71-30	0.01555	0.01377	1.0
	6	1.45	1.35	1.15	64-30	0.01677	0.01377	1.2
	8	1.55	1.60	1.25	52-00	0.01885	0.01496	1.6
	11	1.85	1.80	1.25	55-00	0.02185	0.01496	2.2
	14	2.05	2.00	1.20	52-00	0.02425	0.01437	2.8
	17	2.25	2.15	1.20	37-15	0.02637	0.01437	3.4
	21	2.50	2.40	1.25	46-00	0.02937	0.01496	4.2
	26	2.70	2.60	1.30	50-15	0.03177	0.01555	5.2
	31	2.95	2.85	1.30	45-00	0.03476	0.01555	6.2
	38	3.25	3.05	1.25	45-15	0.03775	0.01496	7.6
	46	3.55	3.30	1.40	37-00	0.04106	0.01677	9.2
	55	3.85	3.50	1.30	32-30	0.04405	0.01555	11.0

TABLE D-2 (continued)

Bubble No.	Frame No.	a cm	b cm	c cm	Contact Angle θ Deg-Min	Actual Bubble Diameter D in.	Actual Base Diameter D_b in.	Time Milli-seconds
8	65	4.00	3.75	1.40	35-00	0.04645	0.01677	13.0
	75	4.20	3.90	1.30	39-15	0.04854	0.01555	15.0
	85	4.25	4.20	1.40	33-45	0.05062	0.01677	17.0
	100	4.60	4.45	1.45	33-45	0.05425	0.01736	20.0
	110	5.10	4.50	1.30	44-00	0.05751	0.01555	22.0
	120	5.25	4.55	1.30	43-00	0.05874	0.01555	24.0
	133	5.05	5.00	1.60	34-00	0.06023	0.01917	26.6
	140	5.00	5.40	2.15	27-30	0.06232	0.02574	28.0
	150	5.60	5.80	2.23	35-30	0.06830	0.02673	30.0
	155	6.05	5.80	1.70	36-15	0.07102	0.02035	31.0
	159	6.40	5.60	1.60	42-15	0.07192	0.01917	31.8
	164	6.85	5.60	1.45	46-00	0.07460	0.01736	32.8
	169	7.05	5.55	1.25	41-00	0.07551	0.01496	33.8
	174	7.10	5.55	1.10	32-30	0.07582	0.01318	34.8
	180	6.75	5.65	1.15	36-00	0.07433	0.01377	36.0
	185	6.40	5.75	1.20	32-15	0.07283	0.01437	37.0
	190	5.75	6.00	1.85	20-30	0.07043	0.02216	38.0
	195	5.30	6.35	2.40	22-30	0.06984	0.02870	39.0
	202	5.60	6.90	3.80	27-30	0.07492	0.04555	40.4
	207	6.05	7.30	3.60	33-15	0.08000	0.04314	41.4
	212	6.60	7.25	2.50	27-00	0.08303	0.02996	42.4
	217	7.40	7.15	1.55	37-30	0.08720	0.01858	43.4
	221	7.90	7.00	1.40	38-00	0.08929	0.01677	44.2
	224	8.25	7.10	1.05	33-30	0.09200	0.01255	44.8
	226	8.70	7.05	0.65	35-45	0.09440	0.00775	45.2

TABLE D-3

VIBRATING SURFACE

Amplitude = 0.125 in.

RPM = 1200.00

(Q/A) = 7×10^3 Btu/(hr)(ft^2) approx.

Camera speed = 5000 frames/sec

Magnification on the projection table = 32.834X

Bubble No.	Frame No.	a cm	b cm	c cm	Contact Angle θ Deg-Min	Actual Bubble Diameter D in.	Actual Base Diameter D_b in.	Time Milli-Seconds
4	1	0.40	0.97	0.97	90-00	0.00818	0.01101	0.2
	2	0.55	1.00	1.00	90-00	0.00929	0.01196	0.4
	3	0.70	1.05	1.05	90-00	0.01047	0.01255	0.6
	4	0.85	1.05	1.00	83-00	0.01137	0.01196	0.8
	5	1.00	1.20	1.05	73-00	0.01318	0.01255	1.0
	8	1.60	1.60	1.10	55-00	0.01917	0.01318	1.6
	11	2.05	2.00	1.20	48-30	0.02407	0.01437	2.2
	16	2.70	2.60	1.25	45-15	0.03177	0.01496	3.2
	22	3.40	3.10	1.18	43-45	0.03893	0.01413	4.4
	30	3.75	3.60	1.25	42-30	0.04405	0.01496	6.0
	40	4.30	3.95	1.25	38-30	0.04944	0.01496	8.0
	50	4.30	4.55	1.75	33-00	0.05303	0.02094	10.0
	56	4.95	4.65	1.38	35-00	0.05751	0.01653	11.2
	60	5.40	4.60	1.15	44-30	0.05992	0.01377	12.0
	66	5.90	4.47	1.10	48-30	0.06216	0.01318	13.0

TABLE D-3 (continued)

Bubble No.	Frame No.	a cm	b cm	c cm	Contact Angle Θ Deg -Min	Actual Bubble Diameter D in.	Actual Base Diameter D_b in.	Time Milli-seconds
4	71	6.05	4.60	0.95	42-00	0.06381	0.01137	14.2
	77	5.90	4.75	1.13	48-30	0.06381	0.01354	15.4
	82	4.88	5.00	1.20	34-30	0.05921	0.01437	16.4
	88	4.65	5.20	1.80	30-00	0.05901	0.02157	17.6
	83	4.80	5.55	3.00	34-00	0.06204	0.03594	16.6
	90	5.15	5.85	2.40	34-00	0.06594	0.02874	18.0
	95	6.00	5.65	1.45	49-30	0.06984	0.01736	19.0
	100	6.70	5.80	1.05	46-00	0.07492	0.01255	20.0
	103	7.00	5.75	0.45	42-30	0.07641	0.00539	20.6

APPENDIX E

FORCES ACTING ON A BUBBLE DURING GROWTH PERIOD

TABLE E-1

STATIONARY SURFACE

Time Milli-seconds	$F_{inertia}$ lbf x 10^5	$F_{buoyancy}$ lbf x 10^5	$F_{surface\ tension}$ lbf x 10^5	F_{drag} lbf x 10^5
0.25	0.0407	0.2170	0.4335	0.0037
0.50	0.1308	0.3441	0.6847	0.0061
0.75	0.2380	0.4257	0.8415	0.0083
1.00	0.3638	0.4759	0.9307	0.0102
1.25	0.5057	0.5066	0.9754	0.0121
1.50	0.6618	0.5277	0.9946	0.0138
1.75	0.8309	0.5472	1.0036	0.0155
2.00	1.0118	0.5711	1.0135	0.0171
2.25	1.2039	0.6034	1.0319	0.0186
2.50	1.4064	0.6463	1.0624	0.0202
2.75	1.6188	0.6998	1.1045	0.0216
3.00	1.8406	0.7621	1.1540	0.0230
5.00	0.0027	0.7878	1.0400	0.0052
7.50	0.0018	0.8947	1.0586	0.0043
10.00	0.0014	0.9926	1.0742	0.0037
12.50	0.0011	1.0838	1.0860	0.0033
15.00	0.0009	1.1694	1.0959	0.0030
17.50	0.0008	1.2504	1.1021	0.0028
20.00	0.0007	1.3272	1.1051	0.0026
22.50	0.0006	1.4002	1.1049	0.0025
25.00	0.0006	1.4698	1.1016	0.0024
27.50	0.0005	1.5362	1.0952	0.0023
30.00	0.0005	1.5995	1.0855	0.0022
32.50	0.0004	1.6600	1.0728	0.0021
35.00	0.0004	1.7176	1.0569	0.0020
37.50	0.0004	1.7726	1.0378	0.0019
40.00	0.0004	1.8250	1.0156	0.0019
42.50	0.0003	1.8749	1.9902	0.0018
45.00	0.0003	1.9224	0.9617	0.0018
47.50	0.0003	1.9675	0.9200	0.0017
50.00	0.0003	2.0103	0.8951	0.0017
52.50	0.0003	2.0508	0.8571	0.0016
55.00	0.0003	2.0890	0.8160	0.0016
57.50	0.0002	2.1251	0.7717	0.0016
60.00	0.0002	2.1590	0.7243	0.0015
62.50	0.0002	2.1908	0.6736	0.0015

TABLE E-2

VIBRATING SURFACE

Amplitude = 0.125 in.

RPM = 600.0

Q/A = 7×10^3 Btu/(hr)(ft^2)

Camera Speed = 5000 frames/sec.

TIME Milli-seconds	$F_{INERTIA}$ lbf x 10^5	$F_{BUOYANCY}$ lbf x 10^5	$F_{SURFACE\ TENSION}$ lbf x 10^5	F_{DRAG} lbf x 10^5
0.20	0.0454	0.6322	1.2628	0.0047
0.40	0.0384	0.6978	1.3916	0.0043
0.60	0.0348	0.6477	1.2886	0.0041
0.80	0.0325	0.6477	1.2854	0.0039
1.00	0.0308	0.6962	1.3790	0.0038
1.20	0.0295	0.6648	1.3125	0.0037
1.60	0.0275	0.6350	1.2450	0.0036
2.20	0.0254	0.6661	1.2942	0.0035
2.80	0.0240	0.6240	1.1960	0.0034
3.40	0.0229	0.4930	0.9187	0.0033
4.20	0.0218	0.6128	1.1366	0.0032
5.20	0.0207	0.6903	1.2627	0.0031
6.20	0.0198	0.6550	1.1613	0.0031
7.60	0.0189	0.6583	1.1221	0.0030
9.20	0.0180	0.6582	1.0660	0.0029
11.00	0.0173	0.6000	0.8825	0.0029
13.00	0.0106	0.7055	1.0160	0.0028
15.00	0.0155	0.7734	0.9841	0.0027
20.00	0.0149	0.8550	1.0187	0.0027
22.00	0.0146	0.9657	1.1409	0.0026
24.00	0.0143	1.0034	1.1201	0.0026
26.60	0.0140	1.0740	1.1322	0.0026
28.00	0.0138	1.1710	1.2554	0.0026

continued...

TABLE E-2 (continued)

TIME Milli- second	$F_{INERTIA}$ lbf x 10^5	$F_{BUOYANCY}$ lbf x 10^5	$F_{SURFACE\ TENSION}$ lbf x 10^5	F_{DRAG} lbf x 10^5
30.00	0.0135	1.4148	1.6395	0.0025
31.00	0.0134	1.2569	1.2710	0.0025
31.80	0.0134	1.3233	1.3613	0.0025
32.80	0.0133	1.3289	1.3189	0.0025
33.80	0.0132	1.2148	1.0366	0.0025
34.80	0.0131	1.0978	0.7480	0.0025
36.00	0.0136	1.1834	0.8549	0.0025
37.00	0.0129	1.1900	0.8100	0.0025
38.00	0.0128	1.2227	0.8200	0.0025
39.00	0.0127	1.4212	1.1601	0.0025
40.80	0.0126	2.0035	2.2215	0.0025
41.40	0.0125	2.1593	2.4983	0.0024
42.40	0.0125	1.6576	1.4360	0.0024
43.40	0.0124	1.5659	1.1946	0.0024
44.20	0.0123	1.5374	1.0905	0.0024
44.80	0.0123	1.3760	0.7316	0.0024
45.20	0.0123	1.2610	0.4782	0.0024

TABLE E-3

VIBRATING SURFACE

Amplitude = 0.125 in.

RPM = 1200

Q/A = 3×10^7 Btu/(hr)(ft^2)

Camera Speed = 5000 frames/sec.

TIME Milli-seconds	$F_{INERTIA}$ lbf x 10^5	$F_{BUOYANCY}$ lbf x 10^5	$F_{SURFACE\ TENSION}$ lbf x 10^5	F_{DRAG} lbf x 10^5
0.20	0.0350	0.6133	1.2258	0.0036
0.60	0.0425	0.6650	1.3251	0.0040
0.80	0.0447	0.6310	1.2535	0.0041
1.00	0.0465	0.6400	1.2674	0.0042
1.60	0.0505	0.5822	1.1402	0.0044
2.20	0.0534	0.5886	1.1367	0.0045
3.20	0.0570	0.5984	1.1221	0.0047
4.40	0.0603	0.5789	1.0320	0.0048
6.00	0.0637	0.6380	1.0675	0.0049
8.00	0.0670	0.6586	0.9836	0.0050
10.00	0.0700	0.8923	1.2046	0.0051
11.20	0.0711	0.7895	1.0014	0.0052
12.00	0.0720	0.8329	1.0194	0.0052
13.20	0.0732	0.8989	1.0426	0.0053
14.20	0.0741	0.8272	0.8035	0.0053
15.40	0.0752	1.0211	1.0710	0.0053
16.40	0.0760	0.9680	0.8597	0.0054
16.60	0.0762	1.6102	2.1227	0.0054
17.60	0.0770	1.1734	1.1391	0.0054
18.00	0.0773	1.4751	1.6975	0.0054
19.00	0.0780	1.3813	1.3942	0.0054
20.00	0.0787	1.2207	0.9535	0.0055
20.60	0.0791	0.9731	0.3848	0.0055